Non-Equilibrium Dynamics of Interacting Many-Body Quantum Systems in One Dimension

Bruno Bertini
St Hugh's College
University of Oxford

A thesis submitted for the degree of
Doctor of Philosophy
Trinity Term 2015

Non-Equilibrium Dynamics of Interacting Many-Body Quantum Systems in One Dimension

Bruno Bertini

St Hugh's College, University of Oxford

A thesis submitted for the degree of *Doctor of Philosophy*

Trinity Term 2015

Abstract

In this thesis we study three examples of interacting many-body systems undergoing a non equilibrium time evolution.

Firstly we consider the time evolution in an integrable system: the sine-Gordon field theory in the repulsive regime. We will focus on the one point function of the semi-local vertex operator $e^{i\beta\phi(x)/2}$ on a specific class of initial states. By analytical means we show that the expectation value considered decays exponentially to zero at late times and we determine the decay time. The method employed is based on a form-factor expansion and uses the "Representative Eigenstate Approach" of Ref. [73] (a.k.a. "Quench Action").

In a second example we study the time evolution in models close to "special" integrable points characterised by hidden symmetries generating infinitely many local conservation laws that do not commute with one another, in addition to the infinite commuting family implied by integrability. We observe that both in the case where the perturbation breaks the integrability and when it breaks only the additional symmetries maintaining integrability, the local observables show a crossover behaviour from an initial to a final quasi stationary plateau. We investigate a weak coupling limit, identify a time window in which the effects of the perturbations become significant and solve the time evolution through a mean-field mapping. As an explicit example we study the XYZ spin-1/2 chain with additional perturbations that break integrability.

Finally, we study the effects of integrability breaking perturbations on the non-equilibrium evolution of more general many-particle quantum systems, where the unperturbed integrable model is generic. We focus on a class of spinless fermion models with weak interactions. We employ equation of motion techniques that can be viewed as generalisations of quantum Boltzmann equations. We benchmark our method against time dependent density matrix renormalisation group computations and find it to be very accurate as long as interactions are weak. For small integrability breaking, we observe robust prethermalisation plateaux for local observables on all accessible time scales. Increasing the strength of the integrability breaking term induces a "drift" away from the prethermalisation plateaux towards thermal behaviour. We identify a time scale characterising this crossover.

To Caterina and my parents.

Acknowledgements

Firstly I would like to thank my supervisor: Prof. Fabian Essler. I will never forget his strenuous exhortations to follow always the proper path instead of taking short-cuts and to "do the calculation" instead of attempting premature physical interpretations. During these three years in Oxford he managed to teach me a great amount of new things ranging from techniques to extract the asymptotic time dependence of a form-factor expansion to the difference between "analogue" and "analogous", which in Italian are the same word. I also thank him for having provided a generous amount of feedback for this thesis, helping to make it "more clear than it was before".

I thank Maurizio Fagotti, who can be considered a sort of additional supervisor, given the number of questions he answered and advices he gave during these three years. Talking with him it has been instructive, offered a different perspective on the topics and gave me the possibility of discussing physics in my mother language.

I am grateful to all the other collaborators that I had the pleasure to work with: Neil Robinson, Dirk Schuricht and Stefan Groha. I particularly thank Neil for everything he taught me and also for having provided me with the ED data for the Chapter 5 of this thesis.

I also sincerely thank my examiners: Paul Fendley and Jean-Sébastien Caux, for their detailed reading of this thesis, for their helpful comments and observations, and for the enjoyable viva they conducted.

The Rudolf Peierls Centre for Theoretical Physics has been my second home here in Oxford and I wish to thank all the people that contributed to make this place so friendly and inspiring: John Cardy, John Chalker, Steve Simon, Zohar Rigel, Stefanie Thiem, Imke Schneider, Pablo Serna, Gabor Halasz, Dillon Liu, Thomas Scaffidi, Richard Fern, Michelle Bosher, Sara Loving, Stephanie Shen, Sara Williams and Ethna Davey. In particular I want to thank my officemates: Thomas Veness and Fenner Harper, for having helped me several times, for all the interesting discussions we had, and for having introduced me to crucial aspects of the British culture. I am grateful to Thomas also for having proofread many parts of this thesis, making always useful comments and observations: if some of the "also" are now in the right place it is due to him.

Getting used to the English weather and being deprived of the Italian food has been really hard, among the factors that helped me to carry on I really need to mention my friends: Mira Zorkot, Mohamad Fahes, Gianluca Laghezza and Giada Nuzzo. In particular, I am sincerely grateful to my house-mates/best friends: Viviana Ponta, Mattia Sormani and Arnold Mathijssen. I thank Viviana for all the Jaffa cakes she offered me, Mattia for having taught me how not to play Street Fighter and Arnold for having cheered me up (together with the entire neighbourhood) singing the opera during his morning shower. I also want to thank my course mates in Pisa, in particular: Guido, Ivan, Tommaso, Silvio, Guglielmo and Andrea. I really miss the discussions about physics and movies with them.

Undoubtedly, I would like to thank my family: my (three) parents and my grandmother. Every one of them in his own way managed to give me a really invaluable

amount of support, during my life in general and these three years in particular.

Most importantly I thank Caterina. These have been three significant years in our lives, she became a doctor and I will hopefully do the same, of course living in two different countries for three years has been really tough some times, but we managed to overcome all the difficult moments and our relation is now even more tight than it was before. We are now ready to open the next chapter of our life together.

The work presented in this thesis is based on three published papers [1–3]. My work in Oxford has been supported by the EPSRC under grant EP/I032487/1.

Contents

1. Introduction

Many-body systems are arguably the most interesting subject to study in physics, showing an incredibly rich phenomenology and giving rise to the most unexpected effects. Unexpected because generically the behaviour of many-body systems can not be understood just by extrapolating that of few body systems, on the contrary they show some phenomena that are revealed only when the number of degrees of freedom in play becomes enormous (infinite for any practical purpose), so called *emergent phenomena*. An example worth mentioning is undoubtedly the phenomenon of *spontaneous symmetry breaking*, the physical mechanism behind the appearance of different phases of a condensed matter system but also behind the Higgs-Anderson mechanism in particle physics, to name but two remarkable examples.

The study of many-body systems is ubiquitous in physics, its applications range from astrophysics to biophysics, from particle physics to condensed matter. The question that every scientist dealing with these complicated objects is trying to answer is whether she or he can find some *universal* properties, *i.e.* some properties that do not depend on the particular configuration of every degree of freedom constituting the system, but instead on a few key attributes characterising it. The existence of these properties is what makes the study of a many-body system possible on the one hand and useful on the other.

The equilibrium properties of many-body systems, both classical and quantum, have been extensively and successfully studied during the twentieth century, leading for example to the elegant concept of the *Renormalisation Group*. In essence the idea is to identify which are the measurable properties of the systems under investigation and find some transformations that simplify the problem while keeping these properties fixed. In particular, in the case of many body systems near to the critical point, these concepts have been put on a more quantitative ground allowing one to extract a substantial amount of information [4–6].

The dynamics of (closed) many-body systems, however, turned out to be an even more difficult problem to study. On the classical side some progress has been achieved. For example the seminal paper [7] stimulated an intensive study on the validity of the *ergodicity hypothesis*, which assumes the trajectory of the system in Phase Space passes close enough to any point of the Phase Space with the same energy. It was understood that the *ergodic hypothesis* does not generally hold in systems with a finite number of degrees of freedom; even if anharmonic potentials are included. In order for the system to display statistical properties the anarmonicity must be above some threshold [8], which guarantees the majority of initial conditions show

chaotic behaviour [9]. The generic presence of cross-over behaviour from regular to chaotic motion depending on the strength of the perturbation added to integrable systems has been described by the celebrated KAM theory [10].

The study of the dynamics in closed quantum many-body systems was considered in the early days of quantum mechanics by John von Neumann [11], who proved a quantum version of the ergodic theorem. After his work, however, this field of research has been set aside: some worth mentioning studies of these kind of problems have been carried out [12–15] but they remain essentially isolated. The reason for the lack of a systematic theoretical investigation on such an interesting problem has been, besides its fundamental difficulty, the impossibility to experimentally test any prediction. Historically, the standard condensed matter systems considered in laboratories were strongly affected by decoherence and dissipation effects, due to the coupling to the external environment. As a consequence, their coherence time was shorter than the measurement time: any theoretical prediction had to take into account the effect of the environment making the comparison much less definite and clear. In addition, effective dissipation mechanisms are present also if the coupling with the environment could be neglected. For example, together with the electronic degrees of freedom, solid state systems have phonons: neglecting their effect on the electronic problem produce effective dissipation. This situation experienced a profound modification during the last decade, when some drastic improvements in experimental techniques allowed the realisation in laboratories of systems of ultra cold atoms, whose dynamics are very close to be unitary and are excellently described by models simple enough to be studied by theoreticians [16–26]. The breakthrough in experimental techniques stimulated intensive theoretical activity on both the numerical and purely analytical side, aiming at understanding the universal physical properties of time evolving quantum many-body systems. In the majority of the cases the physical situation considered has been a so called *quantum quench* [27], *i.e.* the system is taken in the ground state of a locally interacting Hamiltonian H_0 and at a certain time, which can be taken to be $t = 0$, the Hamiltonian is suddenly replaced with a different locally interacting one, H. Generically the two Hamiltonians are related by the change of some parameters. If the two Hamiltonians differ only in a finite region of the real space the quench is called a *local quench* and a *global quench* otherwise. In this thesis we will be interested in the case of global quenches.

The simplest question to ask about time evolving systems regards their stationary properties, *i.e.* do those systems reach some sort of stationary state? If so, can this stationary state be determined from some macroscopic properties of the system? In order to answer questions of this kind, the first step is to correctly identify what we mean by relaxing to stationary

state. Since the systems under consideration are subject to a closed unitary evolution, it is always possible to find some observables whose expectation values keep oscillating indefinitely. However, in the thermodynamic limit (where the volume of the system goes to infinity keeping constant all the densities), observables restricted to finite subsystems can reach stationary values, in this case the rest of the system plays the role of a bath. This suggests a simple definition: we say that a system relaxes to a stationary state if for every finite subsystem A in the thermodynamic limit

$$\exists \lim_{t\to+\infty} \rho_A(t) \equiv \rho_A(\infty)\,, \tag{1.1}$$

where $\rho_A(t) \equiv \mathrm{Tr}_{\bar{A}}\left[\rho(t)\right]$ is the density matrix reduced to the subsystem A [28].

The current belief is to link the values that the observables reach in these stationary states with their local conservation laws, *i.e.* the conservation laws that can be expressed as a sum (an integral in the continuum models) of some local densities. The main distinction is then between generic models which typically have only the Hamiltonian $I_0 = H$ as a local conservation law and *integrable models* possessing an infinite number of local conservation laws $\{I_i\}_{i=0,1,\dots}$. In generic models, the stationary values reached by local observables at late times can be described by a *Gibbs ensemble* [14, 15, 28–34]

$$\rho_A(\infty) = \mathrm{tr}_{\bar{A}}\left[\rho_{\mathrm{GE}}\right]\,, \qquad \rho_{\mathrm{GE}} = \frac{1}{Z} e^{-\beta_{\mathrm{eff}} H}\,, \tag{1.2}$$

which, as only memory of the initial state, retains the information about the energy density through β_{eff}

$$\lim_{L\to\infty} \frac{1}{L} \langle H \rangle_0 = \lim_{L\to\infty} \frac{1}{L} \left[H \rho_{\mathrm{GE}}\right]\,. \tag{1.3}$$

In integrable models on the other hand, observables reach stationary values that are described by a so called *generalized Gibbs ensemble* (GGE) [35] and [28, 29, 36–41]

$$\rho_A(\infty) = \mathrm{tr}_{\bar{A}}\left[\rho_{\mathrm{GGE}}\right]\,, \qquad \rho_{\mathrm{GGE}} = \frac{1}{Z} e^{-\sum_i \lambda_i I_i}\,, \tag{1.4}$$

which retains memory of all the initial values of the infinite local conservation laws, through the Lagrange multipliers λ_i

$$\lim_{L\to\infty} \frac{1}{L} \langle I_i \rangle_0 = \lim_{L\to\infty} \frac{1}{L} \left[I_i \rho_{\mathrm{GGE}}\right]\,. \tag{1.5}$$

This picture has been fully established for many models that are free or can be mapped into free models [42–46]. The logical step forward would be to establish the validity of the GGE also

for interacting integrable models; in some cases has been possible to derive expectation values of local observables in the stationary state after a quantum quench in those models [47–53]. Recent results [54–57], however, have shown that the situation might be more complicated, pointing out that the current GGE predictions do not reproduce the correct stationary values in some cases. However a "conservative" interpretation of these results remains on the scene: the observed disagreement might be due to the existence of some local (or even quasi-local, meaning that the density is decaying exponentially) conservation laws that are still unknown and so are not included in the current GGE prediction, this interpretation is strongly encouraged by very recent findings [58, 59]. We stress that the last developments described are still subject of intensive ongoing research.

Understanding the stationary properties of a time evolving system is clearly very important, but is not the only interesting aspect to study: the dynamics can reveal an even richer spectrum of interesting phenomena. An intriguing example of these, which will be considered in detail in this thesis, is the so-called *prethermalisation* [60, 61], where time evolving weakly non-integrable systems show a transient behaviour, during which local observables reach non-thermal plateaux reminiscent of the underlying integrable theory. This mechanism has been theoretically predicted in several cases [2, 60–70] and, most importantly, observed in experiments [18–20]. The prethermalisation phenomenon drastically widens the application of the results on the dynamics of integrable models: a very large class of systems which are close enough to integrable points will show an "integrable-like" behaviour, at least in a certain time window. This key observation allows one to realise that the study of integrable models out of equilibrium is necessary to understand "real-world" situations and it is not only an academic matter. The common belief is to consider the prethermalization as a transient effect, expecting the non-purely elastic processes typical of non integrable models to become effective at late enough times and bring the system to the thermal stationary state. Reaching times that are long enough to see the system moving from a pre-thermal to a thermal state has revealed to be impractical for most of the numerical [71] and analytical [2, 60, 61, 66] approaches. Until very recently, the only example of a weakly interacting system eventually approaching the thermal plateau has been given in the infinite dimensional case [72]. In [3] we presented what, to the best of our knowledge, represents the first example of a weakly non-integrable one-dimensional model showing prethermalisation behaviour and then approaching the thermal state. In particular, we considered a model with tuneable integrability breaking; for small integrability breaking, we observed robust prethermalisation plateaux for local observables on all accessible timescales. Increasing the strength of the integrability breaking term induces a drift away from

the prethermalisation plateaux towards thermal behaviour.

Importantly, prethermalisation-like behaviour is not limited only to non-integrable models, in Ref. [2] we showed that something very similar can happen in integrable models when one weakly breaks some hidden symmetries which generate additional families of local conservation laws not commuting with one another. In this case, local observables first reach quasi-stationary plateaux reminiscent of the unperturbed model and then move away towards different plateaux described by the perturbed model, which can be still integrable. We call this process *pre-relaxation* since thermalisation is not expected to occur in all these cases. A difference between this case and the one described above is the timescale on which the drifting from the initial plateaux occurs; when there is the standard prethermalisation, the findings of Ref. [3] suggest this to happen at times $t \sim g^{-2}$, where g is the strength of the perturbation. In the case of pre-relaxation on the other hand the drifting takes place at times $t \sim g^{-1}$.

More generally, the main objective of the research in time evolving quantum many body systems is, once again, to find some universal behaviour and concomitantly a method of studying it, which can be applied to a large class of systems, depending only on some basic properties of the class. Currently only very few general techniques are known which allow one to cope with this kind of question for *interacting models*, examples worth mentioning of these are the *Representative Eigenstate Approach* (a.k.a. *Quench Action*) [73] and *Linked Cluster Expansion Approaches* (developed in the the study of equilibrium properties at finite temperature [74]) applicable to the cases where the interaction is integrable. In Ref. [1] we presented the first application of those methods to the determination of the time evolution in the sine-Gordon field theory, a paradigmatic example of interacting integrable model. When the interaction becomes non-integrable the situation complicates even further, however some cases are still analytically tractable. In Ref. [2], we show that the time evolution under weakly-interacting (integrable or non-integrable) Hamiltonians in the time window $gt \sim g^0$ can be mapped into the one generated by free, although time-dependent Hamiltonians which fulfil some self consistency conditions. In Ref. [3] on the other hand, we studied a weakly-interacting non integrable model by means equation of motion techniques that can be viewed as generalisations of quantum Boltzmann equations [75,76]. The purpose of this thesis is to illustrate these methods and their applications to physically relevant cases.

1.0.1 Organisation of the thesis

The rest of this thesis is structured as follows. Chapter 2 reviews some properties of two well known integrable models and introduces some concepts that will be used in the rest of the work.

Chapter 3 contains the study of time evolution in the sine-Gordon model. In particular, there we describe how to determine the time evolution (for large but finite times) of the one-point function of a particular (and highly non-trivial) operator on a class of initial states. This chapter is based on the work [1]. Chapter 4 studies the time evolution of weakly interacting models in the time window $gt \sim g^0$, where g is the strength of the interaction. Together with the general discussion, an application of the formalism to a perturbed XYZ spin-1/2 chain is considered. This chapter draws heavily on the work [2]. Chapter 5 considers the prethermalisation regime and the eventual moving to the thermal one in a weakly interacting model, that can be viewed as a perturbed version of the Peierls insulator [77]. Some of the material presented here is taken from [3], there are however also some results which will be published in the future. Finally Chapter 6 contains a summary of the material presented and some outlook.

2. Two integrable models

In Chapter 1 we discussed the key role of integrable models and their weak deformations in understanding the non-equilibrium time evolution of many-body systems. The goal of this chapter is to examine two outstanding examples of integrable models which will turn out to be of great interest in the course of this thesis: the XY spin chain and the sine-Gordon model.

The first represents a prominent example of a *noninteracting* integrable model, it is noninteracting because it can be mapped into a free fermionic system via a Jordan-Wigner transformation. A typical reason to study free systems is that their exact solvability helps to understand some features that are expected to be generic. Later in this thesis, however, we will see that understanding free models also allows one to extract information on the time evolution of their interacting deformations. The sine-Gordon model on the other hand is the paradigmatic example of an *integrable* interacting field theory (on both the classical and the quantum level [6,78]). Interacting integrable models represent a further step towards the understanding of the "real world" cases, in particular interacting integrable field theories give a universal description of the low energy behaviour of several experimentally relevant systems [79]. Some of their properties, such as the spectrum of the excitations and the scattering matrix are accessible while others, such as correlation functions, are difficult to compute and cannot be generally determined exactly.

The purpose of this chapter is to explain the physical relevance of these models and review some of their mathematical properties, as those will prove to be useful in the rest of the thesis.

2.1 The XY model

The XY model is described by the following Hamiltonian

$$H_{\mathrm{XY}}(\gamma,h)=J\sum_{\ell=1}^{L}\left(\frac{1+\gamma}{4}\sigma_\ell^x\sigma_{\ell+1}^x+\frac{1-\gamma}{4}\sigma_\ell^y\sigma_{\ell+1}^y\right)+\frac{Jh}{2}\sum_{\ell=1}^{L}\sigma_\ell^z\,, \tag{2.1}$$

acting on the Hilbert space $\mathcal{H}=\bigotimes_{i=1}^{L}\mathbb{C}^2$. Here σ_j^α acts as the Pauli matrix σ^α on the site j (j-th component of $\mathcal{H}$) and as the identity matrix elsewhere; we consider the case of periodic boundary conditions $\sigma_{L+1}^\alpha=\sigma_1^\alpha$, where $\alpha=x,y,z$. The Hamiltonian (2.1) is invariant under the $\mathbb{Z}_2$ transformation defined as

$$\sigma_i^\alpha\to-\sigma_i^\alpha\,,\qquad\qquad \alpha=x,y,\qquad\qquad \sigma_i^z\to\sigma_i^z\,, \tag{2.2}$$

for all values of γ and h. For $\gamma = 0$, the Hamiltonian exhibits a O(2) invariance under rotations of σ_j^α in the x-y plane.

As we will show in the following, the Hamiltonian (2.1) is mapped to free fermions by the application of a Jordan-Wigner transformation and then diagonalised by the subsequent application of a Fourier and a Bogoliubov transformation. Excitations over the ground state are gapless for $|h| < 1$ and $\gamma = 0$, or $|h| = 1$ and any possible value of γ. The fact that the model is mappable to free fermions was the main reason behind its introduction in [80], where the authors used this feature to obtain a better understanding of the role of the anisotropy γ in the Heisenberg interaction. The isotropic case $\gamma = 0$, for $|h| < 1$, shows the same qualitative behaviour as the interacting integrable XXZ spin-1/2 chain [81] in the "Luttinger liquid phase" (for zero external magnetic field it corresponds to values of the anisotropy $|\Delta| \leq 1$). In both cases the excitations are gapless and correlation functions show a power law decay; when h reaches a critical value h_c there is a phase transition to a gapped phase which lies in the universality class of *commensurate-incommensurate transition* (see [79] and references therein). Experimentally this regime of the XXZ spin chain has been investigated using for example Cs_2CoCl_4 [82]. An other interesting limiting case of the XY model is $\gamma = 1$ where it corresponds to the transverse field Ising chain (TFIC), which has been extensively studied both in the context of equilibrium quantum phase transitions [6,83,84] and the non-equilibrium dynamics [38,44,45,85–89]. Recently, the Ising limit of the XY model has been experimentally realised using $CoNb_2O_6$ [90].

In this thesis we will be interested in the case of zero external magnetic field $h = 0$, as in this case a symmetry of the dispersion relation will cause the appearance of additional sets of local conserved charges. From now on we adopt the shorthand notation $H_{\mathrm{XY}} \equiv H_{\mathrm{XY}}(\gamma, 0)$.

2.1.1 Diagonalization of the Hamiltonian

The first step to carry out in order to diagonalise the Hamiltonian H_{XY} is to map it to free fermions, as previously mentioned, this is done by means of a Jordan-Wigner transformation [91]. First we introduce

$$c_i^\dagger \equiv \prod_{j=1}^{i-1} \left(\sigma_j^z\right) \sigma_i^+ , \qquad c_i \equiv \prod_{j=1}^{i-1} \left(\sigma_j^z\right) \sigma_i^- . \tag{2.3}$$

Here we used the notation $\sigma_i^{\pm} \equiv (\sigma_i^x \pm i\sigma_i^y)/2$. It is easy to verify that the operators defined satisfy the canonical anti-commutation relations (CAR)

$$\{c_i^\dagger, c_j\} = \delta_{i,j}\,, \qquad \{c_i, c_j\} = 0 = \{c_i^\dagger, c_j^\dagger\}\,. \tag{2.4}$$

Expressing the Hamiltonian in terms of the new variables gives

$$\begin{aligned} H_{XY} =& -\frac{J}{2}\sum_{i=1}^{L}\left\{c_i^\dagger c_{i+1} + c_{i+1}^\dagger c_i + \gamma c_i^\dagger c_{i+1}^\dagger + \gamma c_{i+1} c_i\right\} \\ &+ \frac{J(e^{i\pi N}+1)}{2}\left\{c_L^\dagger c_1 + c_1^\dagger c_L + \gamma c_L^\dagger c_1^\dagger + \gamma c_1 c_L\right\}\,. \end{aligned} \tag{2.5}$$

Here we introduced the fermionic number operator $N \equiv \sum_{i=1}^{L} c_i^\dagger c_i$. The operator $e^{i\pi N}$ commutes with the Hamiltonian (it represents the symmetry (2.2)), so the two can be simultaneously diagonalised and the Hamiltonian can be written in the block diagonal form $H_{XY} = P_e H_{XY}^e P_e + P_o H_{XY}^o P_o$. Here P_e (P_o) projects on the sector of the Hilbert space with even (odd) number of fermions. It turns out that the lowest energy states in the two sectors become degenerate in the thermodynamic limit and a linear combination of those is chosen as a ground state by spontaneous symmetry breaking. This effect, as all the others caused by the boundary term (2.5), play an important role when one has to consider the action of operators which are *non-local* with respect to the fermions, for example in the study of the quantum phase transition happening at $|h| = 1$ or in the determination of the time evolution of σ^x after a quench in the magnetic field in the TFIC [88]; in this thesis, however, we will be interested only in the thermodynamic limit behaviour of operators that are local with respect to the fermions, so we can neglect the boundary term in the second line of (2.5) and assume periodic boundary conditions (PBC) on the fermions; in Appendix 2.A we discuss the relation between the infinite volume and the finite volume spectrum of (2.5), as this will be a useful reference when considering the finite volume realisation of the sine-Gordon model in Chapter 3. Taking PBC on the fermions we reduce ourselves to consider the following modified Hamiltonian

$$\tilde{H}_{XY} = -\frac{J}{2}\sum_{i}\left\{c_i^\dagger c_{i+1} + c_{i+1}^\dagger c_i + \gamma c_i^\dagger c_{i+1}^\dagger + \gamma c_{i+1} c_i\right\}\,, \qquad c_{L+i} = c_i\,, \tag{2.6}$$

this Hamiltonian has always a *unique* ground state. The next step required to diagonalise (2.6) is to take its Fourier transform: since the Hamiltonian is one-site shift invariant the most natural choice would be to consider the unit cell composed by one site. Nevertheless, later in this thesis we will be interested in situations where the initial state or the Hamiltonian are

invariant only under the shift of two sites, hence it is instructive take our elementary cell to contain two sites instead of one[1]. This results in having two different species of fermions f_k and e_k where the momentum k varies in the range $]0,\pi]$. Specifically we define

$$e_{k_n} = \sqrt{\frac{2}{L}} \sum_j e^{ik_n(2j)} c_{2j}\,, \qquad f_{k_n} = \sqrt{\frac{2}{L}} \sum_j e^{ik_n(2j-1)} c_{2j-1}\,, \tag{2.7}$$

$$k_n \equiv \frac{2\pi n}{L} \qquad n = 1, \ldots, \frac{L}{2}\,. \tag{2.8}$$

Writing the Hamiltonian (2.6) in terms of the fermions (2.7) we obtain

$$\tilde{H}_{XY} = -\,J \sum_{k>0} \Big\{ \cos(k) \left(f_k^\dagger e_k + \text{h.c.} \right) + i\gamma \sin(k) \left(f_k^\dagger e_{\pi-k}^\dagger - \text{h.c.} \right) \Big\}\,. \tag{2.9}$$

Here we adopted the notation

$$\sum_{k>0} f(k) \equiv \sum_{n=1}^{L} f(\frac{2\pi n}{L})\,. \tag{2.10}$$

The last step of the diagonalisation process is achieved by means of the Bogoliubov transformation

$$\alpha_\mp(k) = \frac{1}{\sqrt{2}} \left\{ e^{i\theta_k/2} e_k \pm e^{-i\theta_k/2} f_k + e^{i\theta_k/2} e_{\pi-k}^\dagger \pm e^{-i\theta_k/2} f_{\pi-k}^\dagger \right\}\,, \tag{2.11}$$

$$\alpha_\mp^\dagger(\pi-k) = \frac{1}{\sqrt{2}} \left\{ e^{i\theta_k/2} e_k \pm e^{-i\theta_k/2} f_k - e^{i\theta_k/2} e_{\pi-k}^\dagger \mp e^{-i\theta_k/2} f_{\pi-k}^\dagger \right\}\,, \tag{2.12}$$

where $k \in]0, \pi/2]$[2] and θ_k is the Bogoliubov angle given by

$$e^{i\theta_k} = \frac{\cos k + i\gamma \sin k}{\sqrt{\cos^2 k + \gamma^2 \sin^2 k}}\,. \tag{2.13}$$

In terms of the Bogoliubov fermions $\alpha_+(k), \alpha_-(k)$ the Hamiltonian reads as

$$\tilde{H}_{XY} = \sum_{\eta=\pm} \sum_{k>0} \eta \varepsilon(k) \alpha_\eta^\dagger(k) \alpha_\eta(k)\,, \qquad \varepsilon(k) = J\sqrt{\cos^2 k + \gamma^2 \sin^2 k}\,. \tag{2.14}$$

From the expression of the dispersion relation we see that the model describes gapless excitations only for $\gamma = 0$, as stated above for the case $h = 0$. The dispersion relation allows us also to make an other observation: the symmetry $\varepsilon(k) = \varepsilon(\pi - k)$ enables one to construct conserved quantities in momentum space which can not be expressed as a function of the occupation numbers, such as $\alpha_-^\dagger(k)\alpha_+^\dagger(\pi-k)$. Considering linear combinations of these conserved quantities it

[1] L is assumed to be even in this case.

[2] The π mode is treated separately giving $\alpha_-(\pi) = \frac{1}{\sqrt{2}}\{e_\pi^\dagger - f_\pi^\dagger\}$, $\alpha_+(\pi) = \frac{1}{\sqrt{2}}\{e_\pi + f_\pi\}$.

is possible to construct additional local conservation laws for the model. A detailed analysis of this case can be found in Ref. [68] where is also shown that the set of local conservation laws is now non commuting. It is, however, worth stressing that the additional conservation laws discussed here are two-site shift invariant, so they give a non vanishing constraint on the time evolution only if the initial state is not invariant under translations of one site.

We conclude our analysis of the XY model by briefly reviewing a mathematical formalism based on the expression of the Hamiltonian in terms of Majorana fermions (more details can be found in [68] and [92]), as this occurs to be convenient for calculations in free fermionic models. In particular it can be used to find in a very simple way a close expression for the set of all the local conservation laws [38, 68] of the model and the algebra they form, in particular here we show that the charges satisfy a $\mathrm{sl}(2,\mathbb{C})$-loop algebra. We will encounter an example of the application of this formalism in Chapter 4.

2.1.2 Majorana fermions and circulant matrices

It is useful to introduce a new set of fermionic operators, the so called Majorana fermions, defined as

$$a^x_\ell = \left(c^\dagger_\ell + c_\ell\right) , \qquad a^y_\ell = i\left(c_\ell - c^\dagger_\ell\right) . \tag{2.15}$$

They satisfy the following set of anti-commutation relations

$$\{a^\alpha_\ell, a^\beta_n\} = 2\delta_{\alpha\beta}\delta_{\ell n} , \qquad \alpha,\beta = x,y . \tag{2.16}$$

A characteristic feature of these operators is $a^{\alpha\,\dagger}_\ell = a^\alpha_\ell$.

Let us now consider a generic operator A, which is quadratic in the Majorana fermions. Sometimes we will call *nontinteracting* operators with this property. We focus on the case where A is left invariant by the shift of n-sites, where $n \geq 1$ is a divisor of L. This will be useful to study the additional charges of the XY model, as we have seen that they are invariant only under 2-sites shifts. In this case we can express A as

$$A = \frac{1}{4}\sum_{r,s}^{L/n} \begin{pmatrix} a^x_{nr-n+1} & a^y_{nr-n+1} & \dots & a^x_{nr} & a^y_{nr} \end{pmatrix} [\mathcal{A}^{(n)}]_{rs} \begin{pmatrix} a^x_{ns-n+1} \\ a^y_{ns-n+1} \\ \vdots \\ a^x_{ns} \\ a^y_{ns} \end{pmatrix} . \tag{2.17}$$

Here $\mathcal{A}^{(n)}$ is a block-circulant matrix, *i.e.* it is a block-Toeplitz matrix (the blocks composing

it satisfy $M_{nm} \equiv M_{n-m}$, where M_{nm} is a $2n$-by-$2n$ matrix) in which any block-row (a row of $2n$-by-$2n$ matrices) is a right cyclic shift of the block-row above. We stress that every noninteracting operator admits a representation of the form (2.17) for big enough n, however the formalism developed here will be particularly useful to treat cases where n does not scale with L in the thermodynamic limit. To exploit the fact that the matrix $\mathcal{A}^{(n)}$ is block-circulant it is useful to consider its Fourier decomposition

$$[\mathcal{A}^{(n)}]_{rs} = \frac{n}{L} \sum_m e^{i(r-s)k_m} \mathcal{A}^{(n)}(k)\,, \quad k_m = \frac{2\pi n m}{L}\,, \quad m = -\left\lceil \frac{L}{2n} \right\rceil + 1, \ldots, \left\lfloor \frac{L}{2n} \right\rfloor\,. \tag{2.18}$$

The conventions for the Fourier transform used here are different from the ones in (2.7), here the momentum takes values in the interval $]-\pi, \pi]$. The $2n$-by-$2n$ matrix $\mathcal{A}^{(n)}(k)$ is fully specified by the conditions

$$\mathcal{A}^{(n)^\dagger}(k) = \mathcal{A}^{(n)}(k)\,, \qquad \mathcal{A}^{(n)^t}(k) = -\mathcal{A}^{(n)}(-k)\,. \tag{2.19}$$

The unique matrix $\mathcal{A}^{(n)}(k)$ satisfying (2.18) and (2.19) is called the *symbol* of $\mathcal{A}^{(n)}$ and completely characterises the block-circulant matrix. In the following we will refer to $\mathcal{A}^{(n)}(k)$ also as the symbol of A. It is worth stressing that if the operator is local then the block-circulant matrix associated with it has non vanishing contributions only from blocks near to the diagonal, this imply that the symbol *has only a finite number of Fourier coefficients*. If the operator is quasi-local [93, 94] (its density is exponentially localised) the symbol can have an infinite number of Fourier coefficients but it turns out that it must be a smooth function of k [68].

Importantly, the representation in terms of symbols is well behaved under the commutation algebra, indeed the following property holds

Property 2.1.1 *Let A and B be two operators written as in (2.17) with the same n. Their commutator $[A, B]$ has the form (2.17), with symbol equal to the commutator of the symbols*

$$[A, B] \to [\mathcal{A}^{(n)}(k), \mathcal{B}^{(n)}(k)]\,. \tag{2.20}$$

We note that if an operator admits a representation of the form (2.18) for a fixed n, then it admits the representation (2.18) for every m multiple of n. This turns out to be useful when considering the commutator of two operators invariant under a different number of shifts. In particular the $n = 2$ representation of a one-site shift invariant operator A, possessing a $n = 1$

representation of the symbol $\mathcal{A}^{(1)}(k)$, is given by

$$\mathcal{A}^{(2)}(k) = \frac{\mathbb{1} + \sigma^x e^{i(k/2)\sigma^z}}{2} \otimes \mathcal{A}^{(1)}(k/2) + \frac{\mathbb{1} - \sigma^x e^{i(k/2)\sigma^z}}{2} \otimes \mathcal{A}^{(1)}(k/2 + \pi)\,. \tag{2.21}$$

So far we considered general quadratic operators, a prominent example of these is the XY Hamiltonian $\tilde{H}_{XY}$ (2.6). Since the Hamiltonian is one-site-shift invariant it admits an $n = 1$ representation, its symbol reads as

$$\mathcal{H}^{(1)}_{XY}(k) = -\varepsilon(k)\sigma^y e^{i\theta_k \sigma^z}\,, \tag{2.22}$$

where $\varepsilon(k)$ and θ_k are given in the previous subsection. In the following it will be useful to exploit also the $n = 2$ representation of the symbol of $\tilde{H}_{XY}$. Using (2.21) we find

$$\mathcal{H}^{(2)}_{XY}(k) = -\varepsilon(k/2)\sigma^x e^{ik/2\sigma^z} \otimes \sigma^y e^{i\theta_{k/2}\sigma^z}\,. \tag{2.23}$$

From property 2.1.1 follows that the time evolution under the Hamiltonian (2.6) of a non-interacting operator A in the Heisenberg picture is noninteracting, with symbol

$$e^{iHt} A e^{-iHt} \to e^{i\mathcal{H}^{(n)}(k)t} A^{(n)}(k) e^{-i\mathcal{H}^{(n)}(k)t}\,. \tag{2.24}$$

Finally, the representation in terms of symbols can be used to calculate expectation values of noninteracting operators on a certain class of states, namely the n-site shift invariant states on which the Wick's theorem holds

Property 2.1.2 *If a state ρ is such that the expectation value of any noninteracting operator on it can be expressed in terms of the correlation matrix*

$$\Gamma^{(n)}_{m\ell} = \delta_{\ell m}\mathrm{I} - \langle \begin{pmatrix} a^x_{nm-n+1} \\ a^y_{nm-n+1} \\ \vdots \\ a^x_{nm} \\ a^y_{nm} \end{pmatrix} \begin{pmatrix} a^x_{n\ell-n+1} & a^y_{n\ell-n+1} & \dots & a^x_{n\ell} & a^y_{n\ell} \end{pmatrix} \rangle\,, \tag{2.25}$$

and $\Gamma^{(n)}_{\ell m}$ is circulant with symbol $\Gamma^{(n)}(k)$, then the expectation value of non interacting operator A on ρ can be written as follows

$$\mathrm{tr}\,[\rho A] = \frac{1}{4}\sum_m \mathrm{tr}[\Gamma(k_m)\mathcal{A}(k_m)]\,. \tag{2.26}$$

Here we introduced the notation

$$\langle a_i^\alpha a_j^\beta \rangle \equiv \mathrm{tr}[\rho\, a_i^\alpha a_j^\beta] \qquad i,j=1,\dots,L \quad \alpha,\beta = x,y\,. \tag{2.27}$$

In the thermodynamic limit Eq.(2.26) reads as

$$\lim_{L\to\infty} \frac{1}{L}\mathrm{tr}\,[\rho A] = \frac{1}{4n}\int_{-\pi}^{\pi} \frac{\mathrm{d}k}{2\pi}\mathrm{tr}[\Gamma(k)\mathcal{A}(k)]\,. \tag{2.28}$$

Collecting together all the properties described we conclude that in n-site translation invariant noninteracting models, which include the XY as a particular case, any calculation can be traced back to operations on symbols: this represents a drastic simplification as it reduces the size of the matrices that one has to consider from $2^L \times 2^L$ to $2n \times 2n$.

Following Ref. [38] we can easily construct all the local conserved charges which are invariant under one-site shift. Assuming that the charges have a noninteracting form and that are invariant under the shift of one site we conclude that they can be written in the form (2.17) with $n = 1$. Let $\{\mathcal{Q}_m^{(1)}(k)\}_{m=1,2,\dots}$ be the $n = 1$ representation of their symbols. The conservation of the charges can be written in terms of symbols as

$$[\mathcal{H}^{(1)}(k), \mathcal{Q}_m^{(1)}(k)] = 0\,, \qquad\qquad m = 1, 2 \dots\,. \tag{2.29}$$

Given two commuting hermitian d-by-d matrices N and M, it is easy to prove that if M has distinct eigenvalues then N can be written as a combination of M^p with $p = 0,\dots,d-1$[3]. Since $\mathcal{H}_{XY}^{(1)}(k)$ is a 2-by-2 hermitian matrix with distinct eigenvalues we have

$$\mathcal{Q}_m^{(1)}(k) = a_m(k)\mathbb{1}_2 + b_m(k)\mathcal{H}^{(1)}(k)\,, \qquad m = 1,\dots L/2\,. \tag{2.30}$$

The conditions (2.19) require the real coefficients $a_m(k), b_m(k)$ to be respectively odd and even functions of the momentum. Choosing a convenient basis, we conclude that the symbols of a complete set of one site shift invariant charges can be written as

$$\mathcal{Q}_{m,+}^{(1)}(k) = \cos(mk)\mathcal{H}^{(1)}(k)\,, \qquad \mathcal{Q}_{m,-}^{(1)}(k) = \sin(mk)\mathbb{1}_2\,. \qquad m = 1,\dots L/2. \tag{2.31}$$

These symbols have a finite number of Fourier coefficients so the associated charges are local.

In cases where for any value of n the representation of the symbol of the Hamiltonian remain with distinct eigenvalues, this construction can be repeated giving an $2n$-by-$2n$ dimensional

[3]This can be easily established in the common eigenbasis.

representation of the one-site shift invariant charges. An interesting situation is realised when a higher $n = \bar{n}$ representation of the symbol of the Hamiltonian has some degenerate eigenvalues. In this case, for fixed k, the $2\bar{n}$-by-$2\bar{n}$ symbol of the Hamiltonian commutes with more than $2\bar{n}$ independent matrices accounting for the one-site shift invariant charges, the additional ones give some charges that are invariant only under a shift of a number of sites proportional to $\bar{n}$, so can be expressed only in the $n = p\bar{n}$ representation ($p \in \mathbb{N}$). For example let us consider the XY model, $\mathcal{H}^{(2)}_{XY}(k)$ has two doubly degenerate eigenvalues and it turns out that for a fixed k we can find eight independent matrices commuting with it. Four of them can be written as (2.21) using the symbols (2.31), thus they are the $n = 2$ representation of the charges (2.31); the other four are instead "new" and cannot be expressed in the $n = 1$ representation because are invariant only under the shift of two sites. The former generate the following set of symbols [68]

$$\begin{aligned}
&\mathcal{I}^{(2)(\mathrm{e})}_{m;+}(k) = \cos((m-1)k)\varepsilon(k/2)\,\sigma^x_{k/2}\otimes\sigma^y_{\theta_{k/2}} \qquad && \mathcal{I}^{(2)(\mathrm{o})}_{m;-}(k) = \sin((m-1/2)k)\,\sigma^x_{k/2}\otimes\mathbb{1} \\
&\mathcal{I}^{(2)(\mathrm{o})}_{m;+}(k) = \cos((m-1/2)k)\varepsilon(k/2)\,\mathbb{1}\otimes\sigma^y_{\theta_{k/2}} && \mathcal{I}^{(2)(\mathrm{e})}_{m;-}(k) = \sin(mk)\,\mathbb{1}\otimes\mathbb{1}\,,
\end{aligned} \tag{2.32}$$

while the latter generate [68]

$$\begin{aligned}
&\mathcal{J}^{(2)(\mathrm{e})}_{m;+}(k) = \cos((m-1)k)\varepsilon(k/2)\,\sigma^y_{k/2}\otimes\sigma^x_{\theta_{k/2}} \qquad && \mathcal{J}^{(2)(\mathrm{o})}_{m;-}(k) = \sin((m-1/2)k)\varepsilon(k/2)\,\sigma^z\otimes\sigma^x_{\theta_{k/2}} \\
&\mathcal{J}^{(2)(\mathrm{o})}_{m;+}(k) = \cos((m-1/2)k)\,\sigma^y_{k/2}\otimes\sigma^z && \mathcal{J}^{(2)(\mathrm{e})}_{m;-}(k) = \sin(mk)\,\sigma^z\otimes\sigma^z\,.
\end{aligned} \tag{2.33}$$

Here we introduced $\sigma^j_\theta \equiv e^{-i\frac{\theta}{2}\sigma^z}\sigma^j e^{i\frac{\theta}{2}\sigma^z}$ and $m = 1, \dots L/4$. From these expressions one can find the explicit form of the conserved charges by means of the analogs of (2.17) and (2.18). The symbols $\mathcal{I}^{(2)(\mathrm{e})}_{m;+}(k)$ and $\mathcal{I}^{(2)(\mathrm{e})}_{m;-}(k)$ commute with the entire set; to express the commutation relations of the remaining ones it is convenient to form the following combinations

$$\begin{aligned}
I^1_m(k) &= \mathcal{J}^{(2)(\mathrm{o})}_{m;+}(k) - \frac{i\mathcal{J}^{(2)(\mathrm{o})}_{m;-}(k)}{\varepsilon(k/2)} + \mathcal{J}^{(2)(\mathrm{o})}_{m+1;+}(k) - \frac{i\mathcal{J}^{(2)(\mathrm{o})}_{m+1;-}(k)}{\varepsilon(k/2)} \\
&\quad - i\frac{\mathcal{I}^{(2)(\mathrm{o})}_{m+1;+}(k)}{\varepsilon(k/2)} + \mathcal{I}^{(2)(\mathrm{o})}_{m+1;-}(k) + i\frac{\mathcal{I}^{(2)(\mathrm{o})}_{m;+}(k)}{\varepsilon(k/2)} - \mathcal{I}^{(2)(\mathrm{o})}_{m;-}(k) \\
I^2_m(k) &= \frac{\mathcal{J}^{(2)(\mathrm{e})}_{m+1;+}(k)}{\varepsilon(k/2)} + i\mathcal{J}^{(2)(\mathrm{e})}_{m;-}(k) \\
I^3_m(k) &= \frac{\mathcal{I}^{(2)(\mathrm{o})}_{m;+}(k)}{\varepsilon(k/2)} + i\mathcal{I}^{(2)(\mathrm{o})}_{m;-}(k) + \frac{\mathcal{I}^{(2)(\mathrm{o})}_{m+1;+}(k)}{\varepsilon(k/2)} + i\mathcal{I}^{(2)(\mathrm{o})}_{m+1;-}(k) \\
&\quad + i\mathcal{J}^{(2)(\mathrm{o})}_{m+1;+}(k) + \frac{\mathcal{J}^{(2)(\mathrm{o})}_{m+1;-}(k)}{\varepsilon(k/2)} - i\mathcal{J}^{(2)(\mathrm{o})}_{m;+}(k) - \frac{\mathcal{J}^{(2)(\mathrm{o})}_{m;-}(k)}{\varepsilon(k/2)}\,.
\end{aligned} \tag{2.34}$$

The commutation relations fulfilled by the combinations (2.34) read as

$$\Big[I_n^\alpha(k), I_m^\beta(k)\Big] = i\varepsilon^{\alpha\beta\gamma} I_{n+m}^\gamma(k)\,. \tag{2.35}$$

Equations (2.35) are the defining commutation relations of the $\mathrm{sl}(2,\mathbb{C})$ loop algebra: *we have thus shown that the Hamiltonian (2.1), for $h = 0$, is invariant under loop* $\mathrm{sl}(2,\mathbb{C})$ *transformations.* A $\mathrm{sl}(2,\mathbb{C})$ loop algebra invariance has been shown to occur in the XXZ spin-1/2 chain [95], when the anisotropy satisfies $\Delta = \frac{1}{2}(q + q^{-1})$ with $q^{2N} = 1$ ($N \geq 2$). In particular, the case $N = 2$ corresponds to the XX chain ($\Delta = 0$), which is a particular case of the model studied here: our result shows that this symmetry remains present in the XY model for any value of γ. We stress that the charges associated with the symbols (2.34) (and thus forming a representation of the $\mathrm{sl}(2,\mathbb{C})$ loop algebra) are quasi-local, in contrast to the representation constructed in [95].

2.2 Sine-Gordon model

The sine-Gordon quantum field theory is the $(1+1)$-dimensional bosonic field theory described by the following Hamiltonian

$$\mathcal{H}_{\mathrm{SG}} = \frac{v}{16\pi}\int dx\,\Big[\big(\partial_x\Phi\big)^2 + \frac{1}{v^2}\big(\partial_t\Phi\big)^2\Big] - \lambda\int dx\,\cos(\beta\Phi)\,, \tag{2.36}$$

where the bosonic field $\Phi(x,t)$ fulfils the standard commutation relations

$$[\Phi(x,t), \Pi(y,t)] = i\delta(x-y)\,, \qquad \Pi(x,t) = \frac{\partial\mathcal{H}_{SG}}{\partial\partial_t\Phi(x,t)}\,. \tag{2.37}$$

Inspecting the Hamiltonian (2.36) we see that it is invariant under Lorentz transformations, however in the following we will see that it emerges as an effective description of several non relativistic systems. Interestingly, similar situations arise in numerous physically relevant cases [79].

2.2.1 Realisations of the sine-Gordon model

The field theory (2.36) is known to emerge as the low-energy description in a variety of contexts, both in solids and systems of trapped, ultra-cold atoms.

2.2.1.1 Solids

The sine-Gordon model is obtained as the low-energy limit of a variety of quantum spin chain models, see e.g. Ref. [79]. Perhaps the best experimental realisation in this context is in field-induced gap Heisenberg magnets like CuBenzoate [96–105] and [106–112]. The underlying lattice model in these systems is of the form

$$H = J\sum_{j=1}^{L}\Big[S_j^x S_{j+1}^x + S_j^y S_{j+1}^y + \Delta S_j^z S_{j+1}^z\Big] + h_u\sum_{j=1}^{L} S_j^z + h_s\sum_{j=1}^{L}(-1)^j S_j^x. \tag{2.38}$$

In the thermodynamic limit the low-energy sector is described by a quantum sine-Gordon model (2.36). Typically the sine-Gordon emerging from these chains results in having $\beta^2 < 1/2$, which as we will see corresponds to the so called "attractive regime". In the following we will be interested in the "repulsive regime" $1/2 \leq \beta^2 < 1$, which can be realised as the low-energy limit of the spin-1/2 XYZ chain

$$H = J\sum_{j=1}^{L}\Big[(1+\gamma)S_j^x S_{j+1}^x + (1-\gamma)S_j^y S_{j+1}^y + \Delta S_j^z S_{j+1}^z\Big], \tag{2.39}$$

where we take

$$J > 0\ , \quad 0 < \Delta < 1\ , \quad \gamma \ll 1. \tag{2.40}$$

In this regime we may regard (2.39) as a perturbation of the spin-1/2 XXZ chain by the relevant operator $\sum_j [S_j^x S_{j+1}^x - S_j^y S_{j+1}^y]$. In the low-energy limit this gives a sine-Gordon model (2.36) with

$$-\Delta = \cos(\pi\beta^2)\ ,\ \frac{1}{2} < \beta^2 < 1, \quad v = \frac{J}{2}\frac{\sin(\beta^2)}{1-\beta^2}\ , \quad \lambda \propto \gamma. \tag{2.41}$$

The transverse spin operators are bosonized as follows [79][4]

$$\begin{aligned} S_j^+ &= S_j^x + iS_j^y \sim \mathcal{C}(-1)^j :e^{\mathrm{i}\frac{\beta}{2}\Phi(x)}: + \mathcal{A}\Big[:e^{\mathrm{i}\frac{\beta}{2}\Phi(x)+\frac{\mathrm{i}}{2\beta}\Theta(x)}: + :e^{\mathrm{i}\frac{\beta}{2}\Phi(x)-\frac{\mathrm{i}}{2\beta}\Theta(x)}:\Big] + \dots \\ &\equiv J^+(x) + (-1)^j n^+(x)\ , \quad x = ja_0. \end{aligned} \tag{2.42}$$

In the following we will be interested in the operator $e^{\mathrm{i}\frac{\beta}{2}\Phi(x)}$, from (2.42) follows that in this realisation of the sine-Gordon model it corresponds to the staggered magnetisation. Specifically, $\cos\left(\frac{\beta\Phi(x)}{2}\right)$ corresponds to the staggered magnetisation in the x direction and $\sin\left(\frac{\beta\Phi(x)}{2}\right)$ in

[4] Comparing with Ref. [79] our $\Phi(x)$ and $\Theta(x)$ are flipped.

the y direction. The bosonized form of the longitudinal spin operator is

$$S_j^z \sim \frac{a_0}{4\pi\beta}\partial_x\Theta(x) - \mathcal{B}(-1)^j \sin\left(\frac{\Theta(x)}{2\beta}\right) + \dots \tag{2.43}$$

We note that the constants $\mathcal{A}$, $\mathcal{B}$ and $\mathcal{C}$ are known [113, 114]. In the XYZ realisation the Bose fields are compactified (see *e.g.* [79])

$$\Theta(x) = \Theta(x) + 4\pi\beta\ , \qquad \Phi(x) = \Phi(x) + \frac{4\pi}{\beta}. \tag{2.44}$$

This implies that the only local vertex operators are of the form

$$\mathcal{O}_{n,m} = e^{\mathrm{i}\frac{n}{2\beta}\Theta(x) + \mathrm{i}\frac{\beta m}{2}\Phi(x)}. \tag{2.45}$$

Defining the topological charge as

$$Q = \frac{\beta}{2\pi}\int_{-\infty}^{\infty} dx\ \partial_x\Phi(x), \tag{2.46}$$

we see that $\mathcal{O}_{n,m}$ carry topological charge $2n$.

2.2.1.2 Systems of ultra-cold trapped atoms

Other realisations of the sine-Gordon model can be found in systems of interacting one dimensional bosons [115]. For example, one may consider a single species of bosons in a periodic potential

$$H = \frac{1}{2m_0}\int dx|\partial_x\psi|^2 + \frac{1}{2}\int dx\ dx'\ V(x-x') : \rho(x)\rho(x') : + \int dx\ [V_L(x) - \mu]\rho(x), \tag{2.47}$$

were $\psi(x)$ is a complex scalar field, $V(x)$ describes density-density interactions between bosons, μ a chemical potential, and $V_L(x)$ a periodic lattice potential. Models like (2.47) can be realized in systems of trapped, ultra-cold atoms, where $V_L(x)$ accounts for the optical lattice [116]. "Bosonizing the boson" [117, 118]

$$\begin{aligned}\psi^\dagger(x) &\sim \sqrt{\rho_0}\sum_{p\in\mathbb{Z}} e^{2\mathrm{i}p[\pi\rho_0 x - \sqrt{\frac{K}{8}}\Phi(x)]} e^{-\frac{\mathrm{i}}{\sqrt{8K}}\Theta(x)}\ , \\ \rho(x) &\sim \rho_0 - \sqrt{\frac{K}{8\pi^2}}\partial_x\Phi(x) + \rho_0\sum_{p\neq 0} e^{2\mathrm{i}p[\pi\rho_0 x - \sqrt{\frac{K}{8}}\Phi(x)]},\end{aligned} \tag{2.48}$$

where ρ_0 is the average density, leads to a low-energy description [115] in terms of a sine-Gordon model (2.36). Here the $\cos(\beta\Phi)$ originates from the periodic potential $V_L(x)$, and the Luttinger parameter K characterizes the interactions. In order to access the repulsive regime of the sine-Gordon model ($\beta^2 > 1/2$), the density-density interaction $V(x)$ should be sufficiently long-ranged. Of particular interest for our work is the case where the periodic potential is such that there is on average one boson for every two minima of $V_L(x)$, i.e.

$$V_L(x) \sim V_L \cos(4\pi\rho_0 x), \tag{2.49}$$

which leads to a sine-Gordon model with $\beta^2 = 2K$. As long as $K < 1/2$, the leading oscillating term in the density is

$$\rho_{\rm osc}(x) \sim \cos\left(2\pi\rho_0 x - \frac{\beta}{2}\Phi(x)\right) + \text{higher harmonics.} \tag{2.50}$$

Hence in this realisation of the sine-Gordon model the operator $e^{i\frac{\beta}{2}\Phi(x)}$ describes the leading oscillatory behaviour of the boson density. We note that the Bose fields again are compactified according to (2.44).

A second realisation of the sine-Gordon model with ultra-cold atoms is in terms of coupled one-dimensional condensates [119]. The microscopic Hamiltonian is taken to be

$$H = \int dx \left[\sum_{j=1,2}\left(\frac{1}{2m_0}\left|\partial_x\Psi_j(x)\right|^2 + g:\rho_j^2(x):\right) - t_\perp\left(\Psi_1^\dagger(x)\Psi_2(x) + \text{h.c.}\right)\right], \tag{2.51}$$

where $\rho_j(x) =: \Psi_j^\dagger(x)\Psi_j(x):$. Bosonising[5] [117,118] and then transforming to total and relative phases

$$\Phi_\pm(x) = \left[\frac{\Phi_1(x) \pm \Phi_2(x)}{\sqrt{2}}\right],\ \Theta_\pm(x) = \left[\frac{\Theta_1(x) \pm \Theta_2(x)}{\sqrt{2}}\right], \tag{2.52}$$

one finds a low-energy effective Hamiltonian of the form

$$\begin{aligned} H_+ &= \frac{v}{16\pi}\int dx \left[\left(\partial_x\Phi_+\right)^2 + \left(\partial_x\Theta_+\right)^2\right], \\ H_- &= \frac{v}{16\pi}\int dx \left[\left(\partial_x\Phi_-\right)^2 + \left(\partial_x\Theta_-\right)^2\right] - \lambda\int dx\ \cos\left(\frac{\Phi_-}{\sqrt{4K}}\right). \end{aligned} \tag{2.53}$$

Here $\lambda \propto t_\perp$ and the parameters v and K are functions of g, m_0 and the density ρ_0 of the condensates.

[5] We exchange the roles of Φ_i and Θ_i with respect to (2.48).

2.2.2 Sine-Gordon model as an integrable quantum field theory

The sine-Gordon model is an integrable quantum field theory, this means that it possesses an infinite number of local conserved charges $\{I_n\}_{n=0,1,\dots}$ which are in involution, *i.e.* they are mutually commuting. As every relativistic field theory in Minkovski space (2.36) it admits an interpretation in terms of scattering of relativistic particles corresponding to excitations above a vacuum. The presence of the set $\{I_n\}_{n=0,1,\dots}$ imposes two severe constraints on the allowed scattering processes [6, 78, 79, 120–122]

(i) Pure Elasticity;

(ii) Complete Factorizability;

The first condition requires the number of incoming particles to equate that of the outgoing ones in any scattering process; the set $\{p_i\}$ of incoming momenta and the masses characterising the particles must also be to be preserved during the scattering. The only allowed modifications are permutations of the momenta of particles with the same masses.

The second condition requests that every scattering event can be decomposed in terms of *two-particle* scattering processes and every possible way of decomposing an N-particle scattering process into a sequence of two-particle ones must be equivalent. To characterise completely the scattering, one has to determine the *two-particle scattering matrix* defined as

$$ {}^{\text{out}}_{a_1a_2}\langle\theta_1',\theta_2'|\theta_2,\theta_1\rangle^{\text{in}}_{b_1b_2} = \delta(\theta_1'-\theta_1)\delta(\theta_2'-\theta_2)S^{a_1a_2}_{b_1b_2}(\theta_1-\theta_2)\,, \qquad a_i,b_i=1,\dots,d\,. \tag{2.54}$$

Here d is the number of different particles in the spectrum, the superscripts "in" and "out" indicate that the states are respectively asymptotic *incoming* and *outgoing* states ($\theta_2 \le \theta_1$, $\theta_2' \le \theta_1'$); we parametrised the energy and the momentum of on-shell particles by means of the rapidity θ as follows

$$ E_\theta = \Delta_i \cosh\theta\,, \qquad\qquad p_\theta = \frac{\Delta_i}{v}\sinh\theta\,, \tag{2.55}$$

where Δ_i is the mass of the i-th particle and v is the "velocity of light" in our model (*c.f.* (2.36)). The scattering matrix depends only on the difference of rapidities $\theta = \theta_1 - \theta_2$ because of the Lorentz invariance and is a meromorphic function of θ in the complex plane (poles in the segment $0 \le \operatorname{Im}\theta \le \pi$ $\operatorname{Re}\theta = 0$ correspond to bound states). The equivalence of all the possible decompositions of n-particle scattering processes into two-particle ones imposes the

following condition on $S^{a_1a_2}_{b_1b_2}$

$$S^{b_2b_3}_{a_2a_3}(\theta_2-\theta_3)S^{b_1c_3}_{a_1b_3}(\theta_1-\theta_3)S^{c_1c_2}_{b_1b_2}(\theta_1-\theta_2) = \\ = S^{b_1b_2}_{a_1a_2}(\theta_1-\theta_2)S^{c_1b_3}_{b_1a_3}(\theta_1-\theta_3)S^{c_2c_3}_{b_2b_3}(\theta_2-\theta_3), \tag{2.56}$$

it turns out that this is a sufficient requirement [6]. The condition (2.56) is known as *Yang-Baxter equation*. Further conditions on $S^{a_1a_2}_{b_1b_2}$ are imposed by requiring the unitarity of the scattering

$$S^{c_1c_2}_{a_1a_2}(\theta)S^{b_1b_2}_{c_1c_2}(-\theta) = \delta^{b_1}_{a_1}\delta^{b_2}_{a_2}, \tag{2.57}$$

and demanding that it satisfies the *crossing symmetry*

$$S^{cd}_{ab}(\mathrm{i}\pi-\theta) = S^{\bar{a}d}_{\bar{c}b}(\theta) = S^{c\bar{b}}_{a\bar{d}}(\theta), \qquad \bar{a} = -a. \tag{2.58}$$

The conditions (2.56), (2.57) and (2.58), together with some minimality assumptions on the form of the scattering matrix, sometimes are enough to determine the entire $S^{a_1a_2}_{b_1b_2}$ up to some free parameters, which are fixed by means some dynamical information (for example matching the result obtained with that found via perturbation theory or semiclassical approximations) [123].

The scattering matrix of the sine-Gordon model has been determined exactly [123, 124], the particle content depends on the value of β. It is possible to distinguish two different regimes: the *attractive regime* $0 \leq \beta < 1/\sqrt{2}$ and the *repulsive regime* $1/\sqrt{2} \leq \beta < 1$ (for $\beta > 1$ the cosine perturbation becomes irrelevant). The regime of interest to us here is the repulsive one, where the elementary excitations are massive solitons and antisolitons, having the same mass Δ (this is due to the charge conjugation $\mathbb{Z}_2$ symmetry of the model). In the attractive regime solitons and antisolitons can form bound states known as breathers. At the point $\beta = 1/\sqrt{2}$, known as the "Luther-Emery" point, the model is equivalent to a free massive Dirac theory [125].

A basis of eigenstates of the sine-Gordon model in the repulsive regime is conveniently constructed by employing the Faddeev-Zamolodchikov creation and annihilation operators $Z^\dagger_a(\theta)$, $Z_a(\theta)$ [123,126], where the index $a = \pm$ corresponds to the creation and annihilation of solitons and antisolitons respectively. They are taken to fulfil the algebra

$$\begin{aligned} Z_{a_1}(\theta_1)Z_{a_2}(\theta_2) &= S^{b_1b_2}_{a_1a_2}(\theta_1-\theta_2)Z_{b_2}(\theta_2)Z_{b_1}(\theta_1), \\ Z^\dagger_{a_1}(\theta_1)Z^\dagger_{a_2}(\theta_2) &= S^{b_1b_2}_{a_1a_2}(\theta_1-\theta_2)Z^\dagger_{b_2}(\theta_2)Z^\dagger_{b_1}(\theta_1), \\ Z_{a_1}(\theta_1)Z^\dagger_{a_2}(\theta_2) &= 2\pi\delta(\theta_1-\theta_2)\delta_{a_1,a_2} + S^{b_2a_1}_{a_2b_1}(\theta_2-\theta_1)Z^\dagger_{b_2}(\theta_2)Z_{b_1}(\theta_1)\,. \end{aligned} \tag{2.59}$$

For $1/2 < \beta^2 < 1$ the scattering matrix is given by

$$
\begin{aligned}
S^{++}_{++}(\theta) &= S^{--}_{--}(\theta) = S_0(\theta) = -\exp\left[\mathrm{i}\int_0^\infty \frac{dt}{t}\sin\left(\frac{t\theta}{\pi\xi}\right)\frac{\sinh\left(\frac{\xi-1}{2\xi}t\right)}{\sinh\left(\frac{t}{2}\right)\cosh\left(\frac{t}{2\xi}\right)}\right], \\
S^{+-}_{+-}(\theta) &= S^{-+}_{-+}(\theta) = S_T(\theta)S_0(\theta), \qquad S_T(\theta) = -\frac{\sinh\left(\frac{\theta}{\xi}\right)}{\sinh\left(\frac{\theta-\mathrm{i}\pi}{\xi}\right)}, \\
S^{+-}_{-+}(\theta) &= S^{-+}_{+-}(\theta) = S_R(\theta)S_0(\theta), \qquad S_R(\theta) = -\frac{\mathrm{i}\sin\left(\frac{\pi}{\xi}\right)}{\sinh\left(\frac{\theta-\mathrm{i}\pi}{\xi}\right)},
\end{aligned}
\tag{2.60}
$$

where we have defined $\xi = \frac{\beta^2}{1-\beta^2}$. The S-matrix fulfils the Yang-Baxter equation (2.56), crossing (2.58) and unitarity (2.57) relations; further useful relations are

$$
\left(S^{cd}_{ab}(\theta)\right)^* = S^{cd}_{ab}(-\theta) \quad \text{for} \quad \theta \in \mathbb{R}, \quad S^{cd}_{ab}(\theta) = S^{dc}_{ba}(\theta) = S^{ab}_{cd}(\theta) = S^{\bar{c}\bar{d}}_{\bar{a}\bar{b}}(\theta), \tag{2.61}
$$

the first condition is the so called real analyticity condition and is another standard condition imposed on the the scattering matrix [6]; while the others are demanded by the invariance of the scattering amplitude under parity P, time reversal T and charge conjugation C respectively. The zero temperature ground state $|0\rangle$ is defined by

$$
Z_a(\theta)|0\rangle = 0, \tag{2.62}
$$

and a basis of eigenstates is obtained by acting with creation operators

$$
|\theta_1, \ldots, \theta_N\rangle_{a_1 \ldots a_N} = Z^\dagger_{a_1}(\theta_1) \ldots Z^\dagger_{a_N}(\theta_N)|0\rangle. \tag{2.63}
$$

Energy and momentum of the states (2.63) are given by

$$
E = \Delta \sum_{j=1}^N \cosh\theta_j, \qquad\qquad P = \frac{\Delta}{v}\sum_{j=1}^N \sinh\theta_j. \tag{2.64}
$$

The topological charge operator Q defined in (2.46) acts on the basis (2.63) as

$$
Q\,|\theta_1, \ldots, \theta_N\rangle_{a_1 \ldots a_N} = \left\{\sum_{i=1}^N a_i\right\}|\theta_1, \ldots, \theta_N\rangle_{a_1 \ldots a_N}. \tag{2.65}
$$

Importantly, matrix elements of local operators

$$
f^{\mathcal{O}\,b_1 \ldots b_M}_{\quad a_1 \ldots a_N}(\theta'_1, \ldots, \theta'_M|\theta_1, \ldots, \theta_N) = {}_{b_1 \ldots b_M}\langle\theta'_1, \ldots, \theta'_M|\mathcal{O}(0)|\theta_1, \ldots, \theta_N\rangle_{a_1 \ldots a_N} \tag{2.66}
$$

can be calculated by means of the form-factor bootstrap approach [6,127–133]. We report now the basic axioms underlying this approach.

2.2.2.1 Form-factor axioms

We state here form-factor axioms, following the conventions of Delfino [132]. The n-particle form-factor of an arbitrary operator $\mathcal{O}$ is defined by

$$f^{\mathcal{O}}_{a_1\dots a_n}(\theta_1,\dots,\theta_n) = \langle 0|\,\mathcal{O}\,|\theta_1,\dots,\theta_N\rangle_{a_1\dots a_N} = \langle 0|\,\mathcal{O}\,Z^\dagger_{a_1}(\theta_1)\dots Z^\dagger_{a_N}(\theta_N)\,|0\rangle\,. \tag{2.67}$$

The form-factor axioms read:

1. The form-factors $f^{\mathcal{O}}_{a_1\dots a_N}(\theta_1,\dots,\theta_N)$ are meromorphic functions of θ_N in the physical strip $0 \leq \mathfrak{Im}\,\theta_N \leq 2\pi$. There exist only simple poles in this strip.

2. *Scattering axiom*:

$$\begin{aligned} &f^{\mathcal{O}}_{a_1\dots a_i a_{i+1}\dots a_N}(\theta_1,\dots,\theta_i,\theta_{i+1},\dots,\theta_N) \\ &\qquad = S^{b_i b_{i+1}}_{a_i a_{i+1}}(\theta_i-\theta_{i+1})\, f^{\mathcal{O}}_{a_1\dots b_{i+1} b_i\dots a_N}(\theta_1,\dots,\theta_{i+1},\theta_i,\dots,\theta_N). \end{aligned} \tag{2.68}$$

   This axiom follows by the commutation of two Faddeev-Zamolodchikov operators.

3. *Periodicity axiom*:

$$f^{\mathcal{O}}_{a_1\dots a_N}(\theta_1+2\pi i,\theta_2,\dots,\theta_N) = l_{a_1}(\mathcal{O})\, f^{\mathcal{O}}_{a_2\dots a_N a_1}(\theta_2,\dots,\theta_N,\theta_1)\,, \tag{2.69}$$

   where $l_\pm(\mathcal{O})$ is the *mutual semi-locality* factor between the operator $\mathcal{O}$ and the fundamental fields $\mathcal{O}^\pm_0$, the definition of semi-locality factor is given below. This axiom follows from the crossing symmetry of the form-factors [79,121].

4. *Lorentz transformations*:

$$f^{\mathcal{O}}_{a_1\dots a_N}(\theta_1+\Lambda,\dots,\theta_N+\Lambda) = e^{s(\mathcal{O})\Lambda}\, f^{\mathcal{O}}_{a_1\dots a_N}(\theta_1,\dots,\theta_N), \tag{2.70}$$

   where $s(\mathcal{O})$ denotes the Lorentz spin of $\mathcal{O}$. Here we have $s(e^{i\alpha\Phi}) = 0$, i.e. $\mathcal{O} = e^{i\alpha\Phi}$ is a Lorentz scalar. This axiom expresses the Lorentz covariance of the form-factors, the rapidity variable gets shifted by a constant under Lorentz transformations.

5. *Annihilation pole axiom*:

$$\begin{aligned}\mathrm{Res}\big[f^{\mathcal{O}}_{aba_1\dots a_N}(\theta',\theta,\theta_1,\dots,\theta_N),\theta'=\theta+i\pi\big] &= \\ &= i\,C_{ac}\,f^{\mathcal{O}}_{b_1\dots b_N}(\theta_1,\dots,\theta_N)\big[\delta^{b_1}_{a_1}\dots\delta^{b_N}_{a_N}\delta^{c}_{b} \\ &\quad - l_a(\mathcal{O})S^{c_1b_1}_{b\ \ a_1}(\theta-\theta_1)S^{c_2b_2}_{c_1a_2}(\theta-\theta_2)\dots S^{c\ \ \ b_N}_{c_{N-1}a_N}(\theta-\theta_N)\big], \qquad (2.71)\end{aligned}$$

with the charge conjugation matrix of the sine-Gordon model given by $C_{ab}=\delta_{a+b,0}$. If there are no bound states, i.e. for $1/2\leq\beta^2<1$, these are the only poles of the form-factors. This axiom considers form-factors containing a particle and its own antiparticle, relating them to the form-factors where the particle-antiparticle couple is removed, thus it describes an annihilation process.

We conclude the section by introducing an important concept which we will be used several times in the following and already emerged in the axioms 3 and 5: the *mutual semi-locality* of two fields [134]

Definition Considering a 2-dimensional field theory in imaginary time τ, two operators $\mathcal{O}_1(x,\tau)$ and $\mathcal{O}_2(x,\tau)$ are mutually *semi-local* if they satisfy

$$\mathcal{A}_{\mathcal{C}}[\mathcal{O}_1(x,\tau)\mathcal{O}_2(0,0)]=e^{2\pi i\omega_{12}}\mathcal{O}_1(x,\tau)\mathcal{O}_2(0,0), \qquad (2.72)$$

where $\mathcal{A}_{\mathcal{C}}$ denotes the analytic continuation $x\pm\tau\longrightarrow e^{\pm 2\pi i}(x\pm\tau)$. The phase $l_{12}=e^{2\pi i\omega_{12}}$ is called mutual *semilocality index* of $\mathcal{O}_1(x,\tau)$ and $\mathcal{O}_2(x,\tau)$; we will call $l_\pm(\mathcal{O})$ the semi-locality index of an operator with respect to the operators $\mathcal{O}_0^\pm$ creating the elementary excitations.[6] For example $\mathcal{O}_\alpha=e^{i\alpha\Phi}$ the factor $l_\pm(\mathcal{O}_\alpha)\equiv l^\alpha_\pm=e^{\pm i2\pi\alpha/\beta}$.

As it is clear from the axioms the semi-locality index of an operator $\mathcal{O}$ with respect to the operators creating the elementary excitations play a key role in the determination of the analytic structure of the form-factors of $\mathcal{O}$, as we will see in the following this will reflect on the long time behaviour of the correlation functions of $\mathcal{O}$ after a quantum quench.

[6] The equality (2.72) is intended at the level of the correlation functions.

Appendix

2.A Eigenstates of H_{XY} in finite volume

In this appendix we find the exact eigenstates of the Hamiltonian (2.5) for $\gamma \neq 0$ in a finite volume L, which we take even for definiteness, and study the relation between these and the infinite volume ones. As mentioned in the main text, the Hamiltonian is block diagonal in the sectors with even and odd number of particles $H_{XY} = P_e H^e_{XY} P_e + P_o H^o_{XY} P_o$ ($P_{e(o)}$ projects in the even (odd) particle number sector). The Hamiltonians H^e_{XY} and H^o_{XY} have the same form

$$H^{e,o}_{XY} = -\frac{J}{2}\sum_{i=1}^{L}\left\{c_i^\dagger c_{i+1} + c_{i+1}^\dagger c_i + \gamma c_i^\dagger c_{i+1}^\dagger + \gamma c_{i+1} c_i\right\}, \tag{2.73}$$

the only difference being the boundary conditions on the fermions

$$c_{L+1} = \begin{cases} -c_1 & N = \text{even}\,, \\ \\ c_1 & N = \text{odd}\,. \end{cases} \tag{2.74}$$

Here N is the fermion number and from now on we adopt the standard terminology, calling the periodic and antiperiodic sector Ramond and Neveu-Schwarz respectively; for consistency we rename $P_{e(o)} H^{e(o)}_{XY} P_{e(o)} \equiv H^{\mathrm{NS(R)}}$. The Hamiltonians (2.73) are readily diagonalised by a subsequent application of a (standard) Fourier and Bogoliubov transformations (see for example Appendix A of [88]); the effect of the different boundary conditions is to change the quantisation rules for the momenta, in particular we have

$$p_n = \begin{cases} \frac{2\pi}{L}(n+\frac{1}{2}), & n = -\frac{L}{2}, \dots, \frac{L}{2}-1 \qquad \text{Neveu-Schwarz}\,, \\ \\ \frac{2\pi}{L} n, & n = -\frac{L}{2}, \dots, \frac{L}{2}-1 \qquad \text{Ramond}\,. \end{cases} \tag{2.75}$$

In the following we adopt the notation $p \in \mathrm{NS}$, R to indicate that p is quantised according to the first or the second of (2.75).

Performing a particle-hole transformation in the Ramond sector, the Hamiltonians can be brought in the following form

$$H^{\mathrm{a}} = \sum_{p\in \mathrm{a}} \varepsilon(p) \alpha^\dagger_{\mathrm{a}}(p)\alpha_{\mathrm{a}}(p) + E^{\mathrm{a}}_0\,, \qquad E^{\mathrm{a}}_0 = -\frac{1}{2}\sum_{p\in\mathrm{a}}\varepsilon(p)\,, \qquad \mathrm{a} = \mathrm{R},\, \mathrm{NS}\,, \tag{2.76}$$

where the dispersion is given in (2.14) and the Bogoliubov fermions $\alpha_{\rm a}(p)$, unitarily related to the c_i's, satisfy the CAR.

We indicate by $|0\rangle_{\rm R}$ and $|0\rangle_{\rm NS}$ the lowest energy states in the two sectors, since $\varepsilon(p) > 0$ for $\gamma \neq 0$, these states are defined by

$$\alpha_{\rm a}(p)\,|0\rangle_{\rm a} = 0\,, \qquad\qquad \forall\, p \in {\rm a} = {\rm R},\, {\rm NS}\,. \tag{2.77}$$

Their energies are $E_0^{\rm R}$ and $E_0^{\rm NS}$. States $|s\rangle_{\rm a} \in {\rm a} = {\rm R},\, {\rm NS}$ have a definite parity of the fermion number N, consequently are eigenstates of the unitary operator $e^{i\pi N}$ and satisfy

$$e^{i\pi N}\,|s\rangle_{\rm a} = \sigma_{\rm a}\,|s\rangle_{\rm a}\,, \qquad {\rm a} \in {\rm R},\, {\rm NS} \qquad \sigma_{\rm NS} = -\sigma_{\rm R} = 1\,. \tag{2.78}$$

Using (2.77) and expressing N in terms of the Bogoliubov fermions of the two sectors, it can be shown that the states $|0\rangle_{\rm R}$ and $|0\rangle_{\rm NS}$ fulfil the condition (2.78).

A complete basis of eigenstates of H is readily constructed acting on the lowest energy states with the creation operators $\alpha_{\rm a}^\dagger(p)$, respecting the parity of the fermion number in order to remain in the same sector

$$\left\{ |p_1, \ldots, p_{2n}\rangle_{\rm a} = \prod_{i=1}^{2n} \alpha_{\rm a}^\dagger(p_i)\,|0\rangle_{\rm a}\,, \qquad n \in \mathbb{N}\,, \qquad \{p_i\} \in {\rm a} = {\rm R},\, {\rm NS} \right\}. \tag{2.79}$$

For large but finite L the system has the unique ground state $|0\rangle_{\rm NS}$, however $E_0^{\rm R} - E_0^{\rm NS} = O(e^{-\alpha L})$ thus $|0\rangle_{\rm NS}$ and $|0\rangle_{\rm R}$ become degenerate in the infinite volume limit $L \to \infty$. In this limit the ground state is chosen among one of two orthogonal linear combinations of $|0\rangle_{\rm NS}$ and $|0\rangle_{\rm R}$ which are not connected by spatially local operators. States with this property are indeed the only ones that are stable under small perturbations constructed using local operators [135]. We call $|0\rangle$ and $|1\rangle$ these linear combinations

$$|0\rangle = \alpha\,|0\rangle_{\rm NS} + \beta\,|0\rangle_{\rm R}\,, \qquad |1\rangle = \beta^*\,|0\rangle_{\rm NS} - \alpha^*\,|0\rangle_{\rm R}\,, \qquad |\alpha|^2 + |\beta|^2 = 1\,. \tag{2.80}$$

In our case we need to ensure that

$$\langle 1|\mathcal{O}_{i;n}^{\{\alpha_j\}}|0\rangle \equiv \langle 1|\sigma_i^{\alpha_1} \ldots \sigma_{i+n}^{\alpha_n}|0\rangle = 0\,, \qquad \{\alpha_j\} = 0, x, y, z\,, \tag{2.81}$$

where defined $\sigma^0 \equiv \mathbb{1}$. Note that (2.81) is equivalent to requiring that the states have *cluster decomposition properties* [135]. We say that a state $|\Psi_0\rangle$ possesses cluster decomposition

properties if it satisfies

$$\lim_{\substack{\min \\ i\neq j}|x_i-x_j|\to\infty}\Big(\langle\mathcal{O}_1(x_1)\mathcal{O}_2(x_2)\cdots\mathcal{O}_n(x_n)\rangle-\langle\mathcal{O}_1(x_1)\rangle\langle\mathcal{O}_2(x_2)\rangle\cdots\langle\mathcal{O}_n(x_n)\rangle\Big)=0 \qquad (2.82)$$

where the operators $\mathcal{O}_i(x_i)$ are local (act trivially far away from the site x_i) and the expectation values are taken with respect to $|\Psi_0\rangle$.

Strings of the form $\mathcal{O}_{i;n}^{\{\alpha_j\}}$ can either commute or anti commute with the unitary transformation $e^{i\pi N}$, which represents the $\mathbb{Z}_2$ symmetry (2.2) on the Hilbert space. If $e^{i\pi N}\mathcal{O}_{i;n}^{\{\alpha_j\}}e^{-i\pi N}=O_{i;n}^{\{\alpha_j\}}$ we have

$${}_{\rm R}\langle 0|\mathcal{O}_{i;n}^{\{\alpha_j\}}|0\rangle_{\rm NS}={}_{\rm NS}\langle 0|\mathcal{O}_{i;n}^{\{\alpha_j\}}|0\rangle_{\rm R}=0\,,\qquad {}_{\rm NS}\langle 0|\mathcal{O}_{i;n}^{\{\alpha_j\}}|0\rangle_{\rm NS}={}_{\rm R}\langle 0|\mathcal{O}_{i;n}^{\{\alpha_j\}}|0\rangle_{\rm R}\,. \qquad (2.83)$$

The first condition is required by the symmetry properties of the operator and is true for all L, while the second is fulfilled in the infinite volume limit where the effects of boundary conditions can be neglected as long as symmetries are respected. Equations (2.83) imply that (2.81) is fulfilled for all α and β. If instead $e^{i\pi N}\mathcal{O}_{i;n}^{\{\alpha_j\}}e^{-i\pi N}=-\mathcal{O}_{i;n}^{\{\alpha_j\}}$, then

$${}_{\rm R}\langle 0|\mathcal{O}_{i;n}^{\{\alpha_j\}}|0\rangle_{\rm NS}={}_{\rm NS}\langle 0|\mathcal{O}_{i;n}^{\{\alpha_j\}}|0\rangle_{\rm R}\,,\qquad {}_{\rm NS}\langle 0|\mathcal{O}_{i;n}^{\{\alpha_j\}}|0\rangle_{\rm NS}={}_{\rm R}\langle 0|\mathcal{O}_{i;n}^{\{\alpha_j\}}|0\rangle_{\rm R}=0\,. \qquad (2.84)$$

Imposing the condition (2.81) we find $\alpha^2=\beta^2$, which implies

$$|0\rangle=\frac{1}{\sqrt{2}}\Big(|0\rangle_{\rm NS}+|0\rangle_{\rm R}\Big)\,,\qquad\qquad |1\rangle=\frac{1}{\sqrt{2}}\Big(|0\rangle_{\rm NS}-|0\rangle_{\rm R}\Big)\,. \qquad (2.85)$$

The states $|0\rangle$ and $|1\rangle$ are mapped into each other by the unitary transformation $e^{i\pi N}$. The spontaneous selection of one of the states (2.85) as a ground state constitutes a spontaneous breaking of the $\mathbb{Z}_2$ symmetry [135]. We stress that the combinations (2.85) are eigenstates of the Hamiltonian only in the limit $L\to\infty$.

For the excited states the same correspondence between infinite and finite volume eigenstates holds, the states

$$|p_1,\ldots,p_{2n}\rangle_0=\frac{1}{\sqrt{2}}\Big(|p_1,\ldots,p_{2n}\rangle_{\rm NS}+|p_1,\ldots,p_{2n}\rangle_{\rm R}\Big)\,, \qquad (2.86)$$

$$|p_1,\ldots,p_{2n}\rangle_1=\frac{1}{\sqrt{2}}\Big(|p_1,\ldots,p_{2n}\rangle_{\rm NS}-|p_1,\ldots,p_{2n}\rangle_{\rm R}\Big)\,. \qquad (2.87)$$

are not connected by operators which are local in space.

3. The "Representative Eigenstate Approach" to the sine-Gordon dynamics

In this chapter we present a method that allows to obtain the asymptotic time dependence of the expectation values of observables in cases where the time evolution is defined by an *integrable* Hamiltonian. Importantly, this method allows to deal with *interacting problems* as long as the interaction preserves the integrability. Together with the discussion of the general method we provide a highly non trivial example of its application, computing the time evolution of the one point function of a particular *semi-local* vertex operator for a specific class of initial states in the sine-Gordon model, which involves a *non-diagonal* interaction, *i.e.* the scattering matrix is non diagonal.

3.1 Introduction

In Ref. [73] a novel approach to calculating expectation values of local operators after quantum quenches to integrable models was proposed. It has been subsequently applied to determine the infinite-time behaviour of certain local observables in an interaction quench from free to interacting bosons in the Lieb-Liniger model [52], the XXZ chain [54, 55, 57] and recently to determine the time evolution of observables local with respect to the elementary excitations in the Lieb-Liniger model [136, 137] and more generally integrable models with diagonal interactions [138]; in these works the approach is referred to as "Quench Action". Using thermodynamic arguments it was argued in Ref. [73] that

$$\lim_{L\to\infty} \frac{{}_L\langle\Psi_0|\mathcal{O}(t,x)|\Psi_0\rangle_L}{{}_L\langle\Psi_0|\Psi_0\rangle_L} = \lim_{L\to\infty}\left[\frac{{}_L\langle\Psi_0|\mathcal{O}(t,x)|\Phi\rangle_L}{2\,{}_L\langle\Psi_0|\Phi\rangle_L} + \frac{{}_L\langle\Phi|\mathcal{O}(t,x)|\Psi_0\rangle_L}{2\,{}_L\langle\Phi|\Psi_0\rangle_L}\right], \tag{3.1}$$

where $\mathcal{O}(t,x) = e^{iHt}\mathcal{O}(x)e^{-iHt}$ is a local (in space) operator evolving via the *integrable* Hamiltonian H, $|\Psi_0\rangle_L$ is the initial state in a large, finite volume L, and $|\Phi\rangle_L$ is a *representative state* characterised by the requirements that

1. $|\Phi\rangle_L$ is an eigenstate of a set of a complete set of conserved charges $\{I(\alpha)_L\}$ of the model in a large, finite volume L. The set includes both the "standard" ultra-local charges and quasi-local ones, so we labelled them by means of a continuous index $\alpha \geq 0$. The inclusion of the quasi-local charges is necessary for a correct determination of the representative state in a theory on the continuum, as recently clarified in [139].

2. The expectation values of $\{I(\alpha)_L\}$ are the same in the initial and the representative state in the thermodynamic limit

$$\lim_{L\to\infty}\frac{1}{L}\frac{{}_L\langle\Phi|I(\alpha)_L|\Phi\rangle_L}{{}_L\langle\Phi|\Phi\rangle_L}=\lim_{L\to\infty}\frac{1}{L}\frac{{}_L\langle\Psi_0|I(\alpha)_L|\Psi_0\rangle_L}{{}_L\langle\Psi_0|\Psi_0\rangle_L},\quad \alpha\geq 0\,. \tag{3.2}$$

Equation (3.1) represents a very convenient starting point to construct and evaluate a spectral representation, indeed, given the fact that $|\Phi\rangle_L$ is an eigenstate of the Hamiltonian, the spectral representation of the r.h.s. involves only a single sum over the Hilbert space; moreover, since $\mathcal{O}(x)$ is local in space, only the states "close" enough to $|\Phi\rangle_L$ are expected to contribute [73]. The idea is then to explicitly construct such a spectral expansion of (3.1) in terms of the basis $\{|\theta_1,\ldots,\theta_N\rangle_L^s\}$ and evaluate it using general properties of the matrix elements

$${}_L^s\langle\theta_N,\ldots,\theta_1|\mathcal{O}(0,0)|\Phi\rangle_L\,, \tag{3.3}$$

that can be related to the infinite volume *form-factors*, as will be explained in the following. Our plan of attack can be summarised in the following steps

(i) Construct a basis $\{|\theta_1,\ldots,\theta_N\rangle_L^s|s=1,\ldots,2^N\}$ of N-particle energy eigenstates in the finite volume (in fact these will be eigenstates of all the local conserved charges).

(ii) Construct finite-volume matrix elements of (semi-) local operators $\mathcal{O}$ with respect to these eigenstates.

(iii) Given an initial state $|\Psi_0\rangle$, determine a corresponding representative eigenstate $|\Phi\rangle_L$.

(iv) For a given operator $\mathcal{O}(x)$, work out the time evolution using a Lehmann representation of (3.1) in terms of energy eigenstates, i.e. work out matrix elements of the form

$$\begin{aligned}{}_L\langle\Psi_0|\mathcal{O}(t,0)|\Phi\rangle_L&=\sum_{|\{\theta_k\}\rangle_L^s}{}_L\langle\Psi_0|\theta_1,\ldots,\theta_N\rangle_L^s\ {}_L^s\langle\theta_N,\ldots,\theta_1|\mathcal{O}(t,0)|\Phi\rangle_L\\&=\sum_{|\{\theta_k\}\rangle_L^s}{}_L\langle\Psi_0|\theta_1,\ldots,\theta_N\rangle_L^s\ {}_L^s\langle\theta_N,\ldots,\theta_1|\mathcal{O}(0,0)|\Phi\rangle_L\ e^{it\mathcal{E}_N^\Phi}.\end{aligned} \tag{3.4}$$

Here we assumed the initial state to be translationary invariant and introduced the following shorthand notations

$$\mathcal{E}_N^\Phi\equiv E_\Phi-\sum_{j=1}^N\Delta\cosh\theta_j\,, \tag{3.5}$$

$$\sum_{|\{\theta_k\}\rangle_L^s} \cdots \equiv \sum_{N\geq 0} \sum_{\{|\theta_1,\ldots,\theta_N\rangle_L^s\}} \cdots , \tag{3.6}$$

where E_Φ is the energy of the representative eigenstate. It is worth noting that ultimately we are interested in the limit $L \to \infty$ and use finite L only as a regularization. As a result only the dominant finite-size corrections have to be taken into account throughout the procedure.

A non-trivial application of the outlined strategy has been shown directly in [73]. There this was used to determine the time evolution of the one point function of the order parameter, after a quench of the magnetic field in the ordered phase ($h < 1$) of the transverse field Ising chain (TFIC). The result was found in the limit of small density of excitations after the quench. It is important to stress that, even if the TFIC can be mapped into free fermions by means of a Jordan-Wigner transformation, the time dependence of the one point function of the order parameter σ^x in the ordered phase it is hard to compute, in fact the computation has been carried out for the first time only recently [44]. This is due to the fact that the order parameter field is non local with respect to the elementary excitations of the model; in particular, in the continuum limit of the model the field $\sigma(x)$ representing the order parameter is *semi-local* (*c.f.* Eq. (2.72)) with respect to the elementary excitations [140]. In the spectral representation of the one-point function this fact is reflected by the appearance of an infinite number of terms diverging at late times that one has to re-sum in order to obtain the late time behaviour.

Our scope is to show how to generalise the application of the above strategy to the case where the time evolution is determined by a *non-diagonally interacting* integrable model, specifically the sine-Gordon model (SGM) described by the Hamiltonian (2.36), focussing on the repulsive regime $1/\sqrt{2} \leq \beta < 1$. In analogy with the quench in the TFIC described above, we will consider one point functions of operators that are semi-local with respect to the elementary excitations, specifically $\mathcal{O}(x) = e^{i\beta\Phi(x)/2}$. The physical interpretation of this operator depends on the microscopic setting giving rise to a SGM. Chapter 2 reports two important contexts where an effective SGM description emerges, magnetic solids and ultra-cold trapped atoms: in the first realisation $e^{i\beta\Phi(x)/2}$ corresponds to a staggered magnetisation (*c.f.* Eq. (2.42)) while in the second describes the oscillatory component of the particle density (*c.f.* Eq. (2.50)). Instead of considering a standard quench protocol we will consider the time evolution starting from a given class of initial states $|\Psi_0\rangle$, we discuss this class and its realizability in standard quench protocols in Subsection 3.1.1.

Quantum quenches to the massive regime $\beta < 1$ of the sine-Gordon model were considered by Iucci and Cazalilla [141, 142]. They focussed on two special cases, namely quenches from

the massless regime to the free-fermion point $\beta = 1/\sqrt{2}$ and in the semiclassical regime $\beta \to 0$. These cases are characterised by no or weak interactions respectively, and as a result are amenable to treatment by simpler methods than the ones developed here. The solvability of the model at the free-fermion point was also employed by Foster et al. [143, 144] to investigate the amplification of initial density inhomogeneities.

Gritsev et al. [145] considered the time evolution of the *local* operator $e^{i\beta\Phi}$ after preparing the system in an integrable boundary state similar to ours (*cf.* Subsection 3.1.1). However, they focussed on the attractive regime $\beta < 1/\sqrt{2}$ where, in addition to solitons and antisolitons, breather bound states exist. By employing a form-factor expansion and evaluating the first few terms, they calculated the power spectrum of the vertex operator $e^{i\beta\Phi}$ and showed that it possesses sharp resonances corresponding to the creation of breather states and discussed implications for experiments on split one-dimensional Bose condensates. For the approach Ref. [145] to apply, higher order terms in the Lehmann expansion must be negligible. For general operators this is not the case [44,140]: as previously pointed out for semi-local operators of the kind considered here these terms are in fact divergent at late times. Here we describe a method, introduced in [1], allowing to determine the late-time behaviour in this much more complicated case.

For $\beta > 1$ the cosine perturbation is irrelevant at low energies and quenches in this very different regime have been considered in Refs. [146–148].

In summary, the scope of this chapter is to apply the strategy (i) − (iv) to determine the time dependence of the following expectation value

$$F^{\beta/2}_{\Psi_0}(t) = \frac{\langle\Psi_0|e^{i\mathcal{H}_{\rm SG}t}e^{i\beta\Phi(x)/2}e^{-i\mathcal{H}_{\rm SG}t}|\Psi_0\rangle}{\langle\Psi_0|\Psi_0\rangle}\,. \tag{3.7}$$

Comparing to the case analysed in [73] the complications arising here are severe, first the determination of the representative state becomes substantially harder, as we shall see in the following (*c.f.* Section 2.71) this is mainly caused by the non diagonality of the scattering; a second complication is that the rapidities appearing in Eq. (3.4) obey extremely intricate quantisation conditions (*c.f.* Eq. (3.47)) as a consequence of the fact that an interacting system has been confined in a finite volume. Surprisingly, in spite of these complications, the calculation can be carried out, without having to solve the quantisation conditions and without even requiring the full expression of the matrix elements (3.3) but only the coefficients of their most divergent multidimensional poles, which can be extracted by means of the form-factor annihilation pole axiom (2.71). This fact is remarkable and demonstrates the astonishing power of the representative eigenstate approach, showing that it can be applied not only in principle

but also in practice to determine the long time behaviour of (highly non trivial) observables evolving according to any possible interacting integrable Hamiltonian.

3.1.1 "Integrable" quantum quenches

As shown by Calabrese and Cardy [149], the calculation of expectation values of local operators after a quench can be mapped to a corresponding problem in boundary quantum field upon analytic continuation to imaginary time. In the case where the post-quench Hamiltonian is integrable, there is then a particular class of boundary conditions, and concomitantly initial states, namely those compatible with integrability [150]. Given the relative simplicity of such states, they constitute a natural starting point for quenches to interacting integrable models [151]. A characteristic feature of these states is that they can be cast in the form [150]

$$|\Psi_0\rangle = \exp\left(\int_0^\infty \frac{d\theta}{2\pi} K^{ab}(\theta) Z_a^\dagger(-\theta) Z_b^\dagger(\theta)\right)|0\rangle. \tag{3.8}$$

Here the matrix $K^{ab}(\theta)$ is obtained from a solution of the reflection equations and fulfils

$$\begin{aligned} K^{a_1c_1}(\theta_1)K^{c_2c_3}(\theta_2)S_{c_2c_1}^{a_2c_4}(\theta_1+\theta_2)S_{c_3c_4}^{b_2b_1}(\theta_1-\theta_2) = \\ = K^{c_1b_1}(\theta_1)K^{c_2c_3}(\theta_2)S_{c_3c_1}^{b_2c_4}(\theta_1+\theta_2)S_{c_2c_4}^{a_2a_1}(\theta_1-\theta_2), \end{aligned} \tag{3.9}$$

$$K^{ab}(\theta) = S_{cd}^{ab}(2\theta)K^{dc}(-\theta)\,, \tag{3.10}$$

$$K^{\bar{a}c}(i\frac{\pi}{2}-\theta)K^{\bar{c}b}(i\frac{\pi}{2}+\theta) = \delta_{ab}. \tag{3.11}$$

For our purposes it will be useful to exploit the fact that if $K^{ab}(\theta)$ is a solution to (3.9) and (3.10), other solutions can be obtained by multiplication with an even function $g(\theta)$

$$\widetilde{K}^{ab}(\theta) = K^{ab}(\theta)g(\theta). \tag{3.12}$$

Introducing a function $g(\theta)$ is crucial in the quench context in order to obtain well-defined results (see the discussion below). A particular choice of $g(\theta)$ advocated in Ref. [151] in light of the corresponding situation for conformal field theories [149] is

$$g(\theta) = e^{-2\tau_0\Delta\cosh\theta}, \tag{3.13}$$

which defines an "extrapolation time" τ_0. An immediate question is whether boundary states like (3.8) make for physically meaningful initial states after quenches to a sine-Gordon model.

A particular choice of $K^{ab}(\theta)$ corresponds to fixed boundary conditions

$$\Phi(t=0,x)=0. \tag{3.14}$$

These can be realized by quenching the parameter λ in (2.36) from infinity to a finite value at time $t=0$, i.e.

$$\lambda\Big|_{t<0}=\infty \longrightarrow \lambda\Big|_{t>0}=\lambda_+. \tag{3.15}$$

The problem with such a quench is that it corresponds to an initial state after the quench with infinite energy density, which is clearly undesirable. This problem is reflected in the fact that for integrable boundary conditions one typically has

$$\lim_{\theta\to\infty}\sum_{a,b}|K^{ab}(\theta)|^2=\text{const}, \tag{3.16}$$

which essentially corresponds to having a finite density of excitations even for infinite-energy particles. The simplest way to suppress the presence of such excitations in the initial state is to introduce a function $g(\theta)$, and consider an initial state of the form (3.8) with K replaced by $\widetilde{K}$, which does not fulfil the condition (3.11). The particular choice (3.13) is too restrictive for quenches to integrable massive QFTs [152], and an important question is what kind of initial conditions can be described by an appropriate choice of $\widetilde{K}$ [152,153]. One might hope that an approximate realisation of such an initial state could be obtained in a quantum quench

$$\lambda\Big|_{t<0}=\lambda_- \longrightarrow \lambda\Big|_{t>0}=\lambda_+, \tag{3.17}$$

where $\lambda_\pm$ are both large but finite, and their difference is small. This is clearly an important issue worthy of further investigation, but is beyond the scope of this chapter. Interestingly, a similar regularisation procedure has to be performed in quenches from free to interacting bosons in the Lieb-Liniger (LL) model [50,52], in order to avoid the divergence of the expectation values of all even conserved charges above the Hamiltonian. In this case the initial state has to be multiplied by $e^{-\beta H_{LL}(c)}$ where $H_{LL}(c)$ is the LL Hamiltonian and $c>0$ is the final value of the interaction [154].

In the following we will simply set aside the question of how our initial state can be prepared and impose it to be of the form (3.8), where $K^{ab}(\theta)$ is a solution of the boundary Yang-Baxter equation (3.9) and the boundary crossing-unitarity equation (3.10). We will furthermore use the freedom (3.12) to be able to consider $K^{ab}(\theta)$, and hence the quench, to be small in the sense of Refs. [44, 45, 88].

3.1.2 Organisation of the chapter

The remainder of this chapter is organised as follows: In the next three sections we show how to construct a basis of eigenstates of the Hamiltonian in finite volume, define a correspondence between the expectation values on this basis and the infinite volume form-factors and finally construct the representative eigenstate corresponding to the initial state (3.8). In Section 3.5 we determine the time evolution of the one-point function $F_{\Psi_0}^{\beta/2}(t)$ showing that, at the first order in the density of excitations of the final Hamiltonian, it decays exponentially in time, see Eq. (3.123), with a calculable decay time τ. This result is confirmed by an independent calculation carried out using the "linked cluster expansion" approach [1]. We conclude with a discussion of our results and an outlook for further investigations in Section 3.6. Technical details encountered in the course of our analysis are presented in a number of appendices.

3.2 Basis of energy eigenstates in the finite volume

Our starting point for constructing energy eigenstates in the finite volume are the infinite-volume scattering states (2.63). The idea is to consider appropriate linear combinations of scattering states, and then to impose boundary conditions on these, see e.g. Ref. [155]. To this end, we introduce a *transfer matrix* acting on scattering states as follows

$$\mathcal{T}(\lambda|\{\theta_k\})\,|\theta_1,\dots,\theta_N\rangle_{a_1\dots a_N} = \mathcal{T}(\lambda|\{\theta_k\})_{a_1\dots a_N}^{b_1\dots b_N}\,|\theta_1,\dots,\theta_N\rangle_{b_1\dots b_N}\ , \tag{3.18}$$

where

$$\mathcal{T}(\lambda|\{\theta_k\})_{a_1\dots a_N}^{b_1\dots b_N} = S_{c_N\ a_1}^{c_1 b_1}(\lambda-\theta_1)\cdots S_{c_{N-1}a_N}^{c_N\ b_N}(\lambda-\theta_N)\,. \tag{3.19}$$

As the S-matrix is a solution of the Yang-Baxter equation, the transfer matrices form a commuting family

$$\Big[\mathcal{T}(\lambda|\{\theta_k\}),\mathcal{T}(\mu|\{\theta_k\})\Big] = 0. \tag{3.20}$$

Hence the transfer matrices can be diagonalized simultaneously

$$\mathcal{T}(\lambda|\{\theta_k\})\,|\theta_1,\dots,\theta_N\rangle^s = \Lambda^s(\lambda|\{\theta_k\})\,|\theta_1,\dots,\theta_N\rangle^s\ ,\quad s=1,\dots,2^N. \tag{3.21}$$

We refer to the labels s as *polarisations*. Details of the construction of transfer-matrix eigenstates and explicit expressions for the eigenvalues $\Lambda^s(\lambda|\{\theta_k\})$ are given in Appendix 3.A. By construction energy and momentum of the states (3.21) are still given by Formulae (2.64). The basis transformation between scattering states and transfer matrix eigenstates can be cast in

the form

$$|\theta_1,\ldots,\theta_N\rangle^s = \sum_{a_1\ldots a_N} \Psi^s_{a_1\cdots a_N}(\{\theta_k\})\,|\theta_1,\ldots,\theta_N\rangle_{a_1\ldots a_N}\,, \tag{3.22}$$

$$|\theta_1,\ldots,\theta_N\rangle_{a_1\ldots a_N} = \sum_{s} \Psi^s_{a_1\cdots a_N}(\{\theta_k\})^*\,|\theta_1,\ldots,\theta_N\rangle^s\,, \tag{3.23}$$

where the amplitudes $\{\Psi^s_{a_1\cdots a_N}(\{\theta_k\})\}_{s=1,\ldots,2^N}$ satisfy

$$\mathcal{T}(\lambda|\{\theta_k\})^{b_1\cdots b_N}_{a_1\cdots a_N}\Psi^s_{a_1\cdots a_N}(\{\theta_k\}) = \Lambda^s(\lambda|\{\theta_k\})\Psi^s_{b_1\cdots b_N}(\{\theta_k\})\,, \tag{3.24}$$

$$\sum_{a_1\ldots a_N}\Psi^s_{a_1\cdots a_N}(\{\theta_k\})^*\Psi^r_{a_1\cdots a_N}(\{\theta_k\}) = \delta_{rs}\,, \tag{3.25}$$

$$\sum_{s}\Psi^s_{a_1\cdots a_N}(\{\theta_k\})^*\Psi^s_{b_1\cdots b_N}(\{\theta_k\}) = \prod_{j=1}^{N}\delta_{a_j,b_j}\,. \tag{3.26}$$

The last two equations ensure that $\{|\theta_1,\ldots,\theta_N\rangle^s\}_{s=1,\ldots,2^N}$ is an orthonormal and complete set. Since the topological charge operator Q commutes with the transfer matrix we can choose $\{\Psi^s_{a_1\cdots a_N}(\{\theta_k\})\}_{s=1,\ldots,2^N}$ such that Q is diagonal in the basis $\{|\theta_1,\ldots,\theta_N\rangle^s\}_{s=1,\ldots,2^N}$

$$Q\,|\theta_1,\ldots,\theta_N\rangle^s = Q(s)\,|\theta_1,\ldots,\theta_N\rangle^s\,,\quad Q(s)\in\{N,N-2,\ldots,-N\}\,. \tag{3.27}$$

We are now in a position to consider a large, finite volume L and impose periodic boundary conditions on the transfer matrix eigenstates

$$e^{i\ell\sinh\theta_i}\,|\theta_1,\ldots,\theta_N\rangle^s_L = \mathcal{T}^{-1}(\theta_i|\{\theta_k\})\,|\theta_1,\ldots,\theta_N\rangle^s_L\,,\qquad i=1,\ldots,N, \tag{3.28}$$

where we have introduced a dimensionless length $\ell = L\Delta/v$. Equations (3.28) lead to quantisation conditions for the rapidities in the finite volume and are known as Bethe-Yang equations [155–157]

$$e^{i\ell\sinh\theta_i}\Lambda^s(\theta_i|\{\theta_k\}) = 1\,,\qquad i=1,\ldots,N,\quad s=1,\ldots,2^N. \tag{3.29}$$

For practical purposes the logarithmic version of (3.29) is more convenient

$$2\pi I^s_i = \ell\sinh\theta_i - i\log\Lambda^s(\theta_i|\{\theta_k\}) \equiv Q^s_i(\{\theta_k\})\,,\quad i=1,\ldots,N,\ s=1,\ldots,2^N. \tag{3.30}$$

Here I^s_i are integer or half-odd integer numbers that uniquely specify a given solution and concomitantly the corresponding transfer matrix eigenstate. By virtue of these facts one may use the integers (rather than the rapidities) as labels for constructing a basis of eigenstates [158,

159]. The latter is given by the states

$$|\{I_1,\dots,I_N\}\rangle_L^s \ , \quad I_1<\cdots<I_N \ , \tag{3.31}$$

where we impose normalisation conditions

$${}_L^r\langle\{J_M,\dots,J_1\}|\{I_1,\dots,I_N\}\rangle_L^s = \delta_{MN}\delta_{rs}\delta_{J_1I_1}\cdots\delta_{J_NI_N} \, . \tag{3.32}$$

In a given sector specified by N and s the Jacobian matrix of the (invertible) mapping between rapidities $\{\theta_k\}_{k=1,\dots,N}$ and integers $\{I_k\}_{k=1,\dots,N}$ is given by

$$\mathcal{J}_N^s(\{\theta_k\})_{ij} = \partial_{\theta_j} Q_i^s(\{\theta_k\}) \, . \tag{3.33}$$

The *N-particle density of states with polarisation s* is defined as the Jacobian

$$\rho_N^s(\{\theta_k\}) = \det \mathcal{J}_N^s(\{\theta_k\}) \, . \tag{3.34}$$

3.2.1 2-folded sine-Gordon model

When quantising the theory in the finite volume, care has to be taken to account for the absence of spontaneous symmetry breaking of the discrete symmetry

$$\Phi(x) \longrightarrow \Phi(x) + \frac{2\pi n}{\beta} \ , \ n \in \mathbb{Z} \tag{3.35}$$

of the sine-Gordon Hamiltonian. In the applications of the sine-Gordon model we have in mind, the Bose field is compactified on a ring with radius

$$R = \frac{4\pi}{\beta}. \tag{3.36}$$

This implies that on a classical level there are two vacuum states $|0\rangle$ and $|1\rangle$, with corresponding field expectation values

$$\langle n|\Phi(x,t)|n\rangle = \frac{2\pi}{\beta}n, \qquad n=0,1. \tag{3.37}$$

This theory is known as the 2-folded sine-Gordon model SG(β,2), and has been analysed in some detail in Ref. [160]. We now review some relevant results. On the quantum level, the two ground states are mapped one into the other by the transformation

$$T : \Phi(x) \ \longrightarrow \ \Phi(x) - \frac{2\pi}{\beta}, \tag{3.38}$$

which is a symmetry of the Hamiltonian. The linear combinations of $|0\rangle$ and $|1\rangle$ that are eigenvectors of T are given by

$$|0\rangle_{\mathrm{R,NS}} = \frac{|0\rangle \pm |1\rangle}{\sqrt{2}}, \tag{3.39}$$

Note that here we are slightly abusing the notation: usually (see Appendix 2.A) $|0\rangle_{\mathrm{R}}$ and $|0\rangle_{\mathrm{NS}}$, where R and NS respectively stand for Ramond and Neveu-Schwarz sector, designate ground states of the Hamiltonian in *finite volume*. Here we use the same name for their "infinite volume continuation". As discussed in Appendix 2.A for the case of the XY model: in the infinite volume the system spontaneously selects as ground state one of the states $|0\rangle$ and $|1\rangle$, which satisfy cluster decomposition properties. So it is never in the states $|0\rangle_{\mathrm{R}}$ and $|0\rangle_{\mathrm{NS}}$.

Considering now excited states, in the infinite volume, one can construct scattering states over each of the two ground states. They are denoted by

$$|\theta_1, \ldots, \theta_N\rangle^n_{a_1 \ldots a_N} \tag{3.40}$$

where $a_i = \pm 1$ are topological charge quantum numbers and $n = 0, 1$ label the two ground states. In order to define the SG(β,2) model in a finite volume, one considers eigenstates of the "shift"-operator T defined above

$$|\theta_1, \ldots, \theta_N\rangle^{\mathrm{R}}_{a_1 \ldots a_N} = \frac{1}{\sqrt{2}} \Big\{ |\theta_1, \ldots, \theta_N\rangle^0_{a_1 \ldots a_N} + |\theta_1, \ldots, \theta_N\rangle^1_{a_1 \ldots a_N} \Big\}, \tag{3.41}$$

$$|\theta_1, \ldots, \theta_N\rangle^{\mathrm{NS}}_{a_1 \ldots a_N} = \frac{1}{\sqrt{2}} \Big\{ |\theta_1, \ldots, \theta_N\rangle^0_{a_1 \ldots a_N} - |\theta_1, \ldots, \theta_N\rangle^1_{a_1 \ldots a_N} \Big\}. \tag{3.42}$$

In a finite volume, periodic boundary conditions select only states for which the set $\{a_i\}$ is subject to the constraint

$$\sum_{i=1}^{N} a_i \equiv 0 \bmod 2. \tag{3.43}$$

Condition (3.43) is equivalent to requiring that the number N of particles be even. States involving an odd number of (anti) solitons are incompatible with the boundary conditions and are not part of the Hilbert space. Nevertheless all *local* properties of SG(β,2) coincide with the corresponding quantities in the sine-Gordon model. In order to impose boundary conditions we again go over to transfer matrix eigenstates, which we denote by

$$|\theta_1, \ldots, \theta_N\rangle^s_{\mathtt{a}} \ , \qquad \mathtt{a} = \mathrm{R}, \mathrm{NS}. \tag{3.44}$$

Periodic boundary conditions imply that

$$e^{i\ell \sinh\theta_i}\,|\theta_1,\ldots,\theta_N\rangle^s_{\mathtt{a}} = \sigma_{\mathtt{a}}\mathcal{T}^{-1}(\theta_i|\{\theta_k\})\,|\theta_1,\ldots,\theta_N\rangle^s_{\mathtt{a}}\ , \quad i=1,\ldots,N\ , \tag{3.45}$$

where $\sigma_{\rm R} = 1 = -\sigma_{\rm NS}$. Eqs. (3.45) lead to finite-volume quantisation conditions of the form

$$e^{i\ell \sinh\theta_i}\Lambda^s(\theta_i|\{\theta_k\}) = \sigma_{\mathtt{a}}, \quad i=1,\ldots,N\ , \quad s=1,\ldots,2^N, \quad \mathtt{a}={\rm R},{\rm NS}. \tag{3.46}$$

Taking the logarithm we obtain

$$Q^s_i(\{\theta_k\}) = \ell\sinh\theta_i - i\log\Lambda^s(\theta_i|\{\theta_k\}) = 2\pi\,(I^s_i + \kappa_{\mathtt{a}})\,, \qquad \kappa_{\mathtt{a}} \equiv \frac{1-\sigma_{\mathtt{a}}}{4}. \tag{3.47}$$

Using again the (half-odd) integers $\{I_k\}$ to label the states we denote our basis of transfer matrix eigenstates in a large, finite volume L by

$$\{|\{I_1,\ldots,I_N\}\rangle^s_{\mathtt{a}},\ N \text{ even},\ s=1,\ldots,2^N,\ \mathtt{a}={\rm R},{\rm NS}\}. \tag{3.48}$$

Here distinct sets of I_j give rise to different basis states, and a natural choice would therefore be $I_1 < I_2 < \ldots < I_N$. However, in the following we will be interested in the case where our solutions consist of pairs, i.e. $\{-I_1, I_1, -I_2, I_2, \ldots\}$. Having this situation in mind, we choose the following odd-looking convention for labelling our basis states

$$I_{N-1} < I_{N-3} < \ldots < I_3 < I_1 < I_2 < I_4 \ldots < I_{N-2} < I_N\,. \tag{3.49}$$

Before concluding this subsection we note that the operator $\mathcal{O}(t,x) = e^{i\beta\Phi(t,x)/2}$ has non-vanishing matrix elements only between different sectors. This follows because the operator is odd under the symmetry T

$$T\mathcal{O}(t,x)T^\dagger = -\mathcal{O}(t,x), \tag{3.50}$$

while the states are either even or odd under T.

3.3 Matrix elements of operators in finite volume

A general method for determining matrix elements of local (in space) operators in a large, finite volume was developed in Refs. [155] and [158,159]. The leading corrections to the form factors in the infinite-volume limit arises from the quantisation of the rapidities. Given infinite-volume form-factors $f^{\mathcal{O}a_M\cdots a_1}_{b_1\cdots b_N}(\theta_M,\ldots,\theta_1|\tilde\theta_1,\ldots,\tilde\theta_N)$ of an operator $\mathcal{O}(x)$, one first forms appropriate

linear combinations

$$f^{\mathcal{O}}(\theta_M,\dots,\theta_1|\tilde{\theta}_1,\dots,\tilde{\theta}_N)^s_{\tilde{s}} = \sum_{\substack{a_1\dots a_M\\ b_1\dots b_N}} \Psi^{\tilde{s}}_{b_1\cdots b_N}(\{\tilde{\theta}_k\})\Psi^s_{a_1\cdots a_M}(\{\theta_k\})^* \times f^{\mathcal{O}\,a_M\cdots a_1}_{\quad b_1\cdots b_N}(\theta_M,\dots,\theta_1|\tilde{\theta}_1,\dots,\tilde{\theta}_N), \tag{3.51}$$

where the amplitudes $\Psi^s_{a_1\dots a_M}(\{\theta_k\})$ are defined in (3.22). Matrix elements in the basis (3.48) for operators $\mathcal{O}$ odd under the transformation T are then given by

$${}^{s}_{\mathrm{R}}\langle\{I_M,\dots,I_1\}|\mathcal{O}(0,0)|\{\tilde{I}_1,\dots,\tilde{I}_N\}\rangle^{\tilde{s}}_{\mathrm{NS}} = \frac{f^{\mathcal{O}}(\theta_M,\dots,\theta_1|\tilde{\theta}_1,\dots,\tilde{\theta}_N)^s_{\tilde{s}}}{\sqrt{\rho^s_M(\theta_1,\dots,\theta_M)\rho^{\tilde{s}}_N(\tilde{\theta}_1,\dots,\tilde{\theta}_N)}} + O(e^{-\mu' L}). \tag{3.52}$$

Here N and M are both even in our case.

3.4 Representative eigenstate

The next step requires to find a member of the basis (3.48) which represents the initial state $|\Psi_0\rangle$ in the sense described in Section 3.1. The first ingredient we need to determine such a representative eigenstate is a finite volume realisation of the initial state.

3.4.1 Initial state in finite volume

Given that in the thermodynamic limit we must reproduce the spontaneous breaking of the symmetry (3.35), the appropriate linear combination is given by (*cf.* Eq. (3.39))

$$|\Psi_0\rangle_L = \frac{1}{\sqrt{2}}\big[|\Psi_0\rangle_{\mathrm{R}} + |\Psi_0\rangle_{\mathrm{NS}}\big]. \tag{3.53}$$

We now wish to express $|\Psi_0\rangle_{\mathtt{a}}$ in terms of transfer-matrix eigenstates. This can be done by generalising the results of Ref. [161], which considered finite-volume realisations of integrable boundary states for diagonal scattering theories, for which both the scattering matrix $S^{ab}_{cd}(\theta)$ and the $K^{ab}(\theta)$ are scalars. This leads to an expression of the form

$$|\Psi_0\rangle_{\mathtt{a}} = \sum_{N=0}^{\infty}\sum_{s=1}^{2^{2N}}\sum_{0<I_1<\cdots<I_N} \mathcal{N}^s_{2N}(\{\theta_k\})\mathcal{K}^s_{2N}(\{\theta_k\})\,|\{-I_1,I_1,\dots,-I_N,I_N\}\rangle^s_{\mathtt{a}}\,, \tag{3.54}$$

where $\mathtt{a} = \mathrm{R},\mathrm{NS}$. We emphasize that the rapidities appearing in this formula are the parity symmetric solutions $\{-\theta_1,\theta_1,\dots,-\theta_N,\theta_N\}$ of the Bethe-Yang equations for every fixed N, s

and $\mathtt{a}$, with $0 < \theta_1 < \cdots < \theta_N$. The functions $\mathcal{N}^s_{2N}$ and $\mathcal{K}^s_{2N}$ in (3.54) are defined as

$$\mathcal{K}^s_{2N}(\{\theta_k\}) \equiv K^{a_1 b_2}(\theta_1)\cdots K^{a_N b_N}(\theta_N)\Psi^s_{a_1 b_1 \cdots a_N b_N}(\{\theta_k\})^* \,, \tag{3.55}$$

$$\mathcal{N}^s_{2N}(\{\theta_k\}) \equiv \frac{\sqrt{\rho^s_{2N}(-\theta_1,\theta_1,\ldots,-\theta_N,\theta_N)}}{\bar{\rho}^s_N(\theta_1,\ldots,\theta_N)} \,, \tag{3.56}$$

while $\bar{\rho}^s_N(\{\theta_k\})$ is the constrained N-particle density of states with polarisation s

$$\bar{\rho}^s_N(\{\theta_k\}) = \det \bar{\mathcal{J}}^s_N(\{\theta_k\}) \,, \qquad \bar{\mathcal{J}}^s_N(\{\theta_k\})_{ij} = \partial_{\theta_j}\bar{Q}^s_i(\{\theta_k\}) \,. \tag{3.57}$$

Here $\bar{Q}^s_i(\theta_1,\ldots,\theta_N)$ is the function Q^s_i in the sector with $2N$-particles and polarisation s evaluated for a symmetric rapidity distribution (so it refers to a particular subset of solutions of the Bethe-Yang equations for $2N$ particles)

$$\bar{Q}^s_i(\theta_1,\ldots,\theta_N) = Q^s_i(-\theta_1,\theta_1,\ldots,-\theta_N,\theta_N) \,, \quad i = 1,\ldots,N. \tag{3.58}$$

Expression (3.54) is obtained, following Ref. [161], by imposing that the expectation value of an arbitrary local operator $\mathcal{O}(x)$ (even under T) in the state $|\Psi_0\rangle_{\mathtt{a}}$ must reproduce the infinite-volume result up to exponentially small corrections in system size. Inserting resolutions of the identity in terms of the basis $\{|I_1,\ldots,I_N\rangle^s_{\mathrm{a}}\}$, and then using the analogue of relations (3.52) to compute the matrix elements, we obtain (3.54). A complication that arises compared to the case of diagonal scattering is that not every sector s allows parity symmetric rapidity distributions of the kind used in (3.54). Indeed, such solutions exist only if the transfer matrix eigenvalues fulfil the relation

$$\Lambda^s(-\theta_i|\{-\theta_k,\theta_k\}) = \Lambda^s(\theta_i|\{-\theta_k,\theta_k\})^{-1} \,. \tag{3.59}$$

How about sectors where (3.59) does not hold? It turns out that they do not contribute to the expansion of the boundary state. To see this, let us go back to the infinite volume, where we have [cf. (3.23)]

$$|\Psi_0\rangle = \sum_{N=0}^{\infty}\sum_{s=1}^{2^{2N}} \int_0^\infty \frac{d\theta_1}{2\pi}\cdots\int_{\theta_{N-1}}^\infty \frac{d\theta_N}{2\pi}\mathcal{K}^s_{2N}(\{\theta_k\})\,|-\theta_1,\theta_1,\ldots,-\theta_N,\theta_N\rangle^s \ . \tag{3.60}$$

In Appendix 3.B we demonstrate that

$$\mathcal{K}^s_{2N}(\{\theta_k\})\Lambda^s(-\theta_i|\{-\theta_k,\theta_k\}) = \mathcal{K}^s_{2N}(\{\theta_k\})\Lambda^s(\theta_i|\{-\theta_k,\theta_k\})^{-1} \,. \tag{3.61}$$

This implies that either (3.59) holds, in which case parity-symmetric solutions exist, or the coefficients $\mathcal{K}^s_{2N}(\{\theta_k\})$ must vanish, in which case the corresponding sector s does not contribute to the expansion of the boundary state.

3.4.2 Determination of the representative eigenstate

The final step required to set up our calculation of expectation values of local operators is to obtain an expression for the representative state. In Ref. [73] a method for constructing the representative state for a given $|\Psi_0\rangle$ via a generalized thermodynamic Bethe Ansatz [162] was presented. However, since in this case the overlaps between the initial state and the states of the basis (3.48) are not in a product form (*c.f.* (3.54)), here is more convenient to follow a different route. By definition $|\Phi\rangle_L$ is a finite-volume basis state (3.48), which fulfils the requirements that

$$\lim_{L\to\infty}\frac{1}{L}\frac{{}_L\langle\Phi|I(\alpha)_L|\Phi\rangle_L}{{}_L\langle\Phi|\Phi\rangle_L}=\lim_{L\to\infty}\frac{1}{L}\frac{{}_L\langle\Psi_0|I(\alpha)_L|\Psi_0\rangle_L}{{}_L\langle\Psi_0|\Psi_0\rangle_L}\,,\quad \alpha\geq 1\,. \tag{3.62}$$

As already pointed out in Ref. [73], one may use (3.62) to determine the root density $\rho_\Phi(\theta)$ specifying the representative state. Here the root density corresponding to a solution $\{\theta_1,\ldots,\theta_N\}$ of the Bethe-Yang equations such that $\theta_{j+1}-\theta_j=O(L^{-1})$ for large L is defined as

$$\rho(\theta_j)=\lim_{L\to\infty}\frac{1}{L(\theta_{j+1}-\theta_j)}\,. \tag{3.63}$$

Given the density $\rho_\Phi(\theta)$, a particular representative microstate can be constructed. It takes the form

$$|\Phi\rangle_L=|\{-\tilde{I}_1,\tilde{I}_1,\ldots,-\tilde{I}_N,\tilde{I}_N\}\rangle^{\tilde{s}}_{\rm NS}\equiv|\Phi_{\tilde{s}}\rangle_{\rm NS}\,, \tag{3.64}$$

where

- the number of rapidities N is given by $2N=\lceil\delta L\rceil$, where $\delta=\int_{\mathbb{R}}d\theta\rho_\Phi(\theta)$ is the total density of particles;
- we have chosen the state to occur in the NS sector;
- the set of integers $\{\tilde{I}_k\}$ is such that the corresponding root density is equal to $\rho_\Phi(\theta)$;
- the sector $\tilde{s}$ is chosen such that (3.59) holds, i.e. symmetric solutions of the Bethe-Yang solutions exist. Furthermore we require the topological charge to fulfil $Q(\tilde{s})=2m=\lceil qL\rceil+k$ where $k\in\mathbb{Z}$ fixed and q is the density of the expectation value of the topological charge in the initial state ($|q|\leq\delta$).

It turns out that in the regime we are working in (low densities) we do not require an explicit expression of q in terms of $K^{ab}(\theta)$ (our "initial" data), because at late times the leading contribution to the expectation value (3.1) does not depend on the value of q.

3.4.2.1 Calculation of the root density

We start by rewriting the conditions (3.62) in terms of the root density $\rho_\Phi(\theta)$

$$\lim_{L\to\infty}\frac{1}{L}\frac{{}_L\langle\Psi_0|I(\alpha)_L|\Psi_0\rangle_L}{{}_L\langle\Psi_0|\Psi_0\rangle_L}=\int_{-\infty}^{\infty}d\theta\,\rho_\Phi(\theta)i^{(\alpha)}(\theta)\,,\quad n=1,2,\dots\,, \tag{3.65}$$

where the functions $\{i^{(\alpha)}(\theta)\}$ parameterise the eigenvalues of the conservation laws $\{I(\alpha)_L\}$

$$I(\alpha)_L\,|\{I_1,\dots,I_N\}\rangle^s_{\mathtt{a}}=\left\{\sum_{i=1}^{N}i^{(\alpha)}(\theta_i)\right\}|\{I_1,\dots,I_N\}\rangle^s_{\mathtt{a}}\,. \tag{3.66}$$

Here $\{\theta_1,\dots,\theta_N\}$ is the solution of the Bethe-Yang equations in the sector s corresponding to the integers $I_1,\dots,I_N$. A set of local conservation laws for a lattice regularization of the sine-Gordon model is in principle known [163], one could use these charges to find a set of ultra-local and quasi-local conservation laws for the sine-Gordon following the procedure outlined in [139]. However, the charges [163] do not form a complete set [54–56] and one would have to include additional charges such those introduced in [93,164,165]. In any case, obtaining the root density from an explicit calculation of the expectation values of these conserved charges is a very challenging problem. Here we proceed in a different way. The idea is to use (3.65) in reverse: if the functions $i^{(\alpha)}$ form a complete set, we may determine $\rho_\Phi(\theta)$ from a known complete set of expectation values of conservation laws. Assuming this to be the case, the requirements (3.65) are equivalent to

$$\lim_{L\to\infty}\frac{1}{L}\frac{{}_L\langle\Psi_0|\hat{N}_\zeta|\Psi_0\rangle_L}{{}_L\langle\Psi_0|\Psi_0\rangle_L}=\int_{-\infty}^{\infty}d\theta\,\rho_\Phi(\theta)\zeta(\theta)\,, \tag{3.67}$$

where

$$\hat{N}_\zeta\,|\{I_1,\dots,I_N\}\rangle^s_{\mathtt{a}}=\left\{\sum_{i=1}^{N}\zeta(\theta_i)\right\}|\{I_1,\dots,I_N\}\rangle^s_{\mathtt{a}}\,, \tag{3.68}$$

and $\zeta(x)$ is an *arbitrary* function in the space spanned by the $i^{(\alpha)}(\theta)$. Our procedure essentially amounts to starting with the conserved "mode-occupation numbers" in the thermodynamic limit $I(\theta)=\sum_a Z_a^\dagger(\theta)Z_a(\theta)$. Given that the $I(\theta)$ are conserved, it follows that

$$\hat{N}_\zeta=\int d\theta\;\zeta(\theta)\;\sum_a Z_a^\dagger(\theta)Z_a(\theta) \tag{3.69}$$

are conserved as well. The idea is to find an appropriate finite volume regularization of these operators, which together with the arbitrariness of $\zeta(\theta)$ can be used to determine ρ_Φ from conditions (3.67).

It is convenient to express $\hat{N}_\zeta$ as

$$\hat{N}_\zeta \equiv \sum_{I\in\mathbb{Z}} \hat{n}_\zeta(I)\,, \tag{3.70}$$

where $\hat{n}_\zeta(I)$ acts on the basis (3.48) as follows

$$\hat{n}_\zeta(I)\,|\{I_1,\dots,I_N\}\rangle^s_{\mathtt{a}} = \left\{\sum_{i=1}^{N}\delta_{I_i,I+\kappa_{\mathtt{a}}}\zeta(\theta_i)\right\}|\{I_1,\dots,I_N\}\rangle^s_{\mathtt{a}}\,. \tag{3.71}$$

Here $\kappa_{\mathtt{a}}$ have been defined in (3.47). Using the form (3.53) for the initial state in the finite volume and fixing $I>0$ we obtain

$${}_L\langle\Psi_0|\hat{n}_\zeta(I)|\Psi_0\rangle_L = \frac{1}{2}\sum_{\mathtt{a}}\sum_{N'=1}^{\infty}\sum_{s=1}^{2^{N'}}\sum_{m=1}^{N'}\sum_{\{I_1,\dots,I_{N'}\}_I^m}\mathcal{N}^s_{2N'}(\{\theta_k\})^2|\mathcal{K}^s_{2N'}(\{\theta_k\})|^2\zeta(\theta_m)\,, \tag{3.72}$$

where $\{I_1,\dots,I_{N'}\}_I^m$ denotes the set $\{I_1,\dots,I_{N'}\}$ with I_m removed and the integers are ordered as

$$0<\underbrace{I_1<\cdots<I+\kappa_{\mathtt{a}}}_{m}<\cdots<I_{N'}\,. \tag{3.73}$$

The case $I<0$ is dealt with analogously. Our strategy is now to convert the sum

$$\frac{1}{L}\sum_{I\in\mathbb{Z}}\frac{{}_L\langle\Psi_0|\hat{n}_\zeta(I)|\Psi_0\rangle_L}{{}_L\langle\Psi_0|\Psi_0\rangle_L}\,, \tag{3.74}$$

into an integral in the thermodynamic limit, and then to use the arbitrariness of the function $\zeta(\theta)$ to determine $\rho_\Phi(\theta)$. In order for this to be possible we have to compute

$$\frac{{}_L\langle\Psi_0|\hat{n}_\zeta(I)|\Psi_0\rangle_L}{{}_L\langle\Psi_0|\Psi_0\rangle_L} \tag{3.75}$$

and show that is a function of I/L. The problem of calculating (3.75) exactly still presents a formidable task. We therefore restrict our attention to the case of "small" quenches in the sense of Refs. [44, 45, 88, 140], namely to cases where the densities of excitations of the post-quench Hamiltonian in the initial state are small. Then we may use $|K^{ab}(\theta)|$ as formal expansion parameters, and determine (3.75) by means of a linked-cluster expansion first introduced for

the finite-temperature case in Refs. [74]. We start by expanding the denominator in (3.75) as

$$\begin{aligned} {}_L\langle\Psi_0|\Psi_0\rangle_L &= 1+\sum_{n\geq 1}\Upsilon_{2N}\,, \\ \Upsilon_{2N} &\equiv \frac{1}{2}\sum_{\mathtt{a}}\sum_{s=1}^{2^{2N}}\sum_{0<I_1<\cdots<I_N}\mathcal{N}^s_{2N}(\{\theta_k\})^2|\mathcal{K}^s_{2N}(\{\theta_k\})|^2\,. \end{aligned} \tag{3.76}$$

The rapidities appearing in the expression for Υ_{2N} are solutions of the Bethe-Yang equations in the sector determined by N, s and $\mathtt{a}$. Denoting the contribution at order $2M$ in $|K^{ab}(\theta)|$ in (3.72) by $\mathcal{C}^{2M}_{\zeta,I}$, i.e.

$${}_L\langle\Psi_0|\hat{n}_\zeta(I)_\zeta|\Psi_0\rangle_L=\sum_{M\geq 1}\mathcal{C}^{2M}_{\zeta,I}\,, \tag{3.77}$$

we define *linked clusters* $\mathcal{D}^{2M}_{\zeta,I}$ recursively by

$$\mathcal{C}^{2M}_{\zeta,I}=\mathcal{D}^{2M}_{\zeta,I}+\sum_{N=1}^{M-1}\Upsilon_{2N}\mathcal{D}^{2(M-N)}_{\zeta,I}\,,\qquad M=1,2,\ldots \tag{3.78}$$

In terms of the linked clusters our quantity of interest reads

$$\frac{{}_L\langle\Psi_0|\hat{n}_\zeta(I)|\Psi_0\rangle_L}{{}_L\langle\Psi_0|\Psi_0\rangle_L}=\sum_{N\geq 1}\mathcal{D}^{2N}_{\zeta,I}\,. \tag{3.79}$$

Under the assumption that for small quenches (3.79) has a well-defined low-density expansion, the leading contribution is simply given by the first term in the series

$$\mathcal{D}^2_{\zeta,I}=\frac{1}{2}\sum_{\mathtt{a}}\sum_{s=1}^{2^2}\mathcal{N}^s_2\big(\theta^s_{\mathtt{a}}(I)\big)\,|\mathcal{K}^s_2\big(\theta^s_{\mathtt{a}}(I)\big)|^2\,\zeta\big(\theta^s_{\mathtt{a}}(I)\big)\,. \tag{3.80}$$

Here $\theta^s_{\mathtt{a}}(I)$ is the solution of the Bethe-Yang equations

$$\bar{Q}^s(\theta)=2\pi(I+\kappa_{\mathtt{a}}). \tag{3.81}$$

Up to finite-size corrections, the Bethe-Yang equations can be easily solved

$$\theta^s_{\mathtt{a}}(I)=\theta(I)+O(1/\ell)\;,\quad \theta(I)=\operatorname{arcsinh}\left(2\pi I/\ell\right). \tag{3.82}$$

Noting that $\mathcal{N}^s_2(\theta^s_{\mathtt{a}}(I))=1+O(1/\ell)\;\forall\, s\,,\mathtt{a}$, we have

$$\mathcal{D}^2_{\zeta,I}=\zeta\big(\theta(I)\big)\,G\big(\theta(I)\big)+O(1/\ell)\,, \tag{3.83}$$

where we introduced

$$G(\theta) \equiv \sum_{a,b=\pm} |K^{ab}(\theta)|^2 \,. \tag{3.84}$$

The result for the expectation value (3.74) is then

$$\frac{{}_L\langle\Psi_0|\hat{n}_\zeta(I)|\Psi_0\rangle_L}{{}_L\langle\Psi_0|\Psi_0\rangle_L} = \zeta\big(\theta(I)\big)G\big(\theta(I)\big) + O(K^4)\,. \tag{3.85}$$

The sum of this expression over all integers can be expressed as an integral using contour integration methods

$$\lim_{L\to\infty}\frac{1}{L}\frac{{}_L\langle\Psi_0|\hat{N}_\zeta|\Psi_0\rangle_L}{{}_L\langle\Psi_0|\Psi_0\rangle_L} \simeq \lim_{L\to\infty}\sum_I \oint_{\mathcal{C}_{\theta(I)}} \frac{d\eta}{2\pi}\frac{\Delta}{v}\cosh\eta\frac{G(\eta)\zeta(\eta)}{e^{i\ell\sinh\eta}-1}\,, \tag{3.86}$$

where the contour $\mathcal{C}_{\theta(I)}$ encircles $\theta(I)$. Since the integrand is analytic except for the residues at $\{\theta(I)\}$, we may join the paths $\mathcal{C}_{\theta(I)}$ and obtain a single contour $\mathcal{C}$ encircling the real axis

$$\begin{aligned}\lim_{L\to\infty}\frac{1}{L}\frac{{}_L\langle\Psi_0|\hat{N}_\zeta|\Psi_0\rangle_L}{{}_L\langle\Psi_0|\Psi_0\rangle_L} &\simeq \lim_{L\to\infty}\oint_{\mathcal{C}}\frac{d\theta}{2\pi}\frac{\Delta}{v}\cosh\theta\frac{G(\theta)\zeta(\theta)}{e^{i\ell\sinh\theta}-1}\\ &= \frac{\Delta}{v}\int_{-\infty}^{+\infty}\frac{d\theta}{2\pi}G(\theta)\,\zeta(\theta)\,\cosh\theta.\end{aligned} \tag{3.87}$$

In the last step we have used that the contribution from the path below the real axis is exponentially suppressed in ℓ, and will not contribute in the thermodynamic limit. Finally, equating (3.87) and (3.67) and then using the arbitrariness of $\zeta(\theta)$, we are able to find the root density $\rho_\Phi(\theta)$

$$\rho_\Phi(\theta) = \frac{\Delta}{2\pi v}G(\theta)\,\cosh\theta + O(K^4). \tag{3.88}$$

3.5 Time evolution of the expectation value

With an expression for the representative eigenstate in hand, we are now in a position to write the explicit Lehmann representation for the expectation value (3.1) and work out its time evolution. We focus on the first term on the right hand side of Eq. (3.1), as the other can be obtained by taking complex conjugation combined with the change $\beta \to -\beta$. The Lehmann

representation is given by

$$\frac{{}_{\rm R}\langle\Psi_0|e^{i\beta\Phi(t,x)/2}|\Phi_{\tilde{s}}\rangle_{\rm NS}}{{}_{\rm NS}\langle\Psi_0|\Phi_{\tilde{s}}\rangle_{\rm NS}} = \sum_{M\geq 1}\sum_{s=1}^{2^{2M}}\sum_{0<I_1<\cdots<I_M}\frac{\mathcal{N}^s_{2M}(\{\theta_k\})\mathcal{K}^s_{2M}(\{\theta_k\})}{\mathcal{N}^{\tilde{s}}_{2N}(\{\tilde{\theta}_k\})\mathcal{K}^{\tilde{s}}_{2N}(\{\tilde{\theta}_k\})}$$
$$\times\ {}^{s}_{\rm R}\langle\{I_M,-I_M,\ldots,I_1,-I_1\}|e^{i\beta\Phi(0,0)/2}|\{-\tilde{I}_1,\tilde{I}_1,\ldots,-\tilde{I}_N,\tilde{I}_N\}\rangle^{\tilde{s}}_{\rm NS}$$
$$\times\exp\left[2it\Delta\Big(\sum_{i=1}^{M}\cosh\theta_i-\sum_{i=1}^{N}\cosh\tilde{\theta}_i\Big)\right], \tag{3.89}$$

where $\{I_k\}$ and $\{\tilde{I}_k\}$ are respectively integers and half-odd integers, while the rapidities $\{\theta_k\}_{k=1,\ldots,M}$ and $\{\tilde{\theta}_k\}_{k=1,\ldots,N}$ are the corresponding solutions of the Bethe-Yang equations

$$\bar{Q}^s_i(\theta_1,\ldots,\theta_M)=2\pi I_i\,, \qquad i=1,\ldots,M\,, \tag{3.90}$$
$$\bar{Q}^{\tilde{s}}_j(\tilde{\theta}_1,\ldots,\tilde{\theta}_N)=2\pi\tilde{I}_j\,, \qquad j=1,\ldots,N\,. \tag{3.91}$$

As discussed before, both sectors $(2M,s,\mathrm{R})$ and $(2N,\tilde{s},\mathrm{NS})$ permit parity symmetric solutions. The matrix elements are related to infinite-volume form-factors by (3.52), which in the case of interest reads

$${}^{s}_{\rm R}\langle\{I_M,\ldots,-I_1\}|e^{i\beta\Phi(0,0)/2}|\{-\tilde{I}_1,\ldots,\tilde{I}_N\}\rangle^{\tilde{s}}_{\rm NS}=\frac{f^{\beta/2}(\theta_M,\ldots,-\theta_1|-\tilde{\theta}_1,\ldots,\tilde{\theta}_N)^s_{\tilde{s}}}{\sqrt{\rho^s_{2M}(-\theta_1,\ldots,\theta_M)\rho^{\tilde{s}}_{2N}(-\tilde{\theta}_1,\ldots,\tilde{\theta}_N)}}$$
$$+O(e^{-\mu' L})\,. \tag{3.92}$$

Using the crossing symmetry in the infinite-volume form-factors gives an expression of the form

$$f^{\beta/2}(\theta_M,\ldots,-\theta_1|-\tilde{\theta}_1,\ldots,\tilde{\theta}_N)^s_{\tilde{s}}=\sum_{\substack{a_1\ldots a_{2M}\\ b_1\ldots b_{2N}}}\Psi^{\tilde{s}}_{b_1\cdots b_{2N}}(\{\tilde{\theta}_k\})\Psi^{s}_{a_1\cdots a_{2M}}(\{\theta_k\})^*$$
$$\times f^{\beta/2}_{\bar{a}_{2M}\cdots\bar{a}_1,b_1\cdots b_{2N}}(\theta_M+i\pi,\cdots,-\theta_1+i\pi,-\tilde{\theta}_1,\ldots,\tilde{\theta}_N)$$
$$=f^{\beta/2}(\theta_M+i\pi,\ldots,-\theta_1+i\pi,-\tilde{\theta}_1,\ldots,\tilde{\theta}_N)_{s,\tilde{s}}\,. \tag{3.93}$$

In the following we will take into account only the contribution to (3.89) that arises from states with $N=M$ [73], as this represents the leading one. It is shown in Appendix 3.D that the contribution from states with $N=M$ dominates over those from states with $M>N$ at late times. The same conclusion holds also in the case of contributions from states with $M<N$ and can be proven analogously.

3.5.1 Contributions from states with $M = N$

Retaining only states with $M = N$ we have

$$\frac{{}_{\rm R}\langle\Psi_0|e^{i\beta\Phi(t,x)/2}|\Phi_{\tilde{s}}\rangle_{\rm NS}}{{}_{\rm NS}\langle\Psi_0|\Phi_{\tilde{s}}\rangle_{\rm NS}} \approx \sum_{s=1}^{2^{2N}} \sum_{0<I_1<\cdots<I_N} \frac{\bar{\rho}_N^{\tilde{s}}(\tilde{\theta}_1,\ldots,\tilde{\theta}_N)}{\bar{\rho}_N^{s}(\theta_1,\ldots,\theta_N)\rho_{2N}^{\tilde{s}}(-\tilde{\theta}_1,\ldots,\tilde{\theta}_N)} \frac{\mathcal{K}_{2N}^{s}(\{\theta_k\})}{\mathcal{K}_{2N}^{\tilde{s}}(\{\tilde{\theta}_k\})} \times e^{2i\Delta t\sum_{i=1}^{N}[\cosh\theta_i-\cosh\tilde{\theta}_i]} f^{\beta/2}(\theta_N+i\pi,\ldots,\tilde{\theta}_N)_{s,\tilde{s}}\,. \tag{3.94}$$

Following the method introduced by Pozsgay and Takacs in [166], we rewrite each term in (3.94) as an integral on an appropriate multi-contour $\mathcal{C}$ in $\mathbb{C}^N$ by means of the multidimensional residue calculus

$$\frac{{}_{\rm R}\langle\Psi_0|e^{i\beta\Phi(t,x)/2}|\Phi_{\tilde{s}}\rangle_{\rm NS}}{{}_{\rm NS}\langle\Psi_0|\Phi_{\tilde{s}}\rangle_{\rm NS}} \approx \sum_{s=1}^{2^{2N}} \sum_{0<I_1<\cdots<I_N} \oint_{\mathcal{C}_{\{\theta_\ell\}}} \prod_{k=1}^{N}\frac{d\eta_k}{2\pi} \frac{\bar{\rho}_N^{\tilde{s}}(\tilde{\theta}_1,\ldots,\tilde{\theta}_N)}{\rho_{2N}^{\tilde{s}}(-\tilde{\theta}_1,\ldots,\tilde{\theta}_N)} \frac{\mathcal{K}_{2N}^{s}(\{\eta_k\})}{\mathcal{K}_{2N}^{\tilde{s}}(\{\tilde{\theta}_k\})} \times e^{2i\Delta t\sum_{i=1}^{N}[\cosh\eta_i-\cosh\tilde{\theta}_i]} \frac{f^{\beta/2}(\eta_N+i\pi,\ldots,\tilde{\theta}_N)_{s,\tilde{s}}}{\prod_{k=1}^{N}\left\{e^{i\bar{Q}_k^s(\{\eta_k\})}-1\right\}}\,. \tag{3.95}$$

Here $\mathcal{C}_{\{\theta_\ell\}} = \mathcal{C}_{\theta_1}\otimes\cdots\otimes\mathcal{C}_{\theta_N}$, where the contour $\mathcal{C}_{\theta_i}$ encircles the rapidity θ_i, i.e. the i-th rapidity in the solution $\{\theta_k\}$ of the Bethe-Yang equations in the sector $(2N,\, s,\, \mathrm{R})$. We now wish to express the multiple summations in (3.95) in terms of appropriately defined contour integrals. In the case of a single variable this is straightforward, see Fig. 3.1 for a simple example. Let $f(\eta)$ be a meromorphic function with simple poles at the points $\eta = \theta_j$, and C_{θ_j} a very small contour encircling θ_j. Residue calculus then gives

$$\sum_j \oint_{\mathcal{C}_{\theta_j}} \frac{d\eta}{2\pi} f(\eta) = \oint_{\mathcal{C}_{\rm tot}} \frac{d\eta}{2\pi} f(\eta) - \sum_{i=1}^{N_{\mathcal{R}}} \oint_{\mathcal{C}_{\tilde{\theta}_i}} \frac{d\eta}{2\pi} f(\eta) \tag{3.96}$$

where $\mathcal{C}_{\rm tot}$ is a contour encircling the region $\mathcal{R}$, which contains all points θ_j as well as simple poles of $f(\eta)$ at positions $\tilde{\theta}_1,\ldots,\tilde{\theta}_{N_{\mathcal{R}}}$.

The case of N integration variables $\eta_1,\ldots,\eta_N$ is more involved. Our function of interest is

$$G^{(s,\tilde{s})}(\{\eta_k\}) \equiv \frac{\bar{\rho}_N^{\tilde{s}}(\tilde{\theta}_1,\ldots,\tilde{\theta}_N)}{\rho_{2N}^{\tilde{s}}(-\tilde{\theta}_1,\ldots,\tilde{\theta}_N)} \frac{\mathcal{K}_{2N}^{s}(\{\eta_k\})}{\mathcal{K}_{2N}^{\tilde{s}}(\{\tilde{\theta}_k\})} \times \frac{f^{\beta/2}(\eta_N+i\pi,\ldots,\tilde{\theta}_N)_{s,\tilde{s}}}{\prod_{k=1}^{N}\left\{e^{i\bar{Q}_k^s(\{\eta_k\})}-1\right\}} e^{2i\Delta t\sum_{i=1}^{N}[\cosh\eta_i-\cosh\tilde{\theta}_i]}\,. \tag{3.97}$$

We first consider a contour $\mathcal{C}_{\rm tot}$, which is the N-fold tensor product $\mathcal{C}(\mathbb{R}^+)\otimes\ldots\otimes\mathcal{C}(\mathbb{R}^+)$, where $\mathcal{C}(\mathbb{R}^+)$ is a contour encircling $\mathbb{R}^+$. Introducing $\mathcal{C}_{\tilde{\theta}_i}$ as the contour encircling $\tilde{\theta}_i$, we can express

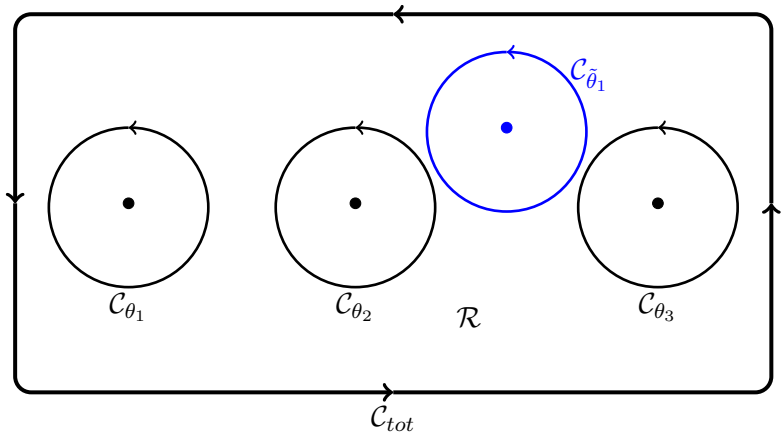

Figure 3.1: Example of the contours in the one-variable case.

$\mathcal{C}_{\rm tot}$ in the form

$$\mathcal{C}_{\rm tot} = \mathcal{G} \otimes \ldots \otimes \mathcal{G} - \sum_{m=1}^{N} (-1)^m \sum_{1 \le j_1 < \cdots < j_m \le N} \sum_{i_1, \cdots, i_m = 1}^{N} \mathcal{C}_{i_1, \cdots, i_m}^{j_1, \cdots, j_m} \,, \tag{3.98}$$

where $\mathcal{G}$ is defined as

$$\mathcal{G} \equiv \mathcal{C}(\mathbb{R}^+) - \sum_{i=1}^{N} \mathcal{C}_{\tilde{\theta}_i} \,, \tag{3.99}$$

and $\mathcal{C}_{i_1, \cdots, i_m}^{j_1, \cdots, j_m}$ is defined as the multi-contour obtained from $\mathcal{C}_{\rm tot}$ by replacing the components $j_1, \cdots, j_m$ in the tensor product by $\mathcal{C}_{\tilde{\theta}_{i_1}}, \cdots, \mathcal{C}_{\tilde{\theta}_{i_m}}$, i.e.

$$\begin{aligned} \mathcal{C}_{i_1, \cdots, i_m}^{j_1, \cdots, j_m} = {} & \otimes_{j=1}^{j_1 - 1} \mathcal{C}(\mathbb{R}^+) \otimes \mathcal{C}_{\tilde{\theta}_{i_1}} \otimes_{j=j_1+1}^{j_2 - 1} \mathcal{C}(\mathbb{R}^+) \otimes \mathcal{C}_{\tilde{\theta}_{i_2}} \otimes_{j=j_2+1}^{j_3 - 1} \mathcal{C}(\mathbb{R}^+) \otimes \ldots \\ & \ldots \otimes_{j=j_{m-1}+1}^{j_m - 1} \mathcal{C}(\mathbb{R}^+) \otimes \mathcal{C}_{\tilde{\theta}_{i_m}} \otimes_{j=j_m+1}^{N} \mathcal{C}(\mathbb{R}^+). \end{aligned} \tag{3.100}$$

We may use (3.98) to rewrite the integral of $G^{(s,\tilde{s})}$ over the multi-contour $\mathcal{C}_{\rm tot}$ as

$$\begin{aligned} \oint_{\mathcal{C}_{\rm tot}} \prod_{i=1}^{N} \frac{d\eta_i}{2\pi} G^{(s,\tilde{s})}(\{\eta_k\}) = {} & \oint_{\mathcal{G} \otimes \cdots \otimes \mathcal{G}} \prod_{i=1}^{N} \frac{d\eta_i}{2\pi} G^{(s,\tilde{s})}(\{\eta_k\}) \\ & - \sum_{m=1}^{N} (-1)^m \sum_{1 \le j_1 < \cdots < j_m \le N} \sum_{\{i_k\}=1}^{N} \oint_{\mathcal{C}_{i_1, \cdots, i_m}^{j_1, \cdots, j_m}} \prod_{i=1}^{N} \frac{d\eta_i}{2\pi} G^{(s,\tilde{s})}(\{\eta_k\}) \,. \end{aligned} \tag{3.101}$$

Let us now focus on the first term in the right-hand side of (3.101). As the singularities of the form-factor $f^{\beta/2}$ lie outside the contour $\mathcal{G} \otimes \cdots \otimes \mathcal{G}$ and all other functions are expected to be well behaved, the only contributions to the integral arise from the regions characterized by

$$e^{i \bar{Q}_k^{\tilde{s}}(\eta_1, \ldots, \eta_N)} - 1 \approx 0 \,, \qquad k = 1, \ldots, N \,. \tag{3.102}$$

By choosing $\mathcal{C}(\mathbb{R}^+)$ sufficiently close to the real axis, we can ensure that (3.102) is fulfilled only when $\{\eta_k\}$ is a real solution of the Bethe-Yang equations in the sector $(2N,\, s,\, \mathrm{R})$ for some set $\{I_k\}$. We can ensure that *all* solutions to the Bethe-Yang equations in the sector $(2N,\, s,\, \mathrm{R})$ are enclosed in $\mathcal{G}\otimes\cdots\otimes\mathcal{G}$ by choosing the contours $\mathcal{C}_{\tilde{\theta}_i}$ to be sufficiently close to $\tilde{\theta}_i$, because $\{\tilde{\theta}_k\}$ is a solution of the Bethe-Yang equations in the NS sector and therefore cannot be arbitrarily close to any solution in the R sector. This allows us to conclude that

$$\oint\limits_{\mathcal{G}\otimes\cdots\otimes\mathcal{G}} \prod_{i=1}^{N}\frac{d\eta_i}{2\pi}G^{(s,\tilde{s})}(\eta_1,\ldots,\eta_N) = \sum_{I_1\ldots,I_N}\oint\limits_{\mathcal{C}_{\{\theta_\ell\}}} \prod_{i=1}^{N}\frac{d\eta_i}{2\pi}G^{(s,\tilde{s})}(\eta_1,\ldots,\eta_N)\,. \tag{3.103}$$

Let us now turn to the contributions with $m = N$ on the right-hand side of Eq. (3.101). For these the relevant multi-contours are of the form

$$\mathcal{C}_{\tilde{\theta}_{\sigma(1)}}\otimes\cdots\otimes\mathcal{C}_{\tilde{\theta}_{\sigma(N)}}\,, \tag{3.104}$$

where $\sigma\in\mathcal{S}_N$ is a permutation. Exploiting again the fact that $\{\tilde{\theta}_k\}$ is a solution of the Bethe-Yang equations in the NS sector, we may conclude that for contours $\mathcal{C}_{\tilde{\theta}_i}$ sufficiently close to the points $\tilde{\theta}_i$ we have for any point $\eta_1,\ldots\eta_N$ inside the multi-contour

$$e^{i\bar{Q}_k^{\tilde{s}}(\eta_1,\ldots,\eta_N)}-1\neq 0\,,\qquad \forall\, k\,. \tag{3.105}$$

Hence the only contributions to the integral arise from the annihilation poles of the form-factor $f^{\beta/2}$. These considerations will be very useful in the following.

Substituting (3.103) into (3.101) we obtain the desired N-variable generalisation of (3.96)

$$\begin{aligned}\sum_{I_1\ldots,I_N}\oint\limits_{\mathcal{C}_{\{\theta_\ell\}}} \prod_{i=1}^{N}\frac{d\eta_i}{2\pi}G^{(s,\tilde{s})}(\{\eta_k\}) &= \oint\limits_{\mathcal{C}_{\mathrm{tot}}} \prod_{i=1}^{N}\frac{d\eta_i}{2\pi}G^{(s,\tilde{s})}(\{\eta_k\})\\ &+\sum_{m=1}^{N}(-1)^m\sum_{1\leq j_1<\cdots<j_m\leq N}\sum_{\{i_k\}=1}^{N}\oint\limits_{\mathcal{C}_{i_1,\cdots,i_m}^{j_1,\cdots,j_m}}\prod_{i=1}^{N}\frac{d\eta_i}{2\pi}G^{(s,\tilde{s})}(\{\eta_k\})\,.\end{aligned} \tag{3.106}$$

In order to deal with Eq. (3.95) we require one more step: since in (3.95) we are considering a fixed order of integers $\{I_k\}$, the corresponding solutions of the Bethe-Yang equations must satisfy $0<\theta_1<\cdots<\theta_N$. In order to accommodate this ordering of rapidities we need to modify our multi-contours such that the i-th component depends on the variable z_{i+1}. For

example, the integral on $\mathcal{C}_{\rm tot}$ changes to

$$\oint_{\mathcal{D}} \frac{dz_N}{2\pi} \oint_{\mathcal{D}(z_N)} \frac{dz_{N-1}}{2\pi} \cdots \oint_{\mathcal{D}(z_2)} \frac{dz_1}{2\pi} f(z_1,\ldots,z_N) \equiv \oint_{\bar{\mathcal{C}}_{\rm tot}} \prod_{i=1}^{N} \frac{dz_i}{2\pi} f(z_1,\ldots,z_N)\,, \tag{3.107}$$

where the contour $\mathcal{D}(z_N)$ encircles the interval $[0, \mathfrak{Re} z_N)$. Reduced multi-contours $\bar{\mathcal{C}}^{j_1,\cdots,j_m}_{i_1,\cdots,i_m}$ are defined in a way analogous to $\mathcal{C}^{j_1,\cdots,j_m}_{i_1,\cdots,i_m}$, but include additional constraints ensuring the ordering $\mathfrak{Re}(z_N) > \mathfrak{Re}(z_{N-1}) > \ldots > \mathfrak{Re}(z_1)$. We may now use these considerations to turn the sums in (3.95) into integrals over appropriate multi-contours in the form

$$\begin{aligned}\frac{{}_{\rm R}\langle\Psi_0|e^{i\beta\Phi(t,x)/2}|\Phi_{\tilde{s}}\rangle_{\rm NS}}{{}_{\rm NS}\langle\Psi_0|\Phi_{\tilde{s}}\rangle_{\rm NS}} \approx & \sum_s \oint_{\bar{\mathcal{C}}_{\rm tot}} \prod_{i=1}^{N} \frac{d\eta_i}{2\pi} G^{(s,\tilde{s})}(\{\eta_k\}) \\ & + \sum_s \sum_{m=1}^{N-1} (-1)^m \sum_{1\le j_1<\cdots<j_m\le N} \sum_{\{i_k\}=1}^{N} \oint_{\bar{\mathcal{C}}^{j_1,\cdots,j_m}_{i_1,\cdots,i_m}} \prod_{i=1}^{N} \frac{d\eta_i}{2\pi} G^{(s,\tilde{s})}(\{\eta_k\}) \\ & + (-1)^N \sum_s \oint_{\mathcal{C}_{\tilde{\theta}_1}\otimes\cdots\otimes\mathcal{C}_{\tilde{\theta}_N}} \prod_{i=1}^{N} \frac{d\eta_i}{2\pi} G^{(s,\tilde{s})}(\{\eta_k\})\,. \end{aligned} \tag{3.108}$$

The crucial simplification occurring at this stage is that in the thermodynamic limit $L\to\infty$ and at late times we need to retain only the last term, as it features the most singular contribution, which occurs when[1]

$$\eta_j \approx \tilde{\theta}_j\ , \qquad\qquad j = 1,\ldots N. \tag{3.109}$$

As we have argued above, the only singularities we need to consider in the last term of (3.108) are those arising from the form-factor. The *leading* singularities of the form-factors can be calculated using the annihilation pole axiom, see Appendix 3.E, and give

$$\begin{aligned} f^{\beta/2}(\eta_N+i\pi,-\eta_N+i\pi,\ldots,-\tilde{\theta}_N,\tilde{\theta}_N)_{s,\tilde{s}}\Big|_{\tilde{\theta}_j\approx\eta_j} = & \mathcal{G}_{\beta/2}\delta_{\tilde{s},s} \prod_{i=1}^{N} \frac{4}{(\eta_i-\tilde{\theta}_i)^2} \\ & + \text{less singular.} \end{aligned} \tag{3.110}$$

An explicit expression for the vacuum expectation value $\mathcal{G}_{\beta/2} \equiv \langle 0|e^{i\beta\Phi/2}|0\rangle$ is given in Ref. [133]. Substituting the expression (3.110) into the last term on the right-hand side of Eq. (3.108) gives

[1] This can be argued using an argument similar to the one employed in Appendix 3.D.

the leading contribution at late times. Carrying out the contour integrals we obtain

$$\frac{{}_{\rm R}\langle\Psi_0|e^{i\beta\Phi(t,x)/2}|\Phi_{\tilde{s}}\rangle_{\rm NS}}{{}_{\rm NS}\langle\Psi_0|\Phi_{\tilde{s}}\rangle_{\rm NS}} \approx (-4i)^N \mathcal{G}_{\beta/2} \frac{\bar{\rho}_N^{\tilde{s}}(\tilde{\theta}_1,\ldots,\tilde{\theta}_N)}{\rho_{2N}^{\tilde{s}}(-\tilde{\theta}_1,\ldots,\tilde{\theta}_N)} \times \partial_{\eta_1}\Big|_{\eta_1=\tilde{\theta}_1} \cdots \partial_{\eta_N}\Big|_{\eta_N=\tilde{\theta}_N} \prod_{i=1}^N \frac{e^{2i\Delta t[\cosh\eta_i-\cosh\tilde{\theta}_i]}}{e^{i\bar{Q}_i^{\tilde{s}}(\{\eta_k\})}-1} + \ldots \tag{3.111}$$

The derivatives can be computed in leading order in the density δ using that $\partial_j \bar{Q}_j^{\tilde{s}} = O(\ell)$, while $\partial_j \bar{Q}_i^{\tilde{s}} = O(1)$ (see Appendix 3.C)

$$\partial_{\eta_1}\Big|_{\eta_1=\tilde{\theta}_1} \cdots \partial_{\eta_N}\Big|_{\eta_N=\tilde{\theta}_N} \prod_{i=1}^N \frac{e^{2i\Delta t[\cosh\eta_i-\cosh\tilde{\theta}_i]}}{e^{i\bar{Q}_i^{\tilde{s}}(\{\eta_k\})}-1} = \left(\frac{i}{4}\right)^N \prod_{i=1}^N \left\{\partial_i \bar{Q}_i^{\tilde{s}}(\{\tilde{\theta}_k\}) - 4\Delta t \sinh\tilde{\theta}_i\right\} + \text{higher order in } \delta. \tag{3.112}$$

Here we have used that

$$e^{i\bar{Q}_i^{\tilde{s}}(\{\tilde{\theta}_k\})} = -1. \tag{3.113}$$

The densities of states $\bar{\rho}_N^{\tilde{s}}$ and $\rho_{2N}^{\tilde{s}}$ are defined in terms of partial derivatives of the functions $\bar{Q}_j^{\tilde{s}}$ and $Q_j^{\tilde{s}}$, see Eqs. (3.57) and (3.30); their ratio can be calculated to leading order in the density δ by using the results derived in Appendix 3.C as well

$$\frac{\bar{\rho}_N^{\tilde{s}}(\tilde{\theta}_1,\ldots,\tilde{\theta}_N)}{\rho_{2N}^{\tilde{s}}(-\tilde{\theta}_1,\ldots,\tilde{\theta}_N)} = \prod_{i=1}^N \frac{1}{\partial_i \bar{Q}_i^{\tilde{s}}(\tilde{\theta}_1,\ldots,\tilde{\theta}_N)} + \text{higher order in } \delta. \tag{3.114}$$

Putting everything together, we obtain

$$\begin{aligned}\frac{{}_{\rm R}\langle\Psi_0|e^{i\beta\Phi(t,x)/2}|\Phi_{\tilde{s}}\rangle_{\rm NS}}{{}_{\rm NS}\langle\Psi_0|\Phi_{\tilde{s}}\rangle_{\rm NS}} &\approx \mathcal{G}_{\beta/2} \prod_{i=1}^N \left\{1 - \frac{4\Delta t\sinh\tilde{\theta}_i}{\partial_i \bar{Q}_i^{\tilde{s}}(\{\tilde{\theta}_k\})}\right\} + \ldots \\ &= \mathcal{G}_{\beta/2} \exp\left[\sum_{i=1}^N \log\left(1 - \frac{4\Delta t\sinh\tilde{\theta}_i}{\partial_i \bar{Q}_i^{\tilde{s}}(\{\tilde{\theta}_k\})}\right)\right] + \ldots\end{aligned} \tag{3.115}$$

Since $\partial_i \bar{Q}_i^{\tilde{s}}(\{\tilde{\theta}_k\}) = O(\ell) \gg \Delta t$, we may expand the logarithm

$$\sum_{i=1}^N \log\left(1 - \frac{4\Delta t\sinh\tilde{\theta}_i}{\partial_i \bar{Q}_i^{\tilde{s}}(\tilde{\theta}_1,\ldots,\tilde{\theta}_N)}\right) = -\frac{4vt}{L}\left\{\sum_{i=1}^N \tanh\tilde{\theta}_i\right\} + \ldots, \tag{3.116}$$

where we used

$$\frac{4\Delta t\sinh\tilde{\theta}_i}{\partial_i \bar{Q}_i^{\tilde{s}}(\{\tilde{\theta}_k\})} = \frac{4\Delta t}{\ell}\tanh\tilde{\theta}_i + \text{higher order in } \delta. \tag{3.117}$$

Finally, we convert the sum over $\tilde{\theta}_j$ into an integral in the $L \to \infty$ limit

$$\begin{aligned}\lim_{L\to\infty} \frac{{}_{\rm R}\langle\Psi_0|e^{i\beta\Phi(t,x)/2}|\Phi_{\tilde{s}}\rangle_{\rm NS}}{{}_{\rm NS}\langle\Psi_0|\Phi_{\tilde{s}}\rangle_{\rm NS}} &\approx \lim_{L\to\infty} \mathcal{G}_{\beta/2} \exp\left[-\frac{4vt}{L}\sum_{i=1}^{N}\tanh\tilde{\theta}_i\right] + \dots \\ &= \mathcal{G}_{\beta/2}\exp\left[-4vt\int_0^\infty d\theta\ \rho_\Phi(\theta)\ \tanh\theta\right] + \dots \\ &= \mathcal{G}_{\beta/2} e^{-t/\tau} + \dots \end{aligned} \tag{3.118}$$

The decay time τ defined in this way is given by

$$\tau^{-1} \equiv \frac{2\Delta}{\pi}\int_0^\infty d\theta\ \left[G(\theta)\sinh\theta + O(K^4)\right]\ . \tag{3.119}$$

Using $\mathcal{G}_a = \mathcal{G}_{-a} = \mathcal{G}_a^*$, we obtain our final result for the time evolution of the one-point function in the thermodynamic limit at late times $\Delta t \gg 1$, and in the low-density limit $\delta \ll 1$

$$\lim_{L\to\infty} \frac{{}_L\langle\Psi_0|e^{i\beta\Phi(t,x)/2}|\Psi_0\rangle_L}{{}_L\langle\Psi_0|\Psi_0\rangle_L} = \mathcal{G}_{\beta/2} e^{-t/\tau} + \dots\ . \tag{3.120}$$

In [1] we compared the result of this calculation with the one obtained by means of a different method: a generalisation of the linked cluster expansion approach first developed for studying finite-temperature dynamics in integrable models [74, 166] and then applied to the TFIM both on the lattice [44, 88] and in the continuum limit [140]. In essence this method consists in constructing a well defined series expansion for the expectation value (3.7) in powers of $K^{ab}(\theta)$; the calculation for the case in exam is extremely involved, however in [1] we managed to find the long-time leading contribution at order $O(K^4)$, using the simplifying assumption of the absence of diagonal terms in the $K^{ab}(\theta)$ matrix, *i.e.* $K^{aa}(\theta) = 0$. The result reads as

$$\frac{\langle\Psi_0|e^{i\beta\Phi(t,x)/2}|\Psi_0\rangle}{\langle\Psi_0|\Psi_0\rangle} = \mathcal{G}_{\beta/2}\left[1 - \frac{t}{\tau} + \frac{1}{2}\left(\frac{t}{\tau}\right)^2 + \dots\right] = \mathcal{G}_{\beta/2} e^{-t/\tau}\left(1 + \dots\right)\ , \tag{3.121}$$

where τ is the one given in (3.119). As we emphasised in the second step of (3.121), the result of the linked cluster expansion approach is compatible with (3.120) up to the order considered, this represents a significant confirmation of (3.120). It is very important to stress that the linked cluster approach *does not rely* on Equation (3.1), thus, the observed agreement represents a further evidence in favour of the findings of [73]. We conclude by noting that, very recently, the result (3.120) has also been confirmed via a semiclassical calculation [167].

3.6 Summary and Conclusions

In this chapter we have considered the time evolution of the semi-local operator $e^{i\beta\Phi/2}$ after an "integrable" quench to the sine-Gordon model. The system was assumed to be initialised in a state of the form

$$|\Psi_0\rangle = \exp\left(\int_0^\infty \frac{d\theta}{2\pi} K^{ab}(\theta) Z_a^\dagger(-\theta) Z_b^\dagger(\theta)\right)|0\rangle, \tag{3.122}$$

with $K^{ab}(\theta)$ satisfying (3.9) and (3.10); we focussed on the behaviour of the expectation value $\langle\Psi_0|e^{\mathrm{i}\beta\Phi(t)/2}|\Psi_0\rangle/\langle\Psi_0|\Psi_0\rangle$ at late times after the quench and developed a novel method to evaluate this expectation value for the case of a "small" quench, defined as involving small densities of excitations of the post-quench Hamiltonian. The approach is based on the concept of a *representative state* [73]. Our main result is that in the thermodynamic limit at late times $\Delta t \gg 1$, and for low densities $\delta \ll 1$

$$\frac{\langle\Psi_0|e^{i\beta\Phi(x,t)/2}|\Psi_0\rangle}{\langle\Psi_0|\Psi_0\rangle} = \mathcal{G}_{\beta/2} e^{-t/\tau} + \ldots, \tag{3.123}$$

where the decay time τ is given in Eq. (3.119). We note that exponential decay has also been observed in numerical simulations [168, 169] of the staggered magnetisation after interaction quenches in the XXZ Heisenberg chain.

To the best of our knowledge this calculation, first reported in [1], provided the first successful analytic calculation of the time dependence of a local observable for a quench to an *interacting* integrable model. In order to be able to carry out our calculations we required several simplifying assumptions:

1. the initial state was taken to be of the form (3.122);
2. we required the functions $K^{ab}(\theta)$ to be uniformly small, which corresponds to the limit of low densities of excitations after the quench;
3. we focussed on the simplest semi-local operator $e^{i\beta\Phi/2}$;
4. we considered the repulsive regime of the sine-Gordon model;
5. the time t was taken to be large.

It clearly would be interesting to go beyond these restrictions. The treatment of more general vertex operators of the form $e^{i\alpha\Phi}$ appears possible, although the results showed in Section 6 of [1] demonstrate that for the local operator $e^{i\beta\Phi}$ the leading term in the linked-cluster

expansion vanishes and thus an analysis of higher orders is necessary. Similarly we believe that the method presented here can be applied with relatively minor extensions to the attractive regime of the sine-Gordon model. To dispense with our other assumptions appears significantly more difficult. Going beyond the leading term in the low-density approximation has proved possible but complicated for the much simpler case of the transverse field Ising chain [44,73,140]. To do the same for the sine-Gordon case appears to be a daunting task. Detailed properties of the solutions of the Bethe-Yang equation entering the Lehmann representation (3.89) will now play a role. Finally, initial states of the form (3.122) are clearly rather special [153]. It is not generally known how to express the initial state in terms of Hamiltonian eigenstates after quenching a system parameter. Given the difficulty of this problem, a more fruitful avenue of research would be to consider special initial states characterised by low entanglement [53–55].

Appendix

3.A Hamiltonian eigenstates in the finite volume and the quantum inverse scattering method

In this appendix we summarize some elements of the quantum inverse scattering method [81], which are used to construct Hamiltonian eigenstates in a large, finite volume [155]. We define a *monodromy matrix* by

$$\mathcal{M}_{ab}(\lambda|\{\theta_k\})^{j_1\dots j_N}_{i_1\dots i_N} = S^{c_1 j_1}_{a\ i_1}(\lambda-\theta_1)\cdots S^{b\ j_N}_{c_{N-1} i_N}(\lambda-\theta_N)\,. \tag{3.124}$$

It can be written as a 2×2 matrix

$$\mathcal{M}(\lambda|\{\theta_k\}) = \begin{pmatrix} \mathcal{A}(\lambda|\{\theta_k\}) & \mathcal{B}(\lambda|\{\theta_k\}) \\ \mathcal{C}(\lambda|\{\theta_k\}) & \mathcal{D}(\lambda|\{\theta_k\}) \end{pmatrix}, \tag{3.125}$$

where $\mathcal{A}(\lambda|\{\theta_k\})$, $\mathcal{B}(\lambda|\{\theta_k\})$, $\mathcal{C}(\lambda|\{\theta_k\})$, $\mathcal{D}(\lambda|\{\theta_k\})$ are operators acting on the 2^N dimensional space of scattering states with N particles and fixed rapidities

$$\mathcal{M}_{ab}(\lambda|\{\theta_k\})\,|\theta_1,\cdots,\theta_N\rangle_{i_1\dots i_N} = \mathcal{M}_{ab}(\lambda|\{\theta_k\})^{i_1\dots i_N}_{j_1\dots j_N}\,|\theta_1,\cdots,\theta_N\rangle_{j_1\dots j_N}\,. \tag{3.126}$$

The rapidities θ_j play the roles of inhomogeneities [81] in the monodromy matrix. The *transfer matrix* is the trace of the monodromy matrix

$$\mathcal{T}(\lambda|\{\theta_k\}) = \sum_a \mathcal{M}_{aa}(\lambda|\{\theta_k\}) = \mathcal{A}(\lambda|\{\theta_k\}) + \mathcal{D}(\lambda|\{\theta_k\}), \tag{3.127}$$

As a consequence of the S-matrix being a solution of the Yang-Baxter equation, the monodromy matrices fulfil the relation

$$\begin{aligned} S^{b_1 b_2}_{c_1 c_2}(\lambda-\mu)\mathcal{M}_{a_1 b_1}(\lambda|\{\theta_k\})\mathcal{M}_{a_2 b_2}(\mu|\{\theta_k\}) = \\ = \mathcal{M}_{d_1 c_1}(\lambda|\{\theta_k\})\mathcal{M}_{d_2 c_2}(\mu|\{\theta_k\})S^{d_1 d_2}_{a_1 a_2}(\lambda-\mu), \end{aligned} \tag{3.128}$$

which implies that the transfer matrices form a commuting family

$$\big[\mathcal{T}(\lambda|\{\theta_k\}),\mathcal{T}(\mu|\{\theta_k\})\big] = 0. \tag{3.129}$$

Simultaneous eigenstates of all transfer matrices can be constructed by algebraic Bethe Ansatz. Starting point is the "reference state"

$$\Omega(\{\theta_k\}) = |\theta_1, \ldots, \theta_N\rangle_{+\cdots+} \,. \tag{3.130}$$

Using the definition of the monodromy matrix, we have

$$\mathcal{M}(\lambda|\{\theta_k\})\Omega(\{\theta_k\}) = \begin{pmatrix} a(\lambda|\{\theta_k\}) & * \\ 0 & d(\lambda|\{\theta_k\}) \end{pmatrix} \Omega(\{\theta_k\}) \,, \tag{3.131}$$

where $*$ denotes a non-zero entry not needed in the following, and

$$a(\lambda|\{\theta_k\}) = \prod_{k=1}^{N} S_0(\lambda - \theta_k) \,, \qquad d(\lambda|\{\theta_k\}) = \prod_{k=1}^{N} S_T(\lambda - \theta_k) \prod_{k=1}^{N} S_0(\lambda - \theta_k) \,. \tag{3.132}$$

Here $S_T(\theta)$ is defined in (2.60). Taking the trace in (3.131) we see that $\Omega(\{\theta_k\})$ is in fact a transfer matrix eigenstate

$$\mathcal{T}(\lambda|\{\theta_k\})\Omega(\{\theta_k\}) = \Big[a(\lambda|\{\theta_k\}) + d(\lambda|\{\theta_k\})\Big]\Omega(\{\theta_k\}). \tag{3.133}$$

The other eigenvectors of the transfer matrix can be constructed by the Ansatz

$$\Psi(\{\lambda_k\}|\{\theta_k\}) = \left[\prod_{j=1}^{r} \mathcal{B}(\lambda_j + \tfrac{i\pi}{2}|\{\theta_k\})\right] \Omega(\{\theta_k\}) \;, \quad 0 \le r \le \frac{N}{2}. \tag{3.134}$$

This gives simultaneous eigenvectors of the transfer matrix and the solitonic charge operator Q with a positive eigenvalue of Q; *cf.* Subsection 3.A.2. States with negative eigenvalues of Q can be obtained acting with the charge conjugation operator C on (3.134). Using the commutation relations for $\mathcal{A}(\lambda|\{\theta_k\}), \mathcal{B}(\lambda|\{\theta_k\}), \mathcal{D}(\lambda|\{\theta_k\})$ that follow from (3.128), one observes that (3.132) are eigenvectors of the transfer matrix with eigenvalues

$$\begin{aligned}\Lambda(\lambda, \{\lambda_k\}|\{\theta_i\}) = \Big\{\prod_{k=1}^{r} S_T(\lambda_k - \lambda + \tfrac{i\pi}{2})^{-1} + \prod_{k=1}^{N} S_T(\lambda - \theta_k) \prod_{k=1}^{r} S_T(\lambda - \lambda_k - \tfrac{i\pi}{2})^{-1}\Big\} \\ \times \prod_{k=1}^{N} S_0(\lambda - \theta_k),\end{aligned} \tag{3.135}$$

if the parameters $\{\lambda_k\}$ satisfy the following set of non-linear algebraic equations

$$\prod_{k=1}^{N} \frac{\sinh\left(\frac{i\pi}{2\xi} - \frac{\lambda_j-\theta_k}{\xi}\right)}{\sinh\left(\frac{i\pi}{2\xi} + \frac{\lambda_j-\theta_k}{\xi}\right)} = \prod_{\substack{k=1\\k\neq j}}^{r} -\frac{\sinh\left(\frac{i\pi}{\xi} - \frac{\lambda_j-\lambda_k}{\xi}\right)}{\sinh\left(\frac{i\pi}{\xi} - \frac{\lambda_k-\lambda_j}{\xi}\right)}\,. \tag{3.136}$$

Since the equations are $i\pi\xi$-periodic we impose the restriction $0 \leq \Im\mathfrak{m}\,\lambda_k \leq \pi\xi\ \forall\ k$. Taking the logarithm of (3.136) results in equations of the form

$$\mathcal{M}_j(\theta_1,\ldots,\theta_N|\lambda_1,\ldots,\lambda_r) = 2\pi I_j\,, \qquad I_j \in \mathbb{Z}\,, \qquad j=1,\ldots,r\,, \tag{3.137}$$

where we defined

$$\begin{aligned}\mathcal{M}_j(\theta_1,\ldots,\theta_N|\lambda_1,\ldots,\lambda_r) \equiv & -i\sum_{k=1}^{N} \log \frac{\sinh\left(\frac{i\pi}{2\xi} - \frac{\lambda_j-\theta_k}{\xi}\right)}{\sinh\left(\frac{i\pi}{2\xi} + \frac{\lambda_j-\theta_k}{\xi}\right)} \\ & + i\sum_{\substack{k=1\\k\neq j}}^{r} \log -\frac{\sinh\left(\frac{i\pi}{\xi} - \frac{\lambda_j-\lambda_k}{\xi}\right)}{\sinh\left(\frac{i\pi}{\xi} - \frac{\lambda_k-\lambda_j}{\xi}\right)}\,.\end{aligned} \tag{3.138}$$

3.A.1 Periodic boundary conditions

Imposing periodic boundary conditions (3.29) on the transfer matrix eigenstates gives rise to the following set of "nested" Bethe Ansatz equations

$$\begin{aligned} e^{i\ell\sinh\theta_i} &= \prod_{m=1}^{N} S_0(\theta_i-\theta_m) \prod_{k=1}^{r} \frac{\sinh\left(\frac{i\pi}{2\xi} + \frac{\lambda_k-\theta_i}{\xi}\right)}{\sinh\left(\frac{i\pi}{2\xi} - \frac{\lambda_k-\theta_i}{\xi}\right)}\,, \qquad i=1,\ldots,N, \\ \prod_{k=1}^{N} \frac{\sinh\left(\frac{i\pi}{2\xi} - \frac{\lambda_j-\theta_k}{\xi}\right)}{\sinh\left(\frac{i\pi}{2\xi} + \frac{\lambda_j-\theta_k}{\xi}\right)} &= \prod_{\substack{k=1\\k\neq j}}^{r} \frac{\sinh\left(\frac{\lambda_j-\lambda_k-i\pi}{\xi}\right)}{\sinh\left(\frac{\lambda_j-\lambda_k+i\pi}{\xi}\right)}\,, \quad j=1,\ldots,r. \end{aligned} \tag{3.139}$$

We recall that $\ell = L\Delta/v$. It is customary to express the logarithmic form of the equations in terms of *counting functions* defined as

$$\begin{aligned} \ell z(\theta) &= \ell\sinh\theta + i\sum_{m=1}^{N} \ln\big[S_0(\theta-\theta_m)\big] + i\sum_{k=1}^{r} \ln\left[\frac{\sinh\left(\frac{\theta-\lambda_k-\frac{i\pi}{2}}{\xi}\right)}{\sinh\left(\frac{\theta-\lambda_k+\frac{i\pi}{2}}{\xi}\right)}\right], \\ \ell y(\lambda) &= i\sum_{k=1}^{N} \ln\left[\frac{\sinh\left(\frac{\lambda-\theta_k}{\xi} - \frac{i\pi}{2\xi}\right)}{\sinh\left(\frac{\lambda-\theta_k}{\xi} + \frac{i\pi}{2\xi}\right)}\right] - i\sum_{k=1}^{r} \ln\left[\frac{\sinh\left(\frac{\lambda-\lambda_k}{\xi} - \frac{i\pi}{\xi}\right)}{\sinh\left(\frac{\lambda-\lambda_k}{\xi} + \frac{i\pi}{\xi}\right)}\right], \end{aligned} \tag{3.140}$$

where the branch cuts of the logarithms need to be chosen appropriately. The Bethe-Yang equations then read

$$\begin{aligned} z(\theta_j) &= \frac{2\pi I_j}{\ell}\,, \quad i=1,\ldots,N, \\ y(\lambda_k) &= \frac{2\pi J_k}{\ell}\,, \quad k=1,\ldots,r, \end{aligned} \tag{3.141}$$

where I_j and J_k are integer or half-odd integer numbers.

3.A.2 Topological charge and charge conjugation operators

It is useful to know how the *solitonic charge operator* Q and *charge conjugation operator* C act of the transfer matrix eigenstates. Their respective actions on scattering states (2.63) are

$$Q\,|\theta_1,\ldots,\theta_N\rangle_{a_1\ldots a_N} = \left\{\sum_{k=1}^{N} a_k\right\} |\theta_1,\ldots,\theta_N\rangle_{a_1\ldots a_N}\,, \tag{3.142}$$

$$C\,|\theta_1,\ldots,\theta_N\rangle_{a_1\ldots a_N} = |\theta_1,\ldots,\theta_N\rangle_{\bar{a}_1\ldots\bar{a}_N}\,. \tag{3.143}$$

It is easily checked that

$$Q\mathcal{M}_{ab}(\lambda|\{\theta_k\}) - \mathcal{M}_{ab}(\lambda|\{\theta_k\})Q = (b-a)\mathcal{M}_{ab}(\lambda|\{\theta_k\}), \tag{3.144}$$

$$C\mathcal{M}_{ab}(\lambda|\{\theta_k\})C^{-1} = C\mathcal{M}_{ab}(\lambda|\{\theta_k\})C = \mathcal{M}_{\bar{a}\bar{b}}(\lambda|\{\theta_k\}). \tag{3.145}$$

This implies that Q and C commute with the transfer matrix, while

$$\big[Q,\mathcal{B}(\lambda|\{\theta_k\})\big] = -2\mathcal{B}(\lambda|\{\theta_k\})\,, \qquad \big[Q,\mathcal{C}(\lambda|\{\theta_k\})\big] = 2\mathcal{C}(\lambda|\{\theta_k\})\,, \tag{3.146}$$

$$C\mathcal{B}(\lambda|\{\theta_k\})C = \mathcal{C}(\lambda|\{\theta_k\})\,, \qquad C\mathcal{C}(\lambda|\{\theta_k\})C = \mathcal{B}(\lambda|\{\theta_k\})\,. \tag{3.147}$$

The action of Q on the reference state is

$$Q\Omega(\{\theta_k\}) = N\Omega(\{\theta_k\})\,, \tag{3.148}$$

and hence (3.134) are eigenstates of Q with eigenvalue $N-2r$.

3.B Proof of property (3.61)

In this appendix we show that the eigenvalues $\Lambda^s(\lambda|\{\theta_k\})$ of the transfer matrix (3.129) satisfy the relations

$$\mathcal{K}^s_{2N}(\theta_1,\dots,\theta_N)\Lambda^s(\theta_i|\{\theta_k\}) = \mathcal{K}^s_{2N}(\theta_1,\dots,\theta_N)\Lambda^s(-\theta_i|\{\theta_k\})^{-1}\ , \tag{3.149}$$

where $\{\theta_k\} = \{-\theta_1,\theta_1,\dots,-\theta_N,\theta_N\}$. The proof of (3.149) is divided into three main steps.

3.B.1 Step I

We first establish the following identity

$$\begin{aligned} &K^{a_1b_1}(\theta_1)\cdots K^{a_Nb_N}(\theta_N)\mathcal{T}(\sigma\theta_i|\{-\theta_1,\theta_1,\dots,-\theta_N,\theta_N\})^{a'_1b'_1\dots a'_Nb'_N}_{a_1b_1\dots a_Nb_N} \\ &\quad = K^{a_1b_1}(\theta_1)\cdots K^{a_Nb_N}(\theta_N)\mathcal{T}(\sigma\theta_i|\{-\theta_N,\theta_N,\dots,-\theta_1,\theta_1\})^{b'_Na'_N\dots b'_1a'_1}_{b_Na_N\dots b_1a_1}\,, \end{aligned} \tag{3.150}$$

where $\sigma = \pm 1$ and $\mathcal{T}$ is the transfer matrix

$$\begin{aligned} &\mathcal{T}(\lambda|\{-\theta_1,\theta_1,\dots,-\theta_N,\theta_N\})^{a'_1\dots b'_N}_{a_1\dots b_N} = \\ &\qquad = S^{c_1a'_1}_{c_{2N}a_1}(\lambda+\theta_1)S^{c_2b'_1}_{c_1b_1}(\lambda-\theta_1)\cdots S^{c_{2N}b'_N}_{c_{2N-1}b_N}(\lambda-\theta_N)\ . \end{aligned} \tag{3.151}$$

We focus on the case $i=1$ in (3.150), all other cases can be proved analogously. Setting $i=1$ and $\sigma=-1$, substituting the expression of $\mathcal{T}$ in terms of scattering matrices (3.151), and finally using that

$$S^{cd}_{ab}(0) = -\delta^d_a\delta^c_b, \tag{3.152}$$

we find that (3.150) is reduced to

$$\begin{aligned} &K^{a_1b_1}(\theta_1)\cdots K^{a_Nb_N}(\theta_N)S^{c_1b'_1}_{a_1b_1}(-2\theta_1)S^{c_2a'_2}_{c_1a'_2}(-\theta_1+\theta_2)\cdots S^{a'_1b'_N}_{c_{2N-1}b_N}(-\theta_1-\theta_N) = \\ &= K^{a_1b_1}(\theta_1)\cdots K^{a_Nb_N}(\theta_N)S^{c_1a'_1}_{b_1a_1}(-2\theta_1)S^{c_2b'_N}_{c_1b_N}(-\theta_1+\theta_N)\cdots S^{b'_1a'_2}_{c_{2N-1}a_2}(-\theta_1-\theta_2)\,. \end{aligned} \tag{3.153}$$

Employing the boundary unitarity property (3.10) of the K-matrix, the left-hand side of (3.153) can be written in the form

$$\begin{aligned} &K^{a_1b_1}(\theta_1)\cdots K^{a_Nb_N}(\theta_N)S^{c_1b'_1}_{a_1b_1}(-2\theta_1)S^{c_2a'_2}_{c_1a'_2}(-\theta_1+\theta_2)\cdots S^{a'_1b'_N}_{c_{2N-1}b_N}(-\theta_1-\theta_N) = \\ &= K^{b'_1c_1}(-\theta_1)\cdots K^{a_Nb_N}(\theta_N)S^{c_2a'_2}_{c_1a'_2}(-\theta_1+\theta_2)\cdots S^{a'_1b'_N}_{c_{2N-1}b_N}(-\theta_1-\theta_N)\,. \end{aligned} \tag{3.154}$$

Now we use the boundary Yang-Baxter equation (3.9) to rewrite the terms involving θ_1 and θ_2

$$\begin{aligned}
&K^{b_1' c_1}(-\theta_1)\cdots K^{a_N b_N}(\theta_N) S^{c_2 a_2'}_{c_1 a_2}(-\theta_1+\theta_2)\cdots S^{a_1' b_N'}_{c_{2N-1} b_N}(-\theta_1-\theta_N) = \\
&= K^{c_1 c_3}(-\theta_1)\cdots K^{a_N b_N}(\theta_N) S^{c_4 a_3'}_{c_3 a_3}(-\theta_1+\theta_3)\cdots S^{a_1' b_N'}_{c_{2N-1} b_N}(-\theta_1-\theta_N) \\
&\qquad\qquad \times S^{c_2 b_2'}_{c_1 b_2}(-\theta_1+\theta_2) S^{b_1' a_2'}_{c_2 a_2}(-\theta_1-\theta_2)\,. \qquad (3.155)
\end{aligned}$$

The index structure on the right-hand side of (3.155) is such that we may use the boundary Yang-Baxter equation to rewrite the terms involving θ_1 and θ_3, then θ_1 and θ_4 and so on. This brings the left-hand side of (3.153) to the form

$$\begin{aligned}
&K^{a_1 b_1}(\theta_1)\cdots K^{a_N b_N}(\theta_N) S^{c_1 b_1'}_{a_1 b_1}(-2\theta_1) S^{c_2 a_2'}_{c_1 a_2}(-\theta_1+\theta_2)\cdots S^{a_1' b_N'}_{c_{2N-1} b_N}(-\theta_1-\theta_N) = \\
&= K^{c_1 a_1'}(-\theta_1)\cdots K^{a_N b_N}(\theta_N) S^{c_2 b_N'}_{c_1 b_N}(-\theta_1+\theta_N)\cdots S^{b_1' a_2'}_{c_{2N-1} a_2}(-\theta_1-\theta_2)\,. \qquad (3.156)
\end{aligned}$$

Finally we use the reflection equations (3.10) and parity invariance of the S-matrix

$$S^{cd}_{ab}(\theta) = S^{dc}_{ba}(\theta)\,, \qquad (3.157)$$

to arrive at

$$\begin{aligned}
&K^{a_1 b_1}(\theta_1)\cdots K^{a_N b_N}(\theta_N) S^{c_1 b_1'}_{a_1 b_1}(-2\theta_1) S^{c_2 a_2'}_{c_1 a_2}(-\theta_1+\theta_2)\cdots S^{a_1' b_N'}_{c_{2N-1} b_N}(-\theta_1-\theta_N) = \\
&= K^{a_1 b_1}(\theta_1)\cdots K^{a_N b_N}(\theta_N) S^{c_1 a_1'}_{b_1 a_1}(-2\theta_1) \\
&\qquad\qquad \times S^{c_2 b_N'}_{c_1 b_N}(-\theta_1+\theta_N)\cdots S^{b_1' a_2'}_{c_{2N-1} a_2}(-\theta_1-\theta_2)\,. \qquad (3.158)
\end{aligned}$$

This establishes (3.153) for $i=1$ and $\sigma=-1$. The case $\sigma=+1$ is proved in the same way.

3.B.2 Step II

Next we establish the following identity

$$\begin{aligned}
&\big[\mathcal{T}(\theta_i|\{-\theta_N,\theta_N,\ldots,-\theta_1,\theta_1\})\big]^{b_N' a_N' \ldots b_1' a_1'}_{b_N a_N \ldots b_1 a_1} = \\
&\qquad\qquad = \big[\mathcal{T}(-\theta_i|\{-\theta_1,\theta_1,\ldots,-\theta_N,\theta_N\})^{-1}\big]^{a_1' b_1' \ldots a_N' b_N'}_{a_1 b_1 \ldots a_N b_N}\,, \qquad (3.159)
\end{aligned}$$

which is equivalent to

$$\sum_{a_1' \ldots b_N'} [\mathcal{T}(\theta_i|\{-\theta_N,\ldots,\theta_1\})]^{b_N' \ldots a_1'}_{b_N \ldots a_1} [\mathcal{T}(-\theta_i|\{-\theta_1,\ldots,\theta_N\})]^{a_1'' \ldots b_N''}_{a_1' \ldots b_N'} = \prod_{i=1}^{N} \delta^{a_i''}_{a_i} \delta^{b_i''}_{b_i}\,. \qquad (3.160)$$

Using the explicit expression of the two transfer matrices

$$[\mathcal{T}(-\theta_i|\{-\theta_1,\dots,\theta_N\})]^{a'_1\dots b'_N}_{a_1\dots b_N} = S^{c_1 b'_i}_{a_i b_i}(-2\theta_i) S^{c_2 a'_{i+1}}_{c_1 a_{i+1}}(-\theta_i-\theta_{i+1})\cdots S^{a'_i b'_{i-1}}_{c_N b_{i-1}}(-\theta_i-\theta_{i-1})\,,$$
$$[\mathcal{T}(\theta_i|\{-\theta_N,\dots,\theta_1\})]^{b'_N\dots a'_1}_{b_N\dots a_1} = S^{c_1 a'_{i-1}}_{b_i a_{i-1}}(\theta_i+\theta_{i-1})\cdots S^{c_N a'_{i+1}}_{c_{N-1} a_{i+1}}(\theta_i-\theta_{i+1}) S^{a'_i b'_i}_{c_N b_i}(2\theta_i)\,, \qquad (3.161)$$

the left-hand side of Eq. (3.160) can be expressed in the form

$$\sum_{a'_1\dots b'_N} S^{c_1 a'_{i-1}}_{b_i a_{i-1}}(\theta_i+\theta_{i-1})\cdots S^{a'_i b'_i}_{c_N b_i}(2\theta_i) S^{c_1 b''_i}_{a'_i b'_i}(-2\theta_i)\cdots S^{a''_i b''_{i-1}}_{c_N b'_{i-1}}(-\theta_i-\theta_{i-1})\,. \qquad (3.162)$$

The product of the two S-matrices involving θ_i can be simplified using the unitarity condition

$$S^{cd}_{ab}(\theta) S^{ef}_{cd}(-\theta) = \delta^e_a \delta^f_b\ . \qquad (3.163)$$

Eq. (3.162) then becomes

$$\delta^{b''_i}_{b_i} \sum_{a'_1\dots b'_N} S^{c_1 a'_{i-1}}_{b_i a_{i-1}}(\theta_i+\theta_{i-1})\cdots S^{c_1 a'_{i+1}}_{c_{N-1} a_{i+1}}(\theta_i-\theta_{i+1})$$
$$\times S^{c_2 a''_{i+1}}_{c_1 a'_{i+1}}(-\theta_i-\theta_{i+1})\cdots S^{a''_i b''_{i-1}}_{c_N b'_{i-1}}(-\theta_i-\theta_{i-1})\,. \qquad (3.164)$$

We observe that now the product of the two S-matrices involving θ_{i+1} can be simplified using (3.163). Repeating this procedure for $\theta_{i+2},\dots,\theta_N,\theta_1,\dots,\theta_{i-1}$ then establishes (3.160).

3.B.3 Step III

We now substitute (3.159) into (3.150) to obtain

$$K^{a_1 b_1}(\theta_1)\cdots K^{a_N b_N}(\theta_N)\,[\mathcal{T}(-\theta_i|\{-\theta_1,\theta_1,\dots,-\theta_N,\theta_N\})]^{a'_1 b'_1\dots a'_N b'_N}_{a_1 b_1\dots a_N b_N} =$$
$$= K^{a_1 b_1}(\theta_1)\cdots K^{a_N b_N}(\theta_N)\,\big[\mathcal{T}(\theta_i|\{-\theta_1,\theta_1,\dots,-\theta_N,\theta_N\})^{-1}\big]^{a'_1 b'_1\dots a'_N b'_N}_{a_1 b_1\dots a_N b_N}\ . \qquad (3.165)$$

Combining the eigenvalue equation (3.24) with the completeness relation (3.26) we have

$$\Psi^s_{a'_1\dots b'_N}(\{\theta_k\})^*\big[\mathcal{T}(-\theta_i|\{-\theta_1,\theta_1,\dots,-\theta_N,\theta_N\})\big]^{a'_1 b'_1\dots a'_N b'_N}_{a_1 b_1\dots a_N b_N} =$$
$$= \Lambda^s(-\theta_i|\{-\theta_1,\dots,\theta_N\})\Psi^s_{a_1\dots b_N}(\{\theta_k\})^*\,. \qquad (3.166)$$

Finally we contract both sides of (3.165) with $\Psi^s_{a'_1\ldots b'_N}(\{\theta_k\})^*$ and then use (3.166) to obtain the desired result

$$\mathcal{K}^s_{2N}(\{\theta_k\})\Lambda^s(-\theta_i|\{-\theta_1,\ldots,\theta_N\}) = \mathcal{K}^s_{2N}(\{\theta_k\})\Lambda^s(\theta_i|\{-\theta_1,\ldots,\theta_N\})^{-1}\,. \tag{3.167}$$

3.C Derivatives of the functions $\bar{Q}^s_i(\theta_1,\ldots,\theta_N)$

The functions $\bar{Q}^s_i(\{\theta_k\})$ are defined by (3.58) and can be written in the form [*cf.* (3.140)]

$$\begin{aligned}\bar{Q}^s_i(\{\theta_k\}) =& \ell\sinh\theta_i + i\sum_{m=1}^{N}\ln\big[S_0(\theta_i-\theta_m)S_0(\theta_i+\theta_m)\big]\\ &+ i\sum_{k=1}^{r}\ln\left[\frac{\sinh\left(\frac{\theta_i-\lambda_k-\frac{i\pi}{2}}{\xi}\right)}{\sinh\left(\frac{\theta_i-\lambda_k+\frac{i\pi}{2}}{\xi}\right)}\right],\end{aligned} \tag{3.168}$$

where the parameters λ_k are obtained by solving the set of equations

$$\begin{aligned}2\pi J^s_m =& i\sum_{k=1}^{N}\ln\left[\frac{\sinh\left(\frac{\lambda_m-\theta_k}{\xi}-\frac{i\pi}{2\xi}\right)\sinh\left(\frac{\lambda_m+\theta_k}{\xi}-\frac{i\pi}{2\xi}\right)}{\sinh\left(\frac{\lambda_m-\theta_k}{\xi}+\frac{i\pi}{2\xi}\right)\sinh\left(\frac{\lambda_m+\theta_k}{\xi}+\frac{i\pi}{2\xi}\right)}\right]\\ &- i\sum_{k=1}^{r}\ln\left[\frac{\sinh\left(\frac{\lambda_m-\lambda_k}{\xi}-\frac{i\pi}{\xi}\right)}{\sinh\left(\frac{\lambda_m-\lambda_k}{\xi}+\frac{i\pi}{\xi}\right)}\right],\quad m=1,\ldots r,\end{aligned} \tag{3.169}$$

for a given set of (half-odd) integers $\{J^s_m\}$ specifying the polarisation s. We are interested in the situation where

$$\theta_j \approx \begin{cases} -\tilde{\theta}_{N+1-j} & j\le N \\ \tilde{\theta}_{j-N} & j>N\end{cases},\quad j=1,\ldots,2N, \tag{3.170}$$

where $\{\tilde{\theta}_j\}$ is the solution of the Bethe-Yang equations corresponding to our representative state, i.e.

$$\bar{Q}^{\tilde{s}}_j(\tilde{\theta}_1,\ldots,\tilde{\theta}_N) = 2\pi\tilde{I}_j\ ,\quad j=1,\ldots,N. \tag{3.171}$$

Crucially, for this solution we have

$$\tilde{\theta}_{j+1}-\tilde{\theta}_j = \frac{1}{\ell\rho_\Phi(\theta_j)} + O(\ell^{-2}), \tag{3.172}$$

where $\rho_\Phi(\theta)$ is the root density (3.88) describing the representative state in the thermodynamic limit. We may use this fact to recast (3.169) in the form

$$\begin{aligned}\frac{2\pi J_m^s}{\ell} =& i\int_{-\infty}^{\infty} d\theta\ \rho_\Phi(\theta)\ln\left[\frac{\sinh\left(\frac{\lambda_m-\theta}{\xi}-\frac{i\pi}{2\xi}\right)}{\sinh\left(\frac{\lambda_m-\theta}{\xi}+\frac{i\pi}{2\xi}\right)}\right]\\ &-\frac{i}{\ell}\sum_{k=1}^{r}\ln\left[\frac{\sinh\left(\frac{\lambda_m-\lambda_k}{\xi}-\frac{i\pi}{\xi}\right)}{\sinh\left(\frac{\lambda_m-\lambda_k}{\xi}+\frac{i\pi}{\xi}\right)}\right]+O(\ell^{-1}),\quad m=1,\dots r.\end{aligned} \tag{3.173}$$

Denoting the solution to Eqs. (3.173) when the $O(\ell^{-1})$ correction terms are dropped by $\{\lambda_m^{(\infty)}\}$, we conclude that

$$\lambda_m = \lambda_m^{(\infty)} + O(\ell^{-1}). \tag{3.174}$$

Importantly, this conclusion holds for any set $\{\theta_j\}$ that is described by the root density $\rho_\Phi(\theta)$ in the thermodynamic limit. For any such set we then have

$$\begin{aligned}\bar{Q}_i^{\tilde{s}}(\theta_1,\dots,\theta_N) =& \ell\sinh\theta_i + i\sum_{m=1}^{N}\ln\big[S_0(\theta_i-\theta_m)S_0(\theta_i+\theta_m)\big]\\ &+ i\sum_{k=1}^{r}\left(\ln\left[\frac{\sinh\left(\frac{\theta_i-\lambda_k^{(\infty)}-\frac{i\pi}{2}}{\xi}\right)}{\sinh\left(\frac{\theta_i-\lambda_k^{(\infty)}+\frac{i\pi}{2}}{\xi}\right)}\right]+\mathcal{O}(\ell^{-1})\right).\end{aligned} \tag{3.175}$$

We conclude that

$$\frac{\partial\bar{Q}_i^{\tilde{s}}(\theta_1,\dots,\theta_N)}{\partial\theta_j} = \begin{cases} O(\ell) & i=j\ , \\ O(1) & i\neq j. \end{cases} \tag{3.176}$$

3.D Contributions from states with $M > N$

In this appendix we use the ideas developed in the Subsection 3.5 to argue that terms with $M > N$ only lead to sub-leading contributions in the Lehmann representation (3.89). Repeating the reasoning employed to arrive at formula (3.108), we obtain

$$\begin{aligned}\left.\frac{{}_{\rm R}\langle\Psi_0|e^{i\beta\Phi(t,x)/2}|\Phi_{\tilde{s}}\rangle_{\rm NS}}{{}_{\rm NS}\langle\Psi_0|\Phi_{\tilde{s}}\rangle_{\rm NS}}\right|_{M>N} =& \sum_{s=1}^{2^{2M}}\oint_{\vec{\mathcal{C}}_{\rm tot}}\prod_{i=1}^{M}\frac{d\eta_i}{2\pi}E(\{\eta_k\})_{\tilde{s},s}\\ &+\sum_{s=1}^{2^{2M}}\sum_{m=1}^{N}(-1)^m\sum_{1\le j_1<\cdots<j_m\le M}\ \sum_{i_1,\cdots,i_m=1}^{N}\ \oint_{\bar{\mathcal{C}}^{j_1,\cdots,j_m}_{i_1,\cdots,i_m}}\prod_{i=1}^{M}\frac{d\eta_i}{2\pi}E(\{\eta_k\})_{\tilde{s},s}\ .\end{aligned} \tag{3.177}$$

Here the multi-contours $\bar{\mathcal{C}}_{\rm tot}$ and $\bar{\mathcal{C}}^{j_1,\cdots,j_m}_{i_1,\cdots,i_m}$ are defined analogously to Subsection 3.5.1, while

$$E(\eta_1,\dots,\eta_M)_{\tilde{s},s} \equiv \frac{\bar{\rho}^{\tilde{s}}_N(\tilde{\theta}_1,\dots,\tilde{\theta}_N)}{\rho^{\tilde{s}}_{2N}(-\tilde{\theta}_1,\dots,\tilde{\theta}_N)} \frac{\mathcal{K}^s_{2M}(\{\eta_k\})}{\mathcal{K}^{\tilde{s}}_{2N}(\{\tilde{\theta}_k\})} \times \frac{f^{\beta/2}(\eta_M+i\pi,\dots,\tilde{\theta}_N)_{s,\tilde{s}}}{\prod_{k=1}^M \left\{e^{i\bar{Q}^s_k(\{\eta_k\})}-1\right\}} e^{2i\Delta t\sum_{i=1}^M \cosh\eta_i - \sum_{i=1}^N \cosh\tilde{\theta}_i}\,. \tag{3.178}$$

As we are dealing with a local operator, we expect that significant contributions in the large-N limit can only arise from states with

$$M-N=O(1). \tag{3.179}$$

The leading contribution to (3.177) arises from the $\binom{M}{N}$ regions where N of the η_j are integrated around the singularities at $\tilde{\theta}_1,\dots,\tilde{\theta}_N$. In order to obtain an estimate for these contributions we consider the case where $\eta_j\approx\tilde{\theta}_j$, $j=1,\dots,N$ in more detail. The leading singularity of the form-factor is given by

$$f^{\beta/2}(\eta_M+i\pi,\dots,\tilde{\theta}_N)_{s,\tilde{s}} \approx f(\eta_1,\dots,\eta_M)_{\tilde{s},s}\prod_{j=1}^N \frac{1}{(\eta_j-\tilde{\theta}_j)^2}\ , \tag{3.180}$$

where $f(\eta_1,\dots,\eta_M)_{s,\tilde{s}}$ is a regular function. Substituting (3.180) back into (3.178) and then carrying out the integrals over $\eta_1,\dots,\eta_N$ gives a leading contribution of the form

$$\sim \oint_{\mathcal{D}^{1,\cdots,N}_{1,\cdots,N}} \left\{ \prod_{i=N+1}^M \frac{d\eta_i}{2\pi} g(\eta_{N+1},\dots,\eta_M)_{\tilde{s},s} \times \prod_{j=1}^N \frac{\partial}{\partial_{\eta_j}}\Big|_{\eta_j=\tilde{\theta}_j} \left[\prod_{i=1}^M \frac{e^{2i\Delta t\cosh\eta_i}}{e^{i\bar{Q}^s_i(\{\eta_k\})}-1}\right] e^{-2i\Delta t\sum_{m=1}^N\cosh\tilde{\theta}_m}\right\}. \tag{3.181}$$

Here $g(\eta_{N+1},\dots,\eta_M)_{\tilde{s},s}$ is a regular function scaling as L^{-N} and $\mathcal{D}^{1,\cdots,N}_{1,\cdots,N}$ is a multi-contour in $\mathbb{C}^{M-N}$ obtained by removing the first N components from $\bar{\mathcal{C}}^{1,\cdots,N}_{1,\cdots,N}$. We may now proceed as in Appendix 3.C. In particular, the nested Bethe-Yang equations for solutions $\{\theta_j\}$ such that

$$\theta_k\approx\tilde{\theta}_k\ ,\quad k=1,\dots,N, \tag{3.182}$$

can still be cast in the form (3.173). Hence we again have

$$\lambda_m=\lambda_m^{(\infty)}+O(\ell^{-1}), \tag{3.183}$$

which in turn implies that

$$\bar{Q}_i^s(\theta_1,\dots,\theta_M) = \ell \sinh\theta_i + i\sum_{m=1}^{M} \ln\big[S_0(\theta_i-\theta_m)S_0(\theta_i-\theta_m)\big] + i\sum_{k=1}^{r} \ln\left[\frac{\sinh\left(\frac{\theta_i-\lambda_k^{(\infty)}-\frac{i\pi}{2}}{\xi}\right)}{\sinh\left(\frac{\theta_i-\lambda_k^{(\infty)}+\frac{i\pi}{2}}{\xi}\right)}\right] + O(1). \tag{3.184}$$

Following the same steps as in Subsection 3.5.1 we then find

$$\prod_{j=1}^{N}\frac{\partial}{\partial_{\eta_j}}\Big|_{\eta_j=\tilde{\theta}_j}\left[\prod_{i=1}^{M}\frac{e^{2i\Delta t\cosh\eta_i}}{e^{i\bar{Q}_i^s(\{\eta_k\})}-1}\right]e^{-2i\Delta t\sum_{m=1}^{N}\cosh\tilde{\theta}_m} \approx$$
$$\approx \left(\frac{i}{4}\right)^N \prod_{i=1}^{N}\Big\{\partial_i\bar{Q}_i^{\tilde{s}}(\{\tilde{\theta}_k\}) - 4\Delta t\sinh\tilde{\theta}_i\Big\}\prod_{j=N+1}^{M}\frac{e^{2i\Delta t\cosh\eta_j}}{e^{i\bar{Q}_j^s(\tilde{\theta}_1,\dots,\tilde{\theta}_N,\eta_{N+1},\dots,\eta_M)}-1}. \tag{3.185}$$

The main difference as compared to the $N = M$ case is the presence of additional integrals over $\eta_{N+1},\dots,\eta_M$. Using that

$$\frac{\partial\bar{Q}_i^{\tilde{s}}(\theta_1,\dots,\theta_M)}{\partial\theta_j} = O(1)\,, \qquad i\neq j\,, \tag{3.186}$$

we see that for small but fixed $\{\epsilon_i\}$

$$\bar{Q}_i^s(\tilde{\theta}_1,\dots\tilde{\theta}_N,\theta_{N+1}+i\epsilon_{N+1},\dots\theta_M+i\epsilon_M) = \bar{Q}_i^s(\tilde{\theta}_1,\dots,\theta_M) + i\epsilon_i\ell\big[\cosh\theta_i + O(1/\ell)\big]\,,$$
$$i = N+1,\dots,M. \tag{3.187}$$

Formula (3.187) implies that for $L\to\infty$ the parts of the paths composing $\hat{\mathcal{C}}_{\rm tot}$ below the real axis will give a vanishing contribution. On the remaining parts of the paths we have $\mathfrak{Im}\,\eta_j > 0$, and assuming that we can deform the integration contours a finite distance up into the upper half plane without encountering singularities, we conclude that the resulting contributions are exponentially suppressed in time.

3.E Most singular parts of the form-factors

In this appendix we determine the most singular contribution to matrix elements of the form

$${}_{b_N\cdots b_1}\langle\theta_N,\dots,\theta_1|e^{i\beta\Phi(0)/2}|\tilde{\theta}_1,\dots,\tilde{\theta}_N\rangle_{a_1\dots a_N} =$$
$$= f^{\beta/2}_{b_N\dots b_1 a_1\dots a_N}(\theta_N+i\pi,\dots,\theta_1+i\pi,\tilde{\theta}_1,\dots,\tilde{\theta}_N). \tag{3.188}$$

We will show by induction that

$$f^{\beta/2}_{b_N\dots b_1 a_1\dots a_N}(\theta_N+i\pi,\dots,\theta_1+i\pi,\tilde\theta_1,\dots,\tilde\theta_N)\Big|_{\substack{\theta_j\approx\tilde\theta_j\\ j=1,\dots,N}} = \mathcal{G}_{\beta/2}\prod_{k=1}^{N}\frac{2i}{\theta_k-\tilde\theta_k}\delta_{a_k,\bar b_k} + \text{less singular}. \tag{3.189}$$

The case $N=1$ is an immediate consequence of the annihilation pole axiom (see chapter 2) for the semi-local operator $e^{i\beta\Phi/2}$. We will now assume that (3.189) holds and consider

$$f^{\beta/2}_{b_{N+1}\dots b_1 a_1\dots a_{N+1}}(\theta_{N+1}+i\pi,\dots,\theta_1+i\pi,\tilde\theta_1,\dots,\tilde\theta_{N+1})\Big|_{\substack{\theta_j\approx\tilde\theta_j\\ j=1,\dots,N+1}}. \tag{3.190}$$

Using the periodicity axiom N times, this can be rewritten as

$$(-1)^N\, f^{\beta/2}_{b_1 a_1\dots a_{N+1}b_{N+1}\dots b_2}(\theta_1+i\pi,\tilde\theta_1,\dots,\tilde\theta_{N+1},\theta_{N+1}-i\pi,\dots,\theta_2-i\pi)\Big|_{\substack{\theta_j\approx\tilde\theta_j\\ j=1,\dots,N+1}}. \tag{3.191}$$

The annihilation pole axiom allows us to extract the leading singularity of (3.191) for $\theta_1\approx\tilde\theta_1$

$$\begin{aligned}(-1)^N\frac{i\delta_{c,\bar b_1}}{\theta_1-\tilde\theta_1}f^{\beta/2}_{a'_2\dots a'_{N+1}b'_{N+1}\dots b'_2}(\tilde\theta_2,\dots,\tilde\theta_{N+1},\theta_{N+1}-i\pi,\dots,\theta_2-i\pi)\Big|_{\substack{\theta_j\approx\tilde\theta_j\\ j=2,\dots,N+1}}\\ \times\ \Big[\delta^c_{a_1}\prod_{j=2}^{N+1}\delta^{a'_j}_{a_j}\delta^{b'_j}_{b_j}+S^{c_2a'_2}_{a_1a_2}(\tilde\theta_1-\tilde\theta_2)\dots S^{c_{N+1}a'_{N+1}}_{c_Na_{N+1}}(\tilde\theta_1-\tilde\theta_{N+1})\\ \times S^{d_Nb'_{N+1}}_{c_{N+1}b_{N+1}}(\tilde\theta_1-\theta_{N+1}-i\pi)\dots S^{cb'_2}_{d_2b_2}(\tilde\theta_1-\theta_2-i\pi)\Big].\end{aligned} \tag{3.192}$$

We now use the periodicity axiom N times to bring the form-factor into a form where we can use the induction assumption (3.189). The most singular contribution is then given by

$$\begin{aligned}\frac{i\delta_{c,\bar b_1}}{\theta_1-\tilde\theta_1}\prod_{k=2}^{N+1}\frac{2i}{\theta_k-\tilde\theta_k}\delta_{a'_k,\bar b'_k}\Big[\delta^c_{a_1}\prod_{j=2}^{N+1}\delta^{a'_j}_{a_j}\delta^{b'_j}_{b_j}+S^{c_2a'_2}_{a_1a_2}(\tilde\theta_1-\tilde\theta_2)\dots S^{c_Na'_N}_{c_{N-1}a_N}(\tilde\theta_1-\tilde\theta_{N+1})\\ \times S^{d_{N-1}b'_N}_{c_Nb_N}(\tilde\theta_1-\tilde\theta_{N+1}-i\pi)\dots S^{cb'_2}_{d_2b_2}(\tilde\theta_1-\tilde\theta_2-i\pi)\Big].\end{aligned} \tag{3.193}$$

The product of S-matrices can be simplified by repeatedly using the identity (starting with the two S-matrices involving $\tilde\theta_{N+1}$ and then moving outwards in the product)

$$S^{c_1c_2}_{a_1a_2}(\theta)S^{b_1\bar c_2}_{c_1\bar b_2}(\theta+i\pi)=\delta^{b_1}_{a_1}\delta^{b_2}_{a_2}. \tag{3.194}$$

This completes the induction step.

4. Pre-relaxation in weakly-interacting models

In this chapter we consider time evolution in models close to integrable points with a special property: at these points, in addition to the infinite set of local conserved charges in involution caused by their integrability, the systems also possess infinitely many *local* conserved charges which satisfy a non-trivial algebra. This property is induced by some hidden symmetries of the Hamiltonians which can be broken with or without breaking the integrability of the models. The described setting is very attractive from the point of view of time evolution: adding a term to the Hamiltonian which weakly breaks these additional symmetries is expected to completely change the stationary state reached; because it drastically modifies the set of conserved charges of the model. The resulting behaviour of local observables is very similar in spirit to the *prethermalisation* phenomenon observed when the integrability is weakly broken. Expectation values first reach quasi-stationary plateaux related to the GGE of the unperturbed model and then move away towards different values. We call "pre-relaxation" the described behaviour because it can also happen when the integrability is not broken and the system is not expected to thermalise; accordingly we call the relevant time window to observing this phenomenon the "pre-relaxation window".

Here we investigate pre-relaxation in the case of a weak-coupling limit, identify the pre-relaxation window and solve the time evolution through a mean-field mapping. Contrary to common situations, the mean-field mapping presented here is not an uncontrolled approximation and arises naturally at the timescale investigated. As an explicit example we study the XYZ spin-1/2 chain with additional perturbations that break integrability; as we shall see in the following, by varying the parameters which characterise the post-quench Hamiltonian, the model presents qualitatively different behaviours.

4.1 Introduction

We consider the time evolution of some initial state $|\Psi_0\rangle$ with cluster decomposition properties (*cf.* Appendix 2.A) under translation invariant Hamiltonians of the form

$$H = H_0 + gV\,, \tag{4.1}$$

where H_0 is non-interacting and translationally invariant, V is a global perturbation and g is a small coupling constant.

The case of interest here is when the limit of infinite time of the expectation value of a local observable $\mathcal{O}$ does not commute with the limit of infinitesimal g

$$\lim_{g\to 0}\lim_{t\to\infty}\langle\Psi_0|e^{i(H_0+gV)t}\mathcal{O}e^{-i(H_0+gV)t}|\Psi_0\rangle \neq \lim_{t\to\infty}\langle\Psi_0|e^{iH_0t}\mathcal{O}e^{-iH_0t}|\Psi_0\rangle\ . \tag{4.2}$$

This is the typical situation in which local degrees of freedom experience a prethermalisation or pre-relaxation behaviour. Indeed, when g is very small, for intermediate times the effect of the perturbation is negligible and the expectation value has time to settle at the stationary value of the unperturbed Hamiltonian. On the other hand, at later times the perturbation can not be ignored any more and the expectation value varies with a typical timescale that depends on the perturbation strength. Importantly, the described behaviour appears also when g is infinitesimal, therefore some important aspects of the pre-relaxation behaviour can be understood in this simplifying limit.

Examples of cases where the situation (4.2) is realised are manifold: probably the most common example is found when the perturbation V breaks the integrability [2, 18–20, 60–67, 69, 70]. There for small but finite g the system relaxes to a Gibbs ensemble for late times, while for $g = 0$ it relaxes to a GGE. It is very easy to see that $\rho_{\rm GE}(g = 0) \neq \rho_{\rm GGE}(g = 0)$ [66]. Interestingly, this is not the only case in which (4.2) can happen: another example is realised when one considers an Hamiltonian H_0 characterised by hidden symmetries, which give rise to an infinite non-abelian set of local conservation laws [68]. This is, for example, the case of the XY model (*cf.* Chapter 2). In this case it is sufficient for V to break these symmetries, while maintaining the integrability, in order to produce behaviour like that of (4.2).

In principle, there could be many pre-relaxation plateaux, depending on how the time t scales with the small parameter g. Here we focus on the limit $g \ll 1$ and large time in such a way that $T = gt \sim O(g^0)$. This defines the "pre-relaxation window": $1 \ll t \ll g^{-\alpha}$ with $\alpha > 1$; the time window of interest in this chapter. For simplicity, throughout this chapter we neglect $O(g)$ corrections to observables.

In the time window considered several simplifications arise, we start by considering the time evolution operator $U(t) = e^{-iHt}$ for the Hamiltonian (4.1). We argue that for $g \ll 1$ and $T = gt \sim O(g^0)$ the following simplification can be performed on $U(t)$

$$U(t) = e^{-iHt} \to e^{-i\bar{V}T}e^{-iH_0t}, \tag{4.3}$$

where $\bar{V}$ is the time average of $V(t) = e^{-iH_0 t} V e^{iH_0 t}$ defined as

$$\bar{V} = \lim_{t\to\infty} \frac{1}{t} \int_0^t \mathrm{d}s\, V(s) = \lim_{t\to\infty} \frac{1}{t} \int_0^t \mathrm{d}s\, e^{-iH_0 s} V e^{iH_0 s} \tag{4.4}$$

which we assume to exist; by construction we have $[\bar{V}, H_0] = 0$. Formula (4.3) has been proven in Ref. [68], in the case of a noninteracting perturbation V. Here we argue that (4.3) holds true also for interacting perturbations. The reasoning is as follows.

We rewrite the time evolution operator as

$$U(t) = e^{-iHt} = U_I(t) e^{-iH_0 t}\,, \tag{4.5}$$

taking the time derivative of (4.5) we find the differential equation for $U_I(t)$

$$i\partial_t U_I(t) = g U_I(t) e^{-iH_0 t} V e^{iH_0 t}\,. \tag{4.6}$$

Solving (4.6) we find

$$U_I(t) = \mathrm{T}^\dagger \exp\Big(-ig \int_0^t \mathrm{d}s e^{-iH_0 s} V e^{iH_0 s}\Big)\,, \tag{4.7}$$

where $\mathrm{T}^\dagger$ is the anti-time-ordering operator. Now we to want find the leading contribution to (4.7) in the limit $g \ll 1$ and large time in such a way that $T = gt \sim O(g^0)$. As $g = T/t$, without the $\mathrm{T}^\dagger$ operator the leading contribution in the limit would simply be found replacing the exponent with $-iT\bar{V}$, obtaining precisely (4.3). The presence of the anti-time-ordering operator complicates the analysis, but expanding (4.7) we see that (4.3) continues to hold. The next order correction in g is given by

$$\lim_{t\to\infty} -ig \int_0^t \mathrm{d}s\, (V(s) - \bar{V}) = \lim_{t\to\infty} -i\frac{T}{t} \int_0^t \mathrm{d}s\, (V(s) - \bar{V})\,, \tag{4.8}$$

and goes to zero in the limit considered according to our assumption on the time average.

It is interesting to understand how the simplification (4.3), valid for $g \ll 1$ with $gt \sim O(g^0)$, can be obtained using well known methods in the study of non-equilibrium time evolution, such as the the continuous unitary transformation (CUT) approach [60, 170–173] or the Keldysh technique [174]. The result (4.3) can be easily derived by means of a perturbative CUT [60] at the lowest order in the perturbation g (*i.e.* $O(g^0)$) for times t of the order g^{-1}. At this order, all the $O(g)$ corrections to the observables are neglected and the only effect of the CUT is a first order correction to the Hamiltonian in the time evolution operator. This correction has to be taken into account because $gt \sim O(g^0)$. The correction to the Hamiltonian is exactly $g\bar{V}$, so

one obtains precisely (4.3). From the point of view of Keldysh perturbation theory, the regime $g \ll 1$ with $gt \sim O(g^0)$ is more complicated to access, indeed all the secular terms proportional to $(gt)^n$ become $O(g^0)$. Resumming all these contributions and neglecting all the other terms one obtains again Formula (4.3).

Having justified the expression (4.3) we can now use it to simplify expectation values of observables. Let us consider the expectation value of the generic local operator $\mathcal{O}$: in the limit $g \ll 1$ with $T = gt \sim O(g^0)$ we have

$$\langle \Psi_0 | e^{iHt} \mathcal{O} e^{-iHt} | \Psi_0 \rangle \to \mathrm{tr}[(e^{-iH_0 t} |\Psi_0\rangle \langle \Psi_0| e^{iH_0 t}) e^{iT\bar{V}} \mathcal{O} e^{-iT\bar{V}}] \,. \tag{4.9}$$

Since the time t is large ($t \sim g^{-1}$) we would like to further simplify (4.9) replacing the state $\rho(t) \equiv e^{-iH_0 t} |\Psi_0\rangle \langle \Psi_0| e^{iH_0 t}$ with the corresponding GGE, *i.e.* the stationary state that the system is supposed to reach in the sense discussed in the Introduction

$$e^{-iH_0 t} |\Psi_0\rangle \langle \Psi_0| e^{iH_0 t} \to \rho_{\mathrm{GGE}} = \lim_{|S|\to\infty} \lim_{t\to\infty} \mathrm{tr}_{\bar{S}}[\rho(t)] \,. \tag{4.10}$$

Here we introduced a finite subsystem S, whose size is sent to infinity after the thermodynamic limit and the infinite time limit have been performed. As discussed in the Introduction the infinite time limit of $\rho(t)$ does not exist, only if the density matrix is reduced to finite subsystems it can have a limit. We stress that, inside the expectation values of local observables, $\rho(t)$ can be directly replaced by $\mathrm{tr}_{\bar{S}}[\rho(t)]$ with a finite S. This is because if $\mathcal{O}$ is local, it acts non-trivially only within a finite subsystem.

In the case under exam ρ_{GGE} is of the form

$$\rho_{\mathrm{GGE}} = \frac{e^{-\sum_j \lambda_j Q_j}}{Z} \,, \tag{4.11}$$

where Q_j are local conservation laws and λ_j are real parameters determined by the initial state [38, 40]. In the following we will be interested in cases where the local conserved charges $\{Q_j\}$ in (4.11) form a non-abelian set. Also in these cases a "standard" GGE can be constructed, where the charges are in involution. These charges, however, will generally depend on the initial state [68].

Since H_0 is a translationally invariant noninteracting Hamiltonian and the state $|\Psi_0\rangle$ has cluster decomposition properties, the validity of the substitution (4.10) for late times is well established when expectation values of local operators are considered. In our case, however, we are dealing with the operator $e^{iT\bar{V}} \mathcal{O} e^{-iT\bar{V}}$, whose locality properties depend on $\bar{V}$. In the

case where $\bar{V}$ is (quasi)-local [93, 94] (its density is exponentially localised), the validity of the replacement has been established in [39]. In the next sections we will show that $\bar{V}$ is in fact non-local, nevertheless its particular form will still allow us to perform the substitution (4.10) (*cf.* Section 4.3). From (4.10) it follows

$$\lim_{g\to 0} \mathrm{tr}[(e^{-iH_0T/g}\left|\Psi_0\right\rangle\left\langle\Psi_0\right| e^{iH_0T/g})e^{iT\bar{V}}\mathcal{O}e^{-iT\bar{V}}] = \mathrm{tr}[\rho_{\mathrm{GGE}}e^{iT\bar{V}}\mathcal{O}e^{-iT\bar{V}}]\,, \tag{4.12}$$

which suggests that the pre-relaxation limit can be described by the time-dependent ensemble

$$\rho_{\mathrm{tGGE}}(t) = e^{-i\bar{V}gt}\rho_{\mathrm{GGE}}e^{i\bar{V}gt}\,. \tag{4.13}$$

The time evolution of observables according to (4.12) represents the main object of study of this chapter.

Both ρ_{GGE} and $\bar{V}$ commute with the Hamiltonian: if the two operators can be written in terms of the same set of local conservation laws in involution, the time dependence disappears $\rho_{\mathrm{tGGE}}(t) = \rho_{\mathrm{GGE}}$. In the next section we will show that in many cases of interest $\bar{V}$ can be approximated by a polynomial of the local conservation laws. Therefore, in order to see some non-trivial pre-relaxation behaviour, the unperturbed Hamiltonian H_0 must have a non-abelian set of local charges. We refer the reader to [68] for an extensive discussion of noninteracting models with that property.

4.1.1 Organisation of the chapter

The rest of this chapter is organised as follows. Section 4.2 is devoted to identifying the class of effective Hamiltonians (*i.e.* the possible $\bar{V}$ *cf.* (4.12)) that emerge in the pre-relaxation limit. We show that they can be written as polynomials of the local conservation laws of the unperturbed model (with the correct scaling factors). In Section 4.3 we introduce mean-field Hamiltonians which, in the thermodynamic limit, generate *exactly* the same dynamics as the effective Hamiltonians. The formalism is explicitly applied to the XYZ spin-1/2 chain in Section 4.4, where pre-relaxation is also investigated in the presence of interactions that break integrability. Section 4.5 contains our conclusions. Several appendices complement the main text with the proofs of the theorems and additional details.

4.2 Effective Hamiltonians

Let us consider the XY model without magnetic field. The Hamiltonian is given by (*cf.* (2.1))

$$H_{\rm XY} = J\sum_{\ell}(\frac{1+\gamma}{4}\sigma^x_\ell\sigma^x_{\ell+1} + \frac{1-\gamma}{4}\sigma^y_\ell\sigma^y_{\ell+1})\,, \tag{4.14}$$

where σ^α_ℓ act like Pauli matrices on the site ℓ and like the identity elsewhere. If the initial state $|\Psi_0\rangle$ breaks one-site shift invariance, the latter symmetry is generally not restored in the GGE that describes local observables at infinite time after the quench.

On the other hand, an infinitesimally small one-site shift invariant perturbation that breaks the non-abelian integrability of (4.14) is expected to catalyse symmetry restoration (similar issues of symmetry restoration have been pointed out long ago, *e.g.* in [175]).

A perturbation that preserves the noninteracting character of the Hamiltonian was already considered in [68]. Here we investigate perturbations that have a 4-fermion representation in terms of the noninteracting fermions that diagonalise (4.14), namely

$$V \sim \sum_{\ell} a^{\alpha_1}_{\ell+n_1}a^{\alpha_2}_{\ell+n_2}a^{\alpha_3}_{\ell+n_3}a^{\alpha_4}_{\ell+n_4}\,, \tag{4.15}$$

where a^α_ℓ are the Majorana fermions (*cf.* Subsection 2.1.2).

The argument presented in Section 4.1 indicates that the relevant Hamiltonian in the pre-relaxation limit is determined by the time average of the perturbation. The calculation of the average in this case is not difficult but rather lengthy. However, a close inspection of the various contributions reveals a hidden structure that helps simplifying the computation. The calculation is carried out in Appendix 4.A, the result is summarised in the following

Property 4.2.1 *The time average under $H_{\rm XY}$ of a one-site shift invariant four fermion operator can be written as follows*

$$\frac{1}{L}\overline{\sum_{\ell} a^{\alpha_1}_{\ell+n_1}a^{\alpha_2}_{\ell+n_2}a^{\alpha_3}_{\ell+n_3}a^{\alpha_4}_{\ell+n_4}} = F^{\{\alpha_1\dots\alpha_4\}}_{\{n_1\dots n_4\}} + A^{\{\alpha_1\dots\alpha_4\}}_{\{n_1\dots n_4\}}\,, \tag{4.16}$$

where $F^{\{\alpha_1\dots\alpha_4\}}_{\{n_1\dots n_4\}}$ is a linear combination of factorised terms and $A^{\{\alpha_1\dots\alpha_4\}}_{\{n_1\dots n_4\}}$ is an anomalous contribution originated by the non-trivial solutions of the energy constraint

$$\varepsilon(k_1)+\varepsilon(k_2) = \varepsilon(k_3)+\varepsilon(k_1+k_2-k_3)\,. \tag{4.17}$$

The latter exists only in the thermodynamic limit and strongly depends on the details of the

dispersion relation, whereas $F^{\{\alpha_1\dots\alpha_4\}}_{\{n_1\dots n_4\}}$ *has a structure that is almost model independent:*

$$F^{\{\alpha_1\dots\alpha_4\}}_{\{n_1\dots n_4\}} = \sum_{s=0}^{1} \underbrace{a^{\alpha_1}_{n_1}a^{\alpha_2}_{n_2}}_{s}\underbrace{a^{\alpha_3}_{n_3}a^{\alpha_4}_{n_4}}_{s} - \underbrace{a^{\alpha_1}_{n_1}a^{\alpha_3}_{n_3}}_{s}\underbrace{a^{\alpha_2}_{n_2}a^{\alpha_4}_{n_4}}_{s} + \underbrace{a^{\alpha_1}_{n_1}a^{\alpha_4}_{n_4}}_{s}\underbrace{a^{\alpha_2}_{n_2}a^{\alpha_3}_{n_3}}_{s}\,, \tag{4.18}$$

where

$$L\,\underbrace{a^{\alpha}_{n_1}a^{\beta}_{n_2}}_{s} = \overline{\sum_{\ell}(-1)^{s\ell}a^{\alpha}_{\ell+n_1}a^{\beta}_{\ell+n_2}} = \sum_{\alpha_1,\alpha_2=1,2}\sum_{\ell_1,\ell_2} d^{\alpha\beta\alpha_1\alpha_2}_{n_1n_2s}(\ell_1,\ell_2)a^{\alpha_1}_{\ell_1}a^{\alpha_2}_{\ell_2}\,, \tag{4.19}$$

is a (quasi)-local operator: $d^{\alpha\beta\alpha_1\alpha_2}_{n_1n_2s}(\ell_1,\ell_2)$ *decays exponentially in* $|\ell_1-\ell_2|$.

Let us consider first the "anomalous term" $A^{\{\alpha_1\dots\alpha_4\}}_{\{n_1\dots n_4\}}$. This conservation law is purely non local: it is possible to show that it can not be written as a function of local ones. We then expect $A^{\{\alpha_1\dots\alpha_4\}}_{\{n_1\dots n_4\}}$ to become important for local observables only at times proportional to the chain length, which are far beyond the pre-relaxation limit. In light of this we argue that anomalous terms are not relevant to our problem, which is equivalent to assume

$$\langle\Psi_0|e^{iHt}[\mathcal{O},A^{\{\alpha_1\dots\alpha_4\}}_{\{n_1\dots n_4\}}]e^{-iHt}|\Psi_0\rangle = 0\,, \tag{4.20}$$

for any local observable $\mathcal{O}$. This will be a working assumption throughout this chapter, in Appendix 4.C we check the self-consistency of our approximation. To support the validity of our assumption, in the next chapter we will compare the results found here with those found by means of a different method, the first order EOM (*cf.* Chapter 5): observing an excellent agreement (*cf.* Fig. 5.29). Additional indications in favour of our assumption have been found in [176], where the results of the approach presented here have been compared with those of infinite time-evolving block-decimation (iTEBD) algorithm: finding a good agreement. Further investigations on the effects of the anomalous terms are left to future works.

The factorised part $F^{\{\alpha_1\dots\alpha_4\}}_{\{n_1\dots n_4\}}$ of the time average has a simple structure: it is written as sum of products of quasi-local operators divided by L, ensuring the correct scaling with L in the thermodynamic limit. This form easily generalises in the case of an arbitrary number of fermions. The factorised part of the time average of a perturbation with $2k$ Majorana fermions, designated by $F^{\{\alpha_1\dots\alpha_k\}}_{\{n_1\dots n_k\}}$, can be written as

$$F^{\{\alpha_1\dots\alpha_k\}}_{\{n_1\dots n_k\}} = \frac{1}{L^{k-1}}H_{1;1}\dots H_{1;k} + \dots + \frac{1}{L^{k-1}}H_{m;1}\dots H_{m;k}\,, \qquad m = \frac{2(2k)!}{2^k k!}\,, \tag{4.21}$$

where $H_{i;j}$ are translation invariant operators (*i.e.* n-site shift invariant for some $n\in\mathbb{N}$) with quasi-local densities, their particular form depends on $\{\alpha_i\}$ and $\{n_i\}$.

Summing all together: the argument of Section 4.1 and our assumption (4.20) suggest that considering general perturbations to the XY model the effective Hamiltonian describing the pre-relaxation limit takes the form

$$H_{\text{eff}} = \frac{1}{L^{n_1-1}} H_{1;1} \dots H_{1;n_1} + \dots + \frac{1}{L^{n_m-1}} H_{m;1} \dots H_{m;n_m} \,, \tag{4.22}$$

where $\{n_i\}, m \in \mathbb{N}$ are finite and $H_{i;j}$ are quasi-local operators.

As a matter of fact, similar factorisations appear whenever the unperturbed Hamiltonian is noninteracting (*e.g.* the model considered in Chapter 5), provided that the anomalous terms in (4.16) can be disregarded. Hamiltonians of the form (4.22) are therefore the perfect workbench for pre-relaxation or pre-thermalisation issues.

The non-equilibrium dynamics generated by a subclass of Hamiltonians of the form (4.22) have been already worked out in [177]. The authors considered "completely connected quantum models", in which the Hamiltonian is symmetric under any permutation of the sites, and exhibited a mapping onto an effective classical Hamiltonian dynamics.

We also point out that the simplest models of the form (4.22) (*e.g.* Curie-Weiss quantum Heisenberg models) have often been used as toy models to investigate the statistical properties in the presence of long range interactions [178].

The rest of the chapter will be focussed on the following points:

1. Solution of the non-equilibrium problem for Hamiltonians of the form (4.22);

2. Characterisation of the pre-relaxation limit in an interacting model, in the presence of perturbations that may or may not break integrability;

The point (2) relies on two assumptions:

(a) In the limit $g \to 0$ with gt finite, the time evolution under $H = H_0 + gV$ can be split in two steps:

   1. infinite time evolution under the unperturbed Hamiltonian H_0, which is supposed to give rise to a generalised Gibbs ensemble $e^{-iH_0 t} |\Psi_0\rangle \langle\Psi_0| e^{iH_0 t} \to \rho_{\text{GGE}}$;

   2. time evolution with rescaled time $T = gt$ under the effective Hamiltonian given by the perturbation V averaged with respect to H_0 (4.4);

$$e^{-i(H_0+gV)t} |\Psi_0\rangle \langle\Psi_0| e^{i(H_0+gV)t} \sim e^{-igt\bar{V}} \rho_{\text{GGE}} e^{igt\bar{V}} \,. \tag{4.23}$$

(b) The "anomalous terms" appearing in the time average of V give a negligible contribution (*cf.* Property 4.2.1 and discussion below).

On the other hand, (1) will be treated as an *ab initio* problem.

4.3 Solution of the non-equilibrium problem

In this section we work out the first point of our plan of attack. We are going to show that, despite the nonlocal appearance, operators of the form (4.22) generate a dynamics which is equivalent to that of a (quasi-)local time-dependent mean-field Hamiltonian. Here only the most relevant results are reported, the details of the derivation can be found in Appendix 4.B.

For the sake of simplicity we only consider cases in which $H_{i;j}$ (*cf.* (4.22)) have local densities, however, as far as we can see, all the results can be generalised to quasi-local operators.

In light of (4.22), we define a class of operators $\mathcal{E}$ as follows:

Definition We say that an operator acting on a spin-1/2 chain belongs to the class $\mathcal{E}$ if it is written as in (4.22), namely as a finite linear combination of operators of the form

$$\frac{1}{L^{n-1}} H_1 \cdots H_n \,, \tag{4.24}$$

where n is finite, H_j are local translation invariant operators, and L is the chain length.

It important to emphasise that we consider cases where the local Hilbert space is finite dimensional. This turns out to be a fundamental assumption for most of our results and includes all the examples mentioned.

One of our goals is to show that the time evolution preserves cluster decomposition properties, which is the key element that allows us to simplify the calculation of expectation values. We have

Lemma 4.3.1 *Let $\mathcal{O} \in \mathcal{E}$ and $|\Psi\rangle$ a state with cluster decomposition properties. The expectation value of $\mathcal{O}/L$ in $|\Psi\rangle$ can be reduced to the expectation values of the local translation invariant operators it consists of:*

$$\lim_{L\to\infty} \langle\Psi| \frac{H_1}{L} \cdots \frac{H_n}{L} |\Psi\rangle = \lim_{L\to\infty} \prod_j \frac{\langle\Psi|H_j|\Psi\rangle}{L} \,. \tag{4.25}$$

Using this lemma it is rather natural to relate the dynamics generated by (4.22) to those generated by the mean-field Hamiltonian defined as follows:

Definition *Mean-field effective Hamiltonian.* Let $H \in \mathcal{E}$ be an operator written as

$$H = \frac{1}{L^{n-1}} H_1 \cdots H_n \,. \tag{4.26}$$

We call $H^{\Psi_0}_{\rm MF}(t)$ the (time dependent) mean field operator associated with H, defined as

$$H^{\Psi_0}_{\rm MF}(t) \equiv \sum_{j=1}^{n} \prod_{\ell \neq j} \left\{ \frac{\langle \Psi_0 | \bar{U}^\dagger(t) H_\ell \bar{U}(t) | \Psi_0 \rangle}{L} \right\} H_j \,, \tag{4.27}$$

where $\bar{U}(t)$ is the time evolution under $H^{\Psi_0}_{\rm MF}(t)$

$$\bar{U}(t) = \mathrm{T} \exp\Big(-i \int_0^t \mathrm{d}\tau H^{\Psi_0}_{\rm MF}(\tau) \Big) \,. \tag{4.28}$$

Consequently, $H^{\Psi_0}_{MF}(t)$ must be generally computed in a self-consistent way.

For example, the Hamiltonian

$$H = -\frac{1}{4} \sum_{\ell}^{L} \Big(\sigma^x_\ell \sigma^x_{\ell+1} + \sigma^y_\ell \sigma^y_{\ell+1} \Big) + \frac{\lambda}{L} \Big(\sum_{\ell}^{L} \sigma^z_\ell \Big)^2 \tag{4.29}$$

belongs to $\mathcal{E}$. In this trivial case $\sum_\ell \sigma^z_\ell$ commutes with H, so the associated mean-field Hamiltonian is independent of time and it is given by

$$H^{\Psi_0}_{\rm MF}(t) = -\frac{1}{4} \sum_{\ell} \Big(\sigma^x_\ell \sigma^x_{\ell+1} + \sigma^y_\ell \sigma^y_{\ell+1} \Big) + 2\lambda \, \langle \Psi_0 | \frac{1}{L} \sum_\ell \sigma^z_\ell | \Psi_0 \rangle \sum_\ell \sigma^z_\ell \,. \tag{4.30}$$

The main result of this section is that the dynamics generated by the mean field Hamiltonian is *exactly equivalent* to that generated by the full Hamiltonian, more precisely:

Lemma 4.3.2 *Let $|\Psi_0\rangle$ be a translation invariant state with cluster decomposition properties and $H, \mathcal{O} \in \mathcal{E}$. Let the expectation value of $\mathcal{O}$ in the state that time evolves with $H^{\Psi_0}_{\rm MF}(t)$ be an analytic function of t in the strip $|\mathrm{Im}[t]| < r$, with r a nonzero constant. In the thermodynamic limit, the time evolution with H can be replaced by the time evolution with the mean-field Hamiltonian:*

$$\lim_{L\to\infty} \langle \Psi_0 | e^{iHt} \frac{\mathcal{O}}{L} e^{-iHt} | \Psi_0 \rangle = \lim_{L\to\infty} \langle \Psi_0 | \bar{U}^\dagger(t) \frac{\mathcal{O}}{L} \bar{U}(t) | \Psi_0 \rangle \,. \tag{4.31}$$

Remark The validity of the hypothesis of analyticity on a strip can be verified *a posteriori*. The idea is the following. The self-consistent mean-field problem can be generally recast into an infinite nonlinear system of ordinary differential equations. The finiteness of n in (4.24) implies that the system can be written as $\dot{\vec{u}} = \vec{F}(\vec{u}, t)$, with $\vec{F}$ a polynomial. If the system was finite, the solution would have been analytic. This is not always the case for an infinite system but, in practice, the numerical solution is obtained by introducing a cutoff parameter N that makes the system finite. If the mean-field time evolution had a point of non-analyticity, the solution of the system of equations should display a non-trivial dependence of the mean-field

parameters on the cutoff as $N \to \infty$.

Corollary 4.3.3 *Lemma 4.3.2 holds true in particular for local operators.*

The local equivalence with the mean-field time evolution can also be expressed in terms of reduced density matrices:

Corollary 4.3.4 *Let $|\Psi_0\rangle$ a translation invariant state with cluster decomposition properties and $H \in \mathcal{E}$. In the thermodynamic limit, the time evolution of the reduced density matrix (RDM) of some spin block S is equal to the RDM in the state that time evolves with the mean-field Hamiltonian:*

$$\rho_S(t) = \mathrm{tr}_{\bar{S}}[e^{-iHt}\,|\Psi_0\rangle\,\langle\Psi_0|\,e^{iHt}] = \mathrm{tr}_{\bar{S}}[\bar{U}(t)\,|\Psi_0\rangle\,\langle\Psi_0|\,\bar{U}^\dagger(t)]\,. \tag{4.32}$$

4.3.1 Time-dependent GGE

We are now in a position to justify (4.10), and in turn (4.12) and (4.13). In the limit of small g the expectation value of a local observable $\mathcal{O}$ reads as (4.9)

$$\langle\Psi_0|e^{iHt}\mathcal{O}e^{-iHt}|\Psi_0\rangle \to \mathrm{tr}[(e^{-iH_0T/g}\,|\Psi_0\rangle\,\langle\Psi_0|\,e^{iH_0T/g})e^{iT\bar{V}}\mathcal{O}e^{-iT\bar{V}}]\,. \tag{4.33}$$

Since H_0 is local, the state $e^{-iH_0T/g}\,|\Psi_0\rangle$ has cluster decomposition properties beyond some typical distance proportional to T/g (in order to be outside of the light cone). Being $\bar{V}$ in $\mathcal{E}$, from Corollary 4.3.3 follows that the time evolution under $\bar{V}$ is equivalent to that under the corresponding mean-field operator. Indeed, introducing the constant J with the dimension of an energy, we only need $JT \ll gL$ (*cf.* (4.122)), which is trivially satisfied in the thermodynamic limit. Thus we obtain

$$\langle\Psi_0|e^{iHt}\mathcal{O}e^{-iHt}|\Psi_0\rangle \to \mathrm{tr}[(e^{-iH_0T/g}\,|\Psi_0\rangle\,\langle\Psi_0|\,e^{iH_0T/g})U^\dagger_{\bar{V}}(T)\mathcal{O}U_{\bar{V}}(T)]\,, \tag{4.34}$$

with

$$U_{\bar{V}}(t) = \mathrm{T}\exp\Big(-i\int_0^t \mathrm{d}\tau \bar{V}^{\Psi_T}_{\mathrm{MF}}(\tau)\Big)\,. \tag{4.35}$$

Incidentally, we note that the time-ordering in (4.35) can not be simplified because $\bar{V}^{\Psi_T}_{\mathrm{MF}}$ is generally written in terms of conservation laws that are not in involution with one another.

For the sake of simplicity we assume that the time-dependent coupling constants of $\bar{V}^{\Psi_T}_{\mathrm{MF}}$ are bounded. The operator $U^\dagger_{\bar{V}}(T)\mathcal{O}U_{\bar{V}}(T)$ is then quasi-local with a typical range ξ proportional to T [179]. On the other hand $e^{-iH_0T/g}\,|\Psi_0\rangle$ is the time evolution of $|\Psi_0\rangle$ at the time ($\infty \leftarrow$

$)T/g \gg T \sim \xi$. In this limit, we can apply the findings of [39] and replace the state with the corresponding GGE

$$\mathrm{tr}[(e^{-iH_0T/g}\,|\Psi_0\rangle\,\langle\Psi_0|\,e^{iH_0T/g})U^\dagger_{\bar V}(T)\mathcal{O}U_{\bar V}(T)] \to \mathrm{tr}[\rho_{\mathrm{GGE}}U^\dagger_{\bar V}(T)\mathcal{O}U_{\bar V}(T)]\,. \tag{4.36}$$

The operator $\bar V^{\Psi_T}_{\mathrm{MF}}$ is obtained self-consistently by computing the expectation values of (quasi-)local conservation laws, which, for late times, can be obtained from (4.36). Therefore, in the definition (4.27) of the mean-field Hamiltonian we can replace $|\Psi_0\rangle$ by ρ_{GGE}

$$H^{\Psi_0}_{\mathrm{MF}}(T) \to \bar H_{\mathrm{MF}}(T) \equiv \sum_{j=1}^{n}\prod_{\ell\neq j}\frac{\mathrm{tr}[\rho_{\mathrm{GGE}}U^\dagger_{\bar V}(T)H_\ell U_{\bar V}(T)]}{L}H_\ell\,. \tag{4.37}$$

4.4 Pre-relaxation in XYZ models

In this section we investigate the pre-relaxation dynamics of a four-parameter family of spin Hamiltonians. This family describes the integrable XYZ spin-1/2 chain in the limit of small anisotropy in the z direction and in presence of small perturbations that can break integrability. Specifically, we consider the time evolution generated by the following Hamiltonian

$$H = J\sum_\ell\Big(\frac{1+\gamma}{4}\sigma^x_\ell\sigma^x_{\ell+1} + \frac{1-\gamma}{4}\sigma^y_\ell\sigma^y_{\ell+1} + \frac{g}{4}\sigma^z_\ell\sigma^z_{\ell+1} + \frac{gU}{4}\sigma^z_\ell\sigma^z_{\ell+2}\Big) + \frac{gh}{2}\sum_\ell\sigma^z_\ell\,, \tag{4.38}$$

which has the form (4.1) with $H_0 = H_{\mathrm{XY}}$ (4.14) and

$$V = \frac{J}{4}\sum_\ell(\sigma^z_\ell\sigma^z_{\ell+1} + U\sigma^z_\ell\sigma^z_{\ell+2}) + \frac{h}{2}\sum_\ell\sigma^z_\ell\,. \tag{4.39}$$

For a fixed $g \neq 0$, the model is integrable for $JU = h = 0$, corresponding to the spin-1/2 XYZ model, and for $JU = \gamma = 0$, corresponding to the XXZ spin-1/2 chain; otherwise it is non-integrable.

Following the results of Sections 4.1 and 4.3, for $g \ll 1$ and large time t in such a way that $T = gt \sim O(g^0)$, the initial state can be replaced by the corresponding GGE of the unperturbed Hamiltonian

$$|\Psi_0\rangle\,\langle\Psi_0| \to \rho_{\mathrm{GGE}} = \lim_{|S|\to\infty}\lim_{t\to\infty}\mathrm{tr}_{\bar S}[e^{-iH_{\mathrm{XY}}t}\,|\Psi_0\rangle\,\langle\Psi_0|\,e^{iH_{\mathrm{XY}}t}]\,, \tag{4.40}$$

and the perturbation V by its time average $\bar V$ (*cf.* (4.4)). We note that the free Hamiltonian H_{XY} does not play any role in the pre-relaxation limit, because it commutes with ρ_{GGE}. In

addition, the results of Sections 4.2 and 4.3 imply that the time evolution generated by $\bar{V}$ is equivalent to the one generated by the associated mean-field Hamiltonian (4.27).

The mapping into a mean-field problem can be decomposed in the following steps:

- Compute the time averaged perturbation $\bar{V}$;

- Construct the mean-field Hamiltonian $\bar{H}_{\rm MF}$;

- Solve the time evolution under $\bar{H}_{\rm MF}$ for *any* local observable.

In this section we will make intense use of the "symbol formalism" introduced in Subsection 2.1.2 of Chapter 2, this will turn out to be of great help in the calculations of the time average of the perturbation $\bar{V}$ and the explicit form of $\bar{H}_{MF}(T)$.

Let us now consider the first step of our plan of attack: compute the time average of the perturbation. We find that the three constituents of the interaction term in (4.39) have the following fermionic representation

$$\frac{1}{4}\sum_{\ell}\sigma^z_\ell\sigma^z_{\ell+j} = \frac{1}{4}\sum_{\ell} i a^y_\ell a^x_\ell i a^y_{\ell+j} a^x_{\ell+j}\,, \qquad j=1,2\,, \tag{4.41}$$

$$\frac{1}{2}\sum_{\ell}\sigma^z_\ell = \frac{1}{2}\sum_{\ell} i a^y_\ell a^x_\ell\,. \tag{4.42}$$

Neglecting the anomalous term (*cf.* 4.2) the time average of the perturbation can thus be written as a sum of products of time averaged quadratic operators as

$$\bar{V}(U,h) = \frac{J}{L}\sum_{s=0}^{1}\sum_{j=1}^{2} U^{j-1}\Big((-1)^{sj}\bar{H}^z_s\bar{H}^z_s + \bar{H}^{xy}_{s,j}\bar{H}^{yx}_{s,j} - \bar{H}^{xx}_{s,j}\bar{H}^{yy}_{s,j}\Big) + h\bar{H}^z_0\,. \tag{4.43}$$

The time averaged quadratic operators appearing on the right hand side of (4.43) are the fundamental blocks of (4.18) and read as

$$\begin{aligned}
\bar{H}^z_s &= \overline{\frac{1}{2}\sum_{\ell}(-1)^{s\ell}\sigma^z_\ell} = \overline{\frac{1}{2}\sum_{\ell}(-1)^{s\ell} i a^y_\ell a^x_\ell}\\
\bar{H}^{xy}_{s,j} &= \overline{\frac{1}{2}\sum_{\ell}(-1)^{s\ell}\sigma^x_\ell(\sigma^z_{\ell+1})^{j-1}\sigma^y_{\ell+j}} = \overline{\frac{1}{2}\sum_{\ell}(-1)^{s\ell}(-i)a^y_\ell a^y_{\ell+j}}\\
\bar{H}^{yx}_{s,j} &= \overline{\frac{1}{2}\sum_{\ell}(-1)^{s\ell}\sigma^y_\ell(\sigma^z_{\ell+1})^{j-1}\sigma^x_{\ell+j}} = \overline{\frac{1}{2}\sum_{\ell}(-1)^{s\ell} i a^x_\ell a^x_{\ell+j}}\\
\bar{H}^{xx}_{s,j} &= \overline{\frac{1}{2}\sum_{\ell}(-1)^{s\ell}\sigma^x_\ell(\sigma^z_{\ell+1})^{j-1}\sigma^x_{\ell+j}} = \overline{\frac{1}{2}\sum_{\ell}(-1)^{s\ell}(-i)a^y_\ell a^x_{\ell+j}}\\
\bar{H}^{yy}_{s,j} &= \overline{\frac{1}{2}\sum_{\ell}(-1)^{s\ell}\sigma^y_\ell(\sigma^z_{\ell+1})^{j-1}\sigma^y_{\ell+j}} = \overline{\frac{1}{2}\sum_{\ell}(-1)^{s\ell} i a^x_\ell a^y_{\ell+j}}\,.
\end{aligned} \tag{4.44}$$

Since we have to compute the time average of quadratic operators evolving according to a noninteracting Hamiltonian (*cf.* (4.14)) we can use the "symbol formalism", in particular Eq. (2.24). This allows to find the following exact result

$$\begin{aligned}\bar{\mathcal{O}}(k) &= \lim_{T\to+\infty}\frac{1}{T}\int_0^T \mathrm{d}t\,\mathcal{O}(k,t) = \lim_{T\to+\infty}\frac{1}{T}\int_0^T \mathrm{d}t\, e^{i\mathcal{H}^{(2)}(k)t}\mathcal{O}(k)e^{-i\mathcal{H}^{(2)}(k)t} \\ &= \frac{1}{2}\mathcal{O}(k,0) + \frac{1}{2}\left[\sigma^x e^{i\frac{k}{2}\sigma^z}\otimes\sigma^y e^{i\theta_{k/2}\sigma^z}\right]\mathcal{O}(k,0)\left[\sigma^x e^{i\frac{k}{2}\sigma^z}\otimes\sigma^y e^{i\theta_{k/2}\sigma^z}\right], \end{aligned} \tag{4.45}$$

where $\mathcal{O}(k)$ is the symbol of a quadratic operator and $\overline{\cdots}$ denotes the time average. Here we used the explicit expression of the symbol of the XY Hamiltonian (2.23) in the two-site translationally invariant representation; we need to use the two-site invariant representation because some of (4.44) are invariant only by a two-site translation. The symbols of the operators (4.44) read

$$\begin{aligned}
\bar{H}^z_s(k) &= \frac{J}{\varepsilon^2(k/2)}(\delta_{s,0}\mathcal{Q}_2(k) - \gamma\delta_{s,1}\mathcal{Q}_8(k)) \\
\bar{H}^{xy}_{s,1}(k) &= \delta_{s,0}\mathcal{Q}_4(k) + \delta_{s,1}\mathcal{Q}_6(k) \\
\bar{H}^{xy}_{s,2}(k) &= \delta_{s,0}\mathcal{Q}_3(k) + \delta_{s,1}\mathcal{Q}_7(k) \\
\bar{H}^{yx}_{s,1}(k) &= -\delta_{s,0}\mathcal{Q}_4(k) + \delta_{s,1}\mathcal{Q}_6(k) \\
\bar{H}^{yx}_{s,2}(k) &= -\delta_{s,0}\mathcal{Q}_3(k) + \delta_{s,1}\mathcal{Q}_7(k) \\
\bar{H}^{xx}_{s,1}(k) &= -\frac{J}{2\varepsilon^2(k/2)}\left((1+\gamma)+(1-\gamma)\cos k\right)(\delta_{s,0}\mathcal{Q}_1(k) - \delta_{s,1}\mathcal{Q}_5(k)) \\
\bar{H}^{xx}_{s,2}(k) &= -\frac{J}{\varepsilon^2(k/2)}\left[\gamma+(1-\gamma)(s+\cos k)\right](\delta_{s,0}\mathcal{Q}_2(k) + \delta_{s,1}\mathcal{Q}_8(k)) \\
\bar{H}^{yy}_{s,1}(k) &= -\frac{J}{2\varepsilon^2(k/2)}\left((1-\gamma)+(1+\gamma)\cos k\right)(\delta_{s,0}\mathcal{Q}_1(k) + \delta_{s,1}\mathcal{Q}_5(k)) \\
\bar{H}^{yy}_{s,2}(k) &= \frac{J}{\varepsilon^2(k/2)}\left(\gamma+s(1-\gamma)-(1+\gamma)(-1)^s\cos k\right)(\delta_{s,0}\mathcal{Q}_2(k) + \delta_{s,1}\mathcal{Q}_8(k)).
\end{aligned} \tag{4.46}$$

Here we expressed the results in terms of the symbols of the local charges of H_{XY} (*cf.* (2.32)

and (2.33))

$$
\begin{aligned}
\mathcal{Q}_1(k) &= \mathcal{I}^{(2)(\mathrm{e})}_{1;+}(k) = \varepsilon(k/2)\left[\sigma^x e^{i\frac{k}{2}\sigma^z}\right]\otimes\left[\sigma^y e^{i\theta_{k/2}\sigma^z}\right]\\
\mathcal{Q}_2(k) &= \mathcal{I}^{(2)(\mathrm{o})}_{1;+}(k) = \cos(k/2)\varepsilon(k/2)\,\mathbb{1}\otimes\left[\sigma^y e^{i\theta_{k/2}\sigma^z}\right]\\
\mathcal{Q}_3(k) &= \mathcal{I}^{(2)(\mathrm{e})}_{1;-}(k) = \sin(k)\,\mathbb{1}\otimes\mathbb{1}\\
\mathcal{Q}_4(k) &= \mathcal{I}^{(2)(\mathrm{o})}_{1;-}(k) = \sin(k/2)\left[\sigma^x e^{i\frac{k}{2}\sigma^z}\right]\otimes\mathbb{1}\\
\mathcal{Q}_5(k) &= \mathcal{J}^{(2)(\mathrm{e})}_{1;+}(k) = \varepsilon(k/2)\left[\sigma^y e^{i\frac{k}{2}\sigma^z}\right]\otimes\left[\sigma^x e^{i\theta_{k/2}\sigma^z}\right]\\
\mathcal{Q}_6(k) &= \mathcal{J}^{(2)(\mathrm{o})}_{1;+}(k) = \cos(k/2)\left[\sigma^y e^{i\frac{k}{2}\sigma^z}\right]\otimes\sigma^z\\
\mathcal{Q}_7(k) &= \mathcal{J}^{(2)(\mathrm{e})}_{1;-}(k) = \sin(k)\,\sigma^z\otimes\sigma^z\\
\mathcal{Q}_8(k) &= \mathcal{J}^{(2)(\mathrm{o})}_{1;-}(k) = \sin(k/2)\varepsilon(k/2)\,\sigma^z\otimes\left[\sigma^x e^{i\theta_{k/2}\sigma^z}\right].
\end{aligned}
\tag{4.47}
$$

As discussed in Chapter 2 (see also [68]), from the symbol of an operator it is possible to infer its local properties. In particular, a smooth symbol is associated with a quasi-local operator. If in addition the symbol has a finite number of nonzero Fourier components the associated operator is local, this is the case of the operators in (4.47) (the dispersion is cancelled by the denominator of the Bogoliubov angle). Equations (4.46) imply that $\bar{H}^{xy}_s, \bar{H}^{yx}_s$ are local while $\bar{H}^{xx}_s, \bar{H}^{yy}_s, \bar{H}^{z}_s$ are quasi-local, thus $\bar{V}$ (*cf.* (4.43)) is a member of the quasi-local extension of the class $\mathcal{E}$ studied in Section 4.3. As previously pointed out, we expect all the theorems of 4.3, in particular corollary 4.3.4, to remain valid also for quasi-local operators. This guarantees the time evolution generated by $H_{XY} + g\bar{V}$ to be *locally* equivalent to the one generated by the following quasi-local mean-field Hamiltonian

$$
\begin{aligned}
\bar{H}_{MF}(T) =& H_{XY} + 2Jg\sum_s (U+(-1)^s)\frac{\langle \bar{H}^z_s\rangle_T}{L}\bar{H}^z_s + Jg\sum_{s,j} U^{j-1}\Big(\frac{\langle \bar{H}^{xy}_{sj}\rangle_T}{L}\bar{H}^{yx}_{sj} + \frac{\langle \bar{H}^{yx}_{sj}\rangle_T}{L}\bar{H}^{xy}_{sj}\Big)\\
&- Jg\sum_{s,j} U^{j-1}\Big(\frac{\langle \bar{H}^{xx}_{sj}\rangle_T}{L}\bar{H}^{yy}_{sj} + \frac{\langle \bar{H}^{yy}_{sj}\rangle_T}{L}\bar{H}^{xx}_{sj}\Big) + hg\bar{H}^z_0\,,
\end{aligned}
\tag{4.48}
$$

where $\langle\mathcal{O}\rangle_T$ is the expectation value of the operator $\mathcal{O}$ in the mean-field description (*cf.* (4.36))

$$
\langle\mathcal{O}\rangle_T = \mathrm{Tr}\left[U_{\bar{V}}(T)\rho_{GGE}U^\dagger_{\bar{V}}(T)\mathcal{O}\right]. \tag{4.49}
$$

To determine the time evolution generated by $\bar{H}_{MF}(T)$ we need to solve the self-consistency conditions encoded in (4.48) and (4.49). To this end it is again convenient to exploit the representation in terms of symbols. Using (4.46), the symbol $\mathcal{H}_{MF}(k,T)$ of the time-dependent mean-field Hamiltonian can be written in terms of the symbols $\{\mathcal{Q}_\alpha(k), \alpha = 1,\dots,8\}$, as

follows[1]

$$\mathcal{H}_{MF}(k,T) = -\mathcal{Q}_1(k) + g\mathcal{V}_{MF}(k,T)\,, \tag{4.50}$$

$$\mathcal{V}_{MF}(k,T) = \frac{h}{\varepsilon^2(k/2)}\mathcal{Q}_2(k) + \sum_{\alpha=1}^{8} c_\alpha(k;\tilde{y}_\alpha)\mathcal{Q}_\alpha(k)\,. \tag{4.51}$$

The coefficients are given by

$$\begin{aligned}
c_1(k;\tilde{y}_1) &= -\frac{1+\cos k}{2\varepsilon^2(k/2)}(\tilde{y}_1^{(0)} + \tilde{y}_1^{(1)}) + \gamma^2\frac{1-\cos k}{2\varepsilon^2(k/2)}(\tilde{y}_1^{(0)} - \tilde{y}_1^{(1)}) \\
c_2(k;\tilde{y}_2) &= 2\frac{1+U}{\varepsilon^2(k/2)}\tilde{y}_2^{(0)} - 2U\frac{\cos k}{\varepsilon^2_{k/2}}\tilde{y}_2^{(1)} + 2U\gamma^2\frac{1-\cos k}{\varepsilon^2(k/2)}(\tilde{y}_2^{(0)} - \tilde{y}_2^{(1)}) \\
c_3(k;\tilde{y}_3) &= -U(1+\gamma^2)\tilde{y}_3^{(0)} - U(1-\gamma^2)\tilde{y}_3^{(1)} \\
c_4(k;\tilde{y}_4) &= -(1+\gamma^2)\tilde{y}_4^{(0)} - (1-\gamma^2)\tilde{y}_4^{(1)} \\
c_5(k;\tilde{y}_5) &= \frac{1+\cos k}{2\varepsilon^2(k/2)}(\tilde{y}_5^{(0)} + \tilde{y}_5^{(1)}) - \gamma^2\frac{1-\cos k}{2\varepsilon^2(k/2)}(\tilde{y}_5^{(0)} - \tilde{y}_5^{(1)}) \\
c_6(k;\tilde{y}_6) &= (1+\gamma^2)\tilde{y}_6^{(0)} + (1-\gamma^2)\tilde{y}_6^{(1)} \\
c_7(k;\tilde{y}_7) &= U(1+\gamma^2)\tilde{y}_7^{(0)} + U(1-\gamma^2)\tilde{y}_7^{(1)} \\
c_8(k;\tilde{y}_8) &= 2\gamma^2\frac{U-1}{\varepsilon^2(k/2)}\tilde{y}_8^{(0)} - 2\gamma^2 U\frac{\cos k}{\varepsilon^2(k/2)}\tilde{y}_8^{(1)} + 2U\frac{1+\cos k}{\varepsilon^2(k/2)}(\tilde{y}_8^{(0)} + \tilde{y}_8^{(1)})\,,
\end{aligned} \tag{4.52}$$

where we defined

$$\tilde{y}_\alpha^{(\ell)}(T) = \int_{-\pi}^{\pi}\frac{\mathrm{d}p}{2\pi}\frac{\cos(\ell p)}{\varepsilon^2(k/2)}y_\alpha(p,T)\,, \tag{4.53}$$

and

$$y_\alpha(k,T) = \frac{1}{8}\mathrm{Tr}\left[U_{\mathcal{H}_{MF}}(k,T)\Gamma_{GGE}(k)U^\dagger_{\mathcal{H}_{MF}}(k,T)\mathcal{Q}_\alpha(k)\right]\,, \tag{4.54}$$

$$U_{\mathcal{H}_{MF}}(k,T) = \mathrm{T}\exp\left[-i\int_0^T \mathrm{d}s\,\mathcal{V}_{MF}(k,s)\right]\,. \tag{4.55}$$

Here we introduced $\Gamma_{\mathrm{GGE}}(k)$: the symbol of the correlation matrix (*cf.* Property 2.1.2) in the unperturbed GGE.

By taking the first derivative of (4.54) with respect to T and using the (closed) commutation algebra of $\mathcal{Q}_\alpha(k)$ we get

$$\dot{y}_\alpha(k,T) = \frac{h}{\varepsilon^2(k/2)}\sum_{\gamma=1}^{8} f_k^{2\alpha\gamma}y_\gamma(k,T) + \sum_{\beta,\gamma=1}^{8} c_\beta(k;\tilde{y}_\gamma)f_k^{\beta\alpha\gamma}y_\gamma(k,T)\,. \tag{4.56}$$

The nonzero structure constants $f_k^{\alpha\beta\gamma}$ that are not connected to one another by symmetry are

[1]From now on we set $J = 1$.

given by

$$f_k^{562} = f_k^{548} = 2f_k^{647} = 2 \qquad f_k^{782} = f_k^{746} = 2f_k^{845} = -2(1-\cos k)$$
$$f_k^{584} = f_k^{526} = 2f_k^{827} = -2\varepsilon^2(k/2) \qquad f_k^{728} = f_k^{764} = 2f_k^{625} = 2(1+\cos k)\,. \tag{4.57}$$

The others follow from $f_k^{\beta\alpha\gamma} = -f_k^{\alpha\beta\gamma}$. In particular $\mathcal{Q}_1(k)$ and $\mathcal{Q}_3(k)$ commute with all the other charges, so $y_1(k)$ and $y_3(k)$ are conserved and the system (4.56) is reduced to 6 first order integro-differential equations that depend on a continuous variable k.

The solution of (4.56) entirely determines the time evolution generated by $\bar{H}_{\rm MF}$. Indeed, the expectation value of any local observable in the pre-relaxation limit can be computed using Wick's theorem with the correlation matrix

$$\left\langle \begin{pmatrix} a^x_{2n-1} \\ a^y_{2n-1} \\ a^x_{2n} \\ a^y_{2n} \end{pmatrix} \begin{pmatrix} a^x_{2\ell-1} & a^y_{2\ell-1} & a^x_{2\ell} & a^y_{2\ell} \end{pmatrix} \right\rangle =$$

$$= \delta_{\ell n}\mathbb{1}_4 + \int_{-\pi}^{\pi} \frac{\mathrm{d}k}{2\pi} e^{-i(n-\ell)k} \sum_{i=1}^{8} \frac{8y_i(k,T)}{\mathrm{tr}(\mathcal{Q}_i(k)^2)}\mathcal{Q}_i(k)\,. \tag{4.58}$$

Here we defined

$$\langle a_i^\alpha a_j^\beta \rangle \equiv \mathrm{tr}[U_{\bar{V}}(T)\rho_{GGE}U_{\bar{V}}^\dagger(T)a_i^\alpha a_j^\beta]\,, \qquad i,j = 1,\dots L\,, \quad \alpha,\beta = x,y\,. \tag{4.59}$$

Eq. (4.58) also means that the reduced density matrices of subsystems are gaussian at any time, so the two assumptions (a) and (b) (see the end of Section 4.2) could be also reformulated as a single hypothesis of RDMs being gaussian.

Equations (4.58) and (4.56) are the main results of this section: they allow us to compute dynamics of the expectation values of local observables in the pre-relaxation limit $g \ll 1$ and $gt \sim O(g^0)$ of the model described by the Hamiltonian (4.38) by solving a nonlinear system of equations, which is rather easy from a numerical point of view. We remind the reader that g measures the strength of the perturbation breaking the symmetry which originates the additional families of conserved charges of the unperturbed model.

Reflection symmetry The Hamiltonian (4.38) is reflection symmetric, that is to say it is invariant under the transformation

$$\sigma^\alpha_\ell \to \sigma^\alpha_{s+L-\ell} \qquad \alpha \in \{x, y, z\}\,, \tag{4.60}$$

where s is odd for reflections about a bond and even for those about a site.

The reflection operator acts on the Majorana fermions as follows

$$\begin{aligned} a^x_\ell &\to i\Big(\prod_j \sigma^z_j\Big) a^y_{s+L-\ell} \\ a^y_\ell &\to -i\Big(\prod_j \sigma^z_j\Big) a^x_{s+L-\ell}\,. \end{aligned} \tag{4.61}$$

Therefore the symbol $\mathcal{H}$ of a one-site shift invariant operator transforms as

$$\mathcal{H}^{(1)}(k) \to \sigma^y \mathcal{H}^{(1)}(-k)\sigma^y\,, \tag{4.62}$$

while for two-site shift invariant operators we find

$$\mathcal{H}^{(2)}(k) \to \begin{cases} \sigma^x \otimes \sigma^y\ \mathcal{H}^{(2)}(-k)\ \sigma^x \otimes \sigma^y & s \text{ odd} \\ e^{-i\frac{k}{2}\sigma^z} \otimes \sigma^y\ \mathcal{H}^{(2)}(-k)\ e^{i\frac{k}{2}\sigma^z} \otimes \sigma^y & s \text{ even}\,. \end{cases} \tag{4.63}$$

The symbols (4.47) of the conservation laws have the simple transformation rules

$$\begin{aligned} \mathcal{Q}_{1,2}(k) &\longrightarrow \mathcal{Q}_{1,2}(k) \\ \mathcal{Q}_{3,4}(k) &\longrightarrow -\mathcal{Q}_{3,4}(k) \\ \mathcal{Q}_{5,6}(k) &\longrightarrow -(-1)^s Q_{5,6}(k) \\ \mathcal{Q}_{7,8}(k) &\longrightarrow (-1)^s \mathcal{Q}_{7,8}(k)\,. \end{aligned} \tag{4.64}$$

Since a shift by one site is equivalent to a reflection about a bond followed by a reflection about a site, we recover the transformation rules pointed out in Chapter 2.

If the initial state is reflection symmetric about a *bond*, $y_j(k,t) = 0$ for $j = 3, 4, 7, 8$ (*cf.*

Eq.(4.54)). Thus, the system of Equations (4.56) can be reduced to

$$\begin{aligned}
\dot{y}_2(k,T) &= -2c_5(k;\tilde{y}_5)\varepsilon^2(k/2)y_6(k,T) + c_6(k;\tilde{y}_6)(1+\cos k)y_5(k,T) \\
\dot{y}_5(k,T) &= -2c_6(k;\tilde{y}_6)y_2(k,T) + 2\Big(\frac{h}{\varepsilon^2(k/2)} + c_2(k;\tilde{y}_2)\Big)\varepsilon^2(k/2)y_6(k,T) \\
\dot{y}_6(k,T) &= 2c_5(k;\tilde{y}_5)y_2(k,T) - \Big(\frac{h}{\varepsilon^2(k/2)} + c_2(k;\tilde{y}_2)\Big)(1+\cos k)y_5(k,T)\,.
\end{aligned} \tag{4.65}$$

We numerically solved these equations for different values of the parameters and identified three distinct qualitative behaviours:

- *Stationarity*: The expectation values of the observables remain equal to the initial values given by the unperturbed GGE (Fig. 4.1a).
- *Local relaxation*: The observables relax to a different stationary value: one-site shift invariance is restored in some cases (Fig. 4.1b) while remaining broken in others (Fig. 4.1c).
- *Persistent oscillations*: The amplitude of the oscillations of the expectation values of the observables does not approach zero (Fig. 4.1d).

It is worth remarking that, even when there is relaxation (at some intermediate times with $Jt \gg g^{-1}$), the stationary state is not thermal, being the local conservation laws of H_{XY} with symbol proportional to $\mathcal{Q}_1(k)$ and $\mathcal{Q}_3(k)$ (namely the charges the preserve non-abelian integrability) conserved also for the perturbed Hamiltonian.

4.4.1 Perturbations preserving integrability

Let us perform a qualitative analysis of the case $U = \gamma = 0$, in which H (4.38) is the Hamiltonian of the XXZ spin-1/2 chain. In this case the Hamiltonian is invariant under U(1) rotations around the z axis, thus $S^z = \frac{1}{2}\sum_\ell \sigma^z_\ell$ commutes with H. This drastically simplifies the dependence on h of the time evolution of observables. In particular, the expectation value of the one-site shift invariant conservation laws is independent of the magnetic field.

In this case, the system of Equations (4.65) can be rewritten as follows:

$$\begin{aligned}
\frac{1}{2}\dot{y}_2^{[n]}(T) &= y_5^{[n]}(T)y_6^{[0]}(T) - y_6^{[n]}(T)y_5^{[0]}(T) \\
\frac{1}{2}\dot{y}_5^{[n]}(T) &= -(2y_2^{[n]}(T) + y_2^{[n-1]}(T) + y_2^{[n+1]}(T))y_6^{[0]}(T) + (h + 4y_2^{[0]}(T))y_6^{[n]}(T) \\
\frac{1}{2}\dot{y}_6^{[n]}(T) &= (2y_2^{[n]}(T) + y_2^{[n-1]}(T) + y_2^{[n+1]}(T))y_5^{[0]}(T) - (h + 4y_2^{[0]}(T))y_5^{[n]}(T)\,,
\end{aligned} \tag{4.66}$$

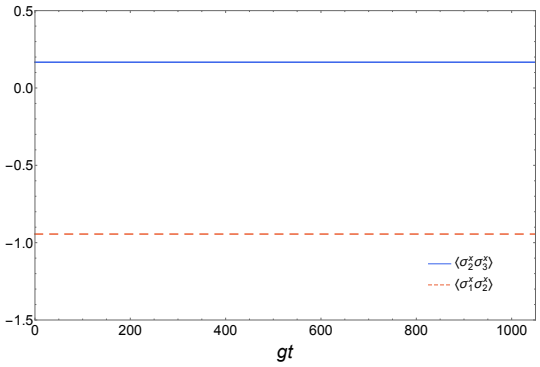

(a) The correlators are stationary. This figure is obtained for $\gamma = 2$, $h = 0$, and $U = 5$. We find stationary behaviour whenever the initial state is reflection symmetric, $y_2(k) = y_6(k) = 0$ (*cf.* (4.54)), and $h = 0$ (*cf.* (4.38)).

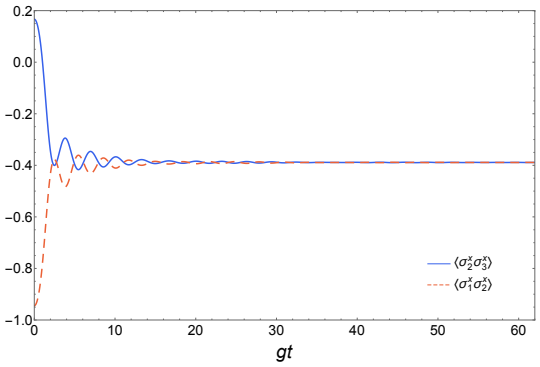

(b) The correlators rapidly relax to the same stationary value, restoring translation invariance. We verified relaxation up to $gt = 1000$. This figure is obtained for $\gamma = 2$, $h = 1$ and $U = -2$ (*cf.* (4.38)).

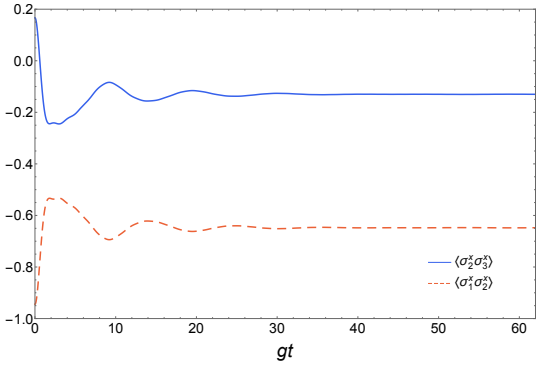

(c) The correlators rapidly relax to different stationary values. We verified relaxation up to $gt = 1000$. This figure is obtained for $\gamma = 2$, $h = 2$ and $U = 2$ (*cf.* (4.38)).

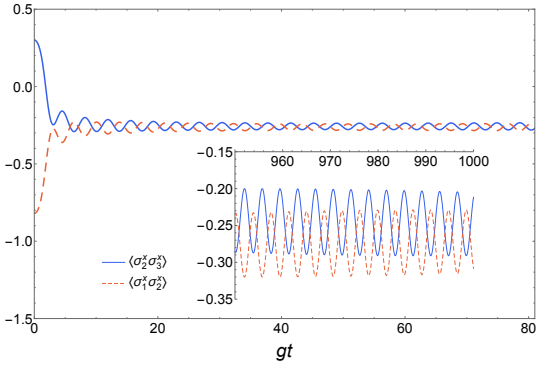

(d) The correlators exhibit persistent oscillations on the time window explored. Inset: the amplitude of the oscillations is still unabated at $gt = 1000$. This figure is obtained for $\gamma = 4$, $h = 1$ and $U = -2$ (*cf.* (4.38)).

Figure 4.1: Time evolution of $\langle \sigma_1^x \sigma_2^x \rangle$ (red dashed) and $\langle \sigma_2^x \sigma_3^x \rangle$ (blue) determined by the Hamiltonian H (4.38) in the pre-relaxation limit $g \ll 1$ with $gt = O(g^0)$; in this limit the observables are functions of the rescaled variable $T = gt$. The figures report four qualitatively different behaviours that one observes varying the parameters of H.

where we defined

$$y_2^{[n]}(T) = \int_{-\pi}^{\pi} \frac{\mathrm{d}p}{2\pi} \frac{\cos(np)}{1+\cos p} y_2(p,T)\,, \qquad y_{5,6}^{[n]}(T) = \int_{-\pi}^{\pi} \frac{\mathrm{d}p}{2\pi} \cos(np) y_{5,6}(p,T)\,. \tag{4.67}$$

We note that, despite the denominator, $y_2^{[n]}$ are expectation values of (quasi)-local operators, as well as $y_{5,6}^{[n]}$. Indeed we have $\lim_{k\to\pm\pi} \mathcal{Q}_2(k)/(1+\cos p) =$ finite.

To understand how the solutions of (4.66) behave in time, it is useful to start considering the $n=0$ components. Inspecting (4.66) we find

$$\begin{aligned}
y_2^{[0]}(T) &= \frac{\langle S^z \rangle}{2L} \equiv \frac{s^z}{2} \\
y_5^{[0]}(T) &= y_5^{[0]}(0) \cos\Big(\int_0^T \mathrm{d}\tau\, (2h + 4m(\tau))\Big) + y_6^{[0]}(0) \sin\Big(\int_0^T \mathrm{d}\tau\, (2h + 4m(\tau))\Big) \\
y_6^{[0]}(T) &= y_6^{[0]}(0) \cos\Big(\int_0^T \mathrm{d}\tau\, (2h + 4m(\tau))\Big) - y_5^{[0]}(0) \sin\Big(\int_0^T \mathrm{d}\tau\, (2h + 4m(\tau))\Big)\,.
\end{aligned} \tag{4.68}$$

Here we defined

$$m(T) \equiv \frac{s^z}{2} - y_2^{[1]}(T) = s^z - \frac{\langle Q_2 \rangle_T}{L} = \frac{1}{4}\langle \sigma_\ell^z \rangle + \frac{1}{8}\left\langle \sigma_{\ell-1}^x \sigma_\ell^z \sigma_{\ell+1}^x + \sigma_{\ell-1}^y \sigma_\ell^z \sigma_{\ell+1}^y \right\rangle_T . \tag{4.69}$$

We see that both $y_2^{[0]}(T)$ and $C \equiv (y_5^{[0]}(T))^2 + (y_6^{[0]}(T))^2$ are conserved. In particular it is convenient to consider the two cases $C=0$ and $C \neq 0$ separately.

If $C=0$, the equations for different values of n are decoupled, and the solution of (4.66) is trivially given by

$$\begin{aligned}
y_2^{[n]}(T) &= y_2^{[n]}(0) \\
y_5^{[n]}(T) &= y_5^{[n]}(0) \cos(2(h+2s^z)T) + y_6^{[n]}(0) \sin(2(h+2s^z)T) \\
y_6^{[n]}(T) &= y_6^{[n]}(0) \cos(2(h+2s^z)T) - y_5^{[n]}(0) \sin(2(h+2s^z)T)\,.
\end{aligned} \tag{4.70}$$

For $h \neq -2s^z$, local observables keep oscillating in time, otherwise, in the pre-relaxation window, the expectation values of local observables do not move from the values reached at times $1 \ll Jt \ll g^{-1}$.

If $C \neq 0$, is sufficient to look at (4.68) to infer that relaxation is possible only if

$$\exists \lim_{T\to\infty} m(T) = -\frac{h}{2}\,, \tag{4.71}$$

$$\exists \lim_{T\to\infty} \Big| \int_0^T \mathrm{d}\tau \Big(m(\tau) + \frac{h}{2} \Big) \Big| < \infty\,. \tag{4.72}$$

We see that $m(T)$ could be interpreted as a sort of 'induced magnetisation' that h must compete with. It turns out that (4.71) and (4.72) are also sufficient conditions for the relaxation of local degrees of freedom. This can be seen as follows. If the conditions (4.71) and (4.72) are verified, $m(T)$, $y_5^{[0]}(T)$ and $y_6^{[0]}(T)$ relax to a time independent value for long times and (4.66) becomes a linear system, which can be easily solved. Doing that, one can verify that all $\{y_i^{[n]}(T)\}$ relax to time independent values.

Therefore the variance

$$\Delta m = \lim_{T\to\infty} \Big(\frac{1}{T} \int_T^{2T} \mathrm{d}t\, m(t)^2 - \Big(\frac{1}{T} \int_T^{2T} \mathrm{d}t\, m(t) \Big)^2 \Big)^{1/2} , \tag{4.73}$$

behaves like an 'order parameter' for the transition, indeed it vanishes in the region of the parameter space where the system relaxes to time independent values and it is not analytic at the boundaries of it (the first derivative is discontinuous).

Some aspects of the solutions of nonlinear systems like (4.66) can be worked out analytically. In the present context this would involve the study of quantum quenches from rather artificial initial states. In Ref. [2], however, we considered the time evolution generated by the non-local Hamiltonian

$$H(\tilde{g},\lambda) = -\sum_{\ell}^{L} (\sigma_\ell^x \sigma_{\ell+1}^x + \tilde{g}\sigma_\ell^z) + \frac{\lambda}{L} \Big(\sum_{\ell}^{L} \sigma_\ell^z \Big)^2 . \tag{4.74}$$

In the thermodynamic limit, the time evolution generated by (4.74) is equivalent to the one generated by

$$H_{\mathrm{MF}}^{\Psi_0}(t) = -\sum_{\ell} (\sigma_\ell^x \sigma_{\ell+1}^x + h(t)\sigma_\ell^z) , \tag{4.75}$$

as a consequence of corollary 4.3.4. The function $h(t)$ is the solution of the self-consistent equation

$$h(t) = \tilde{g} - 2\lambda \, \langle \Psi_0 | \mathrm{T}^\dagger \exp\Big(i \int_0^t \mathrm{d}\tau H_{\mathrm{MF}}^{\Psi_0}(\tau) \Big) \sigma_\ell^z \, \mathrm{T} \exp\Big(-i \int_0^t \mathrm{d}\tau H_{\mathrm{MF}}^{\Psi_0}(\tau) \Big) | \Psi_0 \rangle \ . \tag{4.76}$$

The equations imposed by the self consistency conditions of the mean field solution can be brought in a form which is extremely similar to (4.66). The advantage is that the qualitative analysis can be carried out for more conventional initial states, such as the ground state of the TFIC for a given magnetic field h_0. The results of the analysis can be summarised by the "quench dephasing diagram" in Fig. 4.2, which depicts in white the regions of the parameter space where the relaxation happens and in grey the regions where there is a persistent oscillatory behaviour. The appearance of oscillatory behaviour has been related to the presence of localised excitations in the mean field Hamiltonian (4.75). Finally we note that in Ref. [2] we also

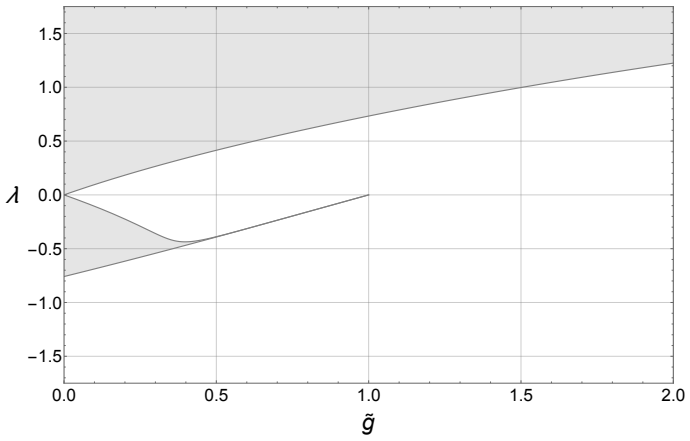

Figure 4.2: Quench dephasing diagram of the model (4.74) in the limit of small quench with energy close to the ground state one. The dark region corresponds to persistent oscillatory behaviour at any time after the quench.

excluded that (4.74) and similar Hamiltonians (for example the one considered in [65]) can lead to thermalisation in the thermodynamic limit.

4.4.2 Perturbations breaking integrability: linearisation

We now move to the case where the Hamiltonian (4.38) is not integrable. In order to make some progress we focus on quantum quenches starting from the dimer product state

$$|\mathrm{MG}\rangle = \frac{|\uparrow\downarrow\rangle - |\downarrow\uparrow\rangle}{\sqrt{2}} \otimes \cdots \otimes \frac{|\uparrow\downarrow\rangle - |\downarrow\uparrow\rangle}{\sqrt{2}}\,, \tag{4.77}$$

which is the ground state of the Majumdar-Ghosh Hamiltonian

$$H_0 = \frac{J}{4}\sum_{\ell=1}^{L} \vec{\sigma}_\ell \cdot \vec{\sigma}_{\ell+1} + \frac{1}{2}\vec{\sigma}_\ell \cdot \vec{\sigma}_{\ell+2}\,. \tag{4.78}$$

Despite the model being interacting, (4.77) is a two-site shift invariant Slater determinant, whose correlation matrix has the following symbol

$$\Gamma_{\mathrm{MG}}(k) = \sigma^x \otimes \sigma^y\,. \tag{4.79}$$

The initial conditions for $\{y_\alpha(k)\}$ (4.54) are determined by the GGE correlation matrix for $g = 0$. They can be obtained by expanding $\Gamma_{\mathrm{MG}}(k)$ in the base of the symbols (4.47) of the conserved charges of H_{XY} (the remaining space is zeroed by the time evolution, as $1 \ll Jt$ *cf.*

(4.36))

$$\Gamma_{\rm GGE}(k;0) = \sum_{i=1}^{8} \frac{{\rm tr}[\Gamma_{\rm MG}(k)\mathcal{Q}_i(k)]}{{\rm tr}[(\mathcal{Q}_i(k))^2]}\mathcal{Q}_i(k)\,. \tag{4.80}$$

We find

$$\Gamma_{\rm GGE}(k;0) = \frac{1+\cos k}{1+\cos k+\gamma^2(1-\cos k)}\mathcal{Q}_1(k) - \gamma\frac{1-\cos k}{1+\cos k+\gamma^2(1-\cos k)}\mathcal{Q}_5(k)\,. \tag{4.81}$$

The only nonzero initial conditions are given by (*cf.* (4.54))

$$\begin{aligned} y_1(k,0) &= \frac{1+\cos k}{4}\,, \\ y_5(k,0) &= -\gamma\frac{1-\cos k}{4}\,. \end{aligned} \tag{4.82}$$

The initial state is reflection symmetric about a bond, so we can use the reduced system (4.65). As only y_5 appears in (4.65), for $\gamma = 0$ (see previous section) the solution is independent of time.

It is easy to see that also for $h = 0$ the system (4.65) with the initial conditions (4.82) has a stationary solution. We therefore assume $\gamma, h \neq 0$. Since $c_j(k;y_j)$ are linear homogeneous functions of y_j, the magnetic field h enters into the equations essentially as a scale factor. It is useful to rescale the variables as follows

$$\tau = 2hT = 2hgt \qquad \epsilon = \frac{\gamma}{2h} \qquad z_j = \frac{2y_j}{\gamma} \qquad \gamma_j = \frac{2c_j}{\gamma}\,. \tag{4.83}$$

From (4.65) we then obtain

$$\begin{aligned} \partial_\tau z_2(k,\tau) &= -\epsilon\,\varepsilon^2(k/2)\gamma_5(k,\tau)z_6(k,\tau) + \epsilon\cos^2\frac{k}{2}\gamma_6(k,\tau)z_5(k,\tau) \\ \partial_\tau z_5(k,\tau) &= -\epsilon\gamma_6(k,\tau)z_2(k,\tau) + (1+\epsilon\,\varepsilon^2(k/2)\gamma_2(k,\tau))z_6(k,\tau) \\ \partial_\tau z_6(k,\tau) &= \epsilon\gamma_5(k,\tau)z_2(k,\tau) - (1+\epsilon\,\varepsilon^2(k/2)\gamma_2(k,\tau))\frac{\cos^2\frac{k}{2}}{\varepsilon^2(k/2)}z_5(k,\tau)\,, \end{aligned} \tag{4.84}$$

with the initial conditions

$$z_2(k,0) = z_6(k,0) = 0 \qquad z_5(k,0) = -\sin^2\frac{k}{2}\,. \tag{4.85}$$

For generic ϵ the system of equations is not exactly solvable, but the limit of small ϵ allows a linear approximation. For not too large rescaled times (we will come back to this point later) the terms that are multiplied by ϵ in the last two equations can be neglected, while the functions that appear on the right hand side of the first equation can be computed at $O(\epsilon^0)$.

For z_5 and z_6 we obtain the simple solution

$$z_5(k,\tau) \approx -\sin^2\frac{k}{2}\cos\Big(\frac{\cos\frac{k}{2}}{\varepsilon(k/2)}\tau\Big)$$
$$z_6(k,\tau) \approx \sin^2\frac{k}{2}\frac{\cos\frac{k}{2}}{\varepsilon(k/2)}\sin\Big(\frac{\cos\frac{k}{2}}{\varepsilon(k/2)}\tau\Big)\,, \tag{4.86}$$

while z_2 is a slightly more complicated function that involves integrals over the momentum of $z_{5,6}$, namely

$$z_2(k,\tau) \approx \epsilon\frac{\sin k\sin\frac{k}{2}}{2}\int_{-\pi}^{\pi}\frac{\mathrm{d}p}{2\pi}\sum_{\sigma=\pm}g_\sigma(k,p)f(\frac{\cos\frac{k}{2}}{\varepsilon(k/2)}+\sigma\frac{\cos\frac{p}{2}}{\varepsilon(p/2)};\tau)\,. \tag{4.87}$$

Here we defined

$$g_\sigma(k,p) \equiv \frac{\sin^2\frac{p}{2}}{\varepsilon(p/2)}\Big[\frac{\cos^2\frac{k}{2}\cos^2\frac{p}{2}-\gamma^2\sin^2\frac{k}{2}\sin^2\frac{p}{2}}{\varepsilon(k/2)\varepsilon(p/2)}+\sigma\cos\frac{k}{2}\cos\frac{p}{2}\Big]\,, \tag{4.88}$$

$$f(x;\tau) \equiv \frac{1-\cos(x\tau)}{x}\,. \tag{4.89}$$

For small ϵ and given γ, $z_2(k,\tau)$ relaxes to the stationary value

$$z_2(k,\infty) = \frac{\epsilon\sin^2 k}{8\gamma^2}\Big[1-3\gamma^2+(2+4\gamma^2)\cos k+(1-\gamma^2)\cos 2k\Big]\,. \tag{4.90}$$

Let us now estimate the time window in which this approximation is appropriate. From (4.86) it follows that γ_5 and γ_6 decay to zero as $\tau^{-\frac{3}{2}}$. Instead, since z_2 approaches a nonzero stationary value, γ_2 is of the same order of z_2. This means that, as the time increases, the first term on the right hand side of the last two equations of (4.84) becomes more and more negligible with respect to the other term multiplied by ϵ. By neglecting the former we obtain essentially the same solution as before (*cf.* (4.86)), with the replacement

$$\tau \to \tau+\epsilon\,\varepsilon^2(k/2)\int_0^\tau \mathrm{d}s\gamma_2(k,s) = \tau\left(1+\epsilon\,\varepsilon^2(k/2)\gamma_2(k,\infty)\right)+\dots\,. \tag{4.91}$$

Being $\gamma_2 \sim O(\epsilon)$, after a rescaled time $\tau \sim \frac{1}{\epsilon^2}$, the correction to $z_{5,6}$ becomes comparable with the function itself. Assuming that the relevant part of the time evolution occurs within this timescale, the linear approximation is justified only if $|z_2| \ll 1$ (and $\epsilon \ll 1$). For $\gamma < 1/2$ we find $|z_2(k,\infty)| < \frac{\epsilon}{6\gamma^2}$, so we obtain the consistency condition

$$\frac{1}{12h} \ll \gamma \ll 2h\,. \tag{4.92}$$

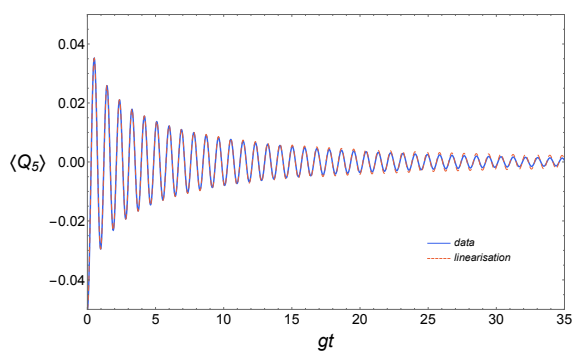

(a) The time evolution of $\langle Q_5 \rangle_t = \gamma \int \frac{\mathrm{d}k}{4\pi} z_5(k,t)$, where Q_5 is the conserved charge of H_{XY} corresponding to the symbol $\mathcal{Q}_5(k)$ (4.47) for a time evolution starting from the state $|MG\rangle$ (4.77). The parameters of the Hamiltonian (4.38) are $\gamma = 0.2$, $h = 3.5$ and $U = -1$, hence $\epsilon \approx 0.029$ (*cf.* (4.83)) and γ fulfils the consistency condition (4.92) of the linearisation procedure. The analytical prediction of (4.86) (red dashed line) is in excellent agreement with the numerical data (blue line).

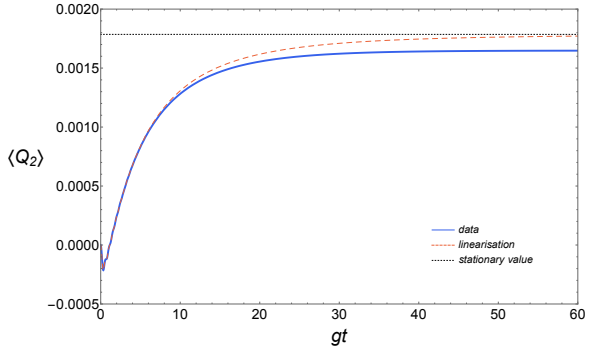

(b) The time evolution of $\langle Q_2 \rangle_t = \gamma \int \frac{\mathrm{d}k}{4\pi} z_2(k,t)$, where Q_2 is the conserved charge of H_{XY} corresponding to the symbol $\mathcal{Q}_2(k)$ (4.47) for a time evolution starting from the state $|MG\rangle$ (4.77). The parameters of the Hamiltonian (4.38) are $\gamma = 0.2$, $h = 3.5$ and $U = -1$, hence $\epsilon \approx 0.029$ (*cf.* (4.83)) and γ fulfils the consistency condition (4.92) of the linearisation procedure. The analytical prediction of (4.86) (red dashed line) is in fairly good agreement with the numerical data (blue line). The stationary value in the linearised approximation (black dotted line) is $\langle Q_2 \rangle = \frac{(1-5\gamma^2)}{128h}$ (*cf.* (4.90)).

Figure 4.3: The results of the linear approximation compared with those of the numerical solution.

Figures 4.3a and 4.3b report a comparison between the solution of the linearised problem and the full numerical solution of system (4.65) for a set of parameters fulfilling (4.92).

From the expressions of $z_5(k,\tau), z_6(k,\tau)$ given in Eq. (4.86) and of $z_2(k,\tau)$ reported in Eq. (4.87), we can directly compute the time evolution of the expectation value of any local observable in the pre-relaxation limit. Corollary 4.3.4, indeed, allows us to apply Wick's theorem at any time (in the limit under examination) and the correlation matrix is given by (4.58).

Any integral involving z_5 and z_6 approaches zero and z_2 becomes independent of time even if not integrated. Therefore, in the limit (4.92) and for large times the expectation value of any local observable relaxes to a stationary value that can be described by the correlation matrix with symbol

$$\lim_{\tau \to \infty^{(*)}} \Gamma(k;\tau) = \frac{\gamma z_1(k,0)}{\varepsilon^2(k/2)} \mathcal{Q}_1(k) + \frac{\gamma z_2(k,\infty)}{\varepsilon^2(k/2)\cos^2(k/2)} \mathcal{Q}_2(k)\,, \tag{4.93}$$

where the infinite time limit $\tau \to \infty^{(*)}$ must be understood within the limits of validity of the linear approximation.

We point out that one-site shift invariance is restored, indeed the only contributions to the correlation matrix at infinite times arise from $\mathcal{Q}_1(k)$ and $\mathcal{Q}_2(k)$, which are symbols of one-site shift invariant operators. The manifestly one-site shift invariant expression of the correlation

matrix in the limit (4.93) reads

$$\lim_{\tau\to\infty^{(*)}} \left\langle \begin{pmatrix} a_n^x \\ a_n^y \end{pmatrix} \begin{pmatrix} a_\ell^x & a_\ell^y \end{pmatrix} \right\rangle = \delta_{\ell n}\mathbb{1}_2 + \int_{-\pi}^{\pi} \frac{\mathrm{d}k}{2\pi} e^{-i(n-\ell)k}\, \Gamma^{(1)}(k)\,, \tag{4.94}$$

with

$$\Gamma^{(1)}(k) = \frac{4h + \tan^2 k \cos k(1 - 3\gamma^2 + (2+4\gamma^2)\cos 2k + (1-\gamma^2)\cos 4k)}{4h \sec^2 k} \sigma^y e^{i\theta_k \sigma^z}\,, \tag{4.95}$$

where θ_k is given in Eq. (2.13).

Despite one-site shift invariance being restored in (4.93), the asymptotic value is not given by the average over a shift of the expectation value of the operator in the GGE of the unperturbed model. Indeed the one-site shift average of (4.81) is proportional to $\mathcal{Q}_1(k)$ (*cf.* (4.64)) but the symbol of the large time correlation matrix (4.93) has also a term proportional to $\mathcal{Q}_2(k)$. Consequently, the shift-averaged stationary values can *not* be recovered from the $g = 0$ ones. For example we have (*cf.* (4.46) and (4.90))

$$\lim_{1\ll t\ll \frac{1}{g}} \left\langle \frac{\sigma_{2\ell-1}^z + \sigma_{2\ell}^z}{2} \right\rangle = O(g) \tag{4.96}$$

$$\lim_{2hgt\to\infty^{(*)}} \left\langle \frac{\sigma_{2\ell-1}^z + \sigma_{2\ell}^z}{2} \right\rangle = -\frac{\gamma^2}{16h}\frac{3+\gamma}{(1+\gamma)^3} + O(g)\,, \tag{4.97}$$

where we highlighted that there are $O(g)$ corrections. Besides this particular quench in a non-integrable model, similar issues can arise also in the integrable case, where it is generally believed that at infinite time after the quench the expectation values can be computed in a GGE constructed with the (quasi-)local conservation laws of the model.

4.5 Conclusions

In this chapter we discussed the *pre-relaxation*, a dynamical phenomenon that arises when small perturbations break symmetries affecting the late time behaviour of local observables. The particular case where the perturbation breaks (abelian) integrability is usually called prethermalisation, which is generally thought as a two-step process where local observables experience virtual relaxation before approaching thermal-like expectation values. The relaxation process, however, can also be more complicated, following many steps of quasi-stationary behaviour. This happens in particular when the model is close to an integrability point characterised by additional, non-commuting, local conserved charges (*cf.* Chapter 2). In order to extract the

pre-relaxation behaviour one must therefore identify the correct timescale of the phenomenon.

We have considered the problem of pre-relaxation after quantum quenches in weakly interacting models, starting from initial states with cluster decomposition properties, focussing on the particular situation where the unperturbed Hamiltonian is one-site shift invariant and has a non-abelian set of local conservation laws that break one-site shift invariance. Specifically, we considered interacting perturbations to the XY spin-1/2 chain and investigated both integrable extensions, like the Heisenberg XYZ model, and the effects of perturbations that break integrability.

We identified the inverse perturbation strength as the relevant timescale of pre-relaxation and studied the dynamics of local observables at times proportional to it.

A key result of our analysis is that, despite the model being interacting, the noninteracting structure remnant of the unperturbed Hamiltonian survives the pre-relaxation limit and it is manifested in the validity of Wick's theorem. However interactions do affect the dynamics by introducing a non-trivial time dependence in the effective noninteracting Hamiltonian that generates the time evolution. The most striking effect is probably that, even if local degrees of freedom approach stationary values, these can not be generally predicted without following the entire dynamics.

We have shown how to recast the non-equilibrium problem into a system of nonlinear differential equations involving expectation values of quasi-local operators. The system of equations has qualitatively distinct solutions, which vary from trivial stationarity to persistent oscillatory behaviour over the entire time window considered. We have not found any relevant difference between integrable and non-integrable perturbations, suggesting that the scenario of thermalisation in generic models arises at much larger times.

For the very nature of the local conservation laws of the XY model, in order to have a non-trivial time evolution the initial state must break one-site shift invariance. For a particular initial state of that kind we considered a limit in which the equations can be linearised and exhibited the analytic solution, in which one-site shift invariance is eventually restored. The regime worked out analytically shows quite clearly the *importance of cluster decomposition* in the non-equilibrium problem. While, as mentioned above, the pre-relaxation limit is trivial for one-site shift invariant states, a shift symmetrisation of the two-site shift invariant initial state has a non-trivial time evolution. This is because cluster decomposition has been lost with the symmetrisation. It is important to take into account such aspect when analytic predictions of the late time stationary behaviour are compared with numerical data at times in which one-site shift invariance is not yet restored.

Finally, we would like to stress that our description of the pre-relaxation limit is based on a few hypotheses. In particular, we neglected some "anomalous terms" (*cf.* (4.20)), proving only the self-consistency of the conjecture. In the next chapter we will compare the results found here with those found with a different technique: the first order EOM; finding an excellent agreement. It is also worth mentioning that a number of careful checks against infinite time-evolving block-decimation (iTEBD) simulations [176] confirmed the validity of the assumptions presented here in the case of the XYZ spin-1/2 chain; a more rigorous analysis of the regimes of validity of our approximations is, however, left to future research.

Appendix

4.A Time averages of interacting operators

In this appendix we show the validity of Property 4.2.1. The Property can be most easily proven for Jordan-Wigner fermions

$$c_j = \frac{1}{2}(a_j^x - i a_j^y)\,; \tag{4.98}$$

the relation for the Majorana fermions a_j^x, a_j^y will then follow by linearity.

In order to proceed it is convenient to introduce the following notation

$$\mathbf{c}_j^\alpha(t) \equiv \begin{cases} c_j^\dagger(t) & \alpha = + \\ c_j(t) & \alpha = -\,. \end{cases} \tag{4.99}$$

The relation between $c^\dagger, c$ and the Bogoliubov fermions $b^\dagger(k), b(k)$ that diagonalise the unperturbed (noninteracting) Hamiltonian H_{XY} (4.14) can be written as

$$\mathbf{c}_j^\alpha(t) = \frac{1}{\sqrt{L}} \sum_k \sum_{\beta=\pm} e^{i\alpha jk} U(k)_\beta^\alpha \mathbf{b}_\beta(k) e^{i\beta\varepsilon(k)t}\,. \tag{4.100}$$

Here $U(k)$ is the 2×2 matrix defining the Bogoliubov transformation, ε_k is the dispersion relation

$$\varepsilon(k) = J\sqrt{\cos^2 k + \gamma^2 \sin^2 k} \tag{4.101}$$

and we set

$$\mathbf{b}_\beta(k) \equiv \begin{cases} b^\dagger(k) & \beta = + \\ b(-k) & \beta = -\,. \end{cases} \tag{4.102}$$

The relation (4.18) is then equivalent to

$$\frac{1}{L}\overline{\sum_j \mathbf{c}_{j+n1}^{\alpha_1}\mathbf{c}_{j+n2}^{\alpha_2}\mathbf{c}_{j+n3}^{\alpha_3}\mathbf{c}_{j+n4}^{\alpha_4}} = \tilde{\mathcal{F}}_{\{n_1\dots n_4\}}^{\{\alpha_1\dots\alpha_4\}} + \tilde{\mathcal{A}}_{\{n_1\dots n_4\}}^{\{\alpha_1\dots\alpha_4\}}\,, \tag{4.103}$$

where $\tilde{\mathcal{F}}_{\{n_1\dots n_4\}}^{\{\alpha_1\dots\alpha_4\}}$ is a factorised term

$$\tilde{\mathcal{F}}_{\{n_1\dots n_4\}}^{\{\alpha_1\dots\alpha_4\}} = \sum_{s=0}^{1} \underbrace{\mathbf{c}_{n_1}^{\alpha_1}\mathbf{c}_{n_2}^{\alpha_2}}_{s}\underbrace{\mathbf{c}_{n_3}^{\alpha_3}\mathbf{c}_{n_4}^{\alpha_4}}_{s} - \underbrace{\mathbf{c}_{n_1}^{\alpha_1}\mathbf{c}_{n_3}^{\alpha_3}}_{s}\underbrace{\mathbf{c}_{n_2}^{\alpha_2}\mathbf{c}_{n_4}^{\alpha_4}}_{s} + \underbrace{\mathbf{c}_{n_2}^{\alpha_2}\mathbf{c}_{n_3}^{\alpha_3}}_{s}\underbrace{\mathbf{c}_{n_1}^{\alpha_1}\mathbf{c}_{n_4}^{\alpha_4}}_{s} \tag{4.104}$$

$$\underbrace{\mathbf{c}^{\alpha}_{n_1}\mathbf{c}^{\beta}_{n_2}}_{s} = \overline{\frac{1}{L}\sum_{\ell}(-1)^{s\ell}\mathbf{c}^{\alpha}_{\ell+n_1}\mathbf{c}^{\beta}_{\ell+n_2}} \tag{4.105}$$

and $\tilde{\mathcal{A}}^{\{\alpha_1\dots\alpha_4\}}_{\{n_1\dots n_4\}}$ is the remaining contribution. Using (4.100) we can explicitly carry out the time average and the sum over ℓ in (4.105). We obtain

$$\underbrace{\mathbf{c}^{\alpha}_{n_1}\mathbf{c}^{\beta}_{n_2}}_{s} = \frac{1}{L}\sum_{k} e^{-i\alpha(n_2-n_1)k}e^{in_2 s\pi}U(k)^{\alpha}_{\gamma}U(\alpha\beta\bar{k}_s)^{\beta}_{\bar{\gamma}}\mathbf{b}_{\gamma}(k)\mathbf{b}_{\bar{\gamma}}(\alpha\beta\bar{k}_s)\,, \tag{4.106}$$

where $\bar{\alpha} = -\alpha$ and we defined $k_s = k + \pi s$. Analogously, (4.103) reads as

$$\begin{aligned}\frac{1}{L}\overline{\sum_{j}\mathbf{c}^{\alpha_1}_{j+n_1}\mathbf{c}^{\alpha_2}_{j+n_2}\mathbf{c}^{\alpha_3}_{j+n_3}\mathbf{c}^{\alpha_4}_{j+n_4}} &= \\ = \frac{1}{L^2}\sum_{\{k_i\}}\prod_{j=1}^{4}\left(e^{i\alpha_j n_j k_j}U(k_j)^{\alpha_j}_{\beta_j}\right)\mathbf{b}_{\beta_1}(k_1)\mathbf{b}_{\beta_2}(k_2)\mathbf{b}_{\beta_3}(k_3)\mathbf{b}_{\beta_4}(k_4)\delta_{\alpha_1 k_1+\alpha_2 k_2+\alpha_3 k_3+\alpha_4 k_4}& \\ \times\,\delta_{\beta_1\varepsilon(k_1)+\beta_2\varepsilon(k_2)+\beta_3\varepsilon(k_3)+\beta_4\varepsilon(k_4)}\,.&\end{aligned} \tag{4.107}$$

In order to compute the sums over the momenta it is necessary to solve the constraints given by the Kronecker deltas, *i.e.*

$$\begin{aligned}&\alpha_1 k_1 + \alpha_2 k_2 + \alpha_3 k_3 + \alpha_4 k_4 = 0\\ &\beta_1\varepsilon(k_1) + \beta_2\varepsilon(k_2) + \beta_3\varepsilon(k_3) + \beta_4\varepsilon(k_4) = 0\,.\end{aligned} \tag{4.108}$$

Some of the solutions to these equations can be found by requiring the terms of (4.108) to cancel in pairs. This would give

$$\delta_{\alpha_1 k_1+\alpha_2 k_2+\alpha_3 k_3+\alpha_4 k_4}\delta_{\beta_1\varepsilon_{k_1}+\beta_2\varepsilon_{k_2}+\beta_3\varepsilon_{k_3}+\beta_4\varepsilon_{k_4}} = \sum_{s=0,1}\Delta_1^s + \Delta_2^s + \Delta_3^s\,, \tag{4.109}$$

with

$$\Delta_1^s = \delta_{\beta_1,\bar{\beta}_2}\delta_{\beta_3,\bar{\beta}_4}\delta_{\bar{\alpha}_1 k_1,\alpha_1 k_{2,s}}\delta_{\bar{\alpha}_3 k_3,\alpha_4 k_{4,s}} \tag{4.110}$$

$$\Delta_2^s = \delta_{\beta_1,\bar{\beta}_3}\delta_{\beta_2,\bar{\beta}_4}\delta_{\bar{\alpha}_1 k_1,\alpha_3 k_{3,s}}\delta_{\bar{\alpha}_2 k_2,\alpha_4 k_{4,s}} \tag{4.111}$$

$$\Delta_3^s = \delta_{\beta_1,\bar{\beta}_4}\delta_{\beta_2,\bar{\beta}_3}\delta_{\bar{\alpha}_1 k_1,\alpha_4 k_{4,s}}\delta_{\bar{\alpha}_2 k_2,\alpha_3 k_{3,s}}\,. \tag{4.112}$$

For a generic dispersion relation it is reasonable to expect these solutions to be the only ones. For the specific dispersion considered, (4.101), Equations (4.108) admit other solutions in the thermodynamic limit. We call these *anomalous solutions* because they depend strongly on the

precise form of the dispersion relation. We now show that the term $\tilde{\mathcal{A}}^{\{\alpha_1\dots\alpha_4\}}_{\{n_1\dots n_4\}}$ in (4.103) is exactly the contribution arising from these solutions, *i.e.*

$$\tilde{\mathcal{F}}^{\{\alpha_1\dots\alpha_4\}}_{\{n_1\dots n_4\}} = \frac{1}{L^2}\sum_{k_1,k_2,k_3,k_4}\sum_{s=0,1}\prod_{j=1}^{4}\left(e^{i\alpha_j n_j k_j}U(k_j)^{\alpha_j}_{\beta_j}\right)\mathbf{b}_{\beta_1}(k_1)\mathbf{b}_{\beta_2}(k_2)\mathbf{b}_{\beta_3}(k_3)\mathbf{b}_{\beta_4}(k_4) \times\{\Delta_1^s+\Delta_2^s+\Delta_3^s\}\,. \quad (4.113)$$

We stress that the operator $\tilde{\mathcal{A}}^{\{\alpha_1\dots\alpha_4\}}_{\{n_1\dots n_4\}}$ will be nonzero only in the thermodynamic limit.

Considering, for example, the term containing Δ_2, we have

$$\begin{aligned}\frac{1}{L^2}\sum_{k_1,k_2,k_3,k_4}\sum_{s=0,1}\prod_{j=1}^{4}\left(e^{i\alpha_j n_j k_j}U(k_j)^{\alpha_j}_{\beta_j}\right)\mathbf{b}_{\beta_1}(k_1)\mathbf{b}_{\beta_2}(k_2)\mathbf{b}_{\beta_3}(k_3)\mathbf{b}_{\beta_4}(k_4)\Delta_2^s &= \\ = \frac{1}{L^2}\sum_{p,q}\sum_{s=0,1} e^{i\alpha_1(n_1-n_3)p+i\alpha_2(n_2-n_4)q}e^{in_3s\pi}e^{in_4s\pi}U(p)^{\alpha_1}_{\beta_1}U(q)^{\alpha_2}_{\beta_2} & \\ \times U(\alpha_1\alpha_3\bar{p}_s)^{\alpha_3}_{\bar{\beta}_1}U(\alpha_2\alpha_4\bar{q}_s)^{\alpha_4}_{\bar{\beta}_2}\mathbf{b}_{\beta_1}(p)\mathbf{b}_{\beta_2}(q)\mathbf{b}_{\bar{\beta}_1}(\alpha_1\alpha_3\bar{p}_s)\mathbf{b}_{\bar{\beta}_2}(\alpha_2\alpha_4\bar{q}_s) & \\ = -\sum_{s=0,1}\underbrace{\mathbf{c}^{\alpha_1}_{n_1}\mathbf{c}^{\alpha_3}_{n_3}}_{s}\underbrace{\mathbf{c}^{\alpha_2}_{n_2}\mathbf{c}^{\alpha_4}_{n_4}}_{s}+O\big(L^{-1}\big)\,, & \quad (4.114)\end{aligned}$$

where we used the commutation relations of the $\{\mathbf{b}_\beta(k)\}$ in the last step. Although the terms $\tilde{\mathcal{F}}^{\{\alpha_1\dots\alpha_4\}}_{\{n_1\dots n_4\}}$ and $\tilde{\mathcal{A}}^{\{\alpha_1\dots\alpha_4\}}_{\{n_1\dots n_4\}}$ are in fact multiplied by L in the time average of (4.15), the possible corrections $O(L^{-1})$ in (4.114) (which would result in corrections $O(L^0)$ in the effective Hamiltonian) are locally irrelevant, because their density approaches zero in the thermodynamic limit.

We obtain analogous results for Δ_1 and Δ_3, that is to say (4.103).

Remark We point out that for other dispersion relations (still with the properties $\varepsilon(k) = \varepsilon(k+\pi)$ and $\varepsilon(k) \neq \varepsilon(k+\pi/n)$ for generic k and $n > 1$) the anomalous terms could be factorised as well. Generally in such situations the factors have a very simple time dependence, *e.g.* a single oscillation frequency. As a consequence, relaxation is ruled out.

4.B Towards a mean-field description

In this appendix we prove the Lemmas of Section 4.3.

Lemma 4.B.1 *If $\mathcal{O} \in \mathcal{E}$, the operator norm (*i.e. *the maximal eigenvalue in absolute value) of $\mathcal{O}/L$ is bounded.*

Proof The proof is straightforward. Let us expand $\mathcal{O}/L$ as in (4.22):

$$\frac{\mathcal{O}}{L} = \sum_{j=1}^{N} \frac{1}{L^{n_j}} \mathcal{O}_1^{(j)} \cdots \mathcal{O}_{n_j}^{(j)} \tag{4.115}$$

where $\mathcal{O}_m^{(j)}$ have local densities, that is to say, they can be written as follows

$$\mathcal{O}_m^{(j)} = \sum_{\ell} o_{m;\ell}^{(j)} , \tag{4.116}$$

with $o_{m;\ell}^{(j)}$ local operators. We immediately find the chain of inequalities

$$\| \frac{\mathcal{O}}{L} \| \leq \sum_{j=1}^{N} \frac{1}{L^{n_j}} \| \mathcal{O}_1^{(j)} \cdots \mathcal{O}_{n_j}^{(j)} \| \leq \sum_{j=1}^{N} \| \frac{\mathcal{O}_1^{(j)}}{L} \| \cdots \| \frac{\mathcal{O}_{n_j}^{(j)}}{L} \| \leq \sum_{j=1}^{N} (\max_{m,\ell} \| o_{m;\ell}^{(j)} \|)^{n_j} . \tag{4.117}$$

The right hand side is clearly $O(L^0)$ because N and n_j are finite by definition and $o_{m;\ell}^{(j)}$ are local.

Lemma 4.B.2 *If $\mathcal{O}, \tilde{\mathcal{O}} \in \mathcal{E}$, then $[\mathcal{O}, \tilde{\mathcal{O}}] \in \mathcal{E}$ as well.*

Proof Without loss of generality, we can restrict to two single terms of the expansions (4.22) of $\mathcal{O}$ and $\tilde{\mathcal{O}}$. The commutator of the two terms reads as

$$\begin{aligned} &[\frac{1}{L^{n_i-1}} \mathcal{O}_1^{(i)} \cdots \mathcal{O}_{n_i}^{(i)}, \frac{1}{L^{n_j-1}} \tilde{\mathcal{O}}_1^{(j)} \cdots \tilde{\mathcal{O}}_{n_j}^{(j)}] = \\ &\quad = \frac{1}{L^{n_j+n_j-2}} \sum_{k,p} \mathcal{O}_1^{(i)} \cdots \mathcal{O}_{k-1}^{(i)} \tilde{\mathcal{O}}_1^{(j)} \cdots \tilde{\mathcal{O}}_{p-1}^{(j)} [\mathcal{O}_k^{(i)}, \tilde{\mathcal{O}}_p^{(j)}] \mathcal{O}_{k+1}^{(i)} \cdots \mathcal{O}_{n_i}^{(i)} \tilde{\mathcal{O}}_{p+1}^{(j)} \cdots \tilde{\mathcal{O}}_{n_j}^{(j)} . \end{aligned} \tag{4.118}$$

Since $[\mathcal{O}_k^{(i)}, \tilde{\mathcal{O}}_p^{(j)}]$ have local densities (the commutator of two local operators is nonzero only if there is a region on which they both act non-trivially; in addition, its range is smaller than the sum of the ranges of the two operators), the number of extensive operators exceeds by one the exponent of $1/L$. Thus, $[\mathcal{O}, \tilde{\mathcal{O}}] \in \mathcal{E}$.

Lemma 4.B.3 *(viz. Lemma 4.3.1) Let $\mathcal{O} \in \mathcal{E}$ and $|\Psi\rangle$ a state with cluster decomposition properties. The expectation value of $\mathcal{O}/L$ in $|\Psi\rangle$ can be reduced to the expectation values of the local translation invariant operators it consists of:*

$$\lim_{L\to\infty} \langle\Psi| \frac{H_1}{L} \cdots \frac{H_n}{L} |\Psi\rangle = \lim_{L\to\infty} \prod_j \frac{\langle\Psi|H_j|\Psi\rangle}{L} . \tag{4.119}$$

Proof Let us consider a term (4.24) of the expansion (4.22). Its expectation value (per unit

of length) is given by

$$\langle\Psi|\frac{H_1}{L}\cdots\frac{H_n}{L}|\Psi\rangle = \frac{1}{L^n}\sum_{\ell_1,\dots,\ell_n}\langle\Psi|h_{1,\ell_1}\cdots h_{n,\ell_n}|\Psi\rangle\ , \tag{4.120}$$

where h_{j,ℓ_j} are local operators acting non-trivially only around ℓ_j and such that

$$H_j = \sum_{\ell} h_{j,\ell_j}\,. \tag{4.121}$$

By cluster decomposition we have

$$\sum_{\substack{\ell_1,\dots,\ell_n\\ |\ell_j-\ell_{j'}|>\xi\gg 1\ (\forall j\neq j')}}\langle\Psi|\frac{h_{1,\ell_1}}{L}\cdots\frac{h_{n,\ell_n}}{L}|\Psi\rangle = \sum_{\substack{\ell_1,\dots,\ell_n\\ |\ell_j-\ell_{j'}|>\xi\gg 1\ (\forall j\neq j')}}\frac{\langle\Psi|h_{1,\ell_1}|\Psi\rangle}{L}\cdots\frac{\langle\Psi|h_{n,\ell_n}|\Psi\rangle}{L} + f(\xi,L)\,, \tag{4.122}$$

where $\lim_{\xi\to\infty}\lim_{L\to\infty} f(\xi,L)=0$. The difference between (4.120) and the left hand side of (4.122) can be bounded from above as follows

$$\Big|\sum_{\substack{\ell_1,\dots,\ell_n\\ |\ell_j-\ell_{j'}|\leq\xi\ (\exists j\neq j')}}\langle\Psi|\frac{h_{1,\ell_1}}{L}\cdots\frac{h_{n,\ell_n}}{L}|\Psi\rangle\Big| \leq \binom{n}{2}\frac{\xi}{L}\max_{\{\ell\}}\Big|\langle\Psi|h_{1,\ell_1}\cdots h_{n,\ell_n}|\Psi\rangle\Big| \to 0\,. \tag{4.123}$$

Analogously

$$\Big|\sum_{\substack{\ell_1,\dots,\ell_n\\ |\ell_j-\ell_{j'}|\leq\xi\ (\exists j\neq j')}}\frac{\langle\Psi|h_{1,\ell_1}|\Psi\rangle}{L}\cdots\frac{\langle\Psi|h_{n,\ell_n}|\Psi\rangle}{L}\Big| \leq \binom{n}{2}\frac{\xi}{L}\max_{\{\ell\}}\Big|\prod_{j=1}^{n}\langle\Psi|h_{j,\ell_j}|\Psi\rangle\Big| \to 0\ , \tag{4.124}$$

so that

$$\Big|\langle\Psi|\frac{H_1}{L}\cdots\frac{H_n}{L}|\Psi\rangle - \prod_j\frac{\langle\Psi|H_j|\Psi\rangle}{L}\Big| \leq |f(\xi,L)| + O(1/L) \tag{4.125}$$

Being ξ arbitrary, we can take the limit $\lim_{\xi\to\infty}\lim_{L\to\infty}$, obtaining (4.119).

Lemma 4.B.4 *If the state $|\Psi_0\rangle$ has cluster decomposition properties and $\mathcal{O}\in\mathcal{E}$, the mean-field Hamiltonian satisfies the following identity:*

$$\lim_{L\to\infty}\langle\Psi_0|\bar{U}^\dagger(t)[H_{\rm MF}(t),\frac{\mathcal{O}}{L}]\bar{U}(t)|\Psi_0\rangle = \lim_{L\to\infty}\langle\Psi_0|\bar{U}^\dagger(t)[H,\frac{\mathcal{O}}{L}]\bar{U}(t)|\Psi_0\rangle\ , \tag{4.126}$$

where $\bar{U}$ was defined in (4.28).

Proof Let us consider a generic term (4.24) of the expansion (4.22) of H

$$\tilde{H} = \frac{1}{L^{n-1}}H_1\cdots H_n\,. \tag{4.127}$$

The corresponding term (4.27) of the mean-field Hamiltonian (4.27) is given by

$$\tilde{H}^{\Psi_0}_{\mathrm{MF}}(t) = \sum_{\ell=1}^{n} \prod_{j\neq\ell} \frac{\langle\Psi_0|\bar{U}^\dagger(t) H_j \bar{U}(t)|\Psi_0\rangle}{L} H_\ell \,. \tag{4.128}$$

By taking the commutators with $\mathcal{O}$ we find

$$[\tilde{H}, \frac{\mathcal{O}}{L}] = \sum_{\ell=1}^{n} \prod_{j=1}^{\ell-1} \frac{H_j}{L} \frac{[H_\ell, \mathcal{O}]}{L} \prod_{j=\ell+1}^{n} \frac{H_j}{L} \tag{4.129}$$

$$[\tilde{H}^{\Psi_0}_{\mathrm{MF}}(t), \frac{\mathcal{O}}{L}] = \sum_{\ell=1}^{n} \prod_{j\neq\ell} \frac{\langle\Psi_0|\bar{U}^\dagger(t) H_j \bar{U}(t)|\Psi_0\rangle}{L} \frac{[H_\ell, \mathcal{O}]}{L} \,. \tag{4.130}$$

Because $|\Psi_0\rangle$ has cluster decomposition properties and the mean-field Hamiltonian is local at any time, the state $\bar{U}(t)\,|\Psi_0\rangle$ has cluster decomposition properties as well (the only difference with respect to $|\Psi_0\rangle$ is that the function f of (4.122) is now time dependent). Finally, by Lemma 4.B.3, in the thermodynamic limit the expectation values of (4.129) and (4.130) in the state $\bar{U}(t)\,|\Psi_0\rangle$ are identical, that is to say (4.126).

Lemma 4.B.5 *Let $|\Psi_0\rangle$ be a translation invariant state with cluster decomposition properties and $H, \mathcal{O} \in \mathcal{E}$. The time derivatives of the expectation value of $\mathcal{O}/L$ in the state evolving with $H^{\Psi_0}_{\mathrm{MF}}(t)$ fulfil*

$$\frac{d^n}{dt^n} \lim_{L\to\infty} \langle\Psi_0|\bar{U}^\dagger(t) \frac{\mathcal{O}}{L} \bar{U}(t)|\Psi_0\rangle = i^n \lim_{L\to\infty} \langle\Psi_0|\bar{U}^\dagger(t) \underbrace{[H, [H, ...[H}_{n}, \frac{\mathcal{O}}{L}]...]\bar{U}(t)|\Psi_0\rangle \tag{4.131}$$

Proof We proceed by induction. First of all we see that for $n = 0$ the property is trivially satisfied; let then the property be true for n, we have

$$\begin{aligned}
\frac{\mathrm{d}^{n+1}}{\mathrm{d}t^{n+1}} \lim_{L\to\infty} \langle\Psi_0|\bar{U}^\dagger(t) \frac{\mathcal{O}}{L} \bar{U}(t)|\Psi_0\rangle &= i^n \frac{\mathrm{d}}{\mathrm{d}t} \lim_{L\to\infty} \langle\Psi_0|\bar{U}^\dagger(t) \underbrace{[H, [H, ...[H}_{n}, \frac{\mathcal{O}}{L}]...]\bar{U}(t)|\Psi_0\rangle \\
&= i^{n+1} \lim_{L\to\infty} \langle\Psi_0|\bar{U}^\dagger(t) [H_{MF}(t), \underbrace{[H, [H, ...[H}_{n}, \frac{\mathcal{O}}{L}]...]]\bar{U}(t)|\Psi_0\rangle \\
&= i^{n+1} \lim_{L\to\infty} \langle\Psi_0|\bar{U}^\dagger(t) \underbrace{[H, [H, ...[H}_{n+1}, \frac{\mathcal{O}}{L}]...]\bar{U}(t)|\Psi_0\rangle \,.
\end{aligned} \tag{4.132}$$

In the second step we used Lemma 4.B.2 and Lemma 4.B.4. This concludes the proof.

Lemma 4.B.6 *(viz. Lemma 4.3.2) Let $|\Psi_0\rangle$ be a translation invariant state with cluster decomposition properties and $H, \mathcal{O} \in \mathcal{E}$. Let the expectation value of $\mathcal{O}$ in the state that time evolves with $H^{\Psi_0}_{\mathrm{MF}}(t)$ be an analytic function of t in the strip $|\mathrm{Im}[t]| < r$, with r a nonzero constant. In the thermodynamic limit, the time evolution with H can be replaced by the time*

evolution with the mean-field Hamiltonian:

$$\lim_{L\to\infty} \langle\Psi_0|e^{iHt}\frac{\mathcal{O}}{L}e^{-iHt}|\Psi_0\rangle = \lim_{L\to\infty} \langle\Psi_0|\bar{U}^\dagger(t)\frac{\mathcal{O}}{L}\bar{U}(t)|\Psi_0\rangle \ . \tag{4.133}$$

Proof We define

$$f(t,s) = \lim_{L\to\infty} \langle\Psi_0|\bar{U}^\dagger(t)e^{iHs}\frac{\mathcal{O}}{L}e^{-iHs}\bar{U}(t)|\Psi_0\rangle \ . \tag{4.134}$$

By Lemma 4.B.5 we have

$$\frac{\partial^n}{\partial t^n} f(t,0) = \frac{\partial^n}{\partial s^n}\Big|_{s=0} f(t,s)\,, \tag{4.135}$$

indeed

$$\frac{\partial^n}{\partial t^n}\Big|_{t=0} e^{iHt}\frac{\mathcal{O}}{L}e^{-iHt} = i^n \underbrace{[H,[H,...[H}_{n},\frac{\mathcal{O}}{L}]...]\,. \tag{4.136}$$

By assumption, $f(t,0)$ (which corresponds to the time evolution with the mean-filed Hamiltonian) is analytic in the strip $|\mathrm{Im}[t]| < r$, so the convergence radius of the Taylor expansion at $t = 0$ is larger than or equal to r. Thus we have

$$f(\tau,0) = \sum_n \frac{\tau^n}{n!}\frac{\partial^n}{\partial t^n}\Big|_{t=0} f(t,0) = \sum_n \frac{\tau^n}{n!}\frac{\partial^n}{\partial t^n}\Big|_{t=0} f(0,t) = f(0,\tau)\,, \qquad |\tau| < r\,. \tag{4.137}$$

Let us call t_* a time such that $f(t,0) = f(0,t)$ for any $0 \le t < t_*$. As before, the function $f(t+\tau,0)$ is analytic in the strip $|\mathrm{Im}[\tau]| < r$, so we have

$$f(t+\tau,0) = \sum_n \frac{\tau^n}{n!}\frac{\partial^n}{\partial t^n} f(t,0) = \sum_n \frac{\tau^n}{n!}\frac{\partial^n}{\partial t^n} f(0,t) = f(0,t+\tau)\,, \qquad |\tau| < r\,. \tag{4.138}$$

That is to say

$$f(t,0) = f(0,t) \quad \forall t < t_* \quad \Longrightarrow \quad f(t,0) = f(0,t) \quad \forall t < t_* + \tau\,. \tag{4.139}$$

Since τ is finite and (4.137) holds, we conclude

$$f(t,0) = f(0,t) \qquad \forall\, t\,, \tag{4.140}$$

which is exactly (4.133).

Corollary 4.B.7 *(viz. Corollary 4.3.3) Lemma 4.B.6 holds true in particular for local operators.*

Proof By translation invariance, the expectation value of any local operator $\mathcal{O}$ is equal to the expectation value per unit of length of the operator $\mathcal{O}_* \in \mathcal{E}$, obtained by shifting $\mathcal{O}$ along the

chain and summing all the (L) terms.

Corollary 4.B.8 *(viz. Corollary 4.3.4) Let $|\Psi_0\rangle$ a translation invariant state with cluster decomposition properties and $H \in \mathcal{E}$. In the thermodynamic limit, the time evolution of the reduced density matrix (RDM) of some spin block S is equal to the RDM in the state that time evolves with the mean-field Hamiltonian:*

$$\rho_S(t) = \mathrm{tr}_{\bar{S}}[e^{-iHt}\,|\Psi_0\rangle\,\langle\Psi_0|\,e^{iHt}] = \mathrm{tr}_{\bar{S}}[\bar{U}(t)\,|\Psi_0\rangle\,\langle\Psi_0|\,\bar{U}^\dagger(t)]\,. \tag{4.141}$$

Proof This is a direct consequence of Corollary 4.B.7.

Corollary 4.B.9 *Let $H \in \mathcal{E}$ and $|\Psi\rangle$ a state with cluster decomposition properties. If $|\Psi\rangle$ is an excited state of the corresponding mean-field Hamiltonian H^Ψ_{MF}*

$$H^\Psi_{\mathrm{MF}}\,|\Psi\rangle = E_\Psi\,|\Psi\rangle\ , \tag{4.142}$$

the expectation value of local observables in $e^{-iHt}\,|\Psi\rangle$ is independent of time. Therefore, $|\Psi\rangle$ behaves locally as an excited state of H.

The reverse is also true. If an excited state of H is locally equivalent to a state with cluster decomposition properties, then the latter is an excited state of the corresponding mean-field Hamiltonian.

Proof Clearly the mean-field Hamiltonian H^Ψ_{MF} is the solution of (4.27). Being $\bar{U}(t)\,|\Psi\rangle \propto |\Psi\rangle$ (*cf.* (4.28)), by Corollary 4.B.7 the expectation value of local observables is independent of time. The reverse holds true for analogous reasons.

4.C Self-consistency check of condition (4.20)

Here we show that neglecting the *anomalous term* $L\mathcal{A}^{\{\alpha_1\ldots\alpha_4\}}_{\{n_1\ldots n_4\}}$ (*cf.* (4.103)) in the time averaged Hamiltonian is a self-consistent approximation. To this aim, we consider the time evolution of a Slater determinant $|\Psi_0\rangle$ under the Hamiltonian $\tilde{H}$, obtained from H by removing $L\mathcal{A}^{\{\alpha_1\ldots\alpha_4\}}_{\{n_1\ldots n_4\}}$. In Section 4.3 and Appendix 4.B we proved that, as long as $\mathcal{O}$ is a local operator (but the class of allowed operators is in fact larger), $e^{-i\tilde{H}t}$ can be replaced by the mean-field time evolution operator $\bar{U}(t)$ (4.28). Here we show that inserting $L\mathcal{A}^{\{\alpha_1\ldots\alpha_4\}}_{\{n_1\ldots n_4\}}$ back at time t does not change the expectation value of local observables. In other words we are going to prove

$$\lim_{L\to\infty} L\,\langle\Psi_0|\bar{U}^\dagger(t)[\mathcal{A}^{\{\alpha_1\ldots\alpha_4\}}_{\{n_1\ldots n_4\}},\mathcal{O}]\bar{U}(t)|\Psi_0\rangle = 0 \qquad\qquad \forall t\,, \tag{4.143}$$

where $\mathcal{O}$ is a generic local operator.

Using the notations of Appendix 4.A, any local operator can be written as a linear combination of operators of the form

$$\mathcal{O} = \mathbf{c}_{\ell_1}^{\gamma_1} \cdots \mathbf{c}_{\ell_n}^{\gamma_n} = \frac{1}{L^{n/2}} \sum_{\{p_i\}} \mathcal{F}_n{}_{\{\sigma_i\}}^{\{\gamma_i\}}(\{\ell_i\}|\{p_i\}) \mathbf{b}_{\sigma_1}(p_1) \cdots \mathbf{b}_{\sigma_n}(p_n)\,, \tag{4.144}$$

where

$$\mathcal{F}_n{}_{\{\beta_i\}}^{\{\alpha_i\}}(\{j_i\}|\{p_i\}) \equiv \prod_{i=1}^{n} \left(e^{i\alpha_i j_i p_i} U(p_i)_{\beta_i}^{\alpha_i} \right)\,. \tag{4.145}$$

If n is odd then (4.143) is trivially satisfied because $\bar{U}(t)\,|\Psi_0\rangle$ is a Slater determinant by assumption and hence the expectation value of an odd number of fermions vanishes. We therefore focus on the case $n = 2m$. The anomalous term $\mathcal{A}_{\{n_1 \dots n_4\}}^{\{\alpha_1 \dots \alpha_4\}}$ of (4.103) can be written as follows

$$\mathcal{A}_{\{n_1 \dots n_4\}}^{\{\alpha_1 \dots \alpha_4\}} = \frac{1}{L^2} \sum_{k_1,k_2} \sum_{\bar{k}_3,\bar{k}_4} \mathcal{F}_2{}_{\{\beta_i\}}^{\{\alpha_i\}}(\{j_i\}|\{k_i\}) \mathcal{F}_2{}_{\{\beta_i\}}^{\{\alpha_i\}}(\{j_i\}|\{\bar{k}_i\}) \mathbf{b}_{\beta_1}(k_1) \mathbf{b}_{\beta_2}(k_2) \mathbf{b}_{\beta_3}(\bar{k}_3) \mathbf{b}_{\beta_4}(\bar{k}_4) \tag{4.146}$$

where $\bar{k}_3$ and $\bar{k}_4$ are the *anomalous solutions* of system (4.108), *i.e.* they are implicit functions of k_1 and k_2 defined by the system (4.108) and in addition fulfilling

$$k_{1,2} \pm \bar{k}_{3,4} \neq 0\,, \qquad\qquad \bar{k}_3 \pm \bar{k}_4 \neq 0\,, \tag{4.147}$$

almost everywhere. Since $|\tilde{\Psi}_t\rangle = \bar{U}(t)\,|\Psi_0\rangle$ is a Slater determinant, we can use Wick's theorem to compute expectation values. We then have

$$\begin{aligned} L\,\langle\tilde{\Psi}_t|\mathcal{A}_{\{n_1 \dots n_4\}}^{\{\alpha_1 \dots \alpha_4\}}\mathcal{O}|\tilde{\Psi}_t\rangle = {} & L\,\langle\tilde{\Psi}_t|\mathcal{A}_{\{n_1 \dots n_4\}}^{\{\alpha_1 \dots \alpha_4\}}|\tilde{\Psi}_t\rangle\,\langle\tilde{\Psi}_t|\mathcal{O}|\tilde{\Psi}_t\rangle \\ & + L\mathcal{C}_2[\mathcal{A}_{\{n_1 \dots n_4\}}^{\{\alpha_1 \dots \alpha_4\}}\mathcal{O}]_t + L\mathcal{C}_4[\mathcal{A}_{\{n_1 \dots n_4\}}^{\{\alpha_1 \dots \alpha_4\}}\mathcal{O}]_t \end{aligned} \tag{4.148}$$

where $\mathcal{C}_2[\mathcal{A}_{\{n_1 \dots n_4\}}^{\{\alpha_1 \dots \alpha_4\}}\mathcal{O}]_t$ contains terms in which two of the $\mathbf{b}$'s in $\mathcal{A}_{\{n_1 \dots n_4\}}^{\{\alpha_1 \dots \alpha_4\}}$ are contracted together and the other two are contracted with two $\mathbf{b}$'s in $\mathcal{O}$; $\mathcal{C}_4[\mathcal{A}_{\{n_1 \dots n_4\}}^{\{\alpha_1 \dots \alpha_4\}}\mathcal{O}]_t$ contains all the terms in which any $\mathbf{b}$ in $\mathcal{A}_{\{n_1 \dots n_4\}}^{\{\alpha_1 \dots \alpha_4\}}$ is contracted with a $\mathbf{b}$ in $\mathcal{O}$.

According to the definition of $\mathcal{A}_{\{n_1 \dots n_4\}}^{\{\alpha_1 \dots \alpha_4\}}$, any Wick's contraction among $\mathbf{b}$'s in it gives zero (because of (4.147)), hence the only non zero contribution to (4.148) arises from $\mathcal{C}_4[\mathcal{A}_{\{n_1 \dots n_4\}}^{\{\alpha_1 \dots \alpha_4\}}\mathcal{O}]_t$. To conclude the proof we will show that the terms in $\mathcal{C}_4[\mathcal{A}_{\{n_1 \dots n_4\}}^{\{\alpha_1 \dots \alpha_4\}}\mathcal{O}]_t$ scale as $O(L^{-2})$ and in the thermodynamic limit their contribution can thus be neglected. To this end it is sufficient

to consider a typical element of $\mathcal{C}_4[\mathcal{A}^{\{\alpha_1\dots\alpha_4\}}_{\{n_1\dots n_4\}}\mathcal{O}]_t$

$$\frac{1}{L^{m+2}}G^{\boldsymbol{\alpha},\boldsymbol{\beta},\boldsymbol{\gamma},\boldsymbol{\sigma}}_{\mathbf{j},\mathbf{k},\boldsymbol{\ell},\mathbf{p}}\mathbf{b}_{\beta_1}(k_1)\mathbf{b}_{\beta_2}(k_2)\mathbf{b}_{\beta_3}(\bar{k}_3)\mathbf{b}_{\beta_4}(\bar{k}_4)\mathbf{b}_{\sigma_1}(p_1)\mathbf{b}_{\sigma_2}(p_2)\mathbf{b}_{\sigma_3}(p_3)\cdots\mathbf{b}_{\sigma_{2m}}(p_{2m})\,, \tag{4.149}$$

where sums over the momenta $\{p_i\},\{k_i\}$ and the indices are understood, and we defined

$$\overbrace{\mathbf{b}_\alpha(p)\mathbf{b}_\beta}(q) = \langle\tilde{\Psi}_t|\mathbf{b}_\alpha(p)\mathbf{b}_\beta(q)|\tilde{\Psi}_t\rangle \tag{4.150}$$

$$G^{\boldsymbol{\alpha},\boldsymbol{\beta},\boldsymbol{\gamma},\boldsymbol{\sigma}}_{\mathbf{j},\mathbf{k},\boldsymbol{\ell},\mathbf{p}} \equiv \mathcal{F}_2{}^{\{\alpha_i\}}_{\{\beta_i\}}(\{j_i\}|\{k_i\})\mathcal{F}_2{}^{\{\alpha_i\}}_{\{\beta_i\}}(\{j_i\}|\{\bar{k}_i\})\mathcal{F}_n{}^{\{\gamma_i\}}_{\{\sigma_i\}}(\{\ell_i\}|\{p_i\})\,. \tag{4.151}$$

The $2m+2$ sums over the momenta are reduced to m by the Kronecker deltas arising from the Wick contractions. Because the number of factors L^{-1} exceeds by two the number of sums, the term turns out to be $O(L^{-2})$. The validity of Equation (4.143) is then established.

5. Prethermalisation and thermalisation in models with weak integrability-breaking

In the previous chapter we studied the effects of weak perturbations on the dynamics of a particular kind of integrable models, here we move to consider the general case where the unperturbed integrable model is generic. As discussed in Chapter 1 this is the physical setting in which *prethermalisation* is expected to occur: the system reaches some quasi-stationary state where local observables show non-thermal plateaux described by the underlying integrable theory. We focus on a class of spinless fermion models with weak interactions which can be thought as interacting Peierls insulators [66, 77] with an additional next-nearest-neighbour hopping term. We attack this problem by means of equations of motion techniques that can be viewed as generalisations of quantum Boltzmann equations. The method presented here is benchmarked against time dependent density matrix renormalisation group computations and is found to be very accurate as long as interactions are weak. For small integrability breaking, we observe robust prethermalisation plateaux for local observables on all accessible time scales. Increasing the strength of the integrability breaking term induces a "drift" away from the prethermalisation plateaux towards thermal behaviour. We identify a time scale characterising this crossover to be proportional to the inverse of the strength of the perturbation squared: much longer than the prerelaxation time-scale of the previous chapter.

5.1 The model

We consider a system described by the three-parameter family of spinless fermion Hamiltonians

$$H(J_2,\delta,U) = -J_1\sum_{l=1}^{L}\Big[1+(-1)^l\delta\Big]\Big(c_l^\dagger c_{l+1}+c_{l+1}^\dagger c_l\Big) - J_2\sum_{l=1}^{L}\Big[c_l^\dagger c_{l+2}+c_{l+2}^\dagger c_l\Big]+U\sum_{l=1}^{L}n_l n_{l+1}\,,\qquad c_{L+1}\equiv c_1\,. \tag{5.1}$$

Here c_i and $c_i^\dagger$ are spinless fermion operators on site i, obeying the CAR algebra (*cf.* Eq. (2.4)); the hopping amplitudes J_1 and J_2 describe nearest-neighbour and next-nearest-neighbour hopping respectively, while $0 \leq \delta < 1$ is a dimerisation parameter. Finally there is a repulsive nearest-neighbour density-density interaction of strength U. From here onwards we set $J_1 = 1$ and measure all the energies in units of J_1.

There are several limits in which (5.1) becomes integrable: (i) $U = 0$ describes a free theory; (ii) $\delta = J_2 = 0$ corresponds to the anisotropic spin-1/2 Heisenberg chain [180] (in external magnetic field along z); (iii) the low-energy degrees of freedom for $J_2 = 0$ and $\delta, U \ll 1$ are described by the quantum sine-Gordon model [79]. Away from these limits, the model is non-integrable.

The Hamiltonian $H(J_2, \delta, U)$ is invariant under the following transformations of the c_i's

a. Global U(1) transformations: $U(\phi)$

$$c_i \to U(\phi) c_i U^\dagger(\phi) = e^{\mathrm{i}\phi} c_i \,, \qquad \phi \in [0, 2\pi] \,, \tag{5.2}$$

b. Two site translations: T_2

$$c_i \to T_2 c_i T_2^\dagger = c_{i+2} \,, \tag{5.3}$$

c. Bond inversion with respect to any bond j: B_j

$$c_i \to B_j c_i B_j^\dagger = c_{2j-i+1} \,. \tag{5.4}$$

Here we will be interested in the weak interaction regime $U \lesssim 1$, a convenient basis for analysing quench dynamics is obtained by diagonalising the quadratic part of the Hamiltonian. This can be done combining a two-site Fourier transformation and a Bogoliubov transformation; the calculation follows the same lines as the one carried out in Chapter 2 and results in

$$\begin{aligned} H(J_2, \delta, U) = \sum_{\eta=\pm} \sum_{k>0} \epsilon_\eta(k) \alpha_\eta^\dagger(k) \alpha_\eta(k) \\ + U \sum_{\boldsymbol{\eta}} \sum_{\boldsymbol{k}>0} V_{\boldsymbol{\eta}}(\boldsymbol{k}) \alpha_{\eta_1}^\dagger(k_1) \alpha_{\eta_2}^\dagger(k_2) \alpha_{\eta_3}(k_3) \alpha_{\eta_4}(k_4) \,. \end{aligned} \tag{5.5}$$

Here we have introduced the notations $\boldsymbol{\eta} = (\eta_1, \eta_2, \eta_3, \eta_4)$, $\boldsymbol{k} = (k_1, k_2, k_3, k_4)$ and $\boldsymbol{k} > 0$ is a shorthand notation for $k_i > 0$ for all $i = 1, \ldots, 4$; the operators $\alpha_\pm(k)$ are momentum space annihilation operators obeying CAR in the form $\{\alpha_\mu(k), \alpha_\nu^\dagger(q)\} = \delta_{\mu\nu}\delta_{k,q}$; the single particle dispersion relation is given by

$$\epsilon_\eta(k) = -2J_2 \cos(2k) + 2\eta \sqrt{\delta^2 + (1-\delta^2)\cos^2(k)} \,, \tag{5.6}$$

and finally the interaction vertex factor can be written in a conveniently antisymmetrised form

$$V_{\boldsymbol{\eta}}(\boldsymbol{k}) = -\frac{1}{4} \sum_{P,Q \in S_2} \mathrm{sgn}(P)\mathrm{sgn}(Q) V'_{\eta_{p_1}\eta_{q_1}\eta_{p_2}\eta_{q_2}}(k_{p_1}, k_{q_1}, k_{p_2}, k_{q_2}) \,, \tag{5.7}$$

where $P = (p_1, p_2)$ and $Q = (q_1, q_2)$ are permutations of $(1, 2)$ and $(3, 4)$ respectively and

$$\begin{aligned} V'_{\boldsymbol{\eta}}(\boldsymbol{k}) =& \frac{e^{i(k_3-k_4)}}{2L}\left(\eta_1\eta_2 e^{i\varphi_{k_1}(\delta)}e^{-i\varphi_{k_2}(\delta)} + \eta_3\eta_4 e^{i\varphi_{k_3}(\delta)}e^{-i\varphi_{k_4}(\delta)}\right)\delta_{k_1-k_2+k_3-k_4,0} \\ &+ \frac{e^{i(k_3-k_4)}}{2L}\left(\eta_1\eta_2 e^{i\varphi_{k_1}(\delta)}e^{-i\varphi_{k_2}(\delta)} - \eta_3\eta_4 e^{i\varphi_{k_3}(\delta)}e^{-i\varphi_{k_4}(\delta)}\right)\delta_{k_1-k_2+k_3-k_4\pm\pi,0}\,. \end{aligned} \tag{5.8}$$

The Bogoliubov angle $\varphi_k(\delta)$ is given by

$$e^{-i\varphi_k(\delta)} = \frac{-\cos k + i\delta \sin k}{\sqrt{\cos^2 k + \delta^2 \sin^2 k}}\,. \tag{5.9}$$

The transformation between the fermions c_i and the Bogoliubov fermions $\alpha_\pm(k)$ can be compactly written as

$$c_l = \frac{1}{\sqrt{L}}\sum_{k>0}\sum_{\eta=\pm}\gamma_\eta(l, k|\delta)\alpha_\eta(k)\ , \tag{5.10}$$

where the coefficients are given by

$$\gamma_\pm(2j-1, k|\delta) = e^{-ik(2j-1)}\,, \qquad \gamma_\pm(2j, k|\delta) = \pm e^{-ik2j}e^{-i\varphi_k(\delta)}\,. \tag{5.11}$$

5.2 Setting of the problem

Our protocol for inducing and analysing non-equilibrium dynamics is as follows. We prepare the system in an initial density matrix ρ_0 that is not an eigenstate of $H(J_2, \delta, U)$ (*i.e.* does not commute with $H(J_2, \delta, U)$) for any value of U, importantly also for $U = 0$. Then, we evolve it in time by means of $H(J_2, \delta, U)$

$$\rho(t) = e^{-itH(J_2,\delta,U)}\rho_0 e^{itH(J_2,\delta,U)}\,. \tag{5.12}$$

For $U = 0$ our model is non-interacting, and concomitantly in the thermodynamic limit expectation values of local operators relax to time independent values described by a generalised Gibbs ensemble (GGE). In the following we analyse how a small integrability breaking interaction $U > 0$, which is expected to drive expectation values of local operators towards stationary values described by a Gibbs ensemble (GE), changes the non-equilibrium evolution. In other words, our main goal is to compare the expectation values of local operators for time evolution with the integrable Hamiltonian $H(J_2, \delta, 0)$ and (weakly) non-integrable $H(J_2, \delta, U)$ respectively.

As mentioned in Section 4.1 of the previous chapter, even when the interaction is zero the stationary values of local observables in the GE and GGE are different, *i.e.* their difference is

$O(U^0)$. Consequently, performing the comparison discussed in the last paragraph, one could expect that the expectation value of the observable evolving according to $H(J_2, \delta, U)$, would immediately separate from the other and evolve towards its thermal value. What happens for small U, however, is instead very different, for long times ($t \sim U^{-1}$ as we will see later) the observables evolving with the two different Hamiltonians remain close, more precisely their difference is $O(U)$. Even more interestingly, they show a quasi-stationary behaviour approaching values which are $O(U)$ close to the one given by the GGE for $U = 0$. This is the realisation in our setting of the *prethermalisation* phenomenon. The first observation of robust prethermalisation after quantum quenches in the model (5.1) with $J_2 = 0$ has been performed in Ref. [66], by numerical and analytical methods. There, no evidence for eventual thermalisation was found on the accessible time scales. Our purpose here is to go beyond the approximations used in that work, in order to understand what happens at even later times: we will show that for $t \sim U^{-2}$ the local observables continuously move away from the quasi-stationary prethermal plateaux towards the values predicted by the GE. To the best of our knowledge, Ref. [3] in which we reported our findings, has been the first work to clearly observe both prethermalisation and thermalisation in a one dimensional model.

We note that in the $J_2 = 0$ case the dispersion has the same form as the one of the XY model (with δ playing the role of γ); in particular it has the symmetry $\epsilon_+(k) = -\epsilon_-(\pi - k)$ which causes combinations like $\alpha_+^\dagger(k)\alpha_-^\dagger(\pi - k)$ to be conserved in the free model. This is thus an other example where one expects the pre-relaxation behaviour to appear; the expectation value of the "anomalous" charges is zero on the initial state considered in Ref. [66] and that is the reason why no pre-relaxation was observed there.

Finally, we stress that our protocol differs in a very important way from the weak interaction quenches analysed previously [72, 181]. In these works there is no dynamics at all for $U = 0$. Hence quenching the interaction from zero to a finite value simultaneously breaks integrability and induces a time dependence into the problem. This masks the interaction induced modification of the integrable post-quench dynamics and is the reason why no prethermalisation in our sense was observed in those works.

Let us now specify the precise form of the initial states used and the observables considered. The time evolution is started from states of the form

$$\rho_0 = \rho(\beta_i, J_{2i}, \delta_i, U_i) = \frac{e^{-\beta_i H(J_{2i}, \delta_i, U_i)}}{\mathrm{Tr}[e^{-\beta H(J_{2i}, \delta_i, U_i)}]}\,, \tag{5.13}$$

these states include, as a particular case, the ground state of the Hamiltonian $H(J_{2i}, \delta_i, U_i)$, however the class (5.13) allows to access the dynamics for a larger range of energy densities. In

this chapter we will focus on the case where the initial state satisfies Wick's theorem, specifically we will consider $\rho_0 = \rho(\beta_i, J_2 = 0, \delta_i, U = 0)$.

We use equation of motion (EOM) techniques [72, 182] analogous to the ones employed in derivations of quantum Boltzmann equations [75,76]; techniques similar to the ones we employ here were also used to analyse quantum quenches in the case $\delta_i = \delta_f = 0$ in Ref. [181]. The EOM technique consists in obtaining evolution equations for the two-point functions

$$n_{\mu\nu}(k,t) = \mathrm{Tr}\left[\rho(t)\alpha^\dagger_\mu(k)\alpha_\nu(k)\right], \tag{5.14}$$

where $\alpha_\pm(k)$ are the Bogoliubov fermions of the final Hamiltonian $H(J_2, \delta_f, U)$; throughout this chapter the quantities (5.14) will be called "occupation numbers". Since ρ_0 is noninteracting, we can easily evaluate (5.14) for $t = 0$, it yields to

$$n_{\mu\mu}(k) = \frac{1}{2} - \frac{1}{2}\cos(\varphi_k(\delta_f) - \varphi_k(\delta_i))\tanh(\beta\epsilon^{(0)}_\mu(k)/2), \qquad \mu = \pm, \tag{5.15}$$

$$n_{\mu\nu}(k) = \frac{i}{2}\sin(\varphi_k(\delta_f) - \varphi_k(\delta_i))\tanh(\beta\epsilon^{(0)}_\mu(k)/2), \qquad \mu \neq \nu\,. \tag{5.16}$$

Here the dispersions $\epsilon^{(0)}_\alpha(k)$ are given by (5.6) with $J_2 = 0$ and $\delta = \delta_i$.

Given the expectation values (5.14), we may readily calculate the single-particle Green's function

$$\mathcal{G}(j,l;t) = \mathrm{Tr}\left[\rho(t)c^\dagger_j c_l\right] = \frac{1}{L}\sum_{k>0}\sum_{\mu,\nu=\pm}\gamma^*_\mu(k,j)\gamma_\nu(k,l)n_{\mu\nu}(k,t)\,. \tag{5.17}$$

The single-particle Green's function represents the main object of interest in this chapter; from the symmetries of the Hamiltonian (and thus of the initial state) the following properties of $\mathcal{G}(j,l;t)$ can be derived

$$\mathcal{G}(j,l;t) = \mathcal{G}(j+2n, l+2n; t), \tag{5.18}$$

$$\mathcal{G}(j,l;t) = \mathcal{G}(j,l;t)^*, \qquad j-l = 2n+1, \tag{5.19}$$

$$\mathcal{G}(j,l;t) = \mathcal{G}(j,2j-l;t)^*, \qquad j-l = 2n, \qquad n \in \mathbb{Z}, \tag{5.20}$$

we note that $\mathrm{Re}\,\mathcal{G}(j,l;t)$, for $j-l = 2n$, is constructed only using diagonal occupation numbers $n_{\mu\mu}(k;t)$.

5.3 Equations of motion

The EOM are derived by considering the time evolution equations of the bilinears $\hat{n}_{\mu\nu}(k,t) = \alpha^\dagger_\mu(k,t)\alpha_\nu(k,t)$ in the Heisenberg picture, a closed system is then obtained by truncating the

expectation value of the Heisenberg equations on the initial state. This is done assuming that the four and six particle connected cumulants in the correlation functions of the fermions $\alpha_{\pm}(k,t)$ can be neglected at all times. In this section we present the derivation of the EOM following the steps set out in Ref. [75], for deriving quantum Boltzmann equations. The Heisenberg equations of motion for $\hat{n}_{\mu\nu}(k,t)$ are of the form

$$\frac{\partial}{\partial t}\hat{n}_{\mu\nu}(k,t) = i\big[H,\hat{n}_{\mu\nu}(k,t)\big] = i\epsilon_{\mu\nu}(k)\hat{n}_{\mu\nu}(k,t) + iU\sum_{\boldsymbol{\eta}}\sum_{\boldsymbol{q}>0} Y^{\boldsymbol{\eta}}_{\mu\nu}(k,\boldsymbol{q})\hat{A}_{\boldsymbol{\eta}}(\boldsymbol{q},t)\ , \tag{5.21}$$

where we have defined $\epsilon_{\mu\nu}(k) = \epsilon_{\mu}(k) - \epsilon_{\nu}(k)$, $\hat{A}_{\boldsymbol{\eta}}(\boldsymbol{q},t) = \alpha^{\dagger}_{\eta_1}(q_1,t)\alpha^{\dagger}_{\eta_2}(q_2,t)\alpha_{\eta_3}(q_3,t)\alpha_{\eta_4}(q_4,t)$, and

$$\begin{aligned} Y^{\boldsymbol{\eta}}_{\mu\nu}(k,\boldsymbol{q}) =& \delta_{\nu,\eta_4}\delta_{k,q_4}V_{\eta_1\eta_2\eta_3\mu}(\boldsymbol{q}) + \delta_{\nu,\eta_3}\delta_{k,q_3}V_{\eta_1\eta_2\mu\eta_4}(\boldsymbol{q}) \\ &- \delta_{\mu,\eta_2}\delta_{k,q_2}V_{\eta_1\nu\eta_3\eta_4}(\boldsymbol{q}) - \delta_{\mu,\eta_1}\delta_{k,q_1}V_{\nu\eta_2\eta_3\eta_4}(\boldsymbol{q})\,. \end{aligned} \tag{5.22}$$

We now consider the Heisenberg equations of motion for the operator $\hat{A}_{\boldsymbol{\eta}}(\boldsymbol{q},t)$, which read as

$$\begin{aligned} \frac{\partial}{\partial t}\hat{A}_{\boldsymbol{\eta}}(\boldsymbol{q},t) = i\left[H,\hat{A}_{\boldsymbol{\eta}}(\boldsymbol{q},t)\right] =& iE_{\boldsymbol{\eta}}(\boldsymbol{q})\hat{A}_{\boldsymbol{\eta}}(\boldsymbol{q},t) \\ &+ iU\sum_{\boldsymbol{\gamma}}\sum_{\boldsymbol{p}>0} V_{\boldsymbol{\gamma}}(\boldsymbol{p})\left[\hat{A}_{\boldsymbol{\gamma}}(\boldsymbol{p},t),\hat{A}_{\boldsymbol{\eta}}(\boldsymbol{q},t)\right]\ , \end{aligned} \tag{5.23}$$

where $E_{\boldsymbol{\eta}}(\boldsymbol{q}) \equiv \epsilon_{\eta_1}(q_1) + \epsilon_{\eta_2}(q_2) - \epsilon_{\eta_3}(q_3) - \epsilon_{\eta_4}(q_4)$. Integrating (5.23) in time and then taking an expectation value with respect to our initial density matrix ρ_0, we have

$$\begin{aligned} \langle\hat{A}_{\boldsymbol{\eta}}(\boldsymbol{q},t)\rangle =& \langle\hat{A}_{\boldsymbol{\eta}}(\boldsymbol{q},0)\rangle\, e^{itE_{\boldsymbol{\eta}}(\boldsymbol{q})} \\ &+ iU\int_0^t ds\sum_{\boldsymbol{\gamma}}\sum_{\boldsymbol{p}>0} e^{i(t-s)E_{\boldsymbol{\eta}}(\boldsymbol{q})}V_{\boldsymbol{\gamma}}(\boldsymbol{p})\left\langle\left[\hat{A}_{\boldsymbol{\gamma}}(\boldsymbol{p},s),\hat{A}_{\boldsymbol{\eta}}(\boldsymbol{q},s)\right]\right\rangle\ . \end{aligned} \tag{5.24}$$

Substituting this back into (5.21) leads to an exact integro-differential equation for the mode occupation numbers $n_{\mu\nu}(k,t) = \mathrm{Tr}[\rho_0\hat{n}_{\mu\nu}(k,t)]$, which takes the form

$$\begin{aligned} \dot{n}_{\mu\nu}(k,t) =& i\epsilon_{\mu\nu}(k)n_{\mu\nu}(k,t) + iU\sum_{\boldsymbol{\eta}}\sum_{\boldsymbol{q}>0} Y^{\boldsymbol{\eta}}_{\mu\nu}(k,\boldsymbol{q})\left\langle\hat{A}_{\boldsymbol{\eta}}(\boldsymbol{q},0)\right\rangle e^{itE_{\boldsymbol{\eta}}(\boldsymbol{q})} \\ &- U^2\int_0^t ds\sum_{\boldsymbol{\eta},\boldsymbol{\gamma}}\sum_{\boldsymbol{q},\boldsymbol{p}>0}\left\langle\hat{A}_{\boldsymbol{\gamma}}(\boldsymbol{p},s)\hat{A}_{\boldsymbol{\eta}}(\boldsymbol{q},s)\right\rangle Y^{\boldsymbol{\eta}}_{\mu\nu}(k,\boldsymbol{q})e^{i(t-s)E_{\boldsymbol{\eta}}(\boldsymbol{q})}V_{\boldsymbol{\gamma}}(\boldsymbol{p}) \\ &+ U^2\int_0^t ds\sum_{\boldsymbol{\eta},\boldsymbol{\gamma}}\sum_{\boldsymbol{q},\boldsymbol{p}>0}\left\langle\hat{A}_{\boldsymbol{\gamma}}(\boldsymbol{p},s)\hat{A}_{\boldsymbol{\eta}}(\boldsymbol{q},s)\right\rangle Y^{\boldsymbol{\gamma}}_{\mu\nu}(k,\boldsymbol{p})e^{i(t-s)E_{\boldsymbol{\gamma}}(\boldsymbol{p})}V_{\boldsymbol{\eta}}(\boldsymbol{q})\,. \end{aligned} \tag{5.25}$$

As Wick's theorem holds for all initial density matrices ρ_0 we consider, the expectation value $\langle \hat{A}_{\boldsymbol{\alpha}}(\boldsymbol{q},0)\rangle$ can be expressed in terms of the mode occupation numbers $n_{\alpha\beta}(k,0)$. The eight-point average in (5.25) can be decomposed as

$$\langle \hat{A}_{\boldsymbol{\gamma}}(\boldsymbol{p},t)\hat{A}_{\boldsymbol{\alpha}}(\boldsymbol{q},t)\rangle = f(\{n_{\alpha\beta}(k,t)\}) + \mathcal{C}[\langle \hat{A}_{\boldsymbol{\gamma}}(\boldsymbol{p},t)\hat{A}_{\boldsymbol{\alpha}}(\boldsymbol{q},t)\rangle]\,,$$

where the first term is the result of applying Wick's theorem, and $\mathcal{C}\,[\cdots]$ denotes terms involving four, six and eight particle cumulants (the eight particle cumulant does not contribute because of the antisymmetric structure of (5.25)). In order to turn (5.25) into a closed system of integro-differential equations we now assume that the four and six particle cumulants can be neglected at all times. This leads to the following system of equations

$$\begin{aligned}
\dot{n}_{\mu\nu}(k,t) &= i\epsilon_{\mu\nu}(k)n_{\mu\nu}(k,t) + 4iU\sum_{\gamma_1\gamma_2\gamma_3}\sum_{q>0} V_{\gamma_1\gamma_2\gamma_3\mu}(k,q,q,k)e^{i\epsilon_{\gamma_1\nu}(k)t}e^{i\epsilon_{\gamma_2\gamma_3}(q)t}n_{\gamma_1\nu}(k,0)n_{\gamma_2\gamma_3}(q,0)\\
&\quad - 4iU\sum_{\gamma_1\gamma_2\gamma_3}\sum_{q>0} V_{\nu\gamma_2\gamma_3\gamma_1}(k,q,q,k)e^{i\epsilon_{\mu\gamma_1}(k)t}e^{i\epsilon_{\gamma_2\gamma_3}(q)t}n_{\mu\gamma_1}(k,0)n_{\gamma_2\gamma_3}(q,0)\\
&\quad - U^2\int_0^t \mathrm{d}t' \sum_{\vec{\gamma}}\sum_{k_1,k_2,k_3>0} L^{\vec{\gamma}}_{\mu\nu}(k_1,k_2,k_3;k;t-t')n_{\gamma_1\gamma_2}(k_1,t')n_{\gamma_3\gamma_4}(k_2,t')n_{\gamma_5\gamma_6}(k_3,t')\\
&\quad - U^2\int_0^t \mathrm{d}t' \sum_{\gamma}\sum_{k_1,k_2>0} K^{\gamma}_{\mu\nu}(k_1,k_2;k;t-t')n_{\gamma_1\gamma_2}(k_1,t')n_{\gamma_3\gamma_4}(k_2,t')\,. \qquad (5.26)
\end{aligned}$$

Here $\vec{\gamma} = (\gamma_1 \ldots \gamma_6)$ and explicit expressions for the kernels are given by

$$\begin{aligned}
K^{\gamma}_{\mu\nu}(k_1,k_2;k;t) &= 4\sum_{k_3,k_4>0}\sum_{\eta,\eta'} X^{\gamma_1\gamma_3\eta\eta';\eta\eta'\gamma_4\gamma_2}_{\boldsymbol{k};\boldsymbol{k}'}(\mu,\nu;k;t),\\
L^{\vec{\gamma}}_{\mu\nu}(k_1,k_2,k_3;k;t) &= 8\sum_{\eta}\sum_{k_4>0} X^{\gamma_1\gamma_3\gamma_6\eta;\eta\gamma_5\gamma_4\gamma_2}_{\boldsymbol{k};\boldsymbol{k}'}(\mu,\nu;k;t) - 16\sum_{\eta} X^{\gamma_1\gamma_3\eta\gamma_4;\gamma_5\eta\gamma_6\gamma_2}_{k_1k_2k_1k_2;k_3k_1k_3k_1}(\mu,\nu;k;t)\,,\\
X^{\boldsymbol{\gamma};\boldsymbol{\eta}}_{\boldsymbol{k};\boldsymbol{q}}(\mu,\nu;q;t) &= Y^{\boldsymbol{\gamma}}_{\mu\nu}(\boldsymbol{k},q)V_{\boldsymbol{\eta}}(\boldsymbol{q})e^{iE_{\boldsymbol{\gamma}}(\boldsymbol{k})t} - (\boldsymbol{\gamma},\boldsymbol{k}) \leftrightarrow (\boldsymbol{\eta},\boldsymbol{q}). \qquad (5.27)
\end{aligned}$$

The solution of the set of integro-differential equations (5.26) is numerically demanding. We designed an algorithm that scales as $L^3 \times T$ where T is the number of time steps and L the number of lattice sites. This allows us to reach long times $J_1 t \sim 80$ on large systems $L \sim 320$ (a similar scaling was proposed in Ref. [181]); the maximum time reachable is set by the appearance of revivals.

We note that Eqs. (5.26) are the result of a "second order" approximation: we approximately take into account the effect of the four-particle connected cumulants in the expectation value of (5.21) (with respect to ρ_0) by means of the Eqs. (5.24). A less accurate approximation would be to completely neglect the four-particle connected cumulant from the expectation

value of (5.21): this would give rise a simpler system of equations that we call "first order equations", it reads as

$$\dot{n}_{\mu\nu}(k,t) = i\epsilon_{\mu\nu}(k)n_{\mu\nu}(k,t) + 4iU \sum_{\gamma_1\gamma_2\gamma_3} \sum_{q>0} V_{\gamma_1\gamma_2\gamma_3\mu}(k,q,q,k)n_{\gamma_1\nu}(k,t)n_{\gamma_2\gamma_3}(q,t)\,,$$
$$- 4iU \sum_{\gamma_1\gamma_2\gamma_3} \sum_{q>0} V_{\nu\gamma_2\gamma_3\gamma_1}(k,q,q,k)n_{\mu\gamma_1}(k,t)n_{\gamma_2\gamma_3}(q,t)\,, \tag{5.28}$$

these equations are analysed in Appendix 5.A. For short times, the right hand sides of (5.28) and (5.26) coincide with the perturbative expansions of $i\mathrm{Tr}\big[\rho_0\big[H,\hat{n}_{\mu\nu}(k,t)\big]\big]$ in U respectively up to first and second order.

The "first order" equations give results which are equivalent to those found in Ref. [66] by means of the first order continuous unitary transformation (CUT) approach [60, 61, 170]. The equivalence is shown in Appendix 5.A, where we analytically solve the first order equations up to $O(U^2)$ corrections. In particular, from our solution it is easy to extract the expectation values of $\hat{n}_{\mu\nu}(k)$ in the "deformed GGE" of Ref. [66].

For short times, the equations (5.26) refine the first order description (obtained by of the first-order EOM or CUT approximation) by going to the next order in perturbation theory. At later times, however, we will see that non-perturbative feedback mechanisms present in the equations cause a drifting away from the prethermalised solution observed using the first order approximations. In this context our most striking "non-perturbative" result is probably the strong J_2 dependence of the solution of (5.26) (see the following) to contrast with the complete J_2 independence that one finds from the first order equations.

5.4 EOM results for the Green's function

In this section we present the results obtained by means of the EOM for the time evolution of the single-particle Green's functions.

We start by providing a crucial check of the accuracy of our approach: the direct comparison to previous time-dependent density-matrix renormalisation-group (t-DMRG) computations [66]. Figs. 5.1 – 5.3 report the time evolution of $\mathcal{G}(L/2, L/2+j)$ with $j = 1, 2, 3, 4, 5$, computed respectively by means of EOM and t-DMRG; for a quench where the system is prepared in the ground state of $H(0, 0.8, 0)$ and time evolved subject to the Hamiltonian $H(0, 0.4, 0.4)$. We see that even for relatively large $U = 0.4$, there is excellent agreement between the two methods for all times accessible by t-DMRG. This agreement suggests that the EOM method is very accurate for small values of U and short and intermediate time scales.

The advantage of the EOM method is that it allows us to access later time scales than the t-DMRG computations reported in Ref. [66]. As long as the interaction strength U is sufficiently small, we observe very long-lived prethermalisation plateaux, as is exemplified in the insets of Figures 5.1 and 5.3: the values of the observables are quasi-stationary for long times, but they remain well separated from the thermal values, which have been computed via exact diagonalisation (ED) on a system of $L = 16$. Specifically we adopt the following procedure. We compute the energy density, given by

$$e = \frac{1}{L}\mathrm{Tr}\left[\rho_0 H(J_2, \delta, U)\right] , \tag{5.29}$$

and determine the effective temperature $1/\beta_{\mathrm{eff}}$ of the thermal ensemble for the post-quench Hamiltonian $H(J_2, \delta, U)$ through

$$e = \frac{1}{L}\mathrm{Tr}\left[\rho(\beta_{\mathrm{eff}}, J_2, \delta, U) H(J_2, \delta, U)\right] , \tag{5.30}$$

where the trace is over states with fixed particle number density $n = \mathrm{Tr}\left[\rho_0 N\right]/L$. Using ED we find β_{eff}, and then use the same method to compute the single-particle Green's function in thermal equilibrium at temperature $1/\beta_{\mathrm{eff}}$. We checked that the ED thermal value of $\mathcal{G}(L/2, L/2+1)$ is consistent the quantum Monte Carlo result reported in [66].

As shown in Fig. 5.A.1 of Appendix 5.A the quasi-stationary values observed are compatible with the CUT ones of Ref. [66] up to $O(U^2)$ corrections. This means that (up to $O(U^2)$ corrections) the values can be described by the ensemble introduced in Ref. [66]: the "deformed GGE", which corrects the stationary value of the free GGE up to $O(U)$.

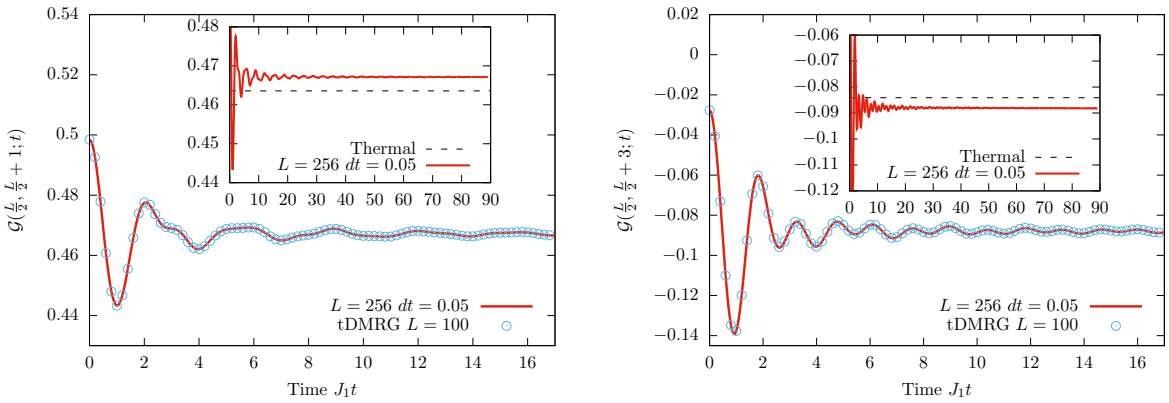

Figure 5.1: $\mathcal{G}(L/2, L/2+j; t)$ with $j = 1$ (left) and $j = 3$ (right) for a quench where the system is prepared in the ground state of $H(0, 0.8, 0)$ and time evolved with $H(0, 0.4, 0.4)$ for a system with $L = 256$ sites. The EOM results (red line) are in excellent agreement with t-DMRG computations [66] (circles). Insets: prethermalised behaviour persists over a large time interval.

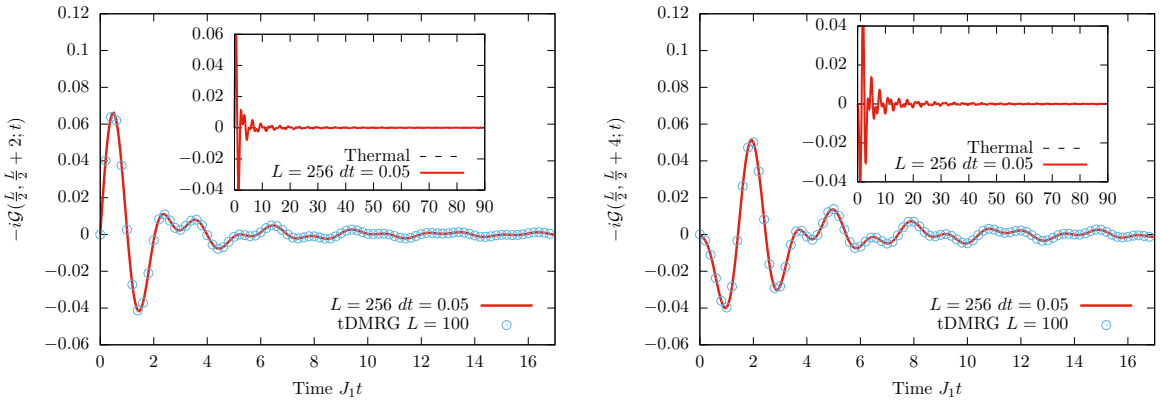

Figure 5.2: $-i\mathcal{G}(L/2, L/2+j; t)$ with $j = 2$ (left) and $j = 4$ (right) (the real parts are zero for all times) for a quench where the system is prepared in the ground state of $H(0, 0.8, 0)$ and time evolved with $H(0, 0.4, 0.4)$ for a system with $L = 256$ sites. The EOM results (red line) are in excellent agreement with t-DMRG computations [66] (circles). Insets: behaviour on a larger time interval (the thermal and prethermal values coincide in this case).

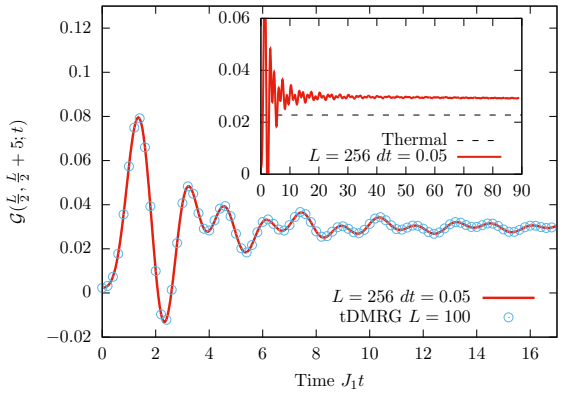

Figure 5.3: $\mathcal{G}(L/2, L/2+5; t)$ for a quench where the system is prepared in the ground state of $H(0, 0.8, 0)$ and time evolved with $H(0, 0.4, 0.4)$ for a system with $L = 256$ sites. The EOM results (red line) are in excellent agreement with t-DMRG computations [66] (circles). Insets: prethermalised behaviour persists over a large time interval.

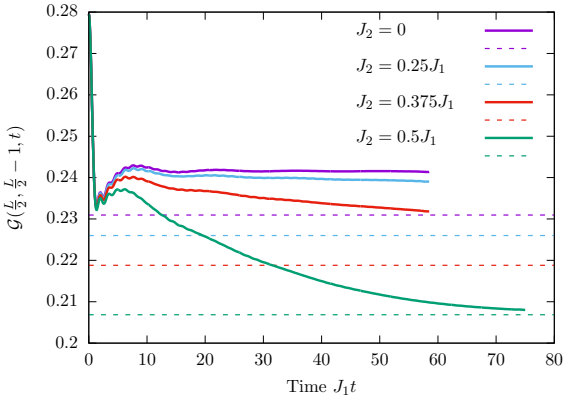

Figure 5.4: $\mathcal{G}(L/2, L/2-1; t)$ for a system with Hamiltonian $H(J_2, 0.1, 0.4)$ and sizes $L = 256, 320$ initially prepared in a thermal state (5.13) with density matrix $\rho(2, 0, 0, 0)$. The different colours correspond to different values of $J_2 = 0, 0.25, 0.375, 0.5$, dashed lines indicate the thermal values.

5.4.1 Next-nearest-neighbour hopping

In order to investigate if and how the prethermalised regime evolves towards thermal equilibrium it is convenient to invoke a non-zero J_2. Fig. 5.4 reports the time evolution of $\mathcal{G}(L/2, L/2-1)$ for a system prepared in the initial state (5.13) with density matrix $\rho_0 = \rho(2, 0, 0, 0)$, and time evolved with Hamiltonian $H(J_2, 0.1, 0.4)$ for $J_2 = 0, 0.25, 0.375, 0.5$. In contrast to the case $J_2 = 0$, $U = 0.4$, we now observe a drift: *the observables continuously leave the prethermal plateau moving towards a thermal steady state.*

For small values J_2 the time window in which the system is in the prethermalised quasi-

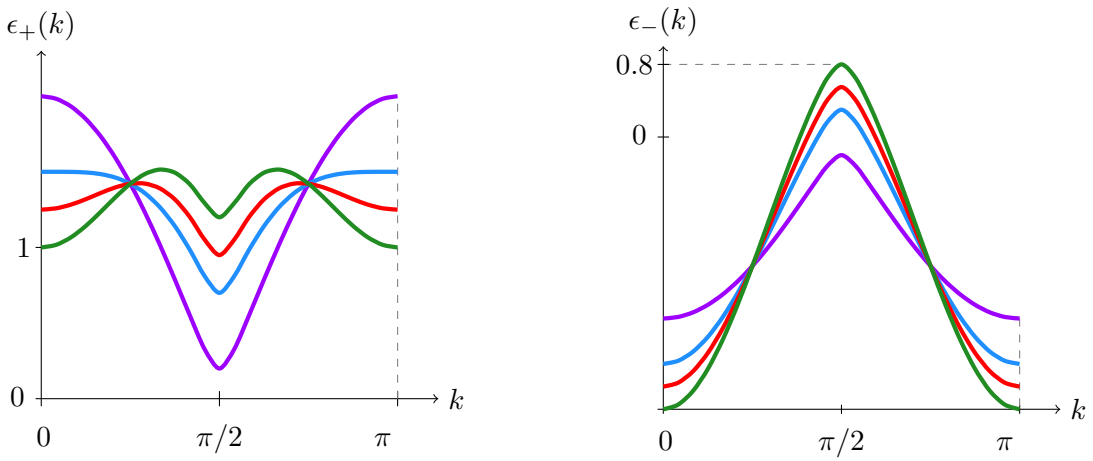

Figure 5.5: Dispersion relations of the free model for $J_1 = 1$, $\delta = 0.1$ and different values of J_2. Violet lines $J_2 = 0$, blue lines $J_2 = 0.25$, red lines $J_2 = 0.375$, green lines $J_2 = 0.5$. From the plot for $\epsilon_+(k)$ we see that increasing J_2 more crossings at fixed energy are developed; for $J_2 > 0.6$ additional fixed energy crossing appear because the ranges of $\epsilon_+(k)$ and $\epsilon_-(k)$ start to overlap.

stationary state remains well visible; increasing J_2 the window substantially reduces and the system rapidly goes towards the thermal value. We stress that the solution of the first order EOM does not show this drift, remaining on the quasi-stationary state and is completely independent of J_2: for large J_2 it is completely unreliable. In summary, J_2 allows us to tune the crossover time scale between the two regimes, effectively gauging the strength of the symmetry breaking. The strong J_2-dependence of the drifting rate can be understood by looking at the band structure of the non-interacting model: large values of J_2 introduce additional crossings at a fixed energy, see Fig. 5.5. This in turn generates additional scattering channels that promote relaxation.

Figures 5.6 – 5.9 show results for the time evolution of the Green's function for different separations and two values of J_2 which generate two qualitatively different evolutions of the local observables: $J_2 = 0.25$, which allows local observables to remain in the prethermalised state for long times, and $J_2 = 0.5$, which instead causes a rapid thermalisation. The thermal values shown in the figures are computed by exact diagonalisation (ED) of small systems up to size $L = 16$.

Let us consider the Green's functions between two sites which are close enough in the chain, such as those showed in Figs. 5.6 and 5.7. Within the reachable times we observe a clear drift towards the thermal values. The observed relaxation is compatible with exponential decay

$$\mathcal{G}(i,j;t) \sim \mathcal{G}(i,j)_{\text{th}} + A_{ij}(J_2,\delta,U)e^{-t/\tau_{ij}(J_2,\delta,U)}\,, \tag{5.31}$$

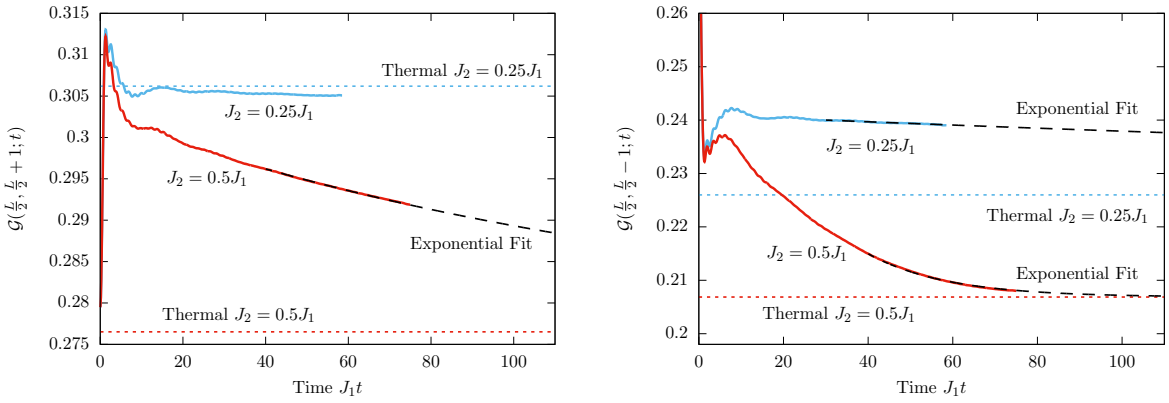

Figure 5.6: $\mathcal{G}(L/2, L/2 \pm 1; t)$ for a system with Hamiltonian $H(J_2, 0.1, 0.4)$ and sizes $L = 256, 320$ initially prepared in a thermal state (5.13) with density matrix $\rho(2, 0, 0, 0)$. The expected steady state thermal values are indicated by dotted lines, while the black dashed lines are exponential fits to (5.31).

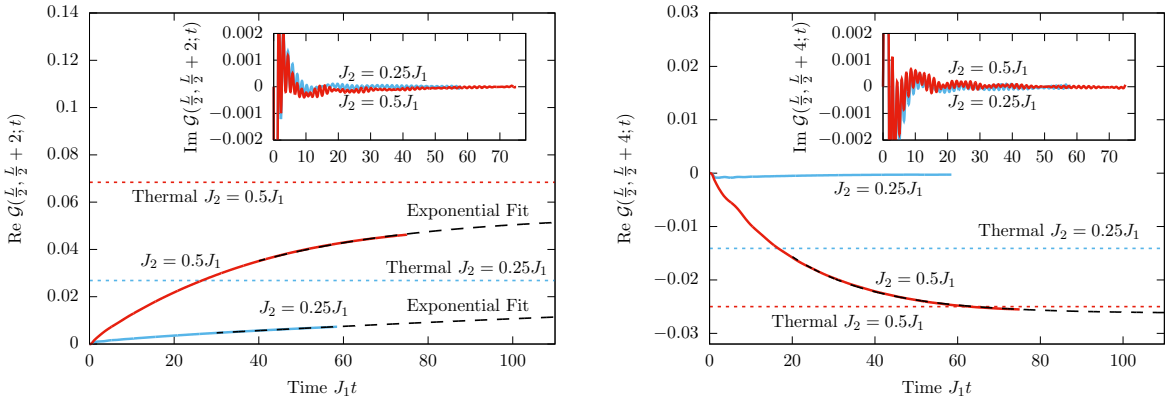

Figure 5.7: $\mathcal{G}(L/2, L/2+j; t)$ with $j = 2$ (left) and $j = 4$ (right) for a system with Hamiltonian $H(J_2, 0.1, 0.4)$ and sizes $L = 256, 320$ initially prepared in a thermal state (5.13) with density matrix $\rho(2, 0, 0, 0)$. The expected steady state thermal values are indicated by dotted lines, while the black dashed lines are exponential fits to (5.31).

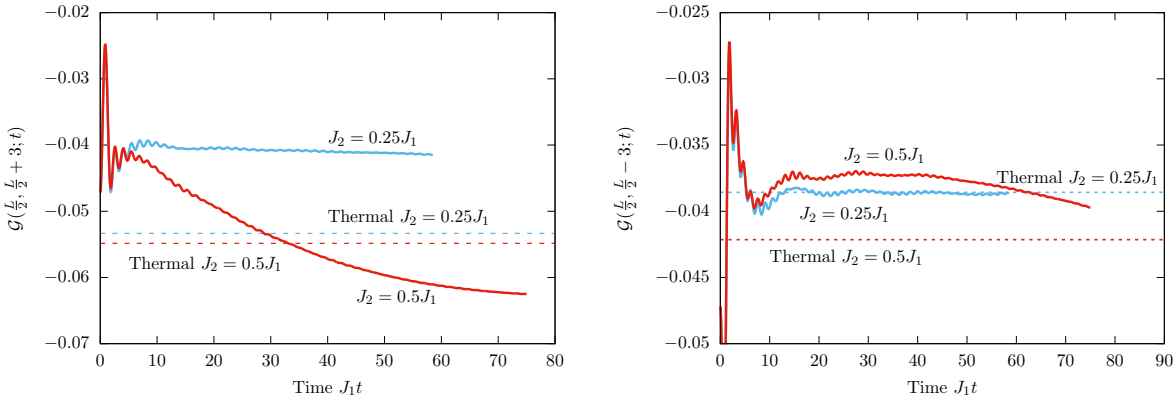

Figure 5.8: $\mathcal{G}(L/2, L/2 \pm 3; t)$ for a system with Hamiltonian $H(J_2, 0.1, 0.4)$ and sizes $L = 256, 320$ initially prepared in a thermal state (5.13) with density matrix $\rho(2, 0, 0, 0)$. The expected steady state thermal values are indicated by dotted lines.

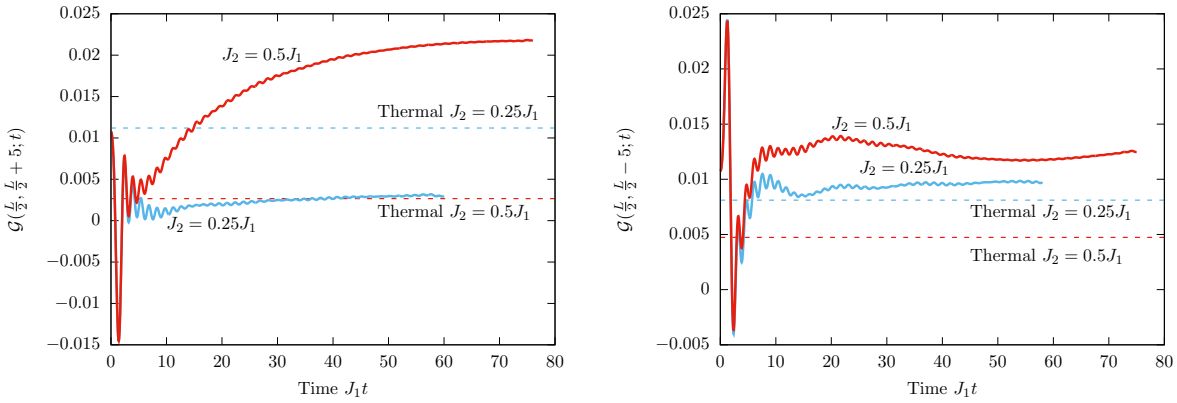

Figure 5.9: $\mathcal{G}(L/2, L/2 \pm 5; t)$ for a system with Hamiltonian $H(J_2, 0.1, 0.4)$ and sizes $L = 256, 320$ initially prepared in a thermal state (5.13) with density matrix $\rho(2, 0, 0, 0)$. The expected steady state thermal values are indicated by dotted lines, while the black dashed lines are exponential fits to (5.31).

where $\mathcal{G}(i,j)_{\text{th}}$ is the thermal Green's function at temperature $1/\beta_{\text{eff}}$ and, in general, the decay times for the real and imaginary part of the Green's function between evenly separated sites are different, we call them $\tau_{ij}(J_2, \delta, U)_{\text{r}}$ and $\tau_{ij}(J_2, \delta, U)_{\text{i}}$. In some cases, for example the $J_2 = 0.5$ case of Fig. 5.7, to obtain a better fit we have to allow the thermal value $\mathcal{G}(i,j)_{\text{th}}$ to deviate from the ED result by a small amount. We believe that this (tiny) discrepancy can be explained by a combination of errors in the EOM and finite size effects on the ED result. As appears clear from the figures, the decay times $\tau_{ij}(J_2, \delta, U)$ are extremely sensitive to the value of J_2.

Increasing the separation between the two sites leads to an increase of the relaxation times, which go beyond the times reached by the numerical solution of (5.26). However, we conjecture that the relation (5.31) describes the relaxation towards the thermal value of the Green's function for any value of the separation if one waits for long enough times. This is in some sense a "minimal" assumption: it is reasonable to think that the relaxation behaviour of the Green's function remains qualitatively the same for any separation of the two sites, providing $|i - j| \ll L$. In the following, however, we will give other elements in favour of this conjecture by exploring the dynamics for longer times with a quantum Boltzmann equation, which can be derived as the scaling limit of the equations (5.26) for the diagonal occupation numbers.

5.5 Quantum Boltzmann equation

It is natural to ask whether the Integral equation (5.26) can be simplified for late times by removing the time integration, in analogy with standard quantum Boltzmann equations (QBE) [75, 76]. The structure of the equations in the situation under exam, however, is profoundly different from the standard case; the EOM presents $O(U^0)$ and $O(U^1)$ terms, which do not

appear in the standard derivation of the QBE and are intimately related to the "prethermalised behaviour". In this case is not *a priori* clear whether the solution of the EOM for late times will depend on t only through the rescaled variable $\tau = U^2 t$, as is common in the QBE framework [75, 76].

The $O(U^0)$ contribution on the r.h.s. of the Equations (5.26) is non-zero only when $\mu = \bar{\nu}$. Numerical integration of the EOM (5.26) suggests that, for small U, the corresponding occupation numbers (*i.e.* $n_{\mu\bar{\mu}}(k;t)$) become negligible at late times: we thus assume $n_{\mu\bar{\mu}}(k,t) \approx 0$ for $t \gg U^{-1}$. If the occupation numbers relax towards their thermal values at late times (see the discussion in Subsection 5.5.2) their infinite time values satisfy $n_{\mu\bar{\mu}}(k,\infty) \sim O(U^1)$ and $n_{++}(k,\infty) \sim n_{--}(k,\infty) \sim O(U^0)$, agreeing with our assumption.

Neglecting the "off-diagonal" occupation numbers, we consider Equations (5.26) only in the diagonal case $\mu = \nu$. The presence of the $O(U^1)$ contribution in the equations, however, still prevents us from performing a standard QBE treatment. A good starting point to attack this problem is when the final Hamiltonian is translationally invariant, *i.e.* $\delta_f = 0$. In this case, although non vanishing, the $O(U^1)$ term does not contribute in the scaling limit: $U \to 0$ and $t \to \infty$ with fixed $\tau = tU^2$. This can be proven by considering the scaling limit of the diagonal Equations (5.26) which gives

$$\begin{aligned}\partial_\tau n_{\mu\mu}(k,\tau) = \lim_{U\to 0} 4iU^{-1} \sum_{\gamma_1\gamma_2\gamma_3} \sum_{q>0} \Big\{ & V_{\gamma_1\gamma_2\gamma_3\mu}(k,q,q,k) e^{i\epsilon_{\gamma_1\nu}(k)t} e^{i\epsilon_{\gamma_2\gamma_3}(q)t} n_{\gamma_1\nu}(k,0) n_{\gamma_2\gamma_3}(q,0) \\ & - V_{\nu\gamma_2\gamma_3\gamma_1}(k,q,q,k) e^{i\epsilon_{\mu\gamma_1}(k)t} e^{i\epsilon_{\gamma_2\gamma_3}(q)t} n_{\mu\gamma_1}(k,0) n_{\gamma_2\gamma_3}(q,0) \Big\} \\ + \lim_{U\to 0} \sum_{\boldsymbol{k}>0} \sum_{\boldsymbol{\nu}} & \int_0^t \mathrm{d}s\, e^{iE_{\boldsymbol{\nu}}(\boldsymbol{k})(t-s)} F^\mu_{\boldsymbol{\nu}}(\boldsymbol{k};k;s)\ , \end{aligned} \tag{5.32}$$

where we have collected most of the integrand of the σ-integral into a single function $F^\mu_{\boldsymbol{\nu}}(\boldsymbol{k};k;s)$ in order to lighten notations.

The first term is the "non-standard" one and is just the $O(U^1)$ term of the original equations divided by U^2 because $\partial_\tau = U^{-2}\partial_t$. The leading contribution at late times is obtained by evaluating the momentum sums by a saddle point approximation. This gives

$$\begin{aligned} & \lim_{U\to 0} \frac{4i}{U} \sum_{\gamma_1} \Big\{ \Big(V_{\gamma_1\gamma_2\gamma_3\mu}(k,q,q,k) e^{i\epsilon_{\gamma_1\nu}(k)t} - V_{\nu\gamma_2\gamma_3\gamma_1}(k,q,q,k) e^{i\epsilon_{\mu\gamma_1}(k)t} n_{\mu\gamma_1}(k,0) \Big) e^{i\epsilon_{\gamma_2\gamma_3}(q)t} n_{\gamma_2\gamma_3}(q,0) \Big\} \\ & = \lim_{U\to 0} U \frac{\sin(\epsilon_{+-}(0)\tau U^{-2} - \pi/4)}{\tau^{3/2}} (A_\mu(k) e^{i\epsilon_{+-}(k)\tau U^{-2}} + \text{c.c.}) = 0\,. \end{aligned} \tag{5.33}$$

Here $A_\mu(k)$ is an amplitude depending on the initial state and the vertex function. The key property that one has to use is $V_{\eta\gamma\gamma\bar{\eta}}(k,q,q,k) = 0$ for $\delta_f = 0$; we also note that the exponent

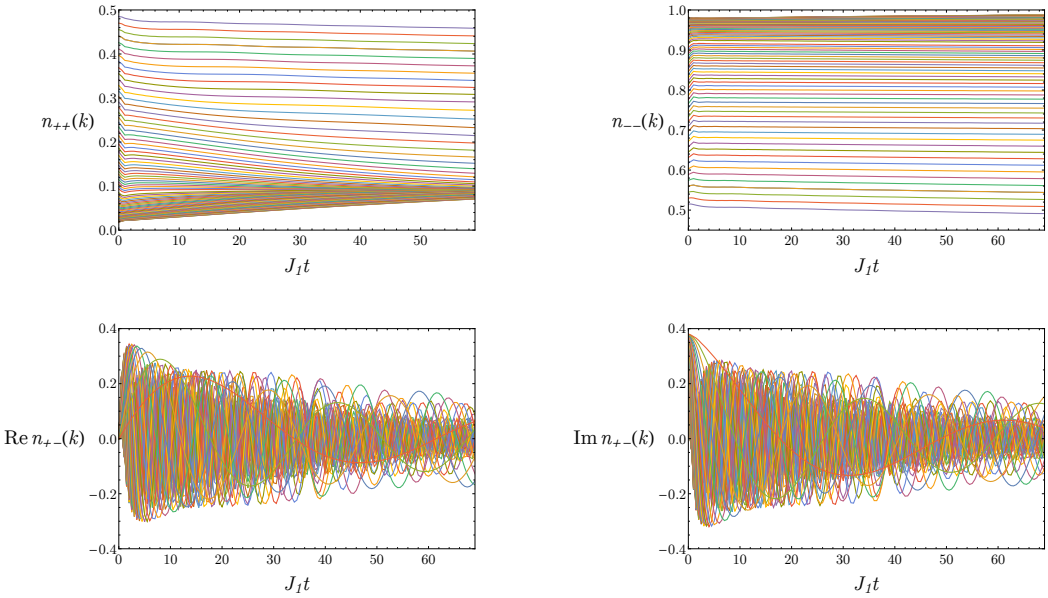

Figure 5.10: The time dependence of the number operators $n_{++}(k)$ (top left), $n_{--}(k)$ (top right), $\mathrm{Re}\, n_{+-}(k)$ (bottom left) and $\mathrm{Im}\, n_{+-}(k)$ (bottom right) evolving from the thermal state of $\rho(2, 0, 0.5, 0)$ according to $H(0.375, 0, 0.4)$ for $L = 320$. The different lines are different k modes (we restricted to $0 \leq k \leq \pi/2$ because the number operators satisfy $n_{\mu\nu}(k,t) = \mu\nu n_{\mu\nu}(\pi - k, t)$).

of the power law decay is $3/2$ because $n_{+-}(k, 0)$ vanish at saddle point 0 (*cf.* (5.16)).

The second contribution on the right hand side is the standard QBE term and can be simplified by using that for, $s \gg U^{-1}$, $n_{\mu\mu}(k, s)$ are functions of sU^2, while $n_{+-}(k, s) \sim 0$. This can be checked by inspecting the numerical solution of the full EOM (5.26), some examples are reported in Figs. 5.10 – 5.11. Using this assumption we have

$$\begin{aligned} &\int_0^t \mathrm{d}s\, e^{iE_{\boldsymbol{\nu}}(\boldsymbol{k})(t-s)} F(\boldsymbol{k}; k; s) \\ &\qquad \approx \int_0^{\bar{t}} \mathrm{d}s\, e^{iE(\boldsymbol{k})(t-s)} F(\boldsymbol{k}; k; s) + F(\boldsymbol{k}; k; \tau) \int_{\bar{t}}^t \mathrm{d}s\, e^{iE(\boldsymbol{k})(t-s)}\,, \end{aligned} \tag{5.34}$$

where we introduced $U^{-1} \ll \bar{t} \ll t$ and removed the dependence on indices, inessential to this discussion; moreover, in the second term, we removed the contribution of $n_{+-}(k, s)$ from $F(\boldsymbol{k}; k; s)$ and used that it is a smooth function of sU^2 to neglect its derivatives with respect to s.

The first term vanishes in our scaling limit. We regularise the integral in the second term by replacing $E(\boldsymbol{k}) \to E(\boldsymbol{k}) + i\eta$, where η is small and positive

$$\lim_{U\to 0} \int_{\bar{t}}^t \mathrm{d}s\, e^{i[E(\boldsymbol{k})+i\eta](t-s)} = \frac{i}{E(\boldsymbol{k}) + i\eta} \equiv D(E(\boldsymbol{k}))\,. \tag{5.35}$$

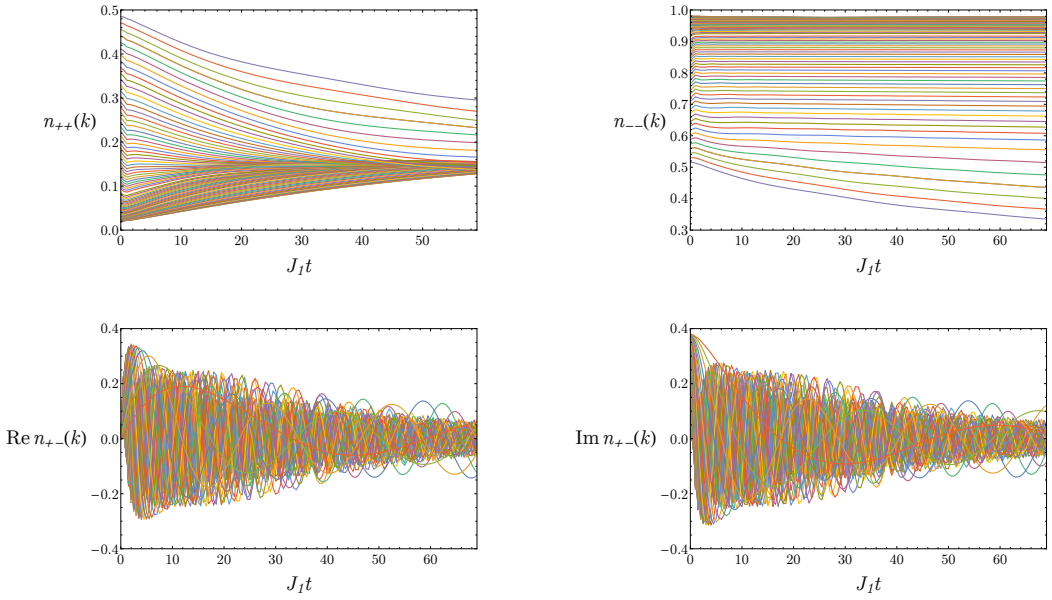

Figure 5.11: The time dependence of the number operators $n_{++}(k)$ (top left), $n_{--}(k)$ (top right), $\mathrm{Re}\, n_{+-}(k)$ (bottom left) and $\mathrm{Im}\, n_{+-}(k)$ (bottom right) evolving from the thermal state of $\rho(2, 0, 0.5, 0)$ according to $H(0.5, 0, 0.4)$ for $L = 320$. The different lines are different k modes (we restricted to $0 \leq k \leq \pi/2$ because the number operators satisfy $n_{\mu\nu}(k,t) = \mu\nu n_{\mu\nu}(\pi - k, t)$).

Putting everything together, we obtain the following QBE for the diagonal occupation numbers in the scaling limit

$$\begin{aligned}\partial_\tau n_{\mu\mu}(k,\tau) = &-\sum_{\gamma,\eta}\sum_{p,q>0} \widetilde{K}^{\gamma\eta}_{\mu\mu}(p,q;k) n_{\gamma\gamma}(p,\tau) n_{\eta\eta}(q,\tau) \\ &-\sum_{\gamma,\eta,\epsilon}\sum_{p,q,r>0} \widetilde{L}^{\gamma\eta\epsilon}_{\mu\mu}(p,q,r;k) n_{\gamma\gamma}(p,\tau) n_{\eta\eta}(q,\tau) n_{\epsilon\epsilon}(r,\tau). \end{aligned} \tag{5.36}$$

Here the kernels are given by

$$\begin{aligned}\widetilde{K}^{\gamma_1\gamma_2}_{\alpha\beta}(k_1,k_2|q) &= 4\sum_{k_3,k_4>0}\sum_{\nu,\nu'} \widetilde{X}^{\gamma_1\gamma_2\nu\nu'|\nu\nu'\gamma_2\gamma_1}_{\boldsymbol{k}|\boldsymbol{k}'}(\alpha,\beta|q), \\ \widetilde{L}^{\gamma_1\gamma_2\gamma_3}_{\alpha\beta}(k_1,k_2,k_3|q) &= 8\sum_{\nu}\sum_{k_4>0} \widetilde{X}^{\gamma_1\gamma_2\gamma_3\nu|\nu\gamma_3\gamma_2\gamma_1}_{\boldsymbol{k}|\boldsymbol{k}'}(\alpha,\beta|q) - 16\sum_{\nu} \widetilde{X}^{\gamma_1\gamma_2\nu\gamma_2|\gamma_3\nu\gamma_3\gamma_1}_{k_1k_2k_1k_2|k_3k_1k_3k_1}(\alpha,\beta|q), \\ \widetilde{X}^{\boldsymbol{\gamma}|\boldsymbol{\alpha}}_{\boldsymbol{k}|\boldsymbol{q}}(\alpha,\beta|q) &= Y^{\boldsymbol{\gamma}}_{\alpha\beta}(\boldsymbol{k}|q) V_{\boldsymbol{\alpha}}(\boldsymbol{q}) D(E_{\boldsymbol{\gamma}}(\boldsymbol{k})) - (\boldsymbol{\gamma},\boldsymbol{k}) \leftrightarrow (\boldsymbol{\alpha},\boldsymbol{q})\,. \end{aligned} \tag{5.37}$$

The Boltzmann equation has to be initialised at a time $t_0 \gg U^{-1}$. We stress that the scaling limit $U \to 0$ and $t \to \infty$ with fixed $\tau = tU^2$, is only a simplification used in the derivation, but is impractical to work with numerically, for example in this limit the time t_0 is formally going to infinity. What we will always do is to keep U small but finite, and initialise the QBE at a (finite!) time $t_0 \gg U^{-1}$; giving as initial values the diagonal occupation numbers computed

up to $t = t_0$ with the full EOM (5.26). This discussion suggests that the quantum Boltzmann equation gives the long-time behaviour of observables at the leading order in U.

To compute the Green's function in the quantum Boltzmann approximation we employ Eq. (5.17), neglecting the contribution of the off-diagonal occupation numbers and using the diagonal ones obtained from the numerical solution of the QBE. Figs. 5.12 – 5.13 compare the results obtained by this procedure with those found computing $\{n_{\mu\nu}(k;t)\}$ by numerical integration to the EOM (5.26); specifically, the results shown are obtained starting from the initial state $\rho(2, 0, 0.5, 0)$ and time evolving with the Hamiltonian $H(J_2, 0, 0.4)$ for $J_2 = 0.375, 0.5$ and $t_0 = 20$.

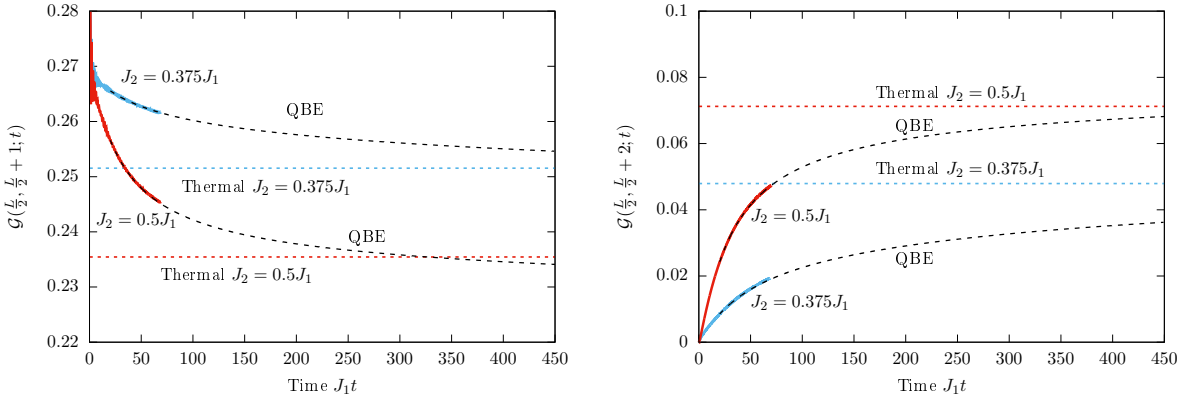

Figure 5.12: $\mathcal{G}(L/2, L/2+j; t)$ with $j = 1$ (left) and $j = 2$ (right) for a system with Hamiltonian $H(J_2, 0, 0.4)$ and size $L = 320$ initially prepared in a thermal state (5.13) with density matrix $\rho(2, 0, 0.5, 0)$. The full lines are the obtained by integrating the EOM (5.26) and the black dashed lines are found by means of the QBE.

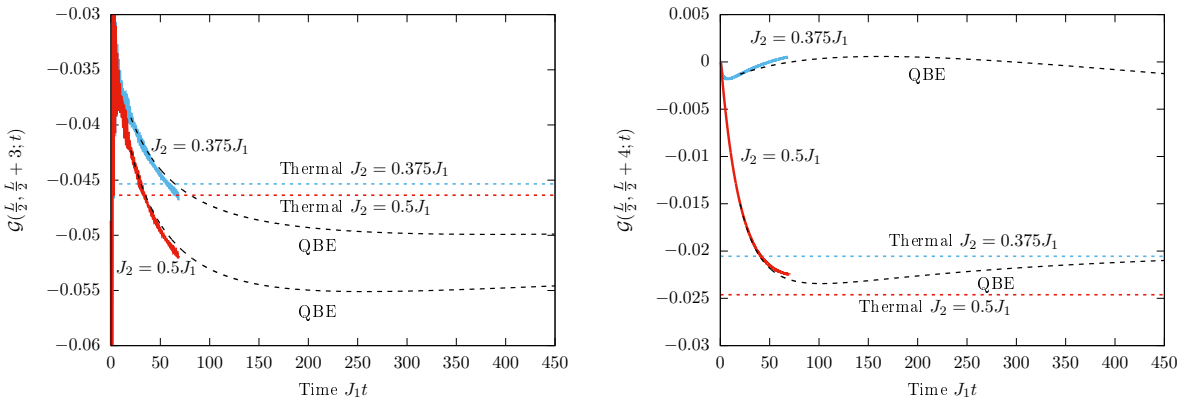

Figure 5.13: $\mathcal{G}(L/2, L/2+j; t)$ with $j = 3$ (left) and $j = 4$ (right) for a system with Hamiltonian $H(J_2, 0, 0.4)$ and size $L = 320$ initially prepared in a thermal state (5.13) with density matrix $\rho(2, 0, 0.5, 0)$. The full lines are the obtained by integrating the EOM (5.26) and the black dashed lines are found by means of the QBE.

Even for a relatively big value of U $(= 0.4)$ the results of Fig. 5.12 show impressive agreement, in Fig. 5.13 we see that for larger values of the separation the agreement worsens (this is

made more visible by the finer resolution of the plots). The figures also report the ED thermal values; for short separations the QBE curves approach the thermal value within the reachable times. For larger separations, the approach towards thermal happens at later times. In particular, $\mathcal{G}(L/2, L/2+3, t)$ are still substantially far from the thermal values in the time interval displayed. For $t \gtrsim 300$, however, they start to slowly drift in the direction of the ED result.

It can be shown (see for example Refs. [76,183]) that the number operators computed with QBE are eventually relaxing to the non-interacting Fermi-Dirac distribution, with an effective temperature set by the kinetic energy at the time the Boltzmann is initialised. This fact implies that the thermal value predicted by the Boltzmann equation is correct only at the order $O(U^0)$ and signals the importance of corrections to the QBE at very late times. Such corrections, arising from higher cumulants, might be responsible for the power law behaviour expected at very late times (for certain observables) after quenches in non-integrable models [184,185] and not captured by the QBE. This is again in accordance with our interpretation of the QBE: it gives the leading contribution for small U.

It is worth noting that when the QBE is implemented for finite L, the parameter η in (5.35) must be kept finite (see for example [183]). Unless otherwise stated we use $\eta = 0.0005$, the time evolution of $\mathcal{G}(L/2, L/2+1; t)$ and $\mathcal{G}(L/2, L/2-1; t)$ for different values of η is compared with the solution of the full EOM in Fig. 5.14.[1]

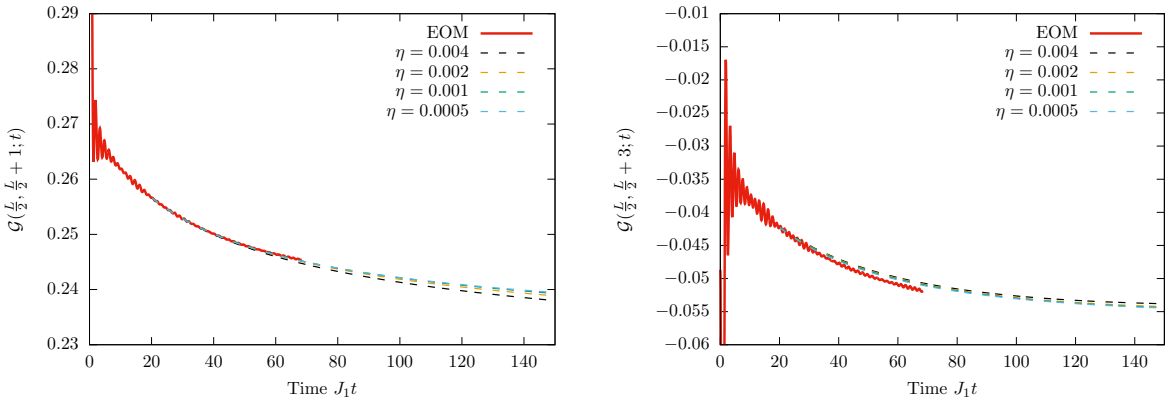

Figure 5.14: Comparison of EOM and QBE for various regularisation parameters. $\mathcal{G}(L/2, L/2+1; t)$ (left) and $\mathcal{G}(L/2, L/2+3; t)$ (right), evolving from the thermal state $\rho(2, 0, 0.5, 0)$ according to $H(0.5, 0, 0.4)$ for $L = 320$.

5.5.1 Scaling of the decay time with U

Due to its simpler structure, the QBE allows us to understand how the exponent (5.31) scales with U. The reasoning is as follows. In the limit $U \ll 1$ at large times such that $\tau \equiv tU^2 =$

[1] While the time evolution of observables can depend on η the stationary values reached are expected to be independent of η [183].

$O(U^0)$, if the Boltzmann description applies, local observables constructed with the diagonal number operators depend on time only through τ. In particular this is true for the Green's functions. The observables, however, can show some additional dependence on U if the initial conditions for the Boltzmann equation (*i.e.* the value of the observable on the prethermalisation plateau) or equivalently their asymptotic values (*i.e.* the thermal values) depend on U. As a consequence the Green's functions take the following scaling form

$$\mathcal{G}(i,j;t,U) = \mathcal{F}_{i,j}(\tau,U)\,, \qquad t > t_0 \gg U^{-1}\,. \tag{5.38}$$

To understand the additional U dependence of $\mathcal{F}_{i,j}$, rather than considering the initial conditions, it is easier to consider the U dependence of the asymptotic values it reaches for large τ. For small U, the energy density of our initial state is $e = O(U^0)$ and so the thermal values $\mathcal{F}_{i,j}(\infty,U) = O(U^0)$. This in turn implies that $\mathcal{F}_{i,j}(\tau,0)$ is not identically zero and expanding in U we have

$$\mathcal{F}_{i,j}(\tau,U) \sim \mathcal{F}_{i,j}(\tau,0) + O(U)\,. \tag{5.39}$$

Combining this expression with (5.31) we then obtain

$$\tau_{i,j}^{-1}(J_2,\delta_f = 0,U) \propto U^2. \tag{5.40}$$

Here we used $U \ll 1$ and $\tau = O(U^0)$. Our numerical findings are in good agreement both with the scaling form (5.39) (see Figs. 5.15 – 5.17) and with scaling (5.40) of the exponent (see Fig. 5.18). The results plotted in Fig. 5.18 depend also on the agreement between the EOM and the ED so we expect stronger deviations.

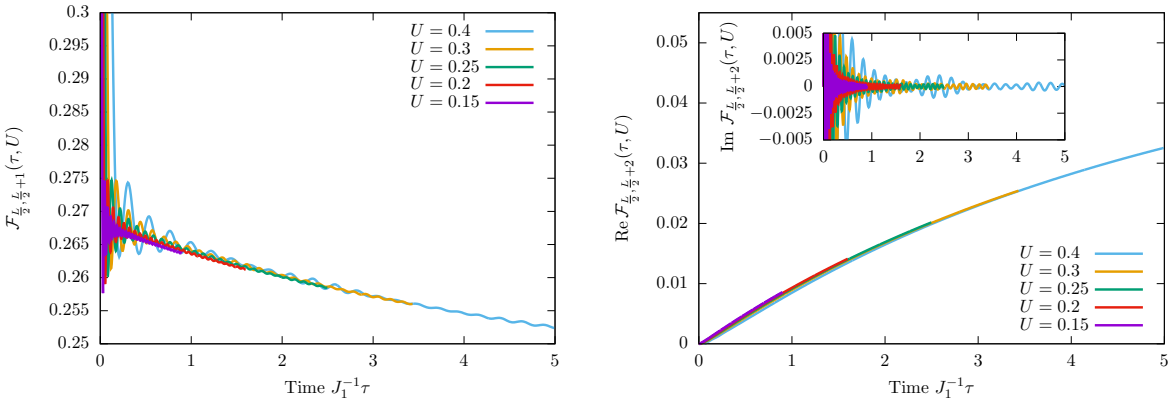

Figure 5.15: $\mathcal{F}_{L/2,L/2+1}(\tau,U) = \mathcal{G}(L/2,L/2+1;t,U)$ (left) and $\mathcal{F}_{L/2,L/2+2}(\tau,U) = \mathcal{G}(L/2,L/2+2;t,U)$ (right) the system is initially prepared in the state $\rho(2,0,0.5,0)$ and evolved with the Hamiltonian $H(0.5,0,U)$, for different values of U. The time evolution is obtained by numerical solution of the full EOM (5.26) and plotted as a function of the rescaled variable $\tau = U^2 t$.

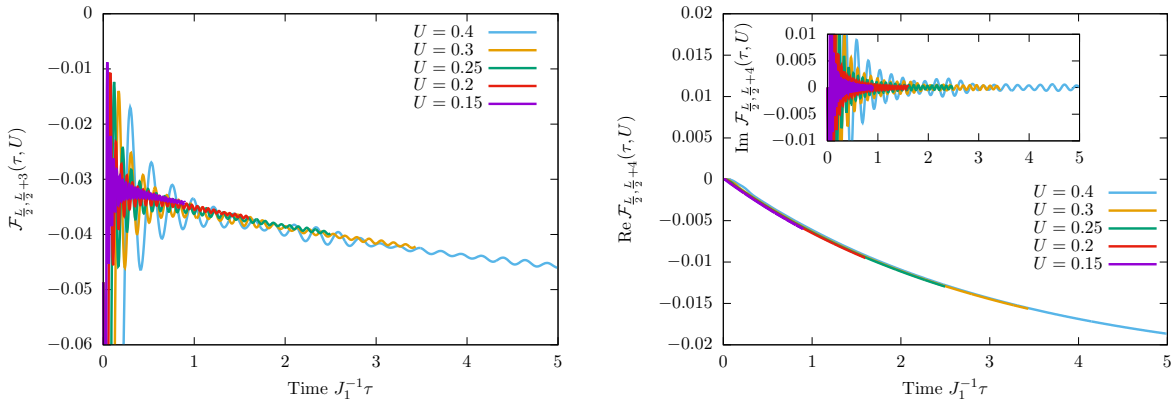

Figure 5.16: $\mathcal{F}_{L/2,L/2+3}(\tau,U) = \mathcal{G}(L/2,L/2+3;t,U)$ (left) and $\mathcal{F}_{L/2,L/2+4}(\tau,U) = \mathcal{G}(L/2,L/2+4;t,U)$ (right) the system is initially prepared in the state $\rho(2,0,0.5,0)$ and evolved with the Hamiltonian $H(0.5,0,U)$, for different values of U. The time evolution is obtained by numerical solution of the full EOM (5.26) and plotted as a function of the rescaled variable $\tau = U^2 t$.

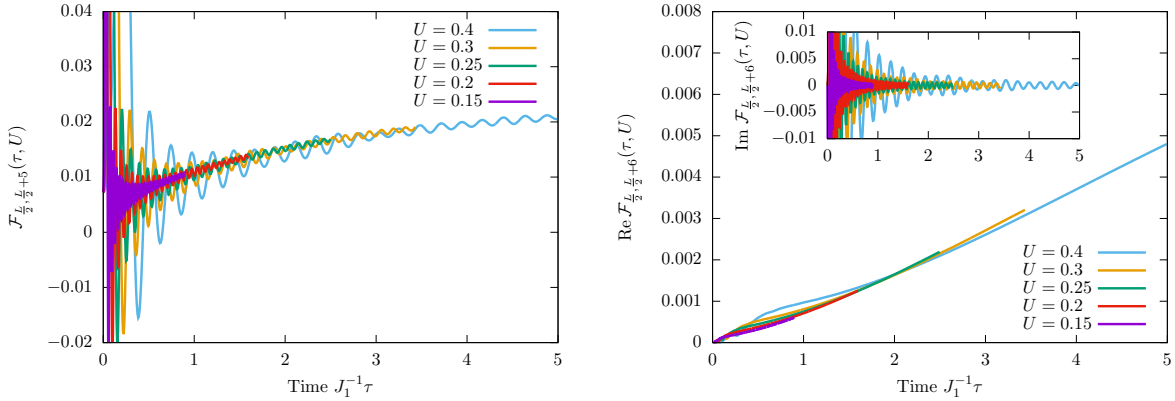

Figure 5.17: $\mathcal{F}_{L/2,L/2+5}(\tau,U) = \mathcal{G}(L/2,L/2+5;t,U)$ (left) and $\mathcal{F}_{L/2,L/2+6}(\tau,U) = \mathcal{G}(L/2,L/2+6;t,U)$ (right) the system is initially prepared in the state $\rho(2,0,0.5,0)$ and evolved with the Hamiltonian $H(0.5,0,U)$, for different values of U. The time evolution is obtained by numerical solution of the full EOM (5.26) and plotted as a function of the rescaled variable $\tau = U^2 t$.

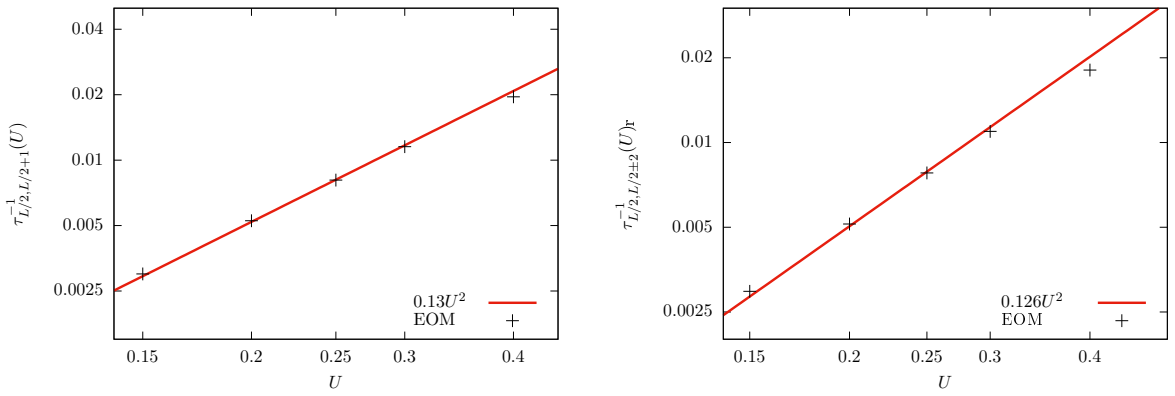

Figure 5.18: Dependence on U of the exponents $\tau^{-1}_{L/2,L/2+1}(U)$ and $\tau^{-1}_{L/2,L/2+2}(U)_{\rm r}$ obtained from the exponential fit (5.31), plotted in logarithmic scale.

The scaling found here differs form the one obtained in Ref. [72], where the exponent was

found to scale as U^{-4}. This is not surprising, in that case the initial energy density is $e = O(U^1)$ for small U and $\mathcal{F}_{i,j}(\tau, 0) = 0$ for every τ, so formula (5.39) does not give any information.

5.5.2 Occupation Numbers

To obtain further indications that the integrability breaking perturbations are causing the thermalisation of the model, it is instructive to study the occupation numbers $n_{\mu\nu}(q,t)$ themselves.

The first question to consider concerns their eventual relaxation: the number operators are localised in momentum space, consequently they are non local in real space. In light of the discussion in Chapter 1 it is then unclear whether we should expect them to relax to a time independent value at late times (see however Ref. [186], where a family of integrable hard-core lattice anyons is considered and the complete relaxation of the one body density matrix is observed, aside from the free-fermion limit).

To answer this question is convenient to write the occupation numbers in terms of the local Green's function by inverting the relation (5.17)

$$n_{\mu\nu}(k,t) = \frac{1}{8}\sum_{j=0}^{L/2} e^{-2ikj}\big\{\mathcal{G}(2j+1,1;t) + \mu\nu\mathcal{G}(2j,0;t) + \nu\mathcal{G}(2j+1,0;t)e^{ik}e^{i\varphi_k} + \mu\mathcal{G}(2j,1;t)e^{-ik}e^{-i\varphi_k}\big\}\,. \tag{5.41}$$

Since we only consider initial states with finite correlation lengths, $\mathcal{G}(j,l;t)$ are exponentially small in $|j-l|$ when $|j-l| \gg J_1 t$, as a consequence of Lieb-Robinson bounds (see Ref. [179] for a more detailed discussion of the applications of Lieb-Robinson bounds to the behaviour of correlation functions). This implies that at time t the sum (5.41) can be well-approximated by truncation at $j_{\max} \sim J_1 t$. Finally, using the fact that $\mathcal{G}(j,l;t)$ decay exponentially fast in time for $|j-l| \leq J_1 t$ we can argue that $n_{\mu\nu}(q,t)$ relax in our regime of interest: $1 \ll J_1 t \ll L$. The numerical solutions of the EOM seem to confirm this reasoning, as shown in Figs. 5.10 – 5.11.

We stress that the exponential decay in time of the correlation functions is necessary in order for the argument given to work. Consider, for example, some occupation numbers that oscillate indefinitely in time

$$n(k,t) = A_k e^{i\varepsilon_k t}\,, \tag{5.42}$$

with some amplitude A_k ensuring a finite correlation length and dispersion ε_k, which is assumed to posses a local minimum. The local Green's function obtained from (5.42) still relaxes (to

zero in this trivial case) in a power law fashion, as can be showed by saddle point approximation

$$G(\ell,t)=\frac{1}{L}\sum_k n(k,t)e^{i\ell k}\sim\int\frac{\mathrm{d}k}{2\pi}n(k,t)e^{i\ell k}\sim\frac{1}{t^\alpha}\,,\qquad\qquad \alpha\geq\frac{1}{2}\,,\tag{5.43}$$

where we considered the limit $L\gg t\gg\ell$.

Having argued that the mode occupation numbers, despite being non-local, relax to their thermal value, it is meaningful to consider their time evolution comparing with the thermal values they are expected to reach. In Figs. 5.19 – 5.20 we present the mode occupation numbers $n_{\mu\mu}(k,t)$ at several different times for a system of size $L=320$, prepared in the density matrix $\rho(2,0,0.5,0)$ and evolved with Hamiltonian $H(J_2,0,0.4)$ with $J_2=0.375,0.5$. For short/intermediate times $J_1t\lesssim 70$ we use the full EOM, while we access later times by means of QBE. In the figures, the QBE is initialised at time $t_0=20$, and is seen to be in good agreement with the full EOM until the latest times accessible by the latter method.

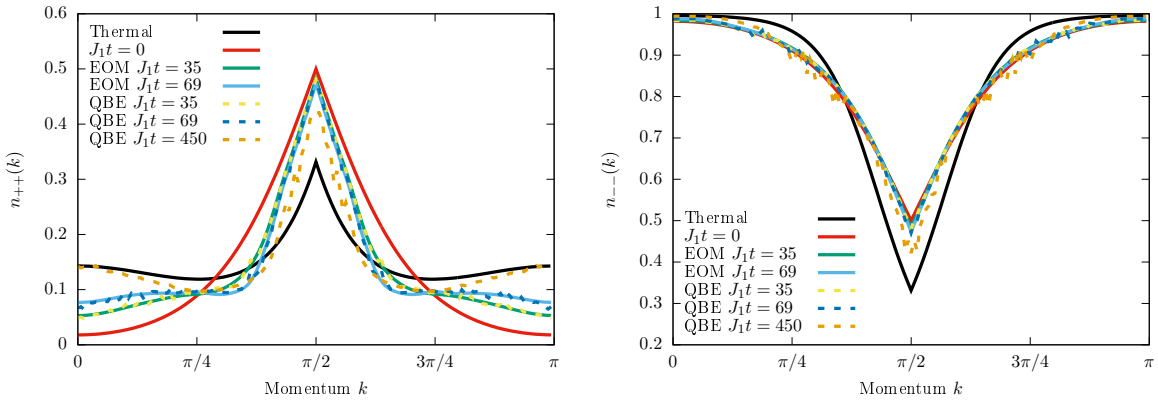

Figure 5.19: Occupation numbers $n_{++}(k,t)$ and $n_{--}(k,t)$ initialised in the thermal state $\rho(2,0,0.5,0)$, and time evolved with $H(0.375,0,0.4)$. The solid lines are the results of the EOM ($L = 320$) for various times. The dotted lines are computed by means of the QBE ($L = 320$). The black solid line is the thermal value found by means of second order perturbation theory in U.

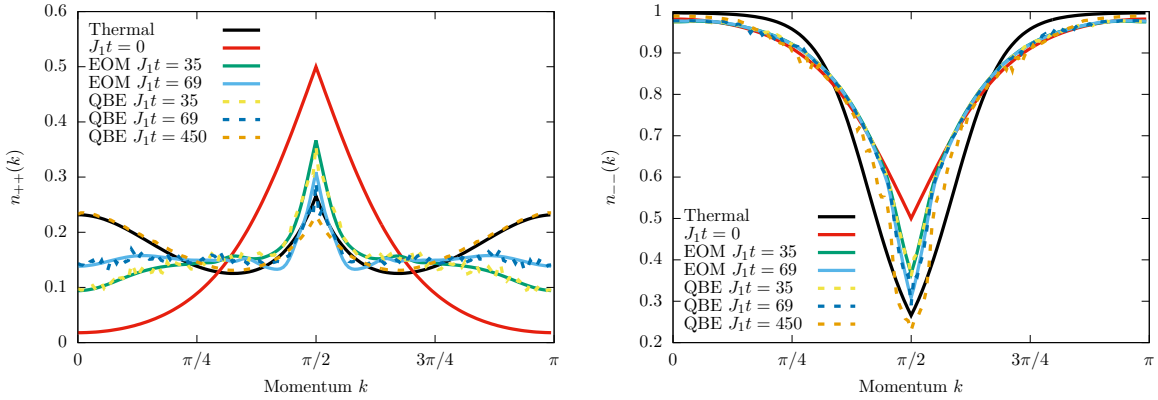

Figure 5.20: Occupation numbers $n_{++}(k,t)$ and $n_{--}(k,t)$ initialised in the thermal state $\rho(2,0,0.5,0)$, and time evolved with $H(0.5,0,0.4)$. The solid lines are the results of the EOM ($L = 320$) for various times. The dotted lines are computed by means of the QBE ($L = 320$). The black solid line is the thermal value found by means of second order perturbation theory in U.

The behaviours reported in the figures represent the main result of this section: at intermediate times, both $n_{++}(k,t)$ and $n_{--}(k,t)$ slowly approach their respective thermal distributions $n_{++}(k,\beta_{\text{eff}},\mu_{\text{eff}})$ and $n_{--}(k,\beta_{\text{eff}},\mu_{\text{eff}})$, calculated by means of perturbation theory (PT) in U, up to $O(U^2)$ (see Appendix 5.B for the details of the calculation). The effective temperature β_{eff}^{-1} and chemical potential μ_{eff} are fixed by

$$e = \frac{\text{Tr}[H(J_2,\delta,U)e^{-\beta_{\text{eff}}(H(J_2,\delta,U)-\mu_{\text{eff}}N)}]}{\text{Tr}[e^{-\beta_{\text{eff}}(H(J_2,\delta,U)-\mu_{\text{eff}}N)}]}\,, \qquad n = \frac{\text{Tr}[Ne^{-\beta_{\text{eff}}(H(J_2,\delta,U)-\mu_{\text{eff}}N)}]}{\text{Tr}[e^{-\beta_{\text{eff}}(H(J_2,\delta,U)-\mu_{\text{eff}}N)}]}\,. \tag{5.44}$$

In particular, at the latest time reached ($t = 450$) the occupation numbers for $J_2 = 0.5$ are almost exactly described by the thermal distribution.

The full integration of EOM (5.26) indicates that the "off-diagonal" occupation numbers

$n_{+-}(k,t)$ approach their thermal value zero in an oscillatory fashion, see Figs. 5.10 – 5.11.

These results strongly suggests that *the weak integrability breaking term induces thermalisation of the system.*

5.5.3 Quantum Boltzmann equation for $\delta_f \neq 0$

Let us now present an heuristic argument which allows us to address the case $\delta_f \neq 0$. We are interested in the long time behaviour ($t \sim U^{-2}$) of observables, with accuracy $O(U^0)$, we can thus neglect the contribution of the off-diagonal occupation numbers and concentrate on the equations for the diagonal ones. When $\delta_f \neq 0$, the Equations (5.26) for $n_{\mu\mu}(k;t)$ present a driving term which displays a persistent oscillatory behaviour, it has the form (*cf.* (5.26))

$$UD(k;t) \equiv -8U \,\mathrm{Im}\left[\sum_{\gamma}\sum_{q>0} V_{\mu\gamma\gamma\bar{\mu}}(k,q,q,k) n_{\gamma\gamma}(q,0) n_{\mu\bar{\mu}}(k,0) e^{i\epsilon_{\mu\bar{\mu}}(k)t}\right] . \tag{5.45}$$

Motivated by the form of this term, we try the following *ansatz* for the late-time ($t \gg U^{-1}$) solution of (5.26)

$$n_{\mu\mu}(k;t) = \tilde{n}_{\mu\mu}(k;\tau) + UI(k;t)\,, \tag{5.46}$$

where $\tau = tU^2$ and

$$I(k;t) \equiv 8\,\mathrm{Re}\left[\sum_{\gamma}\sum_{q>0} V_{\mu\gamma\gamma\bar{\mu}}(k,q,q,k) n_{\gamma\gamma}(q,0) n_{\mu\bar{\mu}}(k,0) \frac{e^{i\epsilon_{\mu\bar{\mu}}(k)t}}{\epsilon_{\bar{\mu}\mu}(k)}\right] . \tag{5.47}$$

Inserting (5.46) into (5.26) we find that $\tilde{n}_{\mu\mu}(k;\tau)$ has to solve a set of equations that differ from (5.32) only by some $O(U^1)$ corrections to the r.h.s. These corrections arise from the cases where $UI(k;t)$ is multiplied by one or two $\tilde{n}_{\mu\mu}(k;\tau)$'s in the quadratic and cubic term of (5.26). Assuming that the $O(U^1)$ corrections are bounded functions of τ we can neglect their contribution in the scaling limit where $\tau = tU^2$ is fixed while $U \to 0$ and $t \to \infty$. In this way we obtain $\tilde{n}_{\mu\mu}(k;\tau) = \tilde{n}^{(0)}_{\mu\mu}(k;\tau) + O(U)$, where $\tilde{n}^{(0)}_{\mu\mu}(k;\tau)$ is a solution of the Boltzmann equation (5.36). Since the only $O(U^0)$ contribution to the solution (5.46) is $\tilde{n}^{(0)}_{\mu\mu}(k;\tau)$ we arrive to the final result: the leading contribution to the solution of (5.26) in the scaling limit is given by the solution of the QBE (5.36) also in the case $\delta_f \neq 0$.

To test the argument presented we considered the time evolution given by $H(J_2, 0.1, U)$, with ($J_2 = 0.25;\ U = 0.2$) and ($J_2 = 0.5;\ U = 0.4$), starting from the thermal state $\rho(2,0,0,0)$. In Figs. 5.21 and 5.22 we show that the scaling form (5.39) is still (approximately) satisfied, however, for some observables the corrections at larger U appear more pronounced then the

$\delta_f = 0$ case.

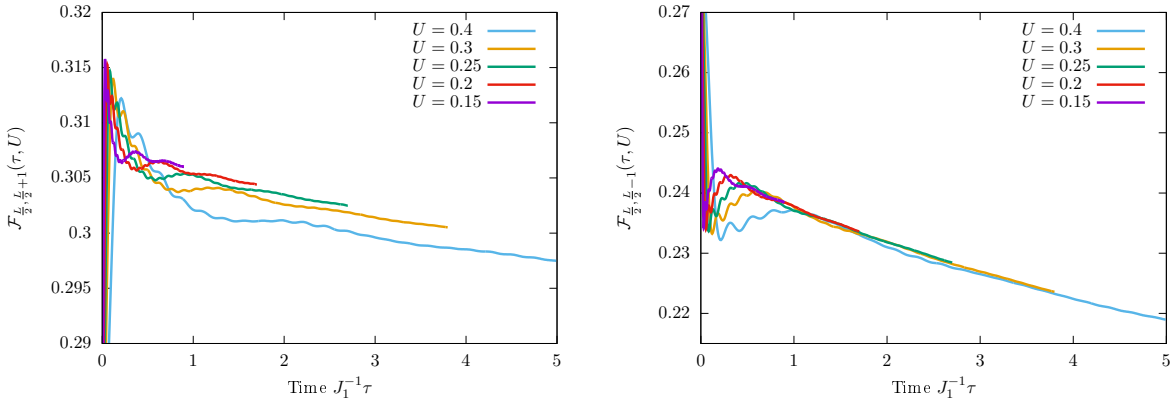

Figure 5.21: $\mathcal{F}_{L/2,L/2+1}(\tau, U) = \mathcal{G}(L/2, L/2+1; t, U)$ (left) and $\mathcal{F}_{L/2,L/2-1}(\tau, U) = \mathcal{G}(L/2, L/2-1; t, U)$ (right), the system is initially prepared in the state $\rho(2, 0, 0, 0)$ and evolved with the Hamiltonian $H(0.5, 0.1, U)$, for different values of U. The time evolution is obtained by numerical solution of the full EOM (5.26) and plotted as a function of the rescaled variable $\tau = U^2 t$.

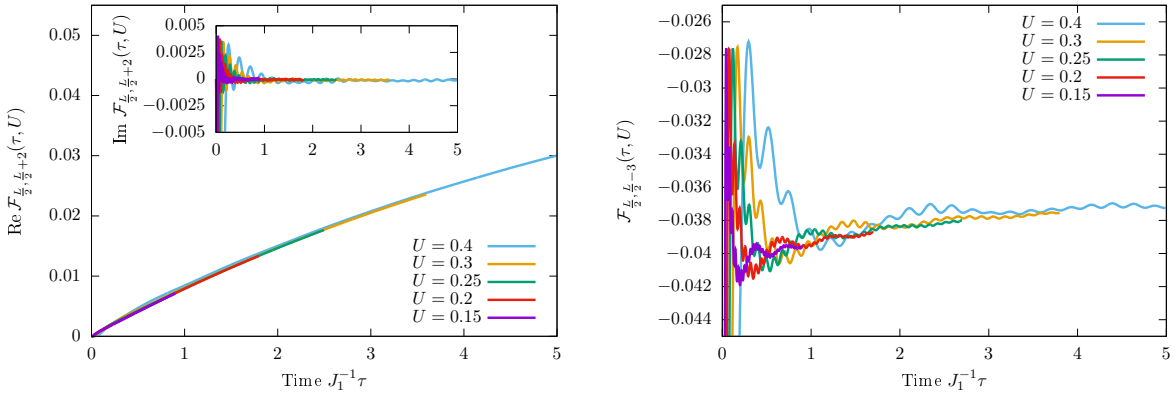

Figure 5.22: $\mathcal{F}_{L/2,L/2+2}(\tau, U) = \mathcal{G}(L/2, L/2+2; t, U)$ (left) and $\mathcal{F}_{L/2,L/2-3}(\tau, U) = \mathcal{G}(L/2, L/2-3; t, U)$ (right), the system is initially prepared in the state $\rho(2, 0, 0, 0)$ and evolved with the Hamiltonian $H(0.5, 0.1, U)$, for different values of U. The time evolution is obtained by numerical solution of the full EOM (5.26) and plotted as a function of the rescaled variable $\tau = U^2 t$.

Figs. 5.23 – 5.24 compare the time evolution obtained via QBE with the one found via EOM. Starting at time $t_0 = 20$, we see that for small U the agreement with the EOM is still very good, for larger U (and larger integrability breaking) it sensibly worsens. Since for observables depending only on diagonal occupation values, such as the real part of the Green's function between evenly separated points, the agreement is better, we argue that the main cause of the disagreement is having neglected the off-diagonal occupation numbers too early in the construction of the observables. If this is the case, however, the disagreement should reduce at later times. Starting the QBE at $t_0 = 40$ when the effect of the off-diagonals is reduced, we see that after a transient the QBE solution exactly agrees with the $t_0 = 20$ one. This suggests that $t_0 = 20$ is late enough to start the QBE.

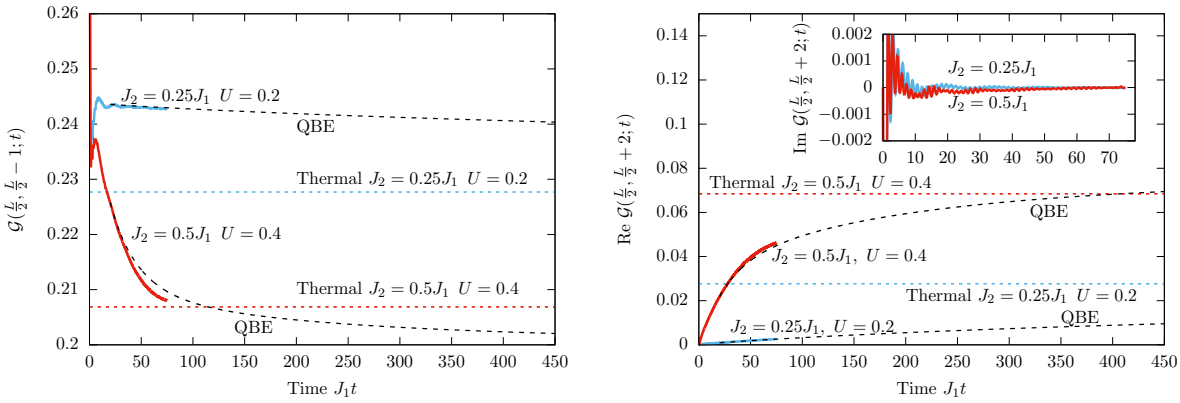

Figure 5.23: $\mathcal{G}(L/2, L/2-1; t)$ (left) and $\mathcal{G}(L/2, L/2+2; t)$ (right) for a system with Hamiltonian $H(J_2, 0.1, U)$ and size $L = 320$ initially prepared in a thermal state (5.13) with density matrix $\rho(2, 0, 0, 0)$. The full lines are the obtained by integrating the EOM (5.26) and the black dashed lines are found by means of the QBE.

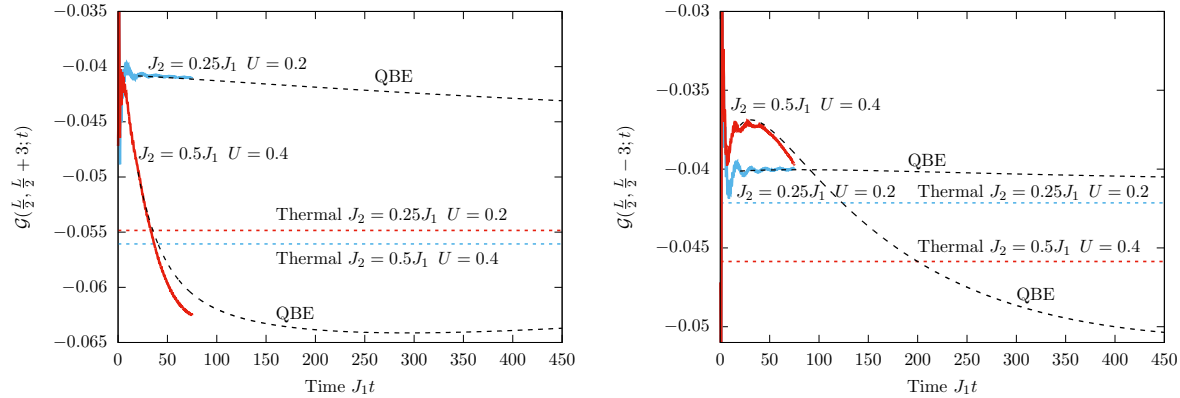

Figure 5.24: $\mathcal{G}(L/2, L/2+3; t)$ (left) and $\mathcal{G}(L/2, L/2-3; t)$ (right) for a system with Hamiltonian $H(J_2, 0.1, U)$ and size $L = 320$ initially prepared in a thermal state (5.13) with density matrix $\rho(2, 0, 0, 0)$. The full lines are the obtained by integrating the EOM (5.26) and the black dashed lines are found by means of the QBE.

In Figs. 5.25 – 5.26 we show the diagonal occupation numbers for various times. The EOM are used for short/intermediate times and QBE for longer times. We see that the agreement between EOM and QBE remains reasonably good until the last times reached by the EOM. At the latest time reached ($t = 450$) the QBE prediction closely approaches the thermal value, for ($J_2 = 0.5$; $U = 0.4$). In the case ($J_2 = 0.25$; $U = 0.2$), on the other hand, we see that the relaxation is much slower. As before, the thermal values are computed by means of perturbation theory (see Appendix 5.B).

In summary, from our findings emerge that the QBE description can be applied also in the $\delta_f \neq 0$ case, even if its derivation from the EOM is less rigorous. For small enough U seems to give good quantitative descriptions and when U becomes larger it still gives a correct qualitative behaviour. We conclude by stressing that the late-time behaviour of $\mathcal{G}(i, j; t)$ predicted by the QBE is compatible with (5.31), where the exponent is proportional to U^{-2} even for $\delta_f \neq 0$.

This is supports our conjecture (5.40).

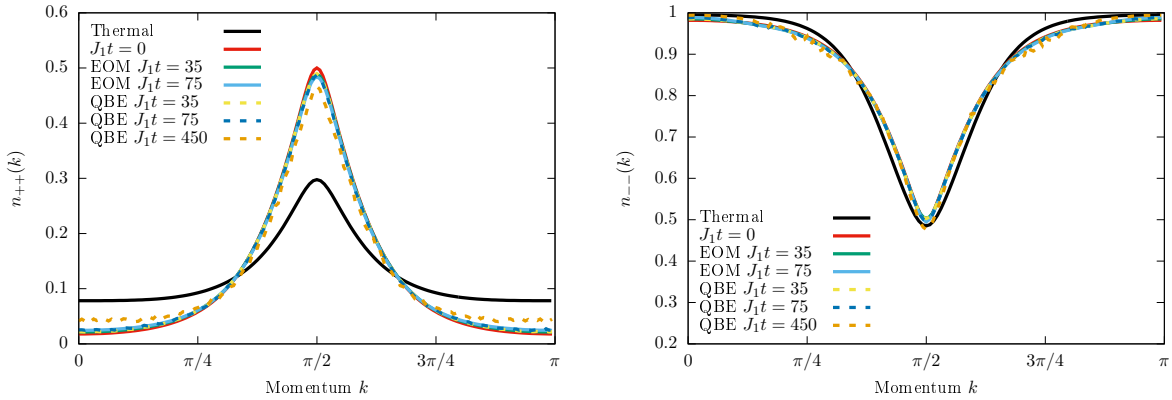

Figure 5.25: Occupation numbers $n_{++}(k,t)$ and $n_{--}(k,t)$ initialised in the thermal state $\rho(2,0,0,0)$, and time evolved with $H(0.25,0.1,0.2)$. The solid lines are the results of the EOM ($L = 320$) for various times. The dotted lines are computed by means of the QBE ($L = 320$). The black solid line is the thermal value found by means of second order perturbation theory in U.

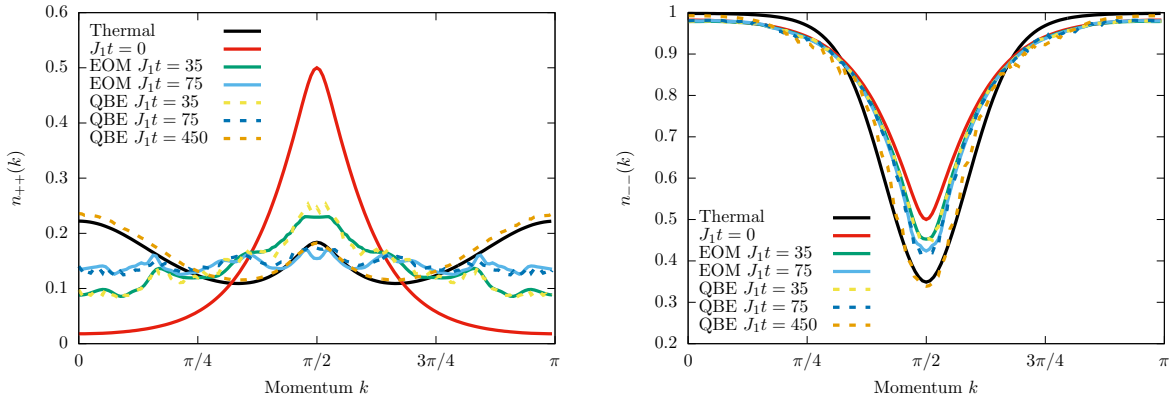

Figure 5.26: Occupation numbers $n_{++}(k,t)$ and $n_{--}(k,t)$ initialised in the thermal state $\rho(2,0,0,0)$, and time evolved with $H(0.5,0.1,0.4)$. The solid lines are the results of the EOM ($L = 320$) for various times. The dotted lines are computed by means of the QBE ($L = 320$). The black solid line is the thermal value found by means of second order perturbation theory in U.

5.6 U(1)-breaking case

So far, we have considered only cases in which the full Hamiltonian possesses a U(1) symmetry (*cf.* Section 5.1). As a consequence the number of particles is conserved during the time evolution. One could think that introducing a perturbation which breaks the U(1) symmetry is, in some sense, a "stronger" way of breaking the integrability, since it reduces the local conserved charges of the model to only the Hamiltonian. Consequently, it is natural to ask: are the phenomena described here a special feature of the U(1)-invariance or do they survive unchanged in the case of a U(1)-breaking perturbation? In this section we start to address this question, focussing on the phenomenon of prethermalisation. Specifically, we show that

prethermalisation survives also in the case of U(1)-breaking perturbations.

We consider the time evolution generated by the Hamiltonian

$$H(\gamma,h,U) = \frac{J}{2}\sum_i \Big[c_i^\dagger c_{i+1} + \gamma c_i^\dagger c_{i+1}^\dagger + \text{h.c.}\Big] + Jh\sum_i c_i^\dagger c_i + U\sum_i c_i^\dagger c_i c_{i+1}^\dagger c_{i+1}\,, \tag{5.48}$$

which is a fermionic XY model, perturbed by a density-density interaction; it is integrable for $U = 0$, where describes free fermions; for $\gamma = 0$ describing a XXZ spin-1/2 chain in external magnetic field; and finally for $h = -U$ where it describes a XYZ spin-1/2 chain; otherwise is non-integrable. The time evolution is started from the thermal state described by the following density matrix

$$\sigma_0 = \sigma(\beta,\gamma_i,h_i,U_i) = \frac{e^{-\beta H(\gamma_i,h_i,U)}}{\text{Tr}\left[e^{-\beta H(\gamma_i,h_i,U)}\right]}\,. \tag{5.49}$$

Performing the two-site Fourier transform (2.7), defined in Chapter 2, we have

$$\begin{aligned} H(\gamma,h,U) =& J\sum_{k>0}\Big[\cos(k) f_k^\dagger e_k + i\gamma\sin(k) f_k^\dagger e_{\pi-k}^\dagger - h(f_k^\dagger f_k + e_k^\dagger e_k) + \text{h.c.}\Big] \\ &+ 4U\sum_{\boldsymbol{k}>0}\tilde{V}(\boldsymbol{k}) e_{k_1}^\dagger e_{k_2} f_{k_3}^\dagger f_{k_4}\,, \end{aligned} \tag{5.50}$$

where

$$\tilde{V}(\boldsymbol{k}) = \frac{1}{L}\left(\delta_{k_1-k_2+k_3-k_4\pm\pi,0} + \delta_{k_1-k_2+k_3-k_4\pm\pi,0}\right)\cos(k_3-k_4)\,. \tag{5.51}$$

In this case, to keep the interaction term simpler, we do not diagonalise the quadratic part of the Hamiltonian and work with the fermions f_k and e_k: to study the prethermalisation of the system we consider the first order EOM for the occupation numbers

$$\begin{aligned} v_1(k;t) &\equiv \langle f_k^\dagger(t) f_k(t)\rangle\,, & v_2(k;t) &\equiv \langle e_k^\dagger(t) e_k(t)\rangle\,, \\ v_3(k;t) &\equiv \langle f_k^\dagger(t) f_{-k}^\dagger(t)\rangle\,, & v_4(k;t) &\equiv \langle e_k^\dagger(t) e_{-k}^\dagger(t)\rangle\,, \\ v_5(k;t) &\equiv \langle f_k^\dagger(t) e_k(t)\rangle\,, & v_6(k;t) &\equiv \langle f_k^\dagger(t) e_{-k}^\dagger(t)\rangle\,. \end{aligned} \tag{5.52}$$

The first order EOM are derived writing the Heisenberg equations for the bilinears $f_k^\dagger(t) f_k(t)$, ... , $f_k^\dagger(t) e_{-k}^\dagger(t)$ and neglecting the four-particles connected cumulants at all times. The result is reported in Appendix 5.C. The local observables are given by

$$\begin{aligned} \mathcal{G}(i,j;t) &= \text{Tr}\left[c_i^\dagger(t) c_j(t)\sigma_0\right] = \frac{1}{L}\sum_{k>0} e^{ik(i-j)} A_{i,j}(\{v_m(k;t)\}) \\ \mathcal{H}(i,j;t) &= \text{Tr}\left[c_i^\dagger(t) c_j^\dagger(t)\sigma_0\right] = \frac{1}{L}\sum_{k>0} e^{ik(i-j)} B_{i,j}(\{v_m(k;t)\})\,, \end{aligned} \tag{5.53}$$

where

$$
\begin{aligned}
&A_{2i-1,2j-1}(\{v_m(k;t)\}) = v_1(k;t)\,, && B_{2i-1,2j-1}(\{v_m(k;t)\}) = v_3(k;t)\,,\\
&A_{2i,2j}(\{v_m(k;t)\}) = v_2(k;t)\,, && B_{2i,2j}(\{v_m(k;t)\}) = v_4(k;t)\,,\\
&A_{2i-1,2j}(\{v_m(k;t)\}) = v_5(k;t)\,, && B_{2i-1,2j}(\{v_m(k;t)\}) = v_6(k;t)\,,\\
&A_{2i,2j-1}(\{v_m(k;t)\}) = v_5^*(k;t)\,, && B_{2i,2j-1}(\{v_m(k;t)\}) = -v_6(k;t)\,.
\end{aligned}
\tag{5.54}
$$

Figs. 5.27 and 5.28 report the time evolution given by the Hamiltonian $H(0.5, 0.1, U)$ starting from the initial state $\sigma(\infty, 0.2, 0, 0)$ for different values of U. For $U \neq 0$ (and the values of γ and h chosen), the Hamiltonian (5.48) describes a non integrable model (a XYZ model in external magnetic field), consequently the stationary values of local observables are described by a GE. Since the GE is different from the GGE also for $U = 0$, the difference between the stationary values reached for $U = 0$ and $U \neq 0$ is finite also for very small U, in other words is $O(U^0)$. From the figures we instead see that the difference between the plateau values goes to zero reducing U, it is thus $O(U)$. This is a clear indication of *prethermalisation*: the quasi-stationary values that the observables are relaxing to are not the thermal ones, but are close to the free GGE. We observe the same behaviour also for different values of γ and h.

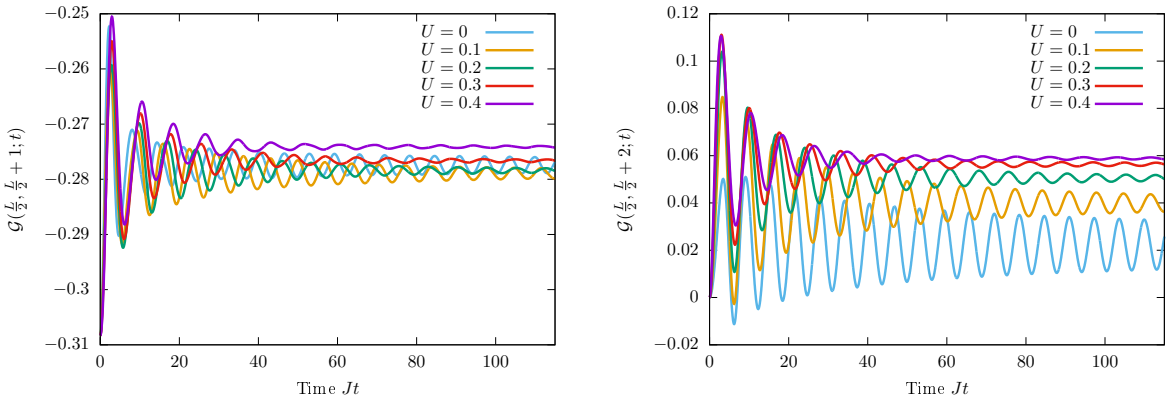

Figure 5.27: $\mathcal{G}(L/2, L/2+1; t)$ (left) and $\mathcal{G}(L/2, L/2+2; t)$ (right), the system is initially prepared in the state $\sigma(\infty, 0.2, 0, 0)$ and evolved with the Hamiltonian $H(0.5, 0.1, U)$, for different values of U. The time evolution is obtained by numerical solution of the first order EOM reported in Appendix 5.C.

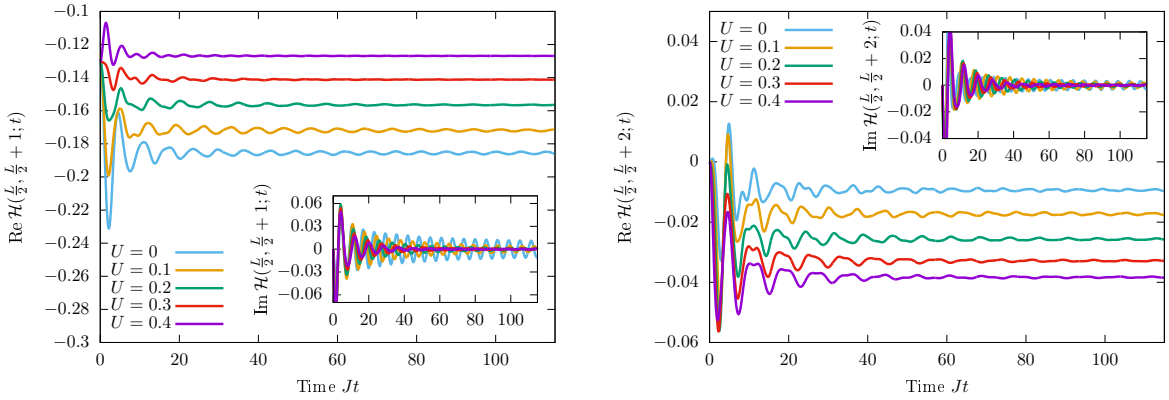

Figure 5.28: $\mathcal{H}(L/2, L/2+1; t)$ (left) and $\mathcal{H}(L/2, L/2+2; t)$ (right), the system is initially prepared in the state $\sigma(\infty, 0.2, 0, 0)$ and evolved with the Hamiltonian $H(0.5, 0.1, U)$, for different values of U. The time evolution is obtained by numerical solution of the first order EOM reported in Appendix 5.C.

For $h = O(U)$, the $O(U^0)$ part of the Hamiltonian possesses the non-abelian infinite set of local conserved quantities (*cf.* Chapter 2), giving rise to the pre-relaxation behaviour studied in 4. In particular, for $h = U(h' - 1)$ the Hamiltonian $H(\gamma, h, U)$ becomes exactly equal to the Hamiltonian (4.38) of Chapter 4. If one identifies $h = h'$, $g = U$ and $U = 0$, where the quantities on the left are those appearing in (4.38). It is then interesting to compare the mean-field results of Chapter 4 with the first order EOM. In Fig. 5.29 we show the time evolution of $\langle \sigma_i^x \sigma_{i+1}^x \rangle$ (which can be easily expressed in terms of $\{v_i(k; t)\}$) as a function of the rescaled time Ut. We see that the mean-field solution, started from the prediction of the unperturbed GGE, excellently captures the behaviour of the EOM in the pre-relaxation window: Ut finite with $U \ll 1$. Even if in this case the agreement is almost perfect, in general we expect $O(U)$ differences, since the EOM are correct up to $O(U^2)$ while the corrections to the mean-field are generally $O(U)$.

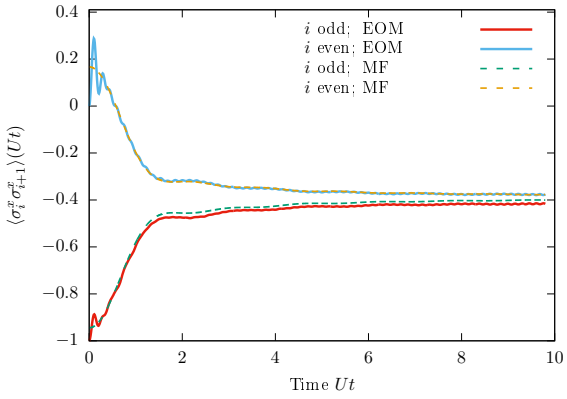

Figure 5.29: $\langle\sigma_i\sigma_{i+1}\rangle$ evolved according to $H(2, 0.1, 0.1)$, starting from the Majumdar-Ghosh state (4.77). The full lines are obtained by integration of the EOM (reported in Appendix 5.C), while the dashed lines are the prediction of the mean-field solution developed in Chapter 4.

5.7 Conclusions

In this chapter we have developed a method for analysing the effects of a weak integrability breaking interaction on the time evolution of local observables after a quantum quench. The method is based on the equations of motion (5.26); its accuracy has been tested by direct comparison with t-DMRG simulations and the agreement found is excellent even for a reasonably large value of the interaction ($U = 0.4J_1$).

We have shown that there is a crossover between a prethermalised regime, characterised by the proximity of our model to an integrable theory and a thermal steady state. The observed drift in time of the two-point function $\mathcal{G}(i, j; t)$ towards its thermal value is exponential in a transient regime and characterised by a time scale proportional to U^{-2}. To find this last result we designed a further approximation of the EOM, reducing (5.26) to a quantum Boltzmann equation [75,76]. This allowed us to reach longer times loosing some accuracy on the result: we argued that the quantum Boltzmann gives the time evolution of local observables up to $O(U)$ corrections.

In the case under consideration it not *a priori* clear whether a QBE-like description can be applied; when the final Hamiltonian is translationally invariant the simplification of the EOM is more rigorous and the results of the QBE show a better agreement with the full answer. When the final Hamiltonian has a dimerised term more assumptions are needed (*cf.* Section 5.5.3) and the agreement with the full answer is worse, especially increasing the strength of the interaction. The QBE, however, apparently gives the correct qualitative behaviour.

All the results discussed have been obtained for Hamiltonians which posses a global U(1) invariance, implying the conservation of the particle number. We carried out an analysis based

on the first order EOM, which showed that a prethermalised regime occurs also in absence of the U(1) symmetry. This suggests that the scenario described above, a crossover from a prethermalised to a thermal steady state occurring at time-scales proportional to U^{-2}, can happen also when the U(1) symmetry is broken. Clearly, to fully prove this conjecture, one would have to solve the second order EOM also in that case. In particular, an interesting situation is realised when the U(1) breaking is combined with the breaking of translationally invariance of the initial state; in this setting, one can study cases where the system shows a "pre-relaxed" behaviour of the kind studied in the previous chapter. Along this line, we verified that the first order EOM are compatible with the results found in Chapter 4. Using the second order EOM will then be possible to go beyond the "pre-relaxation" window of Chapter 4 and investigate the system on time-scales proportional to U^{-2}, where we expect to see the local observables drifting towards their thermal values.

Appendix

5.A First order analysis

Let us consider the first order EOM (5.28), our goal is to find a solution of this system in the limit of small U but for large times $t \sim U^{-1}$ with accuracy up to $O(U)$. We start by finding the solution at order $O(U^0)$. For $t \sim U^{-\alpha}$, with $0 < \alpha < 1$, the zeroth order solution is trivially given by $n^{(0)}_{\mu\nu}(k,t) = n_{\mu\nu}(k,0)e^{i\epsilon_{\mu\bar{\mu}}(k)t}$. When the time becomes $O(U^{-1})$, however, a more detailed analysis is needed: order U corrections become important if multiplied by t. From the structure of the equations we argue at the leading order the off-diagonal occupation numbers will maintain an oscillatory behaviour in time while the diagonal ones will remain constant in time, so we postulate the following *ansatz*

$$n^{(0)}_{\mu\nu}(k,t) = n_{\mu\nu}(k,0)e^{i(\tilde{\epsilon}_\mu(k)-\tilde{\epsilon}_\nu(k))t}\,, \tag{5.55}$$

where the "dressed energy" $\tilde{\epsilon}_\mu(k)$ is determined by imposing (5.55) to solve (5.28) at order $O(U^0)$; consistency with the solution for small t imposes $\tilde{\epsilon}_\mu(k) - \epsilon_\mu(k) \sim O(U)$. Substituting our ansatz into (5.28) we find

$$\begin{aligned}(\tilde{\epsilon}_\mu(k) - \tilde{\epsilon}_{\bar{\mu}}(k))\, n^{(0)}_{\mu\bar{\mu}}(k,t) =& i\Big\{\epsilon_{\mu\bar{\mu}}(k) + 4U\sum_{\gamma_2\gamma_3}\sum_{q>0}\big(V_{\mu\gamma_2\gamma_3\mu}(k,q,q,k) \\ &- V_{\bar{\mu}\gamma_2\gamma_3\bar{\mu}}(k,q,q,k)\big)n^{(0)}_{\gamma_2\gamma_3}(q,t)\Big\}n^{(0)}_{\mu\bar{\mu}}(k,t) + O(U)\,.\end{aligned} \tag{5.56}$$

At the leading order, we can neglect the contribution of $n_{\mu\bar{\mu}}(q,t)$ to sums over q as this vanish for late enough times; this can be easily shown by saddle point arguments for large enough L. Consequently, we conclude that (5.55) solves (5.28) at the leading order, if one chooses

$$\tilde{\epsilon}_\mu(k) \equiv \epsilon_\mu(k) + 4U\sum_{\gamma}\sum_{q>0} V_{\mu\gamma\gamma\mu}(k,q,q,k)n_{\gamma\gamma}(q)\,. \tag{5.57}$$

To find the solution at the order $O(U)$ we now use the following *ansatz*

$$n_{\mu\nu}(k,t) = n_{\mu\nu}(k,0)e^{i(\tilde{\epsilon}_\mu(k)-\tilde{\epsilon}_\nu(k))t} + n^{(1)}_{\mu\nu}(k,t)e^{i(\tilde{\epsilon}_\mu(k)-\tilde{\epsilon}_\nu(k))t} + O(U^2)\,, \tag{5.58}$$

and we determine $n^{(1)}_{\mu\nu}(k,t)$ imposing (5.58) to solve (5.28) up to $O(U^2)$. The final result reads

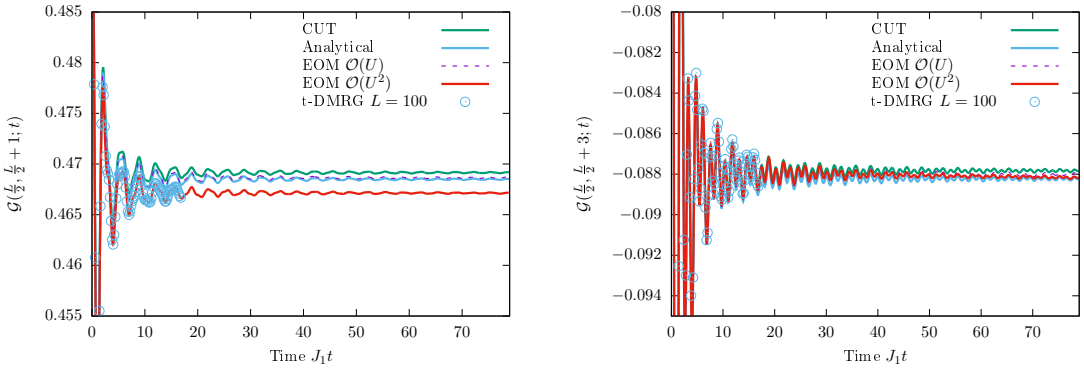

Figure 5.A.1: $\mathcal{G}(L/2, L/2+1; t)$, $\mathcal{G}(L/2, L/2+3; t)$, for a system with Hamiltonian $H(0, 0.4, 0.4)$ and sizes $L = 256$ initially prepared in the ground state of $H(0, 0.8, 0)$. The figures compare the time evolution obtained by means of different techniques: the CUT of Ref. [66] (green line), the analytical solution (5.59) (blue line), the numerical solution of the first order EOM (5.28) (violet dashed line), the numerical solution of the second order Eq. (5.26) (red line) and the t-DMRG (blue circles).

as

$$\begin{aligned} n_{\mu\nu}(k,t) = \;& n_{\mu\nu}(k,0) e^{i(\tilde{\epsilon}_\mu(k) - \tilde{\epsilon}_\nu(k))t} \\ & + 4U \sum_{\gamma_1\gamma_2\gamma_3} \sum_{q>0} W^{\mu\nu}_{\gamma_1\gamma_2\gamma_3\mu}(k,q,q,k;k,t) n^{(0)}_{\gamma_1\nu}(k,t) n^{(0)}_{\gamma_2\gamma_3}(q,t) \\ & - 4U \sum_{\gamma_1\gamma_2\gamma_3} \sum_{q>0} W^{\mu\nu}_{\nu\gamma_2\gamma_3\gamma_1}(k,q,q,k;k,t) n^{(0)}_{\mu\gamma_1}(q,t) n^{(0)}_{\gamma_2\gamma_3}(k,t) + O(U^2)\,, \end{aligned} \tag{5.59}$$

where we used $V_{\boldsymbol{\eta}}(\boldsymbol{k}) = V_{\bar{\boldsymbol{\eta}}}(\boldsymbol{k})$ ($\bar{\boldsymbol{\eta}} \equiv (-\eta_1, \ldots, -\eta_4)$) and defined

$$W^{\mu\nu}_{\boldsymbol{\eta}}(\boldsymbol{k}; k, t) \equiv \lim_{B\to\infty} \frac{1 - e^{-B\tilde{E}_{\boldsymbol{\eta}}(\boldsymbol{k})^2}}{\tilde{E}_{\boldsymbol{\eta}}(\boldsymbol{k})} V_{\boldsymbol{\eta}}(\boldsymbol{k}) (e^{i\tilde{E}_{\boldsymbol{\eta}}(\boldsymbol{k})t} - e^{i(\tilde{\epsilon}_\mu(k) - \tilde{\epsilon}_\nu(k))t})\,. \tag{5.60}$$

Eq. (5.59) differs from the solution for the occupation numbers found in Ref. [66] using the CUT approach only by order $O(U^2)$ contributions. Fig. 5.A.1 reports the time evolution of $\mathcal{G}(L/2, L/2+1; t)$ and $\mathcal{G}(L/2, L/2+3; t)$ comparing the results obtained by various different methods: CUT, Eq. (5.59), numerical solution of (5.28), numerical solution of (5.26) and t-DMRG.

5.B Perturbative calculation of the thermal values

In this appendix we compute the thermal expectation values[2]

$$n_{\mu\nu}(k) \equiv \langle \alpha^\dagger_\mu(k) \alpha_\nu(k) \rangle \equiv \frac{1}{Z} \mathrm{Tr}\left[\alpha^\dagger_\mu(k) \alpha_\nu(k) e^{-\beta(H - \mu N)} \right]\,, \tag{5.61}$$

[2] we omit the dependence of the Hamiltonian on the parameters J_2, δ and U, to lighten the notation.

where $Z \equiv \mathrm{Tr}\left[e^{-\beta(H-\mu N)}\right]$. The inverse temperature β and the chemical potential μ are fixed by requiring

$$\langle H\rangle_0 = \frac{1}{Z}\mathrm{Tr}\left[He^{-\beta(H-\mu N)}\right], \qquad \langle N\rangle_0 = \frac{1}{Z}\mathrm{Tr}\left[Ne^{-\beta(H-\mu N)}\right]. \tag{5.62}$$

In order to compute the finite-temperature mode occupation numbers (5.61), we compute the thermal propagator

$$G_{\mu\nu}(\tau,k) = \langle T_\tau\left[\alpha^\dagger_\mu(\tau,k)\alpha_\nu(0,k)\right]\rangle, \qquad \alpha^\dagger_\mu(s,k) \equiv e^{sH}\alpha^\dagger_\mu(k)e^{-sH}, \tag{5.63}$$

using finite-temperature perturbation theory to order U^2. The calculation of the Fourier transform of this quantity is most convenient; due to the anti-periodicity in imaginary time $G_{\mu\nu}(\tau+\beta,k) = -G_{\mu\nu}(\tau,k)$ the Fourier transformation is discrete

$$G_{\mu\nu}(\tau,k) = \frac{1}{\beta}\sum_{\omega_n} G_{\mu\nu}(\omega_n,k)e^{i\omega_n\tau}, \qquad \omega_n = \frac{(2n+1)\pi}{\beta}. \tag{5.64}$$

The thermal mode occupation numbers can be recovered from the thermal propagator using

$$n_{\mu\nu}(k) = \lim_{\tau\to 0^+} G_{\mu\nu}(\tau,k) = \frac{1}{\beta}\sum_{\omega_n} G_{\mu\nu}(\omega_n,k)e^{i\omega 0^+}. \tag{5.65}$$

5.B.1 Feynman rules

The Feynman rules for the theory under examination read

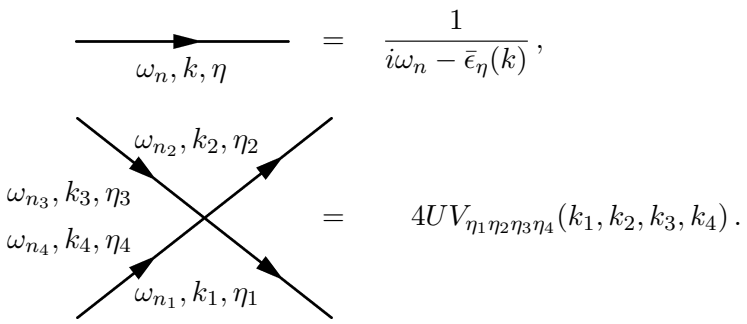

Here we defined $\bar{\epsilon}_\eta(k) \equiv \epsilon_\eta(k) - \mu$. In addition, on each internal line there is a sum over all indices, η, k, ω and at each vertex ω is conserved. Finally, the contribution of every diagram is multiplied by $(-1)^F S^{-1}$, where F is the number of closed loops and S is the *symmetry factor*, *i.e.* the number of ways in which internal lines can be exchanged whilst leaving the diagram invariant.

5.B.2 First order

At first order there is only one diagram which contributes to the thermal propagator

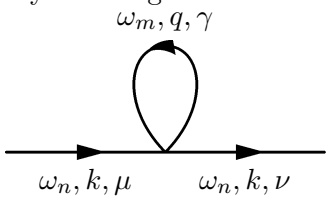

$$= \quad G^{(1)}_{\mu\nu}(\omega_n, k)\,.$$

Which gives the contribution

$$\begin{aligned} G^{(1)}_{\mu\nu}(\omega_n, k) &= \left(\frac{1}{i\omega_n - \bar{\epsilon}_\mu(k)}\right)\left(\frac{1}{i\omega_n - \bar{\epsilon}_\nu(k)}\right)\sum_{q,\gamma} 4U V_{\nu\gamma\gamma\mu}(k,q,q,k)\frac{1}{\beta}\sum_{\omega_m}\frac{1}{i\omega_m - \bar{\epsilon}_\gamma(k)} \\ &= \left(\frac{1}{i\omega_n - \bar{\epsilon}_\mu(k)}\right)\Sigma^{(1)}_{\mu\nu}(k)\left(\frac{1}{i\omega_n - \bar{\epsilon}_\nu(k)}\right)\,, \end{aligned} \tag{5.66}$$

where we introduce the self-energy $\Sigma^{(1)}_{\mu\nu}(k)$ and the Fermi-Dirac distribution function $n(x)$

$$\Sigma^{(1)}_{\mu\nu}(k) = 4U\sum_{q,\gamma} V_{\nu\gamma\gamma\mu}(k,q,q,k)n(\bar{\epsilon}_\gamma(q))\,, \qquad\qquad n(x) \equiv \frac{1}{1+e^{\beta x}}\,.$$

In arriving at Eq. (5.66) we have used

$$0 = \lim_{\eta\to 0^+}\lim_{R\to\infty}\oint_{\mathcal{C}_R}\frac{\mathrm{d}z}{2\pi}\frac{n(iz)e^{i\eta z}}{iz - \bar{\epsilon}_\mu(k)} = n(\bar{\epsilon}_\mu(k)) - \frac{1}{\beta}\sum_{\omega_n}\frac{1}{i\omega_n - \bar{\epsilon}_\mu(k)}\,,$$

where $\mathcal{C}_R$ is the circular path with radius R centred on the origin.

5.B.3 Second order

At second order there are three diagrams which contribute to the thermal propagator

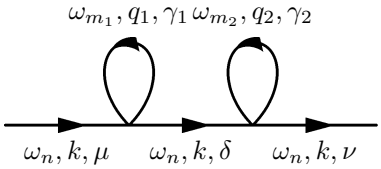

$= G^{(2)}_{\mu\nu}(\omega_n, k)_{[1]}\,,$

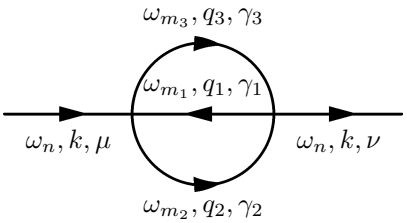

$= G^{(2)}_{\mu\nu}(\omega_n, k)_{[2]}\,,$

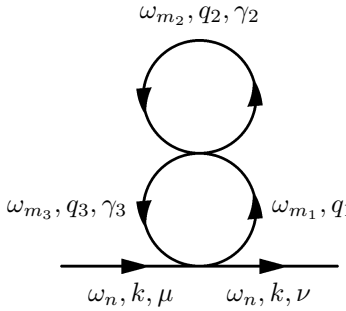

$= G^{(2)}_{\mu\nu}(\omega_n, k)_{[3]}\,.$

Evaluating the contributions of each of the diagrams, we find

$$G^{(2)}_{\mu\nu}(\omega_n,k)_{[1]} = \left(\frac{1}{i\omega_n-\bar{\epsilon}_\mu(k)}\right)\Sigma^{(1)}_{\mu\delta}(k)\left(\frac{1}{i\omega_n-\bar{\epsilon}_\delta(k)}\right)\Sigma^{(1)}_{\delta\nu}(k)\left(\frac{1}{i\omega_n-\bar{\epsilon}_\nu(k)}\right), \tag{5.67}$$

$$G^{(2)}_{\mu\nu}(\omega_n,k)_{[2]} = \left(\frac{1}{i\omega_n-\bar{\epsilon}_\mu(k)}\right)\Sigma^{(2)}_{\mu\nu}(\omega_n,k)_b\left(\frac{1}{i\omega_n-\bar{\epsilon}_\nu(k)}\right), \tag{5.68}$$

$$G^{(2)}_{\mu\nu}(\omega_n,k)_{[3]} = \left(\frac{1}{i\omega_n-\bar{\epsilon}_\mu(k)}\right)\Sigma^{(2)}_{\mu\nu}(k)_a\left(\frac{1}{i\omega_n-\bar{\epsilon}_\nu(k)}\right), \tag{5.69}$$

where we have introduced the self energies

$$\Sigma^{(2)}_{\mu\nu}(k)_a \equiv -4U\sum_{\gamma_1,\gamma_3,q_1}\Sigma^{(1)}_{\gamma_1\gamma_3}(q_1)V_{\nu\gamma_1\gamma_3\mu}(k,q_1,q_1,k)n(\bar{\epsilon}_{\gamma_1}(q_1))\tilde{n}(\bar{\epsilon}_{\gamma_3}(q_1))f(\epsilon_{\gamma_1\gamma_3}(q_1)),$$

$$\Sigma^{(2)}_{\mu\nu}(\omega,k)_b \equiv 8U^2\sum_{\{\gamma_i\}}\sum_{\{q_i\}}\Big\{V_{\nu\gamma_1\gamma_2\gamma_3}(k,q_1,q_2,q_3)V_{\gamma_3\gamma_2\gamma_1\mu}(q_3,q_2,q_1,k)n(\bar{\epsilon}_{\gamma_1}(q_1))$$
$$\times\tilde{n}(\bar{\epsilon}_{\gamma_2}(q_2))\tilde{n}(\bar{\epsilon}_{\gamma_3}(q_3))f(i\omega+\bar{\epsilon}_{\gamma_1}(q_1)-\bar{\epsilon}_{\gamma_2}(q_2)-\bar{\epsilon}_{\gamma_3}(q_3))\Big\}.$$

and the functions

$$\tilde{n}(x)\equiv 1-n(x), \qquad f(x)\equiv\frac{e^{\beta x}-1}{x}.$$

5.B.4 Occupation numbers

Collecting together the corrections to the thermal propagator (5.66–5.69) and inserting into Eq. (5.65), we find the thermal mode occupation numbers up to $O(U^2)$

$$\begin{aligned}n_{\mu\nu}(k,\beta,\mu) =&\delta_{\mu,\nu}\,n(\bar{\epsilon}_\mu(k)) - (\Sigma^{(1)}_{\mu\nu}(k)+\Sigma^{(2)}_{\mu\nu}(k)_a)n(\bar{\epsilon}_\mu(k))\tilde{n}(\bar{\epsilon}_\nu(k))f(\epsilon_{\mu\nu}(k))\\ &+\sum_\delta\frac{\Sigma^{(1)}_{\mu\delta}(k)\Sigma^{(1)}_{\delta\nu}(k)}{\epsilon_{\mu\delta}(k)\epsilon_{\delta\nu}(k)\epsilon_{\mu\nu}(k)}\Big(n(\bar{\epsilon}_\mu(k))\epsilon_{\delta\nu}(k)-n(\bar{\epsilon}_\delta(k))\epsilon_{\mu\nu}(k)+n(\bar{\epsilon}_\nu(k))\epsilon_{\mu\delta}(k)\Big)\\ &+8U^2\sum_{\{\gamma_i\}}\sum_{\{q_i\}}\Big\{V_{\mu\gamma_1\gamma_2\gamma_3}(k,q_1,q_2,q_3)V_{\gamma_3\gamma_2\gamma_1\nu}(q_3,q_2,q_1,k)\tilde{n}(\bar{\epsilon}_{\gamma_3}(q_3))\tilde{n}(\bar{\epsilon}_{\gamma_2}(q_2))\\ &\times n(\bar{\epsilon}_{\gamma_1}(q_1))G_{\mu\nu\gamma_1\gamma_2\gamma_3}(k,q_1,q_2,q_3)\Big\}.\end{aligned} \tag{5.70}$$

where we set

$$G_{\mu\nu\gamma_1\gamma_2\gamma_3}(k,q_1,q_2,q_3) = \frac{1}{\epsilon_{\mu\nu}(k)}\sum_{\eta=\pm}\{(\delta_{\eta,\mu}-\delta_{\eta,\nu})n(\epsilon_\eta(k))f(E_{\eta\gamma_1\gamma_2\gamma_3}(k,q_1,q_2,q_3))\}. \tag{5.71}$$

5.C First order EOM for the U(1)-breaking case

The EOM for the number operators (5.52) read as

$$
\begin{aligned}
\dot{v}_1(k;t) &= 2\cos(k)\mathrm{Im}[v_5(k;t)] + 2\gamma\sin(k)\mathrm{Re}[v_6(k;t)] \\
&\quad - 4Ui\sum_{k_1>0}\tilde{V}(k_1,k,k,k_1)v_5(k_1;t)v_5^*(k;t) + 4Ui\sum_{k_1>0}\tilde{V}(k,k_1,k_1,k)v_5(k;t)v_5^*(k_1;t) \\
&\quad + 4Ui\sum_{k_1>0}\tilde{V}(k_1,\pi-k_1,k,\pi-k)v_6(k_1;t)v_6^*(k;t) - 4Ui\sum_{k_1>0}\tilde{V}(k,\pi-k,k_1,\pi-k_1)v_6(k;t)v_6^*(k_1;t) \\
\dot{v}_2(k;t) &= -2\cos(k)\mathrm{Im}[v_5(k;t)] - 2\gamma\sin(k)\mathrm{Re}[v_6(\pi-k;t)] - 4Ui\sum_{k_1>0}\tilde{V}(k,k_1,k_1,k)v_5(k;t)v_5^*(k_1;t) \\
&\quad + 4Ui\sum_{k_1>0}\tilde{V}(k_1,k,k,k_1)v_5(k_1;t)v_5^*(k;t) - 4Ui\sum_{k_1>0}\tilde{V}(k,\pi-k,k_1,\pi-k_1)v_6(\pi-k;t)v_6^*(k_1;t) \\
&\quad + 4Ui\sum_{k_1>0}\tilde{V}(k_1,\pi-k_1,k,\pi-k)v_6(k_1;t)v_6^*(\pi-k;t) \\
\dot{v}_3(k;t) &= i\cos(k)\left(v_6(k;t)-v_6(\pi-k,t)\right) - \gamma\sin(k)\left(v_5(k;t)+v_5(\pi-k,t)\right) + 2ihv_3(k;t) \\
&\quad + 4Ui\sum_{k_1>0}\tilde{V}(k,k_1,k,k_1)v_2(k_1;t)v_3(k;t) - 4Ui\sum_{k_1>0}\tilde{V}(k_1,\pi-k,\pi-k,k_1)v_5(k_1;t)v_6(k;t) \\
&\quad - 4Ui\sum_{k_1>0}\tilde{V}(\pi-k,k_1,\pi-k,k_1)v_2(k_1;t)v_3(\pi-k;t) + 4Ui\sum_{k_1>0}\tilde{V}(k_1,k,k,k_1)v_5(k_1;t)v_6(\pi-k;t) \\
&\quad + 4Ui\sum_{k_1>0}\tilde{V}(k_1,\pi-k_1,\pi-k,k)v_6(k_1;t)v_5(k;t) - 4Ui\sum_{k_1>0}\tilde{V}(k_1,\pi-k_1,k,\pi-k)v_6(k_1;t)v_5(\pi-k;t) \\
\dot{v}_4(k;t) &= i\cos(k)\left(v_6(k;t)-v_6(\pi-k,t)\right) - \gamma\sin(k)\left(v_5(k;t)+v_5(\pi-k,t)\right) + 2ihv_4(k;t) \\
&\quad - 4Ui\sum_{k_1>0}\tilde{V}(k_1,\pi-k_1,k,\pi-k)v_6(k_1;t)v_5^*(k;t) - 4Ui\sum_{k_1>0}\tilde{V}(\pi-k,k_1,k_1,\pi-k)v_5^*(k_1;t)v_6(\pi-k;t) \\
&\quad - 4Ui\sum_{k_1>0}\tilde{V}(\pi-k,k_1,\pi-k,k_1)v_1(k_1;t)v_4(\pi-k;t) + 4Ui\sum_{k_1>0}\tilde{V}(k,k_1,k,k_1)v_1(k_1;t)v_4(k;t) \\
&\quad + 4Ui\sum_{k_1>0}\tilde{V}(k_1,\pi-k_1,\pi-k,k)v_6(k_1;t)v_5^*(\pi-k;t) + 4Ui\sum_{k_1>0}\tilde{V}(k,k_1,k_1,k)v_5^*(k_1;t)v_6(k;t) \\
\dot{v}_5(k;t) &= i\cos(k)\left(v_2(k;t)-v_1(k;t)\right) + \gamma\sin(k)\left(v_4^*(k;t)+v_3(k;t)\right) \\
&\quad - 4Ui\sum_{k_1>0}\tilde{V}(k_1,k,k_1,k)v_1(k_1;t)v_5(k;t) + 4Ui\sum_{k_1>0}\tilde{V}(k,k_1,k,k_1)v_2(k_1;t)v_5(k;t) \\
&\quad + 4Ui\sum_{k_1>0}\tilde{V}(k_1,k,k,k_1)v_1(k;t)v_5(k_1;t) + 4Ui\sum_{k_1>0}\tilde{V}(k_1,\pi-k_1,k,\pi-k)v_4^*(k_1;t)v_6(\pi-k;t) \\
&\quad + 4Ui\sum_{k_1>0}\tilde{V}(\pi-k,k,k_1,\pi-k_1)v_3(k_1;t)v_6^*(k;t) - 4Ui\sum_{k_1>0}\tilde{V}(k_1,k,k,k_1)v_2(k;t)v_5(k_1;t) \\
\dot{v}_6(k;t) &= i\cos(k)\left(v_4(k;t)+v_3(k;t)\right) - \gamma\sin(k)\left(v_1(k;t)+v_2(\pi-k;t)-1\right) + 2ihv_6(k;t)) \\
&\quad - 4Ui\sum_{k_1>0}\tilde{V}(k_1,\pi-k_1,k,\pi-k)v_6(k_1;t)v_1(k;t) + 4Ui\sum_{k_1>0}\tilde{V}(k,k_1,k,k_1)v_2(k_1;t)v_6(k;t) \\
&\quad + 4Ui\sum_{k_1>0}\tilde{V}(\pi-k,k_1,\pi-k,k_1)v_1(k_1;t)v_6(k;t) - 4Ui\sum_{k_1>0}\tilde{V}(k_1k,k,k_1)v_5(k_1;t)v_4(k;t) \\
&\quad - 4Ui\sum_{k_1>0}\tilde{V}(\pi-k,k_1,k_1,\pi-k)v_5^*(k_1;t)v_3(k;t) \\
&\quad + 4Ui\sum_{k_1>0}\tilde{V}(k_1,\pi-k_1,k,\pi-k)v_6(k_1;t)(1-v_2(\pi-k;t))\,. \qquad (5.72)
\end{aligned}
$$

6. Summary and outlook

Let us now summarise the material presented in this thesis and discuss some open questions which could be a source of future work.

This thesis has been completely devoted to the study of the dynamics in closed many-body systems possessing non-trivial interactions. Finding the exact time evolution in interacting models represents an Herculean task and its complete solution in the general case is completely out of reach. In this thesis we presented three different methods which can be applied to study the dynamics generated by two important subclasses of interacting quantum many-body systems: *integrable models* and *weakly non-integrable models*.

The first class is composed of models of which some properties can be exactly determined (for example the spectrum and the elementary excitations), so they represent a natural starting point in the study of the time evolution. However, the time evolution in integrable models presents a peculiar feature: the stationary state which describes the value that observables reach at late times is expected to be the *Generalised Gibbs ensemble*. In contrast to what happens in non-integrable models, where it is expected to be the *Gibbs ensemble*.

The second class is not only a step forward towards the fully non-integrable case, it is also the situation in which aspects of integrability and non-integrability are expected to coexist at different times during the time evolution. This makes weakly non-integrable models arguably the most interesting case to study.

In Chapter 3 we started by considering the time evolution in an interacting integrable field theory: the sine-Gordon model. In particular we focussed on the repulsive regime and studied the time evolution of the one-point function of the semi-local (*cf.* (2.72)) operator $e^{i\beta\phi(x)/2}$ on a class of initial states (3.8). The approach adopted is fully analytical and can be decomposed in two main steps: first we use the "Representative Eigenstate Approach" (a.k.a. "Quench Action") [73] to simplify the form factor expansion of the expectation value; then we extract its leading contribution for late times. Importantly, to find this contribution we do not need details about the form-factors but only some information about their singularities, which can be extracted using the annihilation pole axiom (2.71). This approach gives the leading order contribution in the density of excitations of the initial state and works in full generality for any integrable field theory, as long as semi-local operators are considered.

Possible generalisations of our work can follow three different routes. The first would be to consider the time evolution of dynamical correlation functions, attempting to generalise the

results found in Ref. [39] to the interacting case; and, in turn, test the results obtained in Ref. [167] by means of a semi-classical approach. A second possible outlook is to consider more general vertex operators of the form $e^{i\alpha\Phi}$ with generic α. Considering generic values of α severely complicates our analysis, in particular the finite volume regularisation of the theory (*cf.* 3.2) becomes much more intricate and the leading singular behaviour of the form factors is no longer given by the expression (3.110). A case of particular interest is the local vertex operator $e^{i\beta\Phi}$: in Ref. [1] we showed the leading term in the linked-cluster expansion vanishes, in general the residues of the most divergent poles always vanish in this case. However, those terms which in the case $\alpha \neq \beta$ give sub leading divergent contributions for late times, become important and might allow us to use a generalisation of our approach. This would go beyond the semiclassical approximation of [167], which found a time independent expectation value. Finally, the method presented can be applied to study the attractive regime of the sine-Gordon model, where bound states of solitons and antisolitons are also present.

In Chapter 4 we considered the effect of weak perturbations to a specific class of integrable models, where in addition to the "standard" infinite family of local conserved charges another infinite non-commuting family of local conserved charges is also present. Adding a perturbation to these models we can either avoid the conservation of the additional charges while maintaining the integrability, or completely break it. To simplify our analysis we considered only cases where these particular integrable models are noninteracting. In a late time window, where the time is proportional to the inverse of the perturbation strength, the time evolution of local operators (at the lowest order in g) can be described by an effective (quasi)-local non-interacting Hamiltonian which is specified by time-dependent parameters found solving some self-consistency conditions. Importantly, in this window we did not observe differences between the case where the perturbation completely breaks integrability and the case in which it does not. This suggest that the effects of integrability breaking are appearing at later times $t \sim g^{-\alpha}$ with $\alpha > 1$, where $g \ll 1$ measures the strength of the perturbation.

Noninteracting models with the additional family of non-commuting local conserved charges are known, an example being the XY model considered in this thesis. In the future it would be interesting to find *interacting* integrable models with the same property: a good candidate is the XXZ spin-1/2 model at the points where the anisotropy satisfies $\Delta = \frac{1}{2}(q + q^{-1})$ with $q^{2N} = 1$ ($N \geq 2$). Indeed, in this case, the model has been shown [95] to possess a $\mathrm{sl}(2, \mathbb{C})$-loop symmetry invariance in addition to its integrability. For the moment, however, only a non-local representation of the charges is known [95]. Another possible outlook of our work is to consider a different scaling limit, for example $t \sim g^{-2}$, which we expect to be the time-scale

in which thermalisation occurs, according to our findings of Ref. [3] (discussed in Chapter 5 of this thesis) and trying to find an effective Hamiltonian also in that case.

Finally, in Chapter 5 we studied the dynamics of a more general class of weakly non-integrable models, that can be thought of as Peierls insulators [66,77], in the presence of a next-nearest-neighbour hopping term with strength J_2 and density-density interactions with strength U. We studied the time evolution numerically solving the second order equations of motion (EOM) for the occupation numbers $n_{\mu\nu}(k,t)$ (5.14), of the Bogoliubov fermions diagonalising the quadratic Hamiltonian. The equations are found in two steps: first we write the Heisenberg equations of motion for the bilinears in the Bogoliubov fermoins; then, we take the expectation value on the initial state, closing the system of equations by assuming the connected higher particle cumulants to be negligible. In particular, we considered a specific truncation scheme which for times of order unity gives the exact results up to $O(U^3)$ corrections; in fact we tested it against the (numerically exact) time-dependent density matrix renormalisation group (t-DMRG) results finding an almost perfect agreement for all the times reached by the t-DMRG, even for not-too-small U. Using the EOM we showed an exponential crossover behaviour of local observables between a prethermalised and the thermalised regime. The crossover is characterised by a time-scale $t \sim U^{-2}$ and has a prefactor which strongly depends on the next-nearest-neighbour hopping strength J_2. To find this scaling and in turn to reach longer times in the evolution of observables we designed a further approximation of the EOM obtaining a quantum Boltzmann equation [75,76], which is expected to describe the time evolution of local observables at the leading order in U.

In Chapter 5 we show that also in absence of the U(1) symmetry, which causes the conservation of the particle number, the systems show a prethermalised behaviour: the local observables stay on quasi-stationary plateaux which are close to those described by the unperturbed GGE up to corrections of order U. This result has been found using a simpler version of the EOM, which is accurate for times $t \sim U^{-1}$. An immediate outlook of our work would be to study this case with the second order EOM, investigating whether the scenario for the approach of the thermal values described in the previous paragraph also applies in this case. In particular, we can investigate cases like those considered in Chapter 4, where the free model possesses an additional non-commuting family of local conservation laws, and explore its time evolution up to times $t \sim U^{-2}$: we expect to see two quasi-stationary plateaux, before the final stationary one, appearing in this case.

Bibliography

[1] B. Bertini, D. Schuricht, and F. H. Essler, J. Stat. Mech. P10035 (2014).

[2] B. Bertini and M. Fagotti, J. Stat. Mech. P07012 (2015).

[3] B. Bertini, F. H. Essler, S. Groha, and N. J. Robinson, Phys. Rev. Lett. **115**, 180601 (2015).

[4] S. Ma, *Modern theory of critical phenomena* (Da Capo Press, New York, 2000), No. 46.

[5] J. Cardy, *Scaling and renormalization in statistical physics* (Cambridge university press, Cambridge, 1996).

[6] G. Mussardo, *Statistical field theory: an introduction to exactly solved models in statistical physics* (OUP, Oxford, 2009).

[7] E. Fermi, J. Pasta, and S. Ulam, Los Alamos Report LA-1940 978 (1955).

[8] F. Izrailev and B. Chirikov, **11**, 30 (1966).

[9] G. Berman and F. Izrailev, Chaos **15**, 015104 (2005).

[10] V. I. Arnold, *Mathematical methods of classical mechanics* (Springer, New York, 1989), Vol. 60.

[11] J. von Neumann, Z. Phys. **57**, 30 (1929).

[12] E. Barouch, B. M. McCoy, and M. Dresden, Phys. Rev. A **2**, 1075 (1970).

[13] E. Barouch and B. M. McCoy, Phys. Rev. A **3**, 786 (1971).

[14] J. Deutsch, Phys. Rev. A **43**, 2046 (1991).

[15] M. Srednicki, Phys. Rev. E **50**, 888 (1994).

[16] M. Greiner *et al.*, Nature **415**, 39 (2002).

[17] T. Kinoshita, T. Wenger, and D. S. Weiss, Nature **440**, 900 (2006).

[18] M. Gring *et al.*, Science **337**, 1318 (2012).

[19] D. A. Smith *et al.*, New J. Phys. **15**, 075011 (2013).

[20] S. Trotzky *et al.*, Nature Physics **8**, 325 (2012).

[21] M. Cheneau *et al.*, Nature **481**, 484 (2012).

[22] U. Schneider *et al.*, Nature Physics **8**, 213 (2012).

[23] F. Meinert *et al.*, Phys. Rev. Lett. **111**, 053003 (2013).

[24] T. Fukuhara *et al.*, Nature Physics **9**, 235 (2013).

[25] T. Fukuhara *et al.*, Nature **502**, 76 (2013).

[26] F. Meinert *et al.*, Phys. Rev. Lett. **112**, 193003 (2014).

[27] P. Calabrese and J. Cardy, J. Stat. Mech. P04010 (2005).

[28] C. Gogolin and J. Eisert, arXiv preprint arXiv:1503.07538 (2015).

[29] A. Polkovnikov, K. Sengupta, A. Silva, and M. Vengalattore, Rev. Mod. Phys. **83**, 863 (2011).

[30] M. Rigol, Phys. Rev. Lett. **103**, 100403 (2009).

[31] L. F. Santos and M. Rigol, Phys. Rev. E **81**, 036206 (2010).

[32] M. Rigol, V. Dunjko, and M. Olshanii, Nature **452**, 854 (2008).

[33] G. Biroli, C. Kollath, and A. M. Läuchli, Phys. Rev. Lett. **105**, 250401 (2010).

[34] M. C. Bañuls, J. I. Cirac, and M. B. Hastings, Phys. Rev. Lett. **106**, 050405 (2011).

[35] M. Rigol, V. Dunjko, V. Yurovsky, and M. Olshanii, Phys. Rev. Lett. **98**, 050405 (2007).

[36] M. A. Cazalilla, Phys. Rev. Lett. **97**, 156403 (2006).

[37] P. Calabrese and J. Cardy, J. Stat. Mech. P06008 (2007).

[38] M. Fagotti and F. H. Essler, Phys. Rev. B **87**, 245107 (2013).

[39] F. H. Essler, S. Evangelisti, and M. Fagotti, Phys. Rev. Lett. **109**, 247206 (2012).

[40] S. Sotiriadis and P. Calabrese, J. Stat. Mech. P07024 (2014).

[41] F. Essler, G. Mussardo, and M. Panfil, Phys. Rev. A **91**, 051602 (2015).

[42] M. Cramer, C. M. Dawson, J. Eisert, and T. J. Osborne, Phys. Rev. Lett. **100**, 030602 (2008).

[43] T. Barthel and U. Schollwöck, Phys. Rev. Lett. **100**, 100601 (2008).

[44] P. Calabrese, F. H. Essler, and M. Fagotti, Phys. Rev. Lett. **106**, 227203 (2011).

[45] P. Calabrese, F. H. Essler, and M. Fagotti, J. Stat. Mech. P07022 (2012).

[46] M. Collura, S. Sotiriadis, and P. Calabrese, Phys. Rev. Lett. **110**, 245301 (2013).

[47] B. Pozsgay, J. Stat. Mech. P07003 (2013).

[48] M. Fagotti and F. H. Essler, J. Stat. Mech. P07012 (2013).

[49] G. Mussardo, Phys. Rev. Lett. **111**, 100401 (2013).

[50] M. Kormos *et al.*, Phys. Rev. B **88**, 205131 (2013).

[51] M. Fagotti, M. Collura, F. H. Essler, and P. Calabrese, Phys. Rev. B **89**, 125101 (2014).

[52] J. De Nardis, B. Wouters, M. Brockmann, and J.-S. Caux, Phys. Rev. A **89**, 033601 (2014).

[53] M. Fagotti, M. Collura, F. H. Essler, and P. Calabrese, Phys. Rev. B **89**, 125101 (2014).

[54] B. Wouters *et al.*, Phys. Rev. Lett. **113**, 117202 (2014).

[55] B. Pozsgay *et al.*, Phys. Rev. Lett. **113**, 117203 (2014).

[56] G. Goldstein and N. Andrei, arXiv preprint arXiv:1405.4224 (2014).

[57] M. Brockmann *et al.*, J. Stat. Mech. P12009 (2014).

[58] E. Ilievski, M. Medenjak, and T. Prosen, arXiv preprint arXiv:1506.05049 (2015).

[59] E. Ilievski *et al.*, arXiv preprint arXiv:1507.02993 (2015).

[60] M. Moeckel and S. Kehrein, Phys. Rev. Lett. **100**, 175702 (2008).

[61] M. Moeckel and S. Kehrein, Annals of Physics **324**, 2146 (2009).

[62] A. Rosch, D. Rasch, B. Binz, and M. Vojta, Phys. Rev. Lett. **101**, 265301 (2008).

[63] M. Kollar, F. A. Wolf, and M. Eckstein, Phys. Rev. B **84**, 054304 (2011).

[64] M. van den Worm, B. C. Sawyer, J. J. Bollinger, and M. Kastner, New J. Phys. **15**, 083007 (2013).

[65] M. Marcuzzi, J. Marino, A. Gambassi, and A. Silva, Phys. Rev. Lett. **111**, 197203 (2013).

[66] F. Essler, S. Kehrein, S. Manmana, and N. Robinson, Phys. Rev. B **89**, 165104 (2014).

[67] N. Nessi, A. Iucci, and M. Cazalilla, Phys. Rev. Lett. **113**, 210402 (2014).

[68] M. Fagotti, J. Stat. Mech. P03016 (2014).

[69] G. Brandino, J.-S. Caux, and R. Konik, arXiv preprint arXiv:1407.7167 (2014).

[70] M. Babadi, E. Demler, and M. Knap, arXiv preprint arXiv:1504.05956 (2015).

[71] U. Schollwöck, Reviews of modern physics **77**, 259 (2005).

[72] M. Stark and M. Kollar, arXiv preprint arXiv:1308.1610 (2013).

[73] J.-S. Caux and F. H. Essler, Phys. Rev. Lett. **110**, 257203 (2013).

[74] F. H. Essler and R. M. Konik, J. Stat. Mech. **2009**, P09018 (2009).

[75] L. Erdős, M. Salmhofer, and H.-T. Yau, J. Stat. Phys. **116**, 367 (2004).

[76] J. Lukkarinen and H. Spohn, J. Stat. Phys. **134**, 1133 (2009).

[77] R. E. Peierls, *Quantum theory of solids* (Oxford University Press, Oxford, 1955), No. 23.

[78] R. Rajaraman, *Solitons and instantons* (North-Holland, Amsterdam, 1982).

[79] F. H. Essler and R. M. Konik, From Fields to Strings: Circumnavigating Theoretical Physics, Editors M. Shifman, A. Vainshtein and J. Wheater, Ian Kogan Memorial Collection, World Scientific (2004).

[80] E. Lieb, T. Schultz, and D. Mattis, Annals of Physics **16**, 407 (1961).

[81] V. E. Korepin, N. M. Bogoliubov, and A. G. Izergin, *Quantum inverse scattering method and correlation functions* (Cambridge university press, Cambridge, 1997).

[82] M. Kenzelmann *et al.*, Phys. Rev. B **65**, 144432 (2002).

[83] G. Delfino, J. Phys. A **37**, R45 (2004).

[84] S. Sachdev, *Quantum phase transitions* (Wiley Online Library, Cambridge, 2007).

[85] F. Iglói and H. Rieger, Phys. Rev. Lett. **106**, 035701 (2011).

[86] K. Sengupta, S. Powell, and S. Sachdev, Phys. Rev. A **69**, 053616_1 (2004).

[87] D. Rossini, A. Silva, G. Mussardo, and G. E. Santoro, Phys. Rev. Lett. **102**, 127204 (2009).

[88] P. Calabrese, F. H. Essler, and M. Fagotti, J. Stat. Mech. P07016 (2012).

[89] L. Bucciantini, M. Kormos, and P. Calabrese, Journal of Physics A: Mathematical and Theoretical **47**, 175002 (2014).

[90] R. Coldea *et al.*, Science **327**, 177 (2010).

[91] P. Jordan and E. P. Wigner, Zeitschrift fur Physik **47**, 631 (1928).

[92] M. Fagotti and P. Calabrese, J. Stat. Mech. P04016 (2010).

[93] E. Ilievski and T. Prosen, Commun. Math. Phys. **318**, 809 (2013).

[94] M. Fagotti, arXiv preprint arXiv:1408.1950 (2014).

[95] T. Deguchi, K. Fabricius, and B. M. McCoy, J. Stat. Phys. **102**, 701 (2001).

[96] D. Dender *et al.*, Phys. Rev. Lett. **79**, 1750 (1997).

[97] M. Oshikawa *et al.*, Journal of the Physical Society of Japan **68**, 3181 (1999).

[98] T. Asano *et al.*, Phys. Rev. Lett. **84**, 5880 (2000).

[99] R. Feyerherm *et al.*, J. Phys.: Condens. Matter **12**, 8495 (2000).

[100] M. Kohgi *et al.*, Phys. Rev. Lett. **86**, 2439 (2001).

[101] H. Nojiri, Y. Ajiro, T. Asano, and J. Boucher, New J. Phys. **8**, 218 (2006).

[102] M. Kenzelmann *et al.*, Phys. Rev. Lett. **93**, 017204 (2004).

[103] S. Zvyagin, A. Kolezhuk, J. Krzystek, and R. Feyerherm, Phys. Rev. Lett. **93**, 027201 (2004).

[104] S. Zvyagin, A. Kolezhuk, J. Krzystek, and R. Feyerherm, Phys. Rev. Lett. **95**, 017207 (2005).

[105] Y. Chen *et al.*, Phys. Rev. B **75**, 214409 (2007).

[106] M. Oshikawa and I. Affleck, Phys. Rev. Lett. **79**, 2883 (1997).

[107] F. H. Essler and A. M. Tsvelik, Phys. Rev. B **57**, 10592 (1998).

[108] F. H. Essler, Phys. Rev. B **59**, 14376 (1999).

[109] I. Affleck and M. Oshikawa, Phys. Rev. B **60**, 1038 (1999).

[110] J. Lou *et al.*, Phys. Rev. B **65**, 064420 (2002).

[111] M. Oshikawa and I. Affleck, Phys. Rev. B **65**, 134410 (2002).

[112] F. H. Essler, A. Furusaki, and T. Hikihara, Phys. Rev. B **68**, 064410 (2003).

[113] S. Lukyanov, Nucl. Phys. B **522**, 533 (1998).

[114] S. Lukyanov, Phys. Rev. B **59**, 11163 (1999).

[115] T. Giamarchi, *Quantum physics in one dimension* (Oxford University Press, Oxford, 2004).

[116] H. Büchler, G. Blatter, and W. Zwerger, Phys. Rev. Lett. **90**, 130401 (2003).

[117] F. Haldane, Phys. Rev. Lett. **47**, 1840 (1981).

[118] M. Cazalilla, J. Phys. B **37**, S1 (2004).

[119] V. Gritsev, A. Polkovnikov, and E. Demler, Phys. Rev. B **75**, 174511 (2007).

[120] P. Dorey, *Conformal field theories and integrable models* (Springer, Berlin, 1997), pp. 85–125.

[121] B. Doyon, lecture notes (unpublished).

[122] G. Delfino, Annals of Physics (2015).

[123] A. B. Zamolodchikov and A. B. Zamolodchikov, Annals of physics **120**, 253 (1979).

[124] V. E. Korepin, Theor. Math. Phys. **41**, 953 (1979).

[125] A. Luther and V. Emery, Phys. Rev. Lett. **33**, 589 (1974).

[126] L. Faddeev, Sov. Sci. Rev. Math. Phys. C **1**, 107 (1980).

[127] F. A. Smirnov, *Form factors in completely integrable models of quantum field theory* (World Scientific, Singapore, 1992), Vol. 14.

[128] J. L. Cardy and G. Mussardo, Nucl. Phys. B **340**, 387 (1990).

[129] V. Yurov and A. B. Zamolodchikov, Int. J. Mod. Phys. A **6**, 3419 (1991).

[130] H. Babujian, A. Fring, M. Karowski, and A. Zapletal, Nucl. Phys. B **538**, 535 (1999).

[131] S. Lukyanov, Modern Physics Letters A **12**, 2543 (1997).

[132] G. Delfino, J. Phys. A **37**, R45 (2004).

[133] S. Lukyanov and A. Zamolodchikov, Nucl. Phys. B **493**, 571 (1997).

[134] S. Lukyanov, Communications in Mathematical Physics **167**, 183 (1995).

[135] S. Weinberg, *The quantum theory of fields* (Cambridge university press, Cambridge, 1996), Vol. 2.

[136] J. De Nardis and J.-S. Caux, J. Stat. Mech. **2014**, P12012 (2014).

[137] R. Berg *et al.*, arXiv preprint arXiv:1507.06339 (2015).

[138] J. De Nardis, L. Piroli, and J.-S. Caux, arXiv preprint arXiv:1505.03080 (2015).

[139] F. H. L. Essler, G. Mussardo, and M. Panfil, Phys. Rev. A **91**, 051602 (2015).

[140] D. Schuricht and F. H. Essler, J. Stat. Mech. P04017 (2012).

[141] A. Iucci and M. Cazalilla, Phys. Rev. A **80**, 063619 (2009).

[142] A. Iucci and M. Cazalilla, New J. Phys. **12**, 055019 (2010).

[143] M. S. Foster, E. A. Yuzbashyan, and B. L. Altshuler, Phys. Rev. Lett. **105**, 135701 (2010).

[144] M. S. Foster, T. C. Berkelbach, D. R. Reichman, and E. A. Yuzbashyan, Phys. Rev. B **84**, 085146 (2011).

[145] V. Gritsev, E. Demler, M. Lukin, and A. Polkovnikov, Phys. Rev. Lett. **99**, 200404 (2007).

[146] J. Sabio and S. Kehrein, New J. Phys. **12**, 055008 (2010).

[147] A. Mitra and T. Giamarchi, Phys. Rev. B **85**, 075117 (2012).

[148] A. Mitra, Phys. Rev. B **87**, 205109 (2013).

[149] P. Calabrese and J. Cardy, J. Stat. Mech. **2007**, P06008 (2007).

[150] S. Ghoshal and A. Zamolodchikov, Int. J. Mod. Phys. A **9**, 3841 (1994).

[151] D. Fioretto and G. Mussardo, New J. Phys. **12**, 055015 (2010).

[152] S. Sotiriadis, G. Takacs, and G. Mussardo, Phys. Lett. B **734**, 52 (2014).

[153] S. Sotiriadis, D. Fioretto, and G. Mussardo, J. Stat. Mech. P02017 (2012).

[154] J.-S. Caux, private communication.

[155] G. Feher and G. Takacs, Nucl. Phys. B **852**, 441 (2011).

[156] C.-N. Yang, Physical Review Letters **19**, 1312 (1967).

[157] T. R. Klassen and E. Melzer, Nuclear Physics B **382**, 441 (1992).

[158] B. Pozsgay and G. Takacs, Nucl. Phys. B **788**, 167 (2008).

[159] B. Pozsgay and G. Takacs, Nucl. Phys. B **788**, 209 (2008).

[160] Z. Bajnok, L. Palla, G. Takács, and F. Wágner, Nucl. Phys. B **587**, 585 (2000).

[161] M. Kormos and B. Pozsgay, J. High Energy Phys. 1 (2010).

[162] J. Mossel and J.-S. Caux, J. Phys. A **45**, 255001 (2012).

[163] C. Destri and T. Segalini, Nucl. Phys. B **455**, 759 (1995).

[164] T. Prosen, Phys. Rev. Lett. **106**, 217206 (2011).

[165] R. Pereira, V. Pasquier, J. Sirker, and I. Affleck, J. Stat. Mech. **2014**, P09037 (2014).

[166] B. Pozsgay and G. Takács, J. Stat. Mech. P11012 (2010).

[167] M. Kormos and G. Zaránd, arXiv preprint arXiv:1507.02708 (2015).

[168] P. Barmettler *et al.*, Phys. Rev. Lett. **102**, 130603 (2009).

[169] P. Barmettler *et al.*, New J. Phys. **12**, 055017 (2010).

[170] F. Wegner, Annalen der physik **506**, 77 (1994).

[171] C. Knetter and G. S. Uhrig, Eur. Phys. J. B **13**, 209 (2000).

[172] C. P. Heidbrink and G. S. Uhrig, Eur. Phys. J. B **30**, 443 (2002).

[173] S. Kehrein, *The flow-equation approach to many-particle systems* (Springer, Berlin, 2007).

[174] A. Kamenev, in *Field theory of nonequilibrium systems*, edited by 1st (Cambridge university press, Cambridge, 2011).

[175] G. Carleo, F. Becca, M. Schiró, and M. Fabrizio, Scientific reports **2**, (2012).

[176] M. Fagotti and M. Collura, arXiv preprint arXiv:1507.02678 (2015).

[177] B. Sciolla and G. Biroli, J. Stat. Mech. P11003 (2011).

[178] M. Kastner, Phys. Rev. Lett. **104**, 240403 (2010).

[179] S. Bravyi, M. Hastings, and F. Verstraete, Phys. Rev. Lett. **97**, 050401 (2006).

[180] R. Orbach, Phys. Rev. **112**, 309 (1958).

[181] N. Nessi and A. Iucci, arXiv preprint arXiv:1503.02507 (2015).

[182] N. Nessi and A. Iucci, J. Phys.: Conf. Ser. **568**, 012013 (2014).

[183] M. L. Fürst, C. B. Mendl, and H. Spohn, Phys. Rev. E **86**, 031122 (2012).

[184] J. Lux, J. Müller, A. Mitra, and A. Rosch, Phys. Rev. A **89**, 053608 (2014).

[185] H. Kim *et al.*, Phys. Rev. E **92**, 012128 (2015).

[186] T. M. Wright, M. Rigol, M. J. Davis, and K. V. Kheruntsyan, Phys. Rev. Lett. **113**, 050601 (2014).